AD-A189 137 COMPILATION OF NRL PUBLICATIONS ON HIGH TEMPERATURE SUPERCONDUCTIVITY(U) NAVAL RESEARCH LAB WASHINGTON DC D U GUBSER 1987 1/3

UNCLASSIFIED F/G 20/3 NL

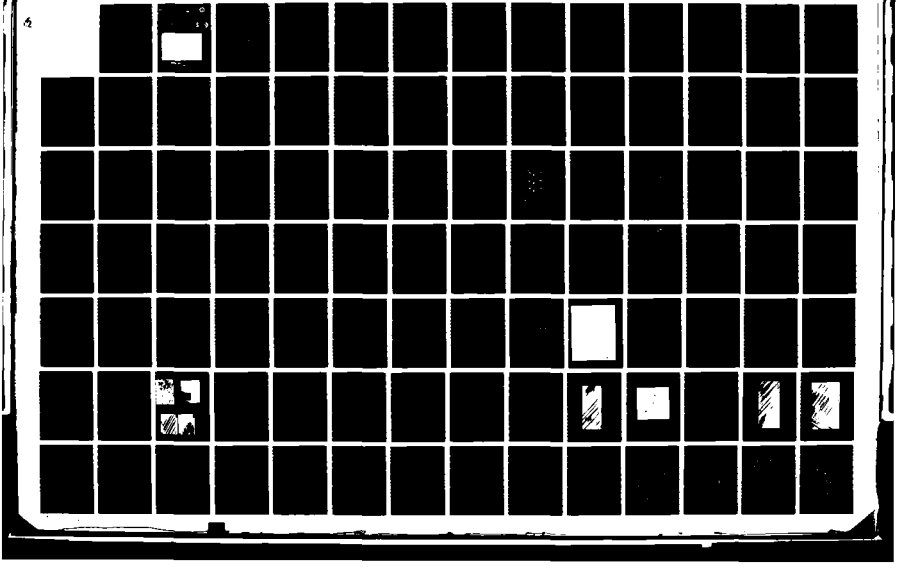

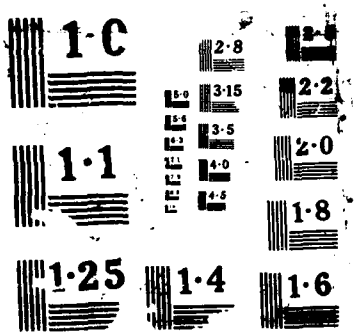
1·C
2·8
3·15
3·5
4·0
4·5
2·2
2·0
1·8
1·1
1·25
1·4
1·6

Naval Research Laboratory
Washington, DC 20375-5000

Compilation of NRL Publications on High Temperature Superconductivity

1 January 1987 — 1 July 1987

Edited by

Donald U. Gubser

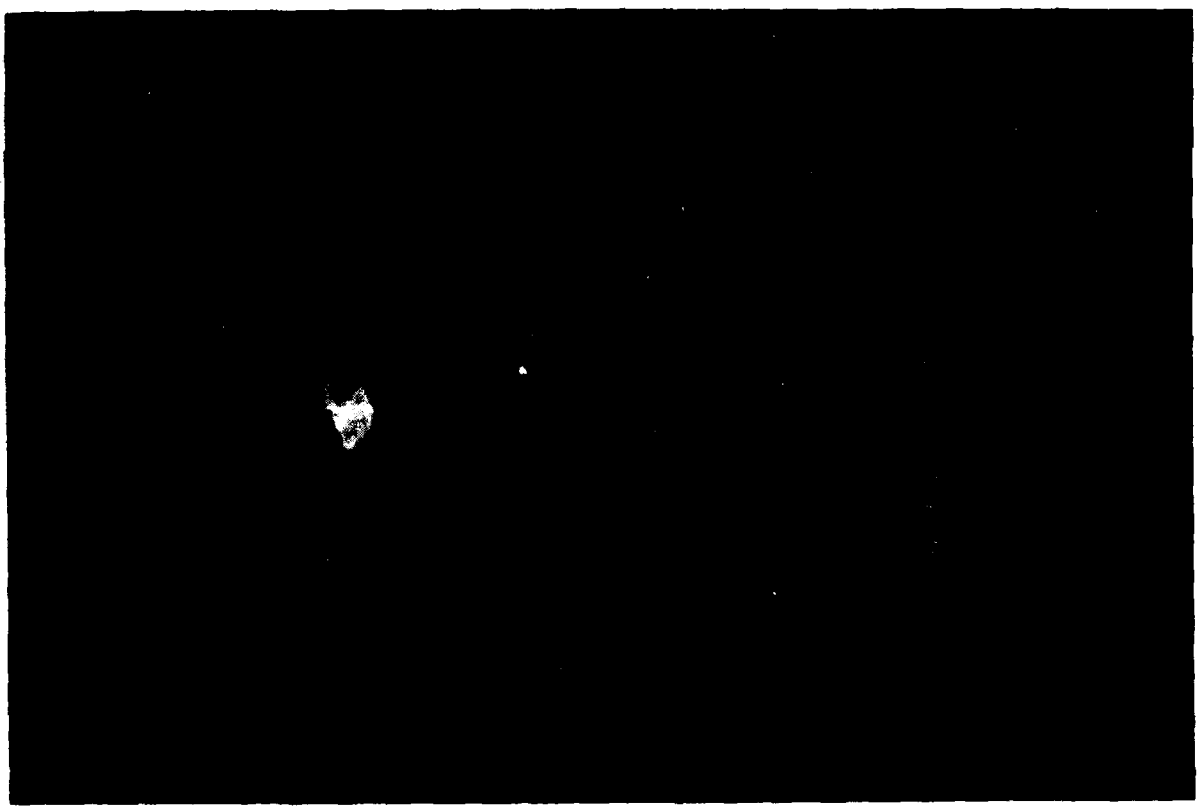

Compilation of NRL Publications on High Temperature Superconductivity

1 January 1987 — 1 July 1987

Edited by

Donald U. Gubser

CONTENTS

PREFACE

The Navy has a long and well established history of research and development in superconducting materials and applications. It was just after World War II that Naval Research Laboratory (NRL) and the Office of Naval Research (ONR) began investigating superconductivity. ONR sponsored two conferences in 1946 to review the status of superconductivity and low temperature physics. By 1950, ONR had sponsored seven conferences on cryogenics, and the ONR program became the focus of much of our nation's effort in the field of superconductivity and low temperature physics. The first volume of Fritz London's famous book, reviewing the macroscopic view of superconductivity, appeared as his fifth ONR technical report. At NRL, the word "cryogenics" first appeared on the organizational chart in 1946. The laboratory acquired one of the first Collins liquifiers in 1948, and began experimental research on superconducting materials shortly thereafter.

In the mid 1950's and 1960's, NRL scientists discovered many new superconducting elements (W and Be) and they were the first to discover superconductivity in low-carrier-density compounds, reporting superconductivity in germanium telluride. Today's new high T_c oxides are also low-carrier-density materials.

In the 1970's, the Navy began programs to develop the use of superconductivity in actual Naval systems. Naval uses for superconductivty range from advanced propulsion systems to sensitive detectors of magnetic fields generated by submarines or other underwater sources, from high power sources of radar to sensitive detectors of electromagnetic radiation, and from high-speed electronic processors to advanced communications systems. Because of these vital interests, the Navy has provided strong support for research on superconducting materials.

Since december 1986, the Navy has been investigating and supporting research on the new high temperature superconducting oxides. Navy scientists are planning the eventual use of the new materials in Naval systems, but not until many materials problems are solved. As these materials become more tractable, however, the Navy will rapidly foster the transition from basic research to the working Navy of the future.

The collection of articles in this report represent research prepared and submitted for publication by scientists at the Naval Research Laboratory during the six months of activity since mid December 1986. It shows the breadth and scope of the materials effort at NRL on the new high temperature superconductors. We expect to see many more exciting research and development results in the near future.

These scientific endeavors at the Naval research Laboratory could not have been done without the support of our management and sponsors. We specifically wish to acknowledge the sponsorship of the Office of Naval Research (ONR), The Strategic Defense Initiative Organization, Office of Innovative Science and Technology (SDIO/IST), and the Defense Advanced Research Project Agency (DARPA).

D.U. Gubser

THE ROCKY ROAD TO HIGH TEMPERATURE SUPERCONDUCTIVITY

E.S. Edelsack,* D.U. Gubser and S.A. Wolf

Naval Research Laboratory
Washington, DC 20375-5000

The story of high temperature superconductivity has its genesis in the stars, particularly in one star, our sun. In the 1860's, unusual spectral lines were observed from the emitted light of the hot incandescent gases in the chromosphere of the sun. These spectral lines appeared unrelated to any then known substance on earth. The gas was given the name "helium" deriving from the Greek word "helios" - sun. At the turn of the century, helium was discovered on earth, and in 1908, the Dutch scientist, Kamerlingh Onnes, succeeded in liquifying helium gas at a temperature a few degrees above absolute zero. This set the stage for the discovery of superconductivity.

In 1911, Onnes observed that below a temperature of 4K, the electrical resistance of mercury completely vanished.[1] He called this a new state of matter and called it superconductivity. Immediately the race was on to discover new materials with higher superconducting transition temperatures, T_c. Initially this meant surveying the elements and simple alloys to determine their superconducting properties. Intermetallic compounds presented more of a materials challenge, but work on these materials also began in the 1920's and 1930's. This work produced a major milestone in 1941 when Aschermann, Friederich, Justi and Kramer[2] reported superconductivity in NbN with a T_c near 16K. In 1937, F. London became the first to speculate that supercurrents might exist in non-metal systems, namely -- aromatic organic molecules.[3] The first experimental high T_c report was made by R. Ogg Jr. in 1946 when he claimed that dilute alkali metal-ammonia solutions became superconducting near 185K[4] if the solution was rapidly cooled. This result was neither reproducible, nor widely accepted by the scientific community.

During the 1950's, efforts in superconductivity revolved around two main themes: 1) development of a microscopic theory, and 2) development of empirical rules to guide the search for new superconducting materials. The first theme included the discovery of the exponential specific heat dependence (energy gap in the electronic spectrum)[5], and the discovery of

*Georgetown Cyrogenics Information Center, 3530 W. Place, Washington, DC

the isotope effect[6] (importance of lattice vibrations), eventually leading to the Bardeen, Cooper, Schrieffer[7] theory of superconductivity and its subsequent refinements. The second theme included development of such empirical rules as the electron per/atom, e/a ratio[8], inverse correlations with Debye temperatures[9], direct correlations with the specific heat[10], and symmetry preferences (cubic symmetry favored over lower symmetry structures)[11]. The search for exotic materials and reports of very high T_c materials were subliminal during this decade. A major materials advance in the 1950's was the discovery of superconductivity in the cubic A15 structure type materials by Hardy and Hulm.[12]

The decade of the 1960's saw rapid advances in superconductivity on four fronts: 1) applied superconductivity was born with the advent of the discoveries of the Josephson effect[13] and high field, high current materials[14]; 2) materials research needed to augment these growing technologies increased significantly; 3) the search for higher T_c materials continued, led primarily by the empirical rules established in the 1950's; and finally 4) a discernable amount of, to paraphrase the words of Alexander Graham Bell, "off the beaten path" theory and experiment began to emerge which would ultimately lead to the discovery of truly high T_c superconductivity in 1986.[15] This paper will briefly discuss the latter two items concerning the search for high T_c materials.

Although the field of superconductivity was growing rapidly in applied areas and in materials processing (films, wires, coatings, etc.), the search for new superconducting materials did not increase concomitantly. In fact, as the push for rapid technology transfer became stronger and stronger, funding of scientific studies to search for new superconducting materials began to decline. Materials research became a secondary goal in many programs. The remainder of this article is dedicated to those scientists who did not let it die!

Although many scientists contributed, one in particular deserves special credit and recognition for keeping the field of superconducting materials research vibrant and healthy for more than 3 decades. His name is Professor BerndMatthias. His contributions during the 1950's, 1960's, 1970's were immense. He is missed today by all.

Materials Search

The majority of researchers searching for high T_c superconductors in the 1960's used empirical rules and stayed within the standard classes of metallic alloys and compounds. Niobium became the favored element and the cubic A15 structure type became the favored structure. Empirical rules such as the e/a ratio[8], atomic volume[16] and atomic mass correlations[17] etc., identified Nb_3Ge and Nb_3Si as candidates to raise T_c above 20K. Neither of these compounds has a stoichiometric equilibrium A15 phase, which was thought to be necessary to obtain the high T_c; thus, researchers began to develop fabrication methods to make metastable phases of the desired compounds.

Rapid cooling techniques leading ultimately to film preparation techniques (sputtering, thermal evaporation, E-beam evaporation, etc.)

were developed leading to the discovery in 1971 of a record high T_c of 23K in Nb_3Ge.[18] Researchers next turned to preparation of Nb_3Si which was expected to have a T_c near 30K. Whereas Nb_3Ge had an off stoichiometric equilibrium A15 phase, Nb_3Si had none. Therefore, the preparation of stoichiometric A15 Nb_3Si was expected to be more difficult than Nb_3Ge, but also more rewarding. In addition to film growth techniques, high pressure synthesis techniques were used in attempts to produce this material. A15 Nb_3Si structures have subsequently been prepared by both techniques in the 1980's, but T_c has been disappointingly low (20K).[19]

Not all research was on A15 structure materials. A significant advance on the road to high T_c materials occurred in 1972 when superconductivity was discovered in $PbMo_6S_8$--a ternary superconductor![20] The significance of this discovery was that it broke the hold of binary superconductors as being the only high T_c materials. Most of the empirical rules developed for the binaries were invalid for the ternaries and synthesis became much more sophisticated. Chemists and material scientists became heavily involved with the search for new materials.

In the late 1970's and early 1980's, superconductivity was discovered in the "heavy Fermion" systems[21] and in nearly magnetic systems.[22] Such research became fashionable even though these systems did not necessarily have high T_c values. New pairing interactions were sought with the hope of eventually using the new interaction for high T_c superconductors.

With the advent of high speed computing, more exact and more precise calculations of T_c in superconducting materials become possible. Theorists began predicting T_c. MoN in the cubic B1 structure was predicted to be a superconductor at 30K.[23] For several years in the mid 1980's a significant amount of experimental research went into attempts to produce this compound. To date, this research has been unsuccessful.

"Off the Beaten Path - Organics"

There were those who decided to forge revolutionary paths in the quest for high T_c. Among the more revolutionary paths was that of looking for superconductivity in organic materials. In 1964, W. Little generated tremendous interest in organic and one dimensional superconductivity when he discussed specific molecular arrangements which would produce superconductivity at room temperature.[24,25] This work generated much excitement, but not much immediate success. Although chemists worked hard to produce structures of the type suggested, and biological and organic molecules of all sorts and types were examined, all of the early reports of superconductivity in these materials proved to be false (or at least nonreproducible and unconfirmed.)

There were many reports of high temperature superconductors in organic materials in the early 1970's. In 1969, Ladik predicted (based on Little's theory) room temperature superconductivity in DNA molecules.[26] In 1972, Wolf claimed superconductivity in bile cholates at temperatures near 140K.[27] Evidence for superconductivity was in magnetic susceptibility anomalies which were not seen in resistance measurements. In 1973, Heeger reported superconducting fluctuations in TTF TCNQ molecules at temperatures as high as 7K.[28] It was claimed that an electronically driven structural transformation (Peierl's instability)

occurred at a temperature slightly higher than the superconducting T_c; hence, bulk superconductivity was not observed. Also in 1971, Cope reported on superconductivity in certain biological systems at temperatures as high as 30C.[29] Evidence for this was the exponential nature of the nerve-muscle response as well as the exponential growth statistics for E. coli. These reponses were claimed to arise from the exponential rise of Josephson currents which followed an energy gap dependence. In 1973, dilute alkali solutions of ammonia were resurrected with a Russian report of superconductivity at 180K.[30] This system is, in certain situations, a very good conductor and at times appeared to exhibit superconductivity. It was unstable, and although several groups tried to reproduce superconductivity, no confirmation was forthcoming.

As reports of very high T_c in organic materials began to fade, significant advances began to occur. In 1975, superconductivity was discovered in a polymeric material SN_x.[31] Although T_c was low (<1K), the discovery did show that superconductivity need not be limited to the conventional alloy systems.

Organic superconductivity was finally discovered in TMTSF-PF_6 by Jerome in 1980.[32] As with SN_x, the T_c was low, but unlike SN_x new organic superconductors were rapidly discovered and T_c began to rise. Research in this field involves significant efforts in organic synthetic chemistry coupled to careful physical measurements. Many new phenomena have been seen in these organic materials in addition to superconductivity. At present the maximum T_c (under pressure) is 8K in β-(BEDT-TTF)$_2I_3$.[33] There is some evidence that the mechanism for superconductivity in the organic materials is not the electron-phonon interaction and there are also speculations that "p" wave pairing interactions are occurring.

"Off The Beaten Path - Layered Compounds"

Later in 1964 (the year that Little revived interest in organic materials), V.L. Ginzburg discussed a new mechanism and a new structure for producing high temperature superconductivity[34] - namely, the excitonic mechanism in layered, or two dimensional structures. Several refinements and variations including the possibility of excitations between two overlapping bands, a three dimensional mechanism proposed by Geilikman,[35] occurred during the next nine years, culminating in the Allender, Bray, Bardeen[36] theory of excitonic superconductivity in 1973. No definitive confirmation of the mechanism has been reported and until recently, there were no high T_c reports in layered structures. Other theories were proposed in this period including various plasmon coupling mechanisms.[37] No experimental demonstration of these models has yet been confirmed.

In 1980, superconductivity was reported in the eutectic Ir-Y at 3K.[38] Since neither Y or Ir have T_c's above 1K, and only these elementary phases were seen in the eutectic, superconductivity was suggested to be a result of the layered nature of the eutectic. This result spurred interest in multilayered metallic systems with the hope of reproducing and improving on what nature had supplied in the eutectics materials. To date no similar enhancements of superconductivity have been reported.

In 1983, Japanese scientists reported superconductivity at temperatures as high as 200K in a Nb layer grown on Si.[39] This result has not gained wide acceptance by the scientific community.

"Off the Beaten Path - Oxides and Hole Carriers"

The last "off the beaten path" that we wish to trace is the path which ultimately led to the recent breakthrough in high temperature superconductivity - namely, the oxides and low carrier density materials. This story begins in 1964 with the publication by M. Cohen predicting superconductivity in semiconducting type materials.[40] The experimental search for superconductivity culminated in 1964 when R. Hein reported superconductivity is p-type GeTe.[41] Shortly thereafter, superconductivity was discovered in $SrTiO_3$ - the first oxide superconductor and the first perovskite superconducting material.[42] Although T_c of these materials were below 1K, history must regard these reports as major milestones in the road to high temperature superconductivity since they started the interest in these types of materials, which persisted on a limited basis until the recent discoveries of superconductivity as in LaBaCuO[15] and YBaCuO.[43]

The next major milestone in this direct route to high T_c occurred in 1973 when Johnston discovered superconductivity in $LiTiO_3$ at temperatures as high as 13K,[44] thus removing the belief that superconductivity in the oxide materials was limited to very low temperatures. In 1975, superconductivity was discovered in $PbBiBaO_3$ at 14K to represent another member to the growing class of higher temperature oxides.[45] $PbBiBaO_3$ had interesting properties which made it potentially useful as sensors of electromagnetic radiation; hence, research on this material persisted over the next eleven years even though T_c was not raised. It was scientists working on these materials who first recognized the significance of the high temperature oxide discoveries and who so rapidly assumed leadership in the early discoveries. But we got ahead of ourselves, for the road to success was not so direct or easy. First came a few false, or at least unconfirmed and nonreproducible results.

In 1975, hints of superconductivity was found in CuCl under high pressures.[46] In 1978, the superconductivity world was rocked by a Russian report of superconductivity in CuCl at temperatures near 140K.[47] This report in fact marked the beginning of the New York Times becoming the premiere journal for reporting high temperature superconductivity discoveries. In the May 9th, 1978 issue of the New York Times, we find reports by B. Matthias "this is a completely false result and probably deliberately meant to deceive", while in the same article we find C.W. Chu suggesting that "there may indeed be some truth to such high temperature superconductivity reports" and that it deserved a further look. Thus, twelve years before the discoveries in LaBaCuO some of the main actors in the eventual explosive discovery were already searching "off the beaten path".

Work on CuCl persisted for years, polarizing many scientists into believers, and nonbelievers. In fact, there is still interest in CuCl even though the results are nonreproducible, thermal history dependent, and subject to a variety of interpretations.

By 1980, interest in the low carrier materials gained new impetus with the report of superconductivity in pressure quenched CdS at temperatures as high as 150K.[48] Like the work on CuCl, the experimental

data were highly nonreproducible, and subject to different interpretation.

In 1980, $TiBe_{1.6}$ was reported to be superconducting at 22C.[49] This result received little scientific interest as, once again, it was nonreproducible and subject to reinterpretation in terms of nonsuperconducting phenomena.

These early reports of high temperature superconductivity are an interesting part of the story of high temperature superconductivity. They set the stage for the discovery which was to come in 1986. The early results and their lack of confirmation had led many scientists to treat such reports as coming from scientists who were more interested in gaining fame than in doing creditable scientific research. It is noteworthy that Bednorz and Mueller[15] waited many months to publish their original discovery, due primarily to this climate of distrust for such reports. It is a credit to them and to those who immediately recognized the importance of their announcement that we now have advanced so far in our understanding of the materials.

Where will the search for high temperature superconductivity lead us next; new materials, new technology, new scientific insights? Yes, probably all of these. But perhaps more important is the realization that the scientific world needs to renew its committment and provide proper recognition and support for those scientists who are not afraid to occasionally stray from the beaten path and delve into the forest. The woods are full of delicious fruit. Let us not be afraid to look for them.

Acknowledgement

We acknowledge W.W. Fuller and R.A. Hein for their critical reading of this manuscript and their many helpful suggestions.

References

1. H.K. Onnes. Leiden comm. 124C (1911).

2. G. Ascherman, E. Friederich, E. Justi and J. Kramer, Phys. Zeir., 42 349 (1941).

3. F.J. London, "Superconductivity in Aromatic Molecules", J. of Chemistry and Physics, 5 (1937).

4. R.A. Ogg, Jr., Phys. Rev. 69, 243 (1946).

5. W.S. Corak, B.B. Goodman, C.B. Satterthwaite and A. Wexter, Phys. Rev. 96, 1442 (1954).

6. E. Maxwell, Phys. Rev. 78, 477 (1950); 79, 173 (1950), Reynolds, Sevin, Wright and Nesbitt, Phys. Rev. 78, 487 (1950).

7. J. Bardeen, L.N. Cooper and J.R. Schrieffer, Phys. Rev. 106, 162 (1957); Phys. Rev. 108, 1175 (1957).

8. B.T. Matthias, Phys., Rev. 97 74 (1955).

9. J. DeLauney and R. Dolecek, Phys., Rev. 72, 141 (1947).

10. H.W. Lewis, Phys. Rev. 101, 939 (1956).

11. B.T. Matthias, T.H. Geballe and V.B. Compton, Reviews of Modern Phys. 35, 1 (1963).

12. G.F. Hardy and J.K. Hulm, Phys. Rev. 93, 1004 (1954).

13. B.D. Josephson, Phys. Lett. 1, 251 (1962).

14. J.E. Kunzler, E. Benkler, F.S.L. Hsu and J.H. Wernick, Phys. Rev. Lett. 6, 89 (1961).

15. J.G. Bednorz and K.A. Mueller, Z. Phys. B64, 189 (1986).

16. L.R. Testardi, J.E. Kunzler, H.G. Levinstein, J.P. Maita and J.E. Wernick, Phys. Rev. B3, 107 (1971).

17. L. Gold. Phys. Stat. Sol. 4, 261 (1964); D. Dew Hughes and V.G. Rivlin, Nature 50, 723 (1974).

18. J.R. Gavaler, App. Phys. Lett. 23, 480 (1973).

19. J.D. Dew Hughes and V.D. Linse, J. Appl. Phys. 50, 3500 (1979); R.E. Somekh and J.E. Evetts, IEEE Trans. Magn. MAG-15, 494 (1979).

20. B.T. Matthias, M. Marezio, E. Corenzwit, A.S. Cooper and H.E. Barz, Science, 175, 1465 (1972).

21. F. Steglich, J. Aarts, C.D. Bredl, W. Lieke, D. Meschede, W. Franz and H. Schafer. Phys. Rev. Lett. 43, 1892 (1979).

22. H.R. Ott, H., Rudiger, Z. Fisk and J.L. Smith, Phys. Rev. Lett. 50, 1595 (1983).

23. W.E. Pickett, B.M. Klein and D.A. Papaconstantopoulos, Physica B&C, 265 (1981).

24. W.A. Little, Phys. Rev. A134, 1416 (1964).

25. W.A. Little, Report on the International Symposium on the Physical and Chemical Problems of Possible Organic Superconductors, 31, (1969).

26. J. Ladik and A. Bierman, Phys. Lett. 29A, 636 (1969).

27. E.H. Halpern and A.A. Wolf, Advanced Cryog. Eng., 17, 109 (1972).

28. L.B. Colemen, M.J. Cohen, D.J. Sandman, F.G. Yamagishi, A.F. Garito and A.J. Heeger, Solid State Commun. 12, 1125 (1973).

29. F.W. Cope, Physiol. Chem. and Physics, 3, 403 (1971).

30. I.M. Dmitrenko and I.S. Shchetkin, Zhetf. Pis. Red. 18, 497 (1973).

31. R.L. Greene, P.M. Grant and G.B. Street, Phys. Rev. Lett. 34, 89 (1975).

32. D. Jerome, A. Mazaud, M. Ribault, and K. Bechgaard, J. Phys. (Paris) Lett. 41, L95 (1980).

33. V.N. Tauklin, E.E. Khostyuchenko, Yu. V. Sushko, I.F. Schnegolve, and E.B. Yagubskii, Pis'ma Zh. Eksp. Teor. Fiz. 41, 68 (1985) (JETP Lett. 41, 81 (1985]. K. Murata, M. Tokumoto, H. Anzai, H. Bando, G. Saito, K. Kajimura, and T. Ishiguro, J. Phys. Soc. Jpn. 54, 1236 (1985).

34. V.L. Ginzburg, Phys. Letters 13, 101 (1964); V.L.Ginzburg and D.A. Kirzuits, Zh. Etisperim, i Theor. Fiz. 46, 397 (1964) [Trans.0:ov. Phys. JETP 19, 269 (1964).]

35. B.T. Geilikman, Usp. Fiz. Nauk. 88, 327 (1966) [Trans.: Sov. Phys. Usp. 9, 142 (1966).

36. D. Allender, J. Bray, and J. Bardeen, Phys. Rev. 7B, 1020 (1973).

37. L.M. Kahn and J.R. Ruvalds, Phys. Rev. B19, 5652 (1979).

38. B.T. Matthias, G.R. Stewart, A.L. Giorgi, J.L. Smith, Z. Fisk and H. Barz, Science, 208, 401 (1980).

39. T. Ogushi, K. Obara, T. Anayama, Jap. J. Appl. Phys. 22, L523 (1983).

40. M.L. Cohen, Phys. Rev. 134, A511 (1964).

41. R.A. Hein, J.W. Gibson, R. Mazelsky, R.C. Miller and J.K. Hulm, Phys. Rev. Lett. 12, 320 (1964).

42. J.F. Schooley, W.R. Hoster, E. Ambler, J.H. Becker, M.L. Cohen and C.S. Koonce, Phys. Rev. Lett. 14, 305 (1965).

43. M.K. Wu, J.R. Ashburn, C.J. Torng, P.H. Hor, R.L.Meng, L. Gao, Z.J. Huang, Y.Q. Wang, and C.W. Chu, Phys. Rev. Lett. 58, 908 (1987).

44. D.C. Johnston, H. Prakash, W.H. Zachariasen and R. Viswanathan, Mat. Res. Bull. 8, 777 (1973).

45. A.W. Sleight, J.L. Gillson and P,.E. Bierstedt, Sol. State Comm. 17, 27 (1975).

46. A.P. Rusakov, V.N. Laukhin and Yu A. Lisovskii, Phys. Stat. Sol (b) 71, K191 (1975); C.W. Chu, S. Early, T.H. Geballe, A.P. Rusakov and R.E. Schwell, J. Phys. C8, L241 (1975).

47. N.B. Brandt, S.V. Kuoshiunikov, A.P. Rusakov, and V.M. Semenor, Pisma Zh. Ehsp. Theor. F12, 27, 37 (1978) [Trans.: JEPT Lett. 27, 33 (1987)]; C.W. Chu, A.P. Rusakov, S. Huang, S. Early, T.H. Geballe, and C.Y Huang, Phys. Rev. B18, 2116 (1978).

48. E. Brown, C.G. Homan and R.K. MacCrone, Phys. Rev. Lett. 45, 478 (1980).

49. F.W. Vahldiek, C & EN, Sept. 8th (1980) pg. 36.

Superconducting phase transitions in the La-M-Cu-O layered perovskite system, M = La, Ba, Sr, and Pb

D. U. Gubser, R. A. Hein,* S. H. Lawrence, M. S. Osofsky, D. J. Schrodt, L. E. Toth,† and S. A. Wolf
Naval Research Laboratory, Washington, D.C. 20375-5000
(Received 5 February 1987)

We report results of our studies of the La-M-Cu-O system, M = La, Ba, Sr, and Pb. T_c and the magnetic moment are correlated with annealing schedules and x-ray structural analyses. The occurrence of superconductivity is associated with the formation of Cu^{3+} ions producing an expansion of the c parameter of the unit cell. We have found magnetic and resistive anomalies near 65 K in some La-Ba-Cu-O samples. These samples show a slight depression of the superconducting transition temperature.

Observation of superconductivity in the La-Ba-Cu-O system[1] at temperatures over 30 K has sparked worldwide enthusiasm and research on this new class of high-temperature superconductors. High-temperature superconductivity ($T_c > 10$ K) had been reported in only two other oxide systems, the Li-Ti-O system possessing a cubic spinel structure,[2] and the Ba-Pb-Bi-O system possessing the perovskite structure,[3] with maximum transition temperatures of 13.7 and 13 K, respectively. The new La-Ba-Cu-O oxide system, with T_c's reported above 40 K,[4-7] possesses a layered perovskite K_2NiF_4-type crystal structure and is metallic at room temperature. The earliest data on the La-Cu-O layered perovskite system date to the early 1960's.[8,9] In 1973, Goodenough, Demazeau, Pouchard, and Hagenmuller reported on an oxygen defect phase in the La-Sr-Cu-O system where the Cu ion assumes a +3 valency.[10] In 1979 Shaplygin, Kakhan, and Lazarev[11] reported metallic conductivities in the compounds $La_{2-x}M_xCuO_4$ with M = Ca, Sr, Ba, and Pb. The initial report of superconductivity in the M = Ba compound has been confirmed by several groups[4-7] and superconductivity has subsequently been observed in the M = Sr (Refs. 12 and 13) and M = Ca (Ref. 13) compounds. Both zero resistance and partial flux expulsion (Meissner effect) have been observed in these samples giving evidence that the compounds are bulk superconductors.

The La-M-Cu-O compounds are prepared either by coprecipitation from aqueous solutions of La, Cu, and M nitrates or by reacting powdered mixtures of oxides and carbonates of La, Cu, and M. Various reaction temperatures and reaction times have been reported as well as various post-reaction annealing schedules which improve the superconducting properties.

Our materials were prepared from reagent-grade powders of La_2O_3, $BaCO_3$, $SrCO_3$, $CaCO_3$, PbO_2, and CuO. These powders were mixed in appropriate ratios to form the desired compounds and calcined in air at temperatures between 1000 °C and 1100 °C for approximately 12 h. The materials were then reground into powder, pressed into small disks (nominally 1-cm diameter by 2-mm height) and sintered in air at temperatures between 1000 °C to 1100 °C for 12 h. The calcined powders and the sintered pellets were x-rayed following each process to ensure the K_2NiF_4 phase was present. In one case the La-Ba-Cu-O powder was calcined a second time before pressing and sintering. This recalcining did improve the structural quality of the compound, as evidenced by the sharpness of the x-ray lines, but slightly lowered the onset of the superconducting transition and produced magnetic and electrical anomalies near 65 K (discussed later). Calcining and/or sintering in a pure oxygen atmosphere at 1100 °C produced substantial phases other than the K_2NiF_4 phase which were not superconducting.

The La-Ba-Cu-O compounds were prepared in three compositions, $La_{2-x}Ba_xCuO_4$ where x = 0.1, 0.2, and 0.3. The resistive transitions were measured on the sintered pellets by attaching four leads with indium solder. The resistivity of the pellets was relatively high (≈10000 $\mu\Omega$ cm), which we assume is due to the granular nature of the loosely compacted and sintered pellet rather than the intrinsic resistivity of the material itself. Similarly, the transition is broadened and the critical current (≈5.0 A/cm^2) is low because of the granularity. Figure 1 shows the resistive and magnetic transition for the x = 0.1 sample which had the sharpest transition and the highest onset

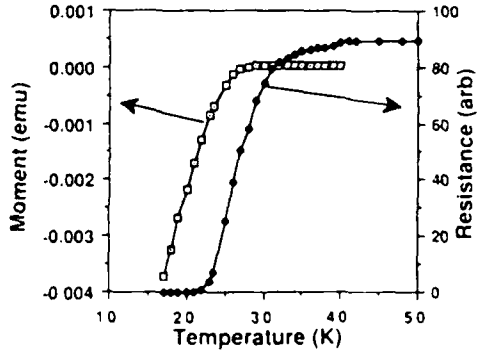

FIG. 1. Resistance and magnetic moment plotted vs temperature of $La_{1.9}Ba_{0.1}CuO_4$. The onset temperature for superconductivity in the resistive transition is 40 K. Magnetic moment was measured cooling in 100 Oe and represents about 10% flux exclusion

temperature. The onset temperature T_0 was 40 K and the $R=0$ point was 24 K. The magnetic moment was measured cooling in a 100-G ambient field and was still changing at 10 K (the lowest temperature measured), but at this point it represented about a 10% flux exclusion (subsequent Sr samples showed over 50% exclusion). T_0, determined magnetically, of this sintered material is about 28 K.

An interesting anomaly in the resistive and magnetic transition appears around 65 K in some of our samples. Figure 2 shows the magnetic moment of two $La_{1.9}Ba_{0.1}CuO_4$ samples, one of which had been reacted only once at 1100 °C for 12 h (a), while the other had been reacted a second time also at 1100 °C for 12 h (b). X-ray spectra of these samples are shown in Fig. 3. The twice-reacted sample (similar thermal history as the sintered samples), which shows the anomaly, has slightly sharper x-ray lines indicating a more homogeneous composition, and the c parameter is smaller. It also has a slightly depressed T_0 (28 vs 32 K).

The anomaly at high temperature in the twice-reacted $La_{1.9}Ba_{0.1}CuO_4$ may be associated with an electronically driven distortion of the lattice similar to a charge-density-wave (CDW) transition. Such transitions remove carriers from the conduction process and are usually detrimental to superconductivity.[14] Similarly, the CDW structural distortion is removed by crystalline defects of various types[15] and may explain the absence of an anomaly in the slightly less homogeneous once-reacted samples. The tendency for a structural instability is often correlated with low-frequency phonon modes that are important for high T_c. The anomalies observed in our samples also suggest that such low-frequency modes may be present and may be responsible for the very high T_c in these materials.[16]

Magnetic transitions for $La_{1.8}Sr_{0.2}CuO_4$ and $La_{1.7}Ca_{0.3}CuO_4$ samples are shown in Fig. 4. T_0, determined magnetically, for these samples are 36 and 24 K, respectively. Samples having the composition Ba, $x=0.1$ and 0.2; Sr, $x=0.1$ and 0.2; and Ca, $x=0.3$, showed x-ray spectra characteristic of nearly single phase K_2NiF_4 structure and had higher and sharper transitions than other compositions.

Three compositions of $La_{2-x}Pb_xCuO_4$ with $x=0.1$, 0.2, and 0.3 were also made. These samples were processed in a similar manner as were the Sr, Ba, and Ca samples. The Pb, $x=0.1$ sample had an x-ray spectrum with nearly single-phase K_2NiF_4 structure. In the lowest resistivity of the three compositions, however, the sample showed no sign of superconductivity and had activated conductivity. Various subsequent annealing procedures were attempted to improve the conductivity of this sample. An inert gas anneal at 750 K for 12 h produced the lowest resistivity of about 30000 Ω cm, but again there was no sign of superconductivity.

Superconductivity in this new class of high T_c compounds appears to be intimately connected with the valence of the Cu^{3+} ion.[12] In La_2CuO_4 the copper is in

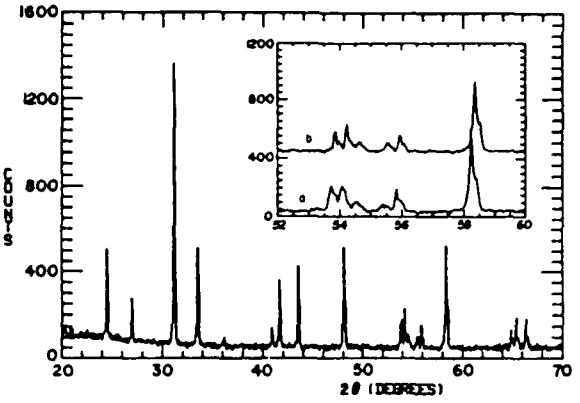

FIG. 3. The x-ray powder diffraction pattern for the twice-calcined sample of $La_{1.9}Ba_{0.1}CuO_4$. The pattern shows a single-phase K_2NiF_4 structure. The inset compares a portion of this pattern [(b) upper trace] with the same region of the x-ray pattern for the (a) singly calcined sample. Note that the singly calcined sample has broader lines at a slightly smaller 2θ (indicating a larger lattice parameter).

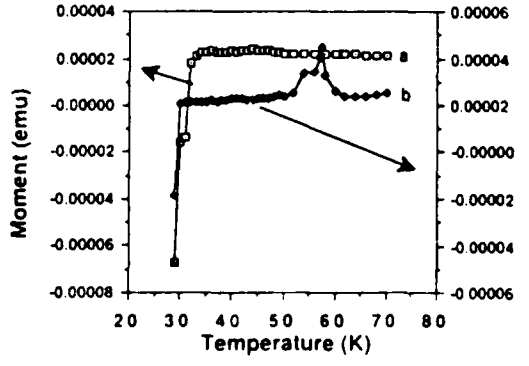

FIG. 2. This figure shows the (a) once-reacted and (b) twice-reacted samples of $La_{1.9}Ba_{0.1}CuO_4$ plotted vs temperature. The anomaly in the twice-reacted sample near 60 K is clearly visible as is the reduction in the onset temperature for superconductivity.

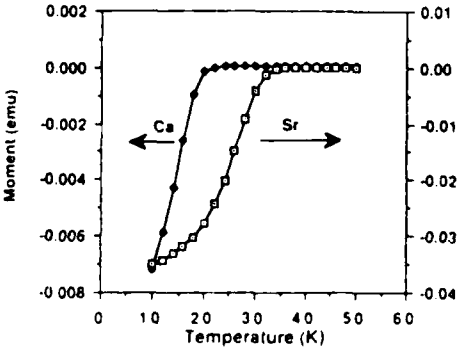

FIG. 4. The magnetic moment of $La_{1.8}Sr_{0.2}CuO_4$ and $La_{1.7}Ca_{0.3}CuO_4$ plotted vs temperature. The magnetic moment for the sample at 10 K represents almost 60% flux expulsion (100-Oe ambient field).

TABLE I. Sample parameters.

Material	a (Å)	c (Å)	c/a	T_0 (K)
$La_{1.8}Ca_{0.2}CuO_4$	3.790	13.159	3.47	22.5
$La_{1.7}Ca_{0.3}CuO_4$	3.782	13.162	3.48	25
$La_{1.9}Ba_{0.1}CuO_4$	3.786	13.238	3.49	30*
$La_{1.9}Ba_{0.1}CuO_4$	3.787	13.256	3.50	33*
$La_{1.8}Ba_{0.2}CuO_4$	3.801	13.301	3.50	31
$La_{1.9}Sr_{0.1}CuO_4$	3.771	13.233	3.51	36.5
$La_{1.8}Sr_{0.2}CuO_4$	3.777	13.261	3.51	37
$La_{1.7}Sr_{0.3}CuO_4$	3.798	13.111	3.45	< 4
$La_{1.9}Pb_{0.1}CuO_4$	3.801	13.191	3.47	. . .
$La_{1.8}Pb_{0.2}CuO_4$	3.772	13.120	3.48	. . .
$La_{1.7}Pb_{0.3}CuO_4$	3.791	13.158	3.47	. . .

*T_0 measured by dc susceptibility.

the +2 valence state. The addition of Ba, Sr, Ca, and Pb either forces some of the Cu ions into the +3 valence state, creating a mixed valence compound, or produced oxygen vacancies.[17,18] The preservation of Cu^{3+} by minimizing the oxygen vacancy formation with suitable processing procedures is essential to superconductivity. The extra electrons from Cu provide carriers which make the material highly conductive and superconductive in some cases. The relative amounts of Cu^{3+} ions can be inferred from the x-ray structural analysis. Cu^{3+} produces an expansion of the c parameter relative to the a parameter if the oxygen content remains constant.[17] Table I lists the a and c parameters for the compounds shown as well as the T_0 values of the samples. The correlation of superconductivity with the size of the c/a ratio is clearly evident.

Reacting or annealing the compounds in oxygen can be either detrimental or beneficial depending on the presence of second-phase higher oxides. If second-phase higher oxides are present, then annealing in oxygen at high temperatures will promote the growth of this phase at the expense of the LaM_xCuO_4 oxide. An associated reduction of the c parameter in the K_2NiF_4 structure is observed. In this situation, annealing in a reducing atmosphere rather than an oxidizing one promotes the growth of LaM_xCuO_4 oxide and enhances the superconducting properties. If, on the other hand, one has a single phase K_2NiF_4 structure or a second phase of lower oxides, then a low-temperature oxygen anneal which does not nucleate a higher oxide second phase will promote the formation of more Cu^{3+} by ensuring that more oxygen vacancies are filled. Thus we see that annealing schedules and procedures may vary significantly depending on the exact chemistry of the compound.

In summary, we have prepared $La_{2-x}M_xCuO_4$ superconducting compounds with M_x = Ba, Sr, and Ca. With M = Pb, the compound of the same structure is not superconducting. The reason for this change in behavior is unclear but is most likely associated with the ability of Pb to promote Cu^{3+} ions versus oxygen vacancies. Correlation of the presence of Cu^{3+} ions with the c/a ratio has been demonstrated, and a reason for the variety of apparently conflicting annealing procedures has been suggested.

The authors thank C. Vold, J. Wallace, S. Qadri, J. Claassen, T. Francavilla, V. Kresin, J. Krebs, D. Papaconstantopoulos, and W. Pickett for their assistance and valuable discussions. One of us (M.S.O.) was partially supported by the Office of Naval Technology.

*Permanent address: Catholic University of America, Washington, DC 20064.

†Permanent address: National Science Foundation, Washington, DC 20550.

[1]J. G. Bednorz and K. A. Muller, Z. Phys. B **64**, 189 (1986).

[2]D. C. Johnston, H. Prakash, W. H. Zachariasen, and R. Viswanathan, Mater. Res. Bull. **8**, 777 (1973).

[3]A. W. Sleight, J. L. Gillson, and P. E. Bierstedt, Solid State Commun. **17**, 27 (1975).

[4]C. W. Chu, P. H. Hor, R. L. Meng, L. Gao, Z. J. Huang, and Y. Q. Wang, Phys. Rev. Lett. **58**, 405 (1987).

[5]S. Uchida, H. Takagi, K. Kitazawa, and S. Tanaka, Jpn. J. Appl. Phys. (to be published).

[6]H. Takagi, S. Uchida, K. Kitazawa, and S. Tanaka (unpublished).

[7]S. Uchida, H. Takagi, K. Kitazawa, and S. Tanaka (unpublished).

[8]M. Foex, A. Mancheron, and L. Line, C. R. Acad. Sci. **250**, 3027 (1960).

[9]J. M. Longo and P. M. Raccah, J. Solid State Chem. **6**, 526 (1963).

[10]J. B. Goodenough, G. Demazeau, M. Pouchard, and P. Hagenmuller, J. Solid State Chem. **8**, 325 (1973).

[11]I. S. Shaplygin, B. G. Kakhan, and V. B. Lazarev, Zh. Neorg. Khim. **24**, 1478 (1979) [J. Inorg. Chem. **24**, 820 (1979)].

[12]R. J. Cava, R. B. van Dover, B. Batlogg, and E. A. Rietman, Phys. Rev. Lett. **58**, 408 (1987).

[13]K. Kishio, K. Kitazawa, S. Kanbe, I. Yasuda, N. Sugii, H. Takagi, S. Uchida, K. Fueki, and S. Tanaka (unpublished).

[14]G. Bilbro and W. L. McMillan, Phys. Rev. B **14**, 1887 (1976).

[15]W. W. Fuller, O. M. Chaikin, and N. P. Ong, Phys. Rev. B **24**, 1333 (1981).

[16]V. Z. Kresin (unpublished).

[17]N. Nguyen, J. Choisnet, M. Hervieu, and B. Raveau, J. Solid State Chem. **39**, 120 (1981).

[18]C. Michel and B. Raveau, Rev. Chim. Miner. **21**, 407 (1984).

TEMPERATURE DEPENDENT X-RAY STUDIES OF THE HIGH-T_c SUPERCONDUCTOR $La_{1.9}Ba_{0.1}CuO_4$

E. F. Skelton, W. T. Elam D. U. Gubser, S. H. Lawrence

M. S. Osofsky[†] L. E. Toth[††] and S. A. Wolf

Condensed Matter and Radiation Sciences Division
Naval Research Laboratory
Washington, DC 20375-5000

Abstract

Simultaneous x-ray diffraction and four-probe electrical resistance measurements have been performed as a function of temperature on a polycrystalline sample of the high-T_c material $La_{1.9}Ba_{0.1}CuO_4$. Comparisons of the diffraction spectra between 290 and 18 K show no evidence of any gross structural distortions. Least-squares refinements of the tetragonal unit cell parameters at several temperatures indicate smooth monotonic thermal expansions of about 0 10±0.05% along the a-axis and about 0.35±0.10% along the c-axis over this temperature range.

[†]On sabbatical leave from the National Science Foundation
[††]ONT Postdoctoral Fellow

Introduction

It has recently been reported[1] and confirmed[2] that superconductivity occurs in La-Ba-Cu-oxides at temperatures (T_c) in excess of 30 K. Subsequent structural studies[3] have identified the superconducting phase as being $(LaBa)_2CuO_{4-y}$, crystallizing in the tetragonal K_2NiF_4-type structure. More recently, a magnetic and resistive anomaly was reported in $La_{1.9}Ba_{0.1}CuO_4$ near 65 K, well above T_c. We have performed a series of x-ray diffraction measurements as a function of temperature to investigate whether this anomaly is associated with a structural distortion and to obtain structural information on this material at low temperatures.

Experimental Procedures

The test specimen was prepared by mixing appropriate proportions of reagent grade powders of La_2O_3, $BaCO_3$ and CuO to yield a product of nominal composition $La_{1.9}Ba_{0.1}CuO_4$. The mixture was calcined twice in air at 1000-1100° C for approximately 12 hours and pressed into a cylindrical pellet.

The pellet was mounted with thermally conducting grease on the cold stage of a Heli-tran cryogenic refrigerator. This refrigerator system is coupled to a computer controlled x-ray diffractometer in a manner similar to that previously described.[5] A calibrated Si-diode thermometer is also bonded to the low-temperature block and coarse temperature control is achieved by regulating the flow rate of He fluid from a remote storage dewar. Fine control is accomplished with an electrical heater and feedback control circuit using either a Pt or Ge sensor, depending on the temperature range. The measured temperatures are estimated to be accurate and stable to within +0.5 K.

Four leads were bonded to the sample with In-solder and the electrical resistance was continuously monitored. A typical resistance curve is shown in Fig. 1. Although the resistive anomaly reported in Ref. 4 was not observed, possibly due to aging effects, a local minimum in the resistance near 70 K was observed to precede the onset of superconductivity which occurs at about 38 K. The superconducting transition is complete at 29 K.

Concurrent with the resistance measurements the sample was illuminated with radiation from a Cu x-ray tube operated at 30 kV and 20 ma. A 9 um thick Ni foil was placed in the incident beam to attenuate the Cu-K-beta radiation.

Results and Discussion

Diffraction spectra recorded at 297.5 and 24.0 K are shown in Fig. 2. All but four of the diffraction peaks can be indexed on the basis of the tetragonal K_2NiF_4-type structure. These four peaks, identified as A through D in Fig. 2, are believed to be associated with a small component of the orthorhombic phase, a distortion of the K_2NiF_4-structure.[6], present in the sample

Based on least-squares analyses of the measured Bragg angles of 15 diffraction peaks between 40° and 80°, the [a;c]-tetragonal unit cell parameters are found to be [3.7873±0.0012 A;13.235±0.019 A] at 297.5 K and [3.7820±0.0025 A;13.168±0.037 A] at 24.0 K. To provide an estimate of the linear thermal expansivities and possibly detect anomalous behavior in the vicinity of the electrical/magnetic anomalies, measurements of five diffraction peaks, the (2,1,7), (2,0,8), (3,0,3), (3,1,0) and (1,1,10) were performed at several different temperatures. The temperature dependence of the fractional change in the unit cell parameters derived from the data are plotted in Fig. 3. There is an overall expansion of about 0.10±0.05%

and 0.35±0.10% in the a and c axes, respectively. To within the uncertainty of the measurements, there is no indication of any unusual behavior in these linear expansivities.

Most recently, neutron powder diffraction measurements have been reported on $La_{1.85}Ba_{0.15}CuO_4$ at 295 and 10 K.[7] The observations reported here are in agreement with the results of the neutron measurements. In summary, the results of these experiments do not indicate any gross low temperature lattice distortions in $La_{1.9}Ba_{0.1}CuO_4$ over the temperature range from 18 to 300 K. It should be noted that this does not rule out the possibility of a charge density wave transition or other less demonstrative effect occuring in these materials. Single crystal samples would be helpful in searching for these possibilities.

Figure Captions

Fig. 1: Temperature dependence of the electrical resistance exhibiting a local minimum near 70 K.

Fig. 2: X-ray diffraction spectra as recorded at 297.5 K (upper curve) and 24.0 K (lower curve).

Fig. 3: Fractional change in the tetragonal a and c lattice parameters on increasing temperature from 18 K.

References

1. J. G. Bednorz and K. A. Müller, Z. Phys. B 64, 189 (1986).

2. S. Uchida, H. Takagi, K. Kitazawa, and S. Tanaka, Japan J. Appl. Phys. Lett. (to be pub.).

3. H. Takagi, S. Uchida, K. Kitazawa, and S. Tanaka, Japan J. Appl. Phys. Lett. (to be pub.).

4. D. U. Gubser, R. A. Hein, S. H. Lawrence, M. S. Osofsky, D. J. Schrodt, L. E. Toth, and S. A. Wolf, submitted to Phys. Rev. Lett.

5. E. F. Skelton, I. L. Spain, S. C. Yu, C. Y. Liu and E. R. Carpenter, Jr., Rev. Sci. Instrum. 55, 849 (1984).

6. J. M. Longo and P. M. Raccah, J. Solid State Chem. 6, 526 (1973).

7. J. D. Jorgensen, H.-B.Schüttler, D. G. Hinks, D. W. Capone II, K. Zhang, M. B. Brodsky, and D. J. Scalapino, Phys. Rev. Lett. 58, 1024 (1987).

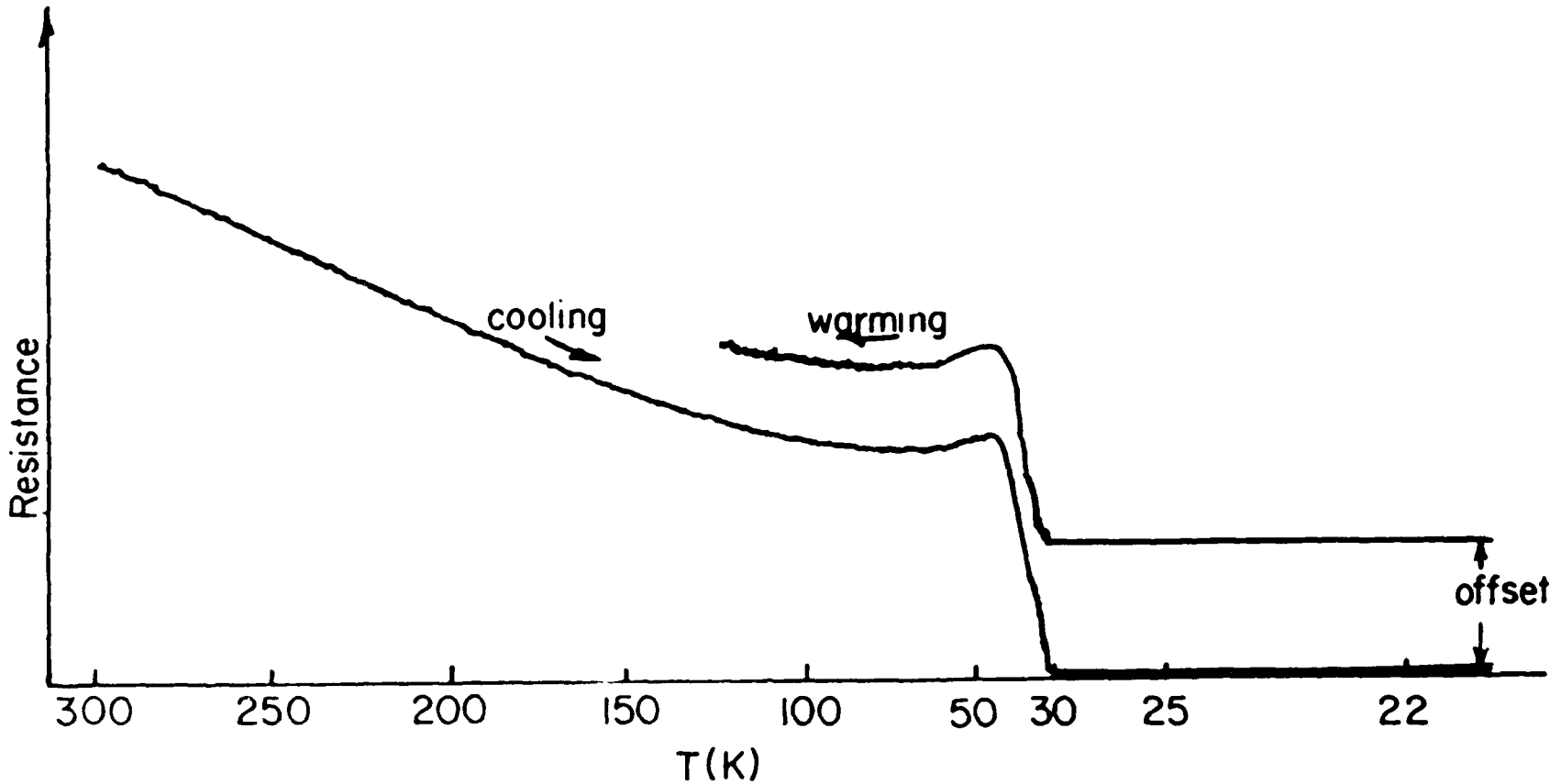
Resistance
cooling
warming
offset
300
250
200
150
100
50
30
25
22
T(K)

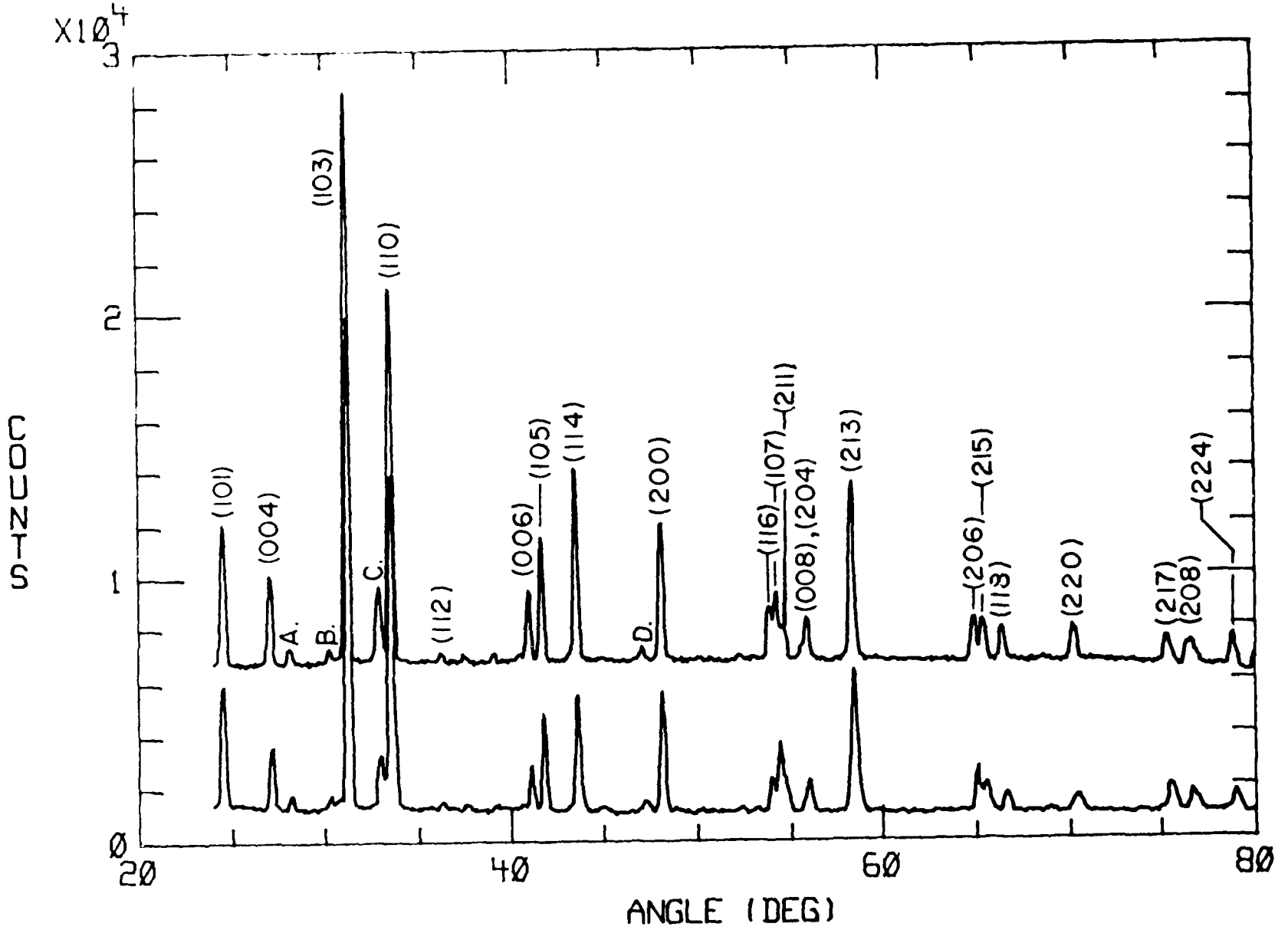
X10^4
3
2
1
0
COUNTS
(101)
(004)
A.
B.
(103)
C.
(110)
(112)
(006)
(105)
(114)
D.
(200)
(116)
(107)
(211)
(008),(204)
(213)
(206)
(215)
(118)
(220)
(217)
(208)
(224)
20
40
60
80
ANGLE (DEG)

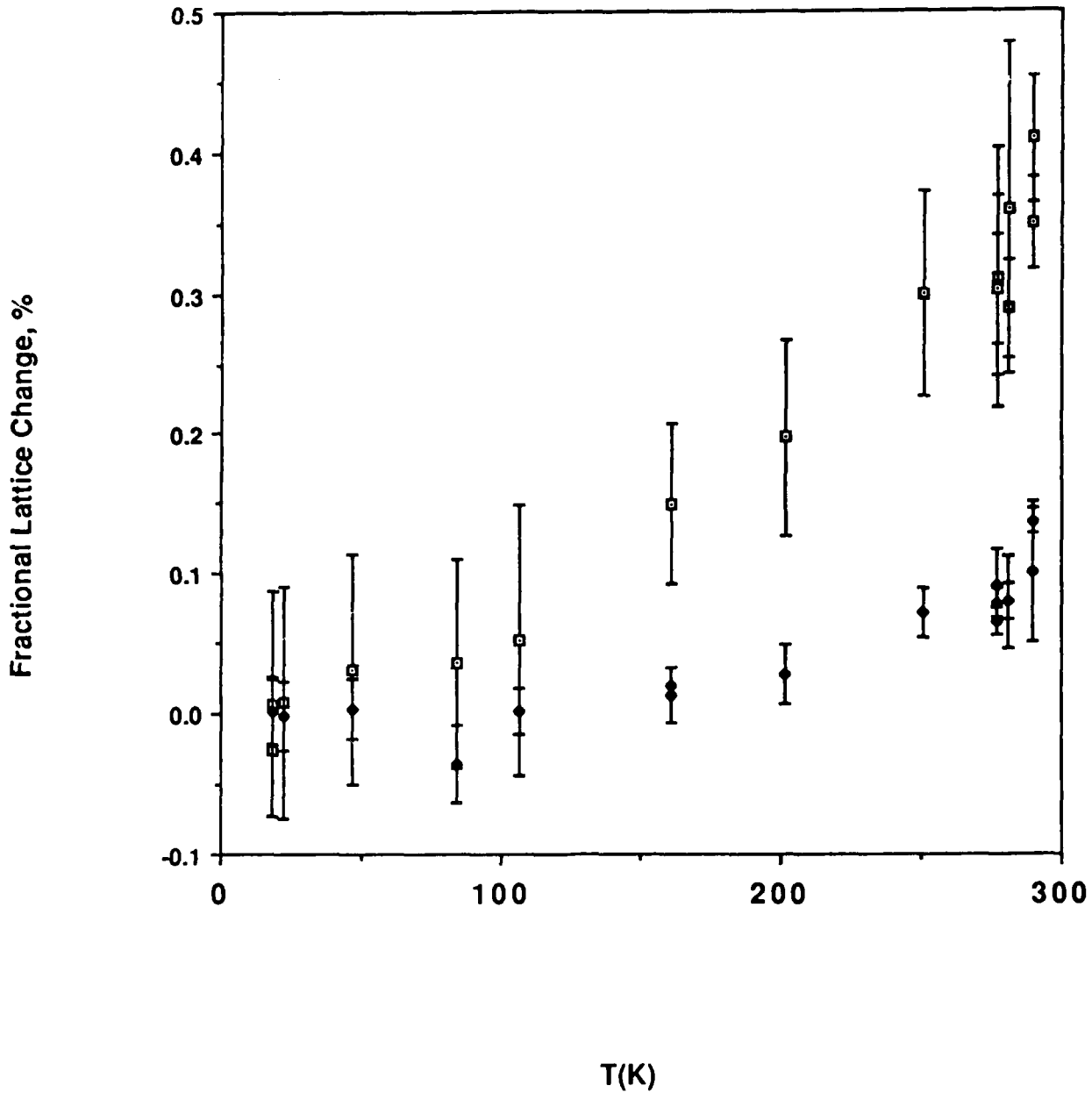
Fractional Lattice Change, %
0.5
0.4
0.3
0.2
0.1
0.0
-0.1
0
100
200
300
T(K)

X-Ray Identification of the Superconducting High T_c Phase in the Y-Ba-Cu-O System

S.B. Qadri, L.E. Toth[†], M. Osofsky, S. Lawrence, D.U. Gubser and S.A. Wolf
Naval Research Laboratory
Washington, DC 20375-5000

Abstract

The phase responsible for superconductivity above 90 K in the Y-Ba-Cu-O system has been tentatively identified as the $La_{3-x}Ba_{3+x}Cu_6O_{14+y}$ type structure through a combination of x-ray diffraction and superconducting transport measurements.

Accepted Phys. Rev. B. Rapid Communications, 1 May 1987.

[†]On Sabbatical leave from the National Science Foundation

Recently Wu *et al.*[1] have reported a remarkably high superconducting transition temperature, T_c, above 90 K in the Y-Ba-Cu-O system. The nominal composition of this high T_c material was $Y_{1.2}Ba_{.8}CuO_{4-y}$. An analysis of the samples' x-ray diffraction yielded at least three phases. The superconducting phase was unidentified. Subsequently Tarascon *et al.*[2] reported the onset of superconductivity above 90 K in the same system but with a distinctly richer yttrium composition, $Y_{1.75}Ba_{.25}CuO_{4-y}$. These samples also contained three or more phases. Two of these phases were identified from the x-ray diffraction spectra as Y_2O_3 and $Y_2Cu_2O_5$. The samples which they reported as superconducting had a unique set of relatively weak diffraction peaks at 2θ = 32.60°, 32.89°, 35.62° and 48.79°. Tarascon *et al.* neither identified the phase responsible for these reflections nor did they unambiguously associate them with the superconductivity of their samples.

The purpose of this communication is to show (1) that superconducting high T_c samples with the nominal composition $Y_{1.2}Ba_{.8}CuO_{4-y}$ also contain these characteristic x-ray peaks, (2) samples of the identical compositions processed differently do not contain these reflections and are <u>not</u> superconducting and (3) to tentatively identify the lines as belonging to a Perovskite related double layered structure $Y_{3-x}Ba_{3+x}Cu_6O_{14+y}$

Samples with nominal compositions $Y_{.4}Ba_{.27}Cu_{.33}O_x$ (Wu's composition), $Y_{.4}Ba_{.2}Cu_{.4}O_x$, $Y_{.3}Ba_{.2}Cu_{.5}O_x$, $Y_{.3}Ba_{.3}Cu_{.4}O_x$, $Y_{.3}Ba_{.4}Cu_{.3}O_x$, and others in the Y-Ba-Cu-O pseudoternary system were prepared from high purity powders of Y_2O_3, $BaCO_3$, and CuO. These powders were mixed and calcined at 900-1000°C for 1 hour, with an intermediate mixing, and then pressed into ½ inch diameter pellets and sintered for 15-24 hours at 900-1000°C in air or oxygen. Several samples with the $Y_{.4}Ba_{.27}Cu_{.33}O_x$ composition were sintered in an atmosphere of 10^{-5} Bar of oxygen pressure (a reducing atmosphere)

Resistance and susceptibility measurements show that the onset of superconductivity in the oxygen sintered samples with the nominal composition $Y_{1.4}Ba_{1.6}Cu_2O_x$ is 94 K with transition widths ~4K (see Fig. 1). In contrast pellets of the calcined powders sintered in the reducing atmosphere were not conducting or superconducting.

X-ray diffraction patterns of the two samples mentioned in the preceding paragraph were quite similar, the significant difference is that the air fired sample contained strong extra lines at 2θ = 32.575° and 32.875° whereas the reduced, non-superconducting samples did not. Significantly, both reflections belong to the set of unidentified lines reported by Tarascon *et al.* for their superconducting samples. Because these lines are not present in the non-superconducting sample we speculated that the extra lines are associated with the high T_c phase. Samples richer in both copper and barium contained more of this unidentified phase and were also superconducting with onsets between 70 and 105 K.

Tentatively we have been able to index this phase with tetragonal symmetry and as belonging to the $La_3Ba_3Cu_6O_{14+y}$ type crystal structure. This structure was studied by Er-Rakho *et. al.*[3] It is a structure related to the cubic perovskites and characterized by ordered vacancies on the oxygen sublattice which occur on planes, perpendicular to the c-axis of the unit cell, and occurring in every other layer of oxygen octahedra (double layer). The lattice parameters for the composition $Y_{.3}Ba_{.2}Cu_{.5}O_x$ are $a = \sqrt{2}\, a_p = 5.438$ and $c = 3\ a_p = 11.711$ with $a_p = 3.864$ for the primitive subcell. These are just slightly smaller than those reported by Er-Rakho *et. al.* for $La_3Ba_3O_6O_{14.1}$.[4] The x-ray pattern for a nearly pure form of the phase is shown in Figure 2. We have been able to index all major lines in the pattern; there is a small amount of $BaCuO_2$ and a few very weak unidentified lines.

In barium rich samples the unit cell contains a cubic primitive subcell and $a = \sqrt{2}a_p$ and $c = 3a_p$. In ytterium rich samples the subcell becomes tetragonal and as a result, many of the diffraction peaks split. Table I gives a complete indexing from $2\theta = 20$ to 70° for two samples with and without splitting. A few of the observed peak intensities are appreciably different from those given by Er-Rakho *et. al.* corresponding to the different composition and indicating a somewhat different arrangement of atoms and vacancies.

We believe that the high T_c is associated with this double layered Perovskite $La_3Ba_3Cu_6O_{14+y}$ structure and that the very high T_c's are possible due to the large number of vacant oxygen sites and also to the very strongly two dimensional nature of the compound.[5]

We acknowledge very useful conversations with D. Papaconstantopoulos, B. Klein, P. Allen, and V. Kresin and the use of the x-ray facilities of Carl Vold.

References

1. M.K. Wu, J.R. Ashburn, C.J. Torng, P.H. Hor, R.L. Meng, L. Gao, Z.J. Huang, Y.Q. Wang, and C.W. Chu, Phys. Rev. Lett. 58, 908 (1087).
2. J.M. Tarascon, L.H. Greene, W.R. McKinnon, and G.W. Hull, Phys. Rev. Lett. submitted.
3. L. Er-Rakho, C. Michel, J. Provost and B. Raveau, J. Solid State Chem. 37, 151 (1981).
4. L. Er-Rakho *et. al.* prepared Y containing samples of this phase and reported a decreasing lattice constant.
5. V.Z. Kresin, Phys. Rev. Rapid Commun., submitted.

Figure Captions

Fig. 1. Resistive transition for a sample with composition $Y_{1.6}Ba_{1.4}Cu_2O_{6+y}$

Fig. 2. X-ray diffraction patterns of two samples with appreciable amounts of the $La_{3-x}Ba_{3+x}Cu_6O_{14+y}$ like structure: $Ba_{.4}Y_{.1}Cu_{.5}O_x$ (top) and $Ba_{.3}Y_{.3}Cu_{.4}O_x$ (bottom).

Fig. 3. Arrangements of atoms and vacancies in the unit cell of $La_3Ba_3Cu_6O_{14+y}$ (after Er-Rakho *et. al.*[3]). Vacancies are ordered in planes perpendicular to c axis at c/2. Planes containing vacancies are separated by a double layer of O_6 octahedra. Atomic arrangements in the present samples are probably different because of discrepancies in intensities of specific x-ray peaks.

TABLE 1: CALCULATED AND OBSERVED D SPACINGS

	Er-Rakho et.al.		$Ba_{.4}Y_{.1}Cu_{.5}O_x$			$Ba_{.3}Y_{.3}Cu_{.4}O_x$		
hkl	I_{obs}	I_{calc}	d_{obs}	d_{calc}	I_{obs}	d_{obs}	d_{calc}	I_{obs}
003	12.9	1.9	3.8833	3.8798	24	3.9044	3.9049	11
110		10.3		3.8766		3.8297	3.8631	1
111	0.6	0.3	---	---	--	---	---	--
112	1.1	0.9	3.2270	3.2263	9	3.2318	3.2249	4
103	---	---	---	---	--	3.2062	3.1769	4
004	---	---	---	---	--	2.9285	2.9287	7
113	100	71.3	2.7417	2.7423	100	2.7487	2.7463	60
200		28.1		2.7411		2.7284	2.7316	100
202	0.3	0.3	---	---	-	2.4698	2.4757	1
005	4.5	1.2				2.3426	2.3429	31
114		2.3	2.3311	2.3272	55			
203	12.9	12.7	2.2361	2.2388	23	2.2365	2.2383	7
115	0.8	0.1				---	---	--
204		0.3	1.9903	1.9953	5			
006	27.1	7.7				1.9539	1.9525	20
220		19.4	1.9420	1.9383	73	1.9440	1.9316	13
221	---	---	---	---	--	1.9141	1.9058	17
205	0.5	0.4	1.7736	1.7744	4	1.7784	1.7784	6
302	---	---	---	---	--	1.7406	1.7390	4
116		2.0		1.7348				
223	6.0	1.4	1.7360	1.7339	13	---	---	--
310		2.3		1.7336				
007	0.5	0.5	1.6640	1.6628	12	---	---	--
312		0.3		1.6615				
206	33.8	9.6	1.5826	1.5835	55	1.5882	1.5884	41
313		25.0		1.5828		1.5718	1.5799	21
117	0.5	0.5	1.5285	1.5281	1	1.5366	1.5356	4
321	---	---	---	---	--	1.5083	1.5027	4
225	2.1	0.9	1.4887	1.4895	11	1.4941	1.4904	2
314		0.9		1.4894		1.4833	1.4880	2
207	0.6	0.7	1.4216	1.4217	5	1.4265	1.4270	4
226	14.7	8.5	1.3693	1.3711	16	1.3746	1.3731	5
400		5.2		1.3706		1.3649	1.3658	17
			a = 5.482			a = 5.463		
			c = 11.639			c = 11.715		

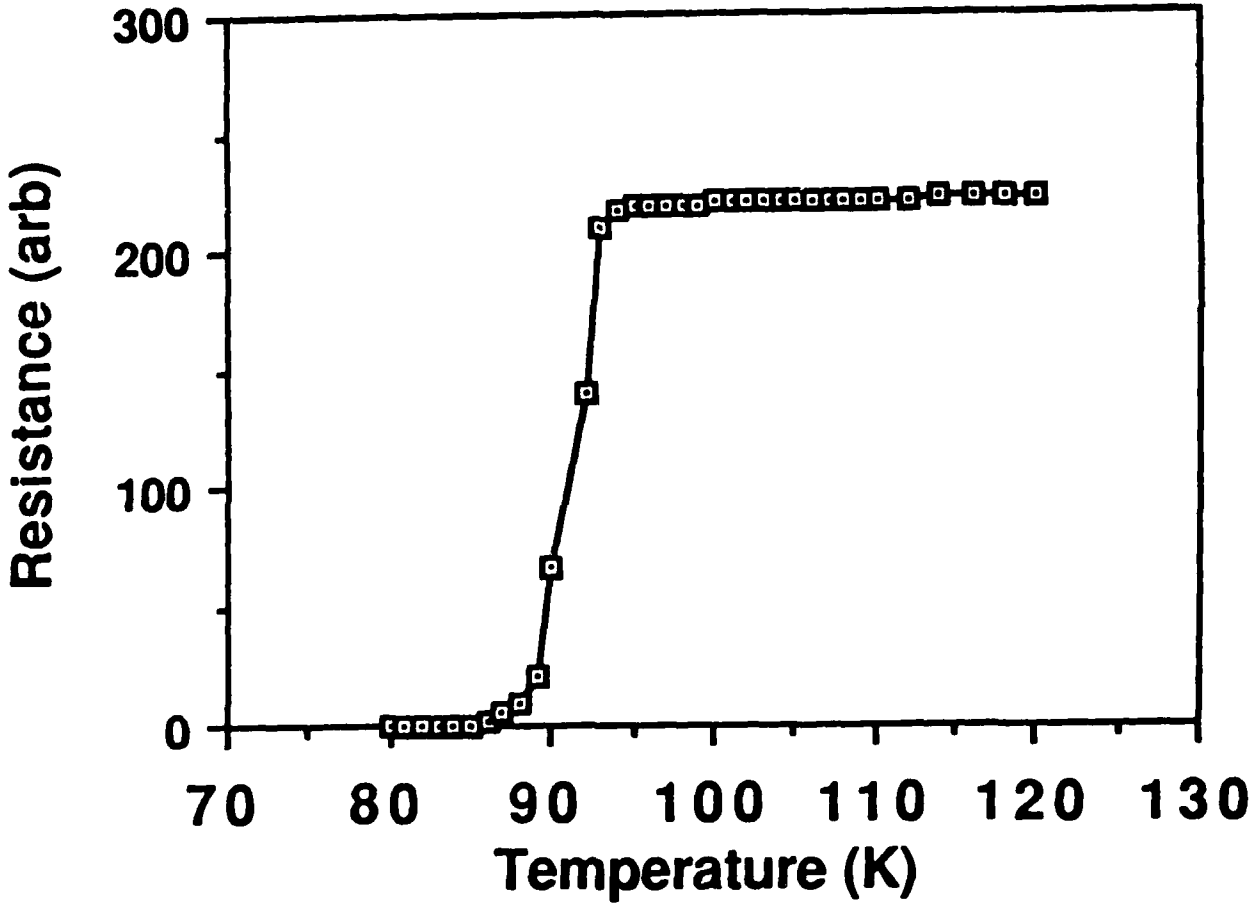
300
200
100
0
Resistance (arb)
70
80
90
100
110
120
130
Temperature (K)

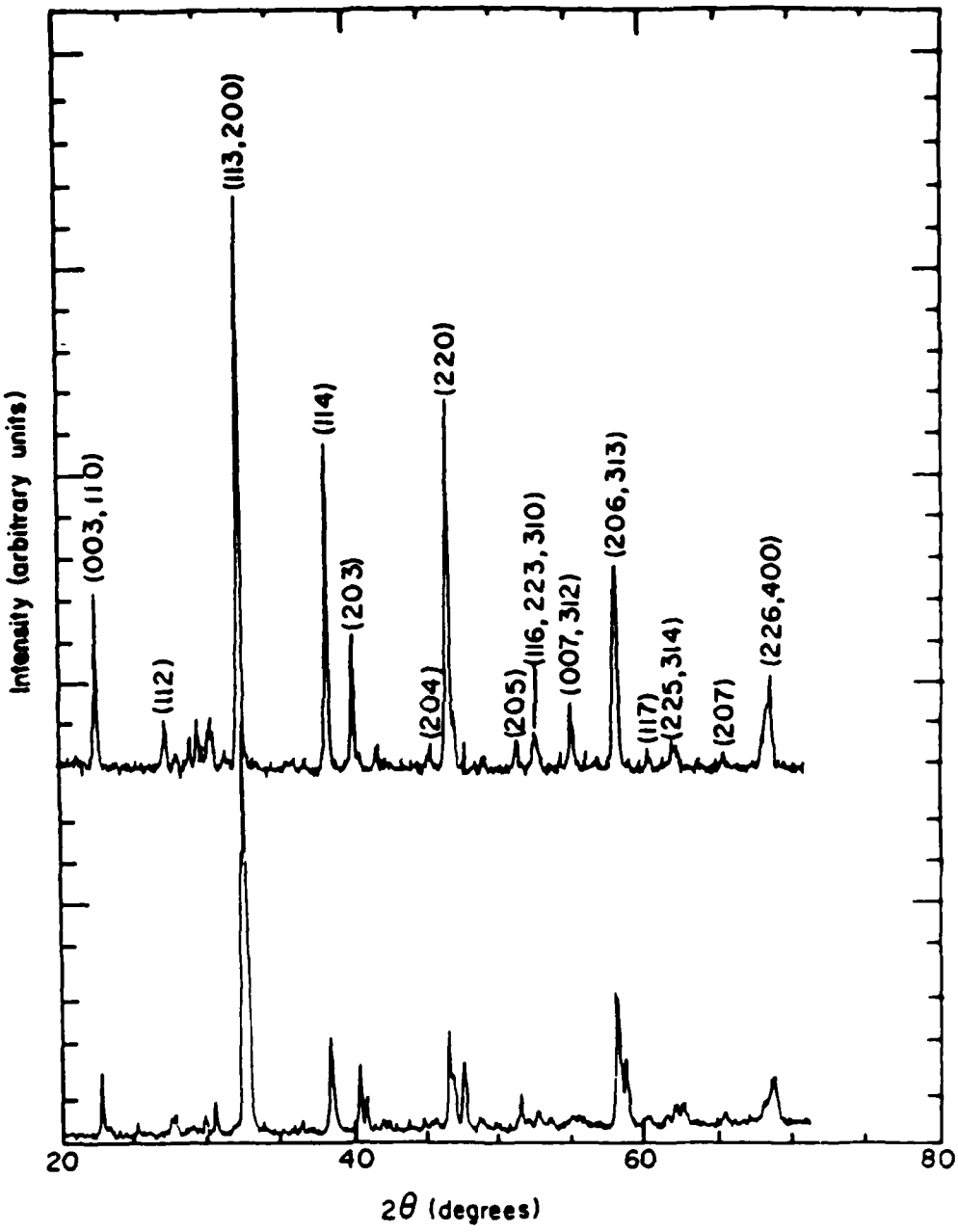
Intensity (arbitrary units)
(003,110)
(112)
(113,200)
(114)
(203)
(204)
(220)
(205)
(116,223,310)
(007,312)
(206,313)
(117)
(225,314)
(207)
(226,400)
20
40
60
80
2θ (degrees)

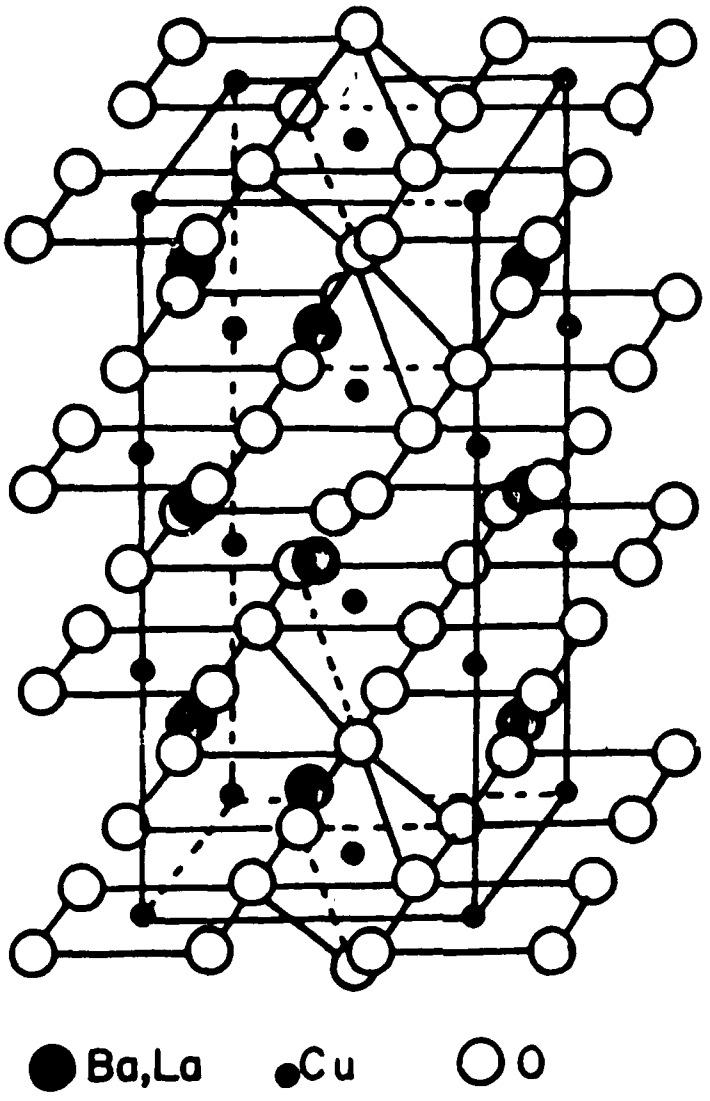
Ba,La
Cu
O

STRUCTURAL CONSIDERATIONS OF Cu-OXIDE BASED HIGH-T_c SUPERCONDUCTORS

E. P. SKELTON, S. B. QADRI, B. A. MENDER, A. S. EDELSTEIN, W. T. ELAM, T. L. FRANCAVILLA, D. U. GUBSER, R. L. HOLTZ, S. H. LAWRENCE, M. S. OSOFSKY†, L. E. TOTH††, and S. A. WOLF

Condensed Matter & Radiation Sciences Division, Naval Research Laboratory, Washington, DC 20375-5000

INTRODUCTION

The discovery of superconductivity in La-Ba-Cu-oxides (LBC) at temperatures in excess of 30 K[1] and in Y-Ba-Cu-oxides (YBC) at temperatures in excess of 90 K[2] has spawned a flurry of research directed toward these and related materials, such as La-Sr-Cu-oxide (LSC). The phase of LBC responsible for superconductivity has been identified as that of the tetragonal-K_2NiF_4 structure[3]. Based on electron and x-ray diffraction measurements, several groups have independently reported on the structure of superconducting YBC. Although there is general agreement in the atomic positions of the metal cations, variances exist in the occupancies and locations of the oxygen anions. Moreover, some researchers find the lattice to be tetragonal [4-6], whereas others find it orthorhombic[7-10]. We believe that both are correct. In this paper, recent structural studies on these materials are correlated with preparation and processing methods.

SAMPLE PREPARATIONS

Test samples of LBC were prepared by mixing appropriate proportions of reagent grade powders of La_2O_3, $BaCO_3$, and CuO to yield a product of nominal composition $La_{1.9}Ba_{0.1}CuO_4$. The mixture was calcined twice in air at 1000-1100° C for about 12 h and pressed into a cylindrical pellet.

A variety of methods were used to prepare the YBC materials; the steps which yielded the $YBa_2Cu_3O_7$ composition and the orthorhombic lattice are as follows: (a) mix appropriate proportions of $BaCO_3$, CuO, and Y_2O_3 powders; (b) ultrasonically pulverize the mixture; (c) calcine for about 6 h at 900-950° C with intermediary grindings; (d) grind and cold press into pellets; (e) air sinter at 925-950° C for about 12 h (f) heat to 950°C in an oxygen atmosphere and slowly cool (1°/min). Additional details are discussed below.

LOW TEMPERATURE MEASUREMENTS

Polycrystalline samples of both LBC and YBC have been measured simultaneously with 4-probe resistance and x-ray diffraction techniques. The onset/completion of superconducting transitions are observed at 38/28 K and 93/91 K for LBC and YBC, respectively. In both cases, detailed comparisons of x-ray diffraction spectra recorded at 290 K and at 18 K reveal no evidence of any gross structural distortions. In the case of the tetragonal structure of LBC, the unit cell parameters exhibit smooth, monotonic thermal expansions of about 0.10±0.05% along the a-axis and about 0.35±0.10% along the c-axis over this temperature range[11]. The linear expansivities of the orthorhombic a,b,c-axes in YBC are all represented by 0.17±0.07%.

---

†ONT Postdoctoral Fellow ††On sabbatical leave from the National Science Foundation

THIN FILM STUDIES OF LSC

Films of LSC were prepared by sputtering from a single inhomogenious target of the three metals, La, Sr, and Cu, onto quartz substrates. In their initial form, the sputtered films exhibited no evidence of crystallinity. However annealing, initially at 350° C and at subsequently higher temperatures, for 15-min produced x-ray diffraction peaks. (See figure at right.) The major peaks could be identified with the aforementioned tetragonal K_2NiF_4-structure. Extending the duration of the anneal at each temperature for up to 1-hour did not appear to increase the amount of crystallization. It is also noted that oxide of the La appears to form at the higher annealing temperatures whereas that of Sr shows up at 350° C.

There is some discrepancy between the measured and calculated intensities of the diffraction peaks from the K_2NiF_4-phase. However, a Read photograph of the film annealed at 600° C indicates that some, if not all, of this is due to preferred orientation.

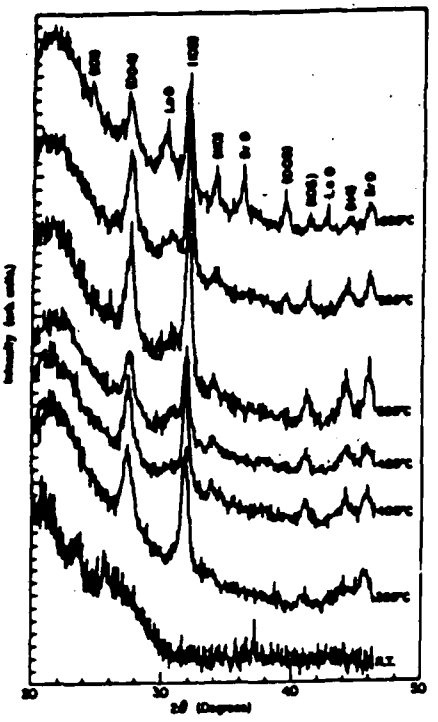

Diffraction Spectra vs. Annealing Temperature

As the annealing temperature is increased, the a-unit cell parameter exhibits a linear increase from about 3.762 to 3.787 A, whereas the c-axis decreases uniformly from about 13.45 to 13.14 A. These correspond to an overall volume reduction of about 1%. The lattice parameters of the 600°-annealed sample are in approximate agreement with our measurements on LBC: a=3.787±0.001; c=13.23±0.02 A., suggesting that the film may have reached the stoichiometric composition. This is further supported by x-ray fluorescence anslyses which indicate that the average metal composition is $(La_{0.959}\ Sr_{0.041})_2\ Cu_1$. Unfortunately resistance measurements did not show the film to be superconducting down to 4.2 K. The reason for this is not clear, compositional or stoichiometric variances may be involved.

YBC: TETRAGONAL VS. ORTHORHOMIC LATTICES

As noted, the aforementioned YBC-processing procedures favor the formation of the orthorhombic structure, concomitant with this are improved superconducting properties: sharp transitions above 90 K and complete flux explusion. However, when the processing was carried out at lower temperatures or for shorter times, the chemical reactions and subsequent grain growth were incomplete and the tetragonal phase was observed. Along with this phase were degraded superconducting properties: broad transitions and poor flux explusion.

The unit cell parameters for a variety of samples and heat treatments were determined from 15 to 20 high angle diffraction peaks by fitting to an orthorhombic lattice. The percent change between the a and b axes was

used as an indication of the orthorhombic distortion. In three cases, this distortion was less than a 0.3%, which is below our detectable limit. For six samples with superior superconducting properties, the fractional differences were between 1.3% and 1.9%, well outside our experimental uncertainty. An interesting observation is that there does not appear to be a continuous gradation from the tetragonal to the orthorhombic phase. We suggest that, based on the correlation between the post-reaction treatments and the lattice parameters, the orthorhombic distortion and the resulting improved superconductivity may be due to an ordered occupation by oxygen anions on one of the initially equivalent tetragonal axes.

CONCLUSIONS

(1) Neither La-Ba-Cu-oxides nor Y-Ba-Cu-oxides exhibit any evidence of gross structural distortions between 290 and 18 K; the linear thermal expansivities are 0.2 ± 0.1% in all cases. (2) Sputter deposited thin films of La-Sr-Cu-oxide are initially noncrystalline, but begin to crystallize in the K_2NiF_4-structure at annealing temperatures as low as 300° C. These films do not exhibit evidence of superconductivity. (3) Preparation procedures can affect whether samples of Y-Ba-Cu-oxide form in the orthorhombic or tetragonal lattice, the former exhibiting superior superconducting properties.

REFERENCES:

1. J. G. Bednorz and K. A. Müller, Z. Phys. B64, 189 (1986).
2. M. K. Wu, J. R. Ashburn, C. J. Torng, P. H. Hor, R. L. Hor, R. L. Meng, L. Gao, Z. J. Huang, Y. Q. Wang, and C. W. Chu, Phys. Rev. Lett. 58, 908 (1987).
3. H. Takagi, S. Uchida, K. Kitazawa, and S. Tanaka, Jpn J. Appl. Phys. Lett. (to be published).
4. S. B. Qadri, L. E. Toth, M. Osofsky, S. Lawrence, D. U. Gubser, S. A. Wolf, Phys. Rev.- Rapid Commun. (to be published).
5. R. M. Hazen, L. W. Finger, R. J. Angel, C. T. Prewitt, N. L. Ross, H. K. Mao, C. G. Hadidiacos, P. H. Hor, R. L. Meng, and C. W. Chu, Phys. Rev.- Rapid Commun. (to be published).
6. M. Hirabayashi, H. Ihara, N. Tereda, K. Senzaki, K. Hayashi, K. Murata, M. Tokumoto, S. Waki, and Y. Kimura, Jpn. J. Appl. Phys. (to be published).
7. R. Beyers, G. Lim, E. M. Engler, R. J. Savoy, T. M. Shaw, T. R. Dinger, W. J. Gallagher, and R. L. Sandstrom, Phys. Rev.- Rapid Commun. (to be published).
8. Y. LePage, W. R. McKinnon, J. M. Tarascon, L. H. Greene, G. W. Hull, and D. M. Hwang, Phys. Rev.- Rapid Commun. (to be published).
9. Y. Syono, M. Kikuchi, K. Oh-ishi, K. Hiraga, H. Arai, Y. Matsui, N. Kobayashi, T. Sassoka, and Y. Muto, (to be published).
10. R. J. Cava, B. Batlogg, R. B. VanDover, D. W. Murphy, S. Sunshine, T. Siegrist, J. P Remeika, E. A. Rietman, S. Zahurak, and G. P. Espinosa, (to be published).
11. R. F. Skelton, W. T. Elam, D. U Gubser, S. H. Lawrence, M. S. Osofsky, L. E. Toth, and S. A. Wolf, Phys. Rev.-B (to be published).

Table I: COMPOSITION, HEAT TREATMENTS, AND LATTICE PARAMETERS FOR Y-Ba-Cu-OXIDES

Sample No.	Nominal Composition	Heat Treatment*	Lattice Parameters a(A)	b(A)	c(A)	vol(A^3)	% Distortion
194	$Y_{0.1}Ba_{0.4}Cu_{0.5}O_y$	A	3.876±0.006	3.877±0.005	11.634±0.013	174.8	0.02
186B	$Y_{0.28}Ba_{0.32}Cu_{0.4}O_y$	B	3.867±0.013	3.872±0.012	11.633±0.030	174.2	0.14
193A	$Y_{0.2}Ba_{0.3}Cu_{0.5}O_y$	A	3.863±0.014	3.873±0.011	11.626±0.027	173.9	0.25
223.3	$YBa_2Cu_3O_7$	C	3.834±0.007	3.884±0.007	11.70±0.02	174.2	1.3
177	$Y_{0.3}Ba_{0.3}Cu_{0.4}O_y$	D	3.835±0.007	3.890±0.008	11.680±0.019	174.3	1.4
183	$Y_{0.3}Ba_{0.2}Cu_{0.5}O_y$	D	3.826±0.013	3.879±0.011	11.739±0.031	174.2	1.4
223.3	$YBa_2Cu_3O_7$†	E	3.8220±0.0001	3.8855±0.0001	11.6797±0.0004	173.4	1.6
223.3	$YBa_2Cu_3O_7$	E	3.822±0.002	3.888±0.002	11.672±0.005	173.4	1.7
187	$Y_{0.24}Ba_{0.36}Cu_{0.4}O_y$	D	3.838±0.015	3.902±0.026	11.755±0.031	176.1	1.7
242	$Y_{0.15}Ba_{0.3}Cu_{0.55}O_y$	D	3.837±0.024	3.911±0.023	11.705±0.074	175.6	1.9

There are six more lines on the page after this line

†Based on neutron diffraction measurements of J. Rhyne et al., to be published

*A = Sinter @ 900° C; air quench
B = Sinter @ 1000° C for 24-96 h; air quench
C = Reheat to 1000° C; quench
D = Sinter @ 950° C; hold @ 700° C
E = Sinter @ 937° C ; cool 1°/min

RELATIONSHIP BETWEEN PROCESSING PROCEDURE, CRYSTAL STRUCTURE AND SUPERCONDUCTING T_c IN THE Y-BA-CU-O SYSTEM

L.E. Toth*, E.F. Skelton, S.A. Wolf, S.B. Qadri,
M.S. Osofsky, B.A. Bender, S.H. Lawrence, and D.U. Gubser
Naval Research Laboratory
Washington, DC 20375-5000

Abstract

Processing procedures producing well ordered orthorhombic structures in $YBa_2Cu_3O_7$ result in T_{onset}'s in excess of 90K, sharp transitions and nearly complete flux expulsion. Procedures producing samples with tetragonal symmetry result in broad transitions and relatively poor flux expulsion. This suggests that superconductivity in $YBa_2Cu_3O_7$ is strongly associated with the ordered orthorhombic structure and one dimensional Cu-O chains in the basal plane, and less influenced by other atoms in the unit cell.

*On leave from NSF

Recently, several groups[1-6] using electron and x-ray diffraction identified the high T_c superconducting phase and its crystal symmetry. Although all investigations agreed on the $YBa_2Cu_3O_{9-\delta}$ stoichiometry for the compound and the position of the metal cations in the unit cell, there was disagreement as to whether the symmetry is tetragonal[1,2,7] or orthorhombic[3-6] and to the location and occupation of the oxygen sites. Neutron diffraction studies[8,9,10] on several different stoichiometric samples refined the crystal structure and identified positions of oxygen atoms showing that the stoichiometric phase is orthorhombic. The orthorhombic structure results from a filling of oxygen positions on 0,1/2,0 and vacancies on 1/2,0,0 positions. The "b" axis is about 1.6% longer than the "a" axis. These investigators of the neutron diffraction studies[8,9] nevertheless suggested that the tetragonal phase observed in previous x-ray difraction studies may reflect true differences in samples prepared by different processing conditions.

Several reports suggest optimum processing conditions for high and sharp T_c's. Most prescriptions favor sintering in flowing oxygen followed by a post anneal at a lower temperature and very slow cooling[11]. Samples more rapidly cooled show a broad transition. There have been no reports that relate processing to structure, i.e. to the conditions favoring orthorhombic versus tetragonal symmetry. The purpose of this communication is to correlate processing with structure and superconducting properties.

In our earlier investigations[1] of superconductivity in the Y-Ba-Cu-O system we studied about 20 samples of different compositions all containing the 1:2:3 (Y:Ba:Cu) phase. As there were no well defined optimum processing procedures at that time, we prepared samples by several different techniques.

We observed the orthorhombic structure in about half of the samples and the tetragonal in the other half. Reviewing these results in light of the refined crystal structure, clarifies the relationships between processing and structure.

Processing conditions which favored the formation of the orthorhombic structure were as follows: (a) Powders of $BaCO_3$, CuO, and Y_2O_3 were premixed. (b) The powders were immersed in alcohol and loose agglomerates pulverized using ultrasonic vibrations. (c) The powders were then calcined for about six hours at 925-950°C with intermediary grindings. (d) Samples were again ground and cold pressed into pellets and sintered in air at 925-950°C for about 12 hours. (e) They were then transferred to a furnace with an oxygen atmosphere, equilibrated for several hours at 950C before the furnace was slowly cooled (1°/min). For step (e) we could also substitute an equilibration in O_2 or air, followed by reducing the temperature to 500-700°C, holding for several hours and a moderately slow cool down.

Two conditions favored tetragonal formation. When the processing was done at relatively low temperatures and shorter times, the chemical reactions and subsequent grain growth were incomplete, the ordering of oxygen atoms did not occur and a tetragonal phase was observed. In cases where reaction was known to have been completed, the tetragonal phase was formed when samples were quenched from 900-1000°C.

Most samples were prepared off the stoichiometric 1:2:3 and we observed the orthorhombic and tetragonal symmetries with nearly equal frequency. We saw no obvious correlation between overall composition and the occurrence of either phase. At the stoichiometric composition we observed only the orthorhombic structure. There is no indication, however, that the tetragonal

phase has a stoichiometry other than 1:2:3.

Table 1 shows the lattice parameters of some of the samples. These parameters were calculated assuming the structure to be orthorhombic and carrying out a least squares fit to 15 to 20 high angle diffraction peaks. If the "a" and "b" parameters were determined to be equivalent to within the uncertainty of the fit, we then called the sample tetragonal. For all the samples determined to be orthorhombic, the b/a ratios lie between 1.014 and 1.019. The "a" lattice parameter varies from 3.822 and 3.838. The "b" parameter varies from 3.879 and 3.911. For nearly tetragonal samples, the orthorhombic distortion ranges from less than measurable to about 0.25%. The "a" lattice parameter varies from 3.863 to 3.876 and "b" from 3.867 to 3.877.

For the samples that we tested, there was no overlap of the b/a ratios between the two groups of samples; i.e. the orthorhombic distortion was 1.4-1.9% in the orthorhombic samples and much smaller, less than 0.3% in the tetragonal samples. The "b" parameter tends to be slightly smaller in the tetragonal structure compared to the orthorhombic, whereas "a" clearly shows the opposite trend. This would indicate at least partial occupancy of both 1/2,0,0 and 0,1/2,0 sites in the tetragonal structure. Thus we regard the tetragonal structure as the disordered form of the orthorhombic lattice.

We inspected three samples with optical microscopy. Two samples with nearly tetragonal symmetry showed elongated grains. One of the samples with tetragonal symmetry had sintered fairly well with typical elongated grains 10 by 50 microns in size and was much more dense than the other sample. These results indicate that the degree of sintering did not affect the crystal symmetry. The microstructure of the sample with orthorhombic symmetry showed significant amounts of twinning as evidence by the striations (see figure 1).

Changing the focal length showed that most of the grains were striated. In some grains the striations are seen running at right angles to each other. It is believed these striations result from twinning associated with the orthorhombic distortion as seen also by Beyers et. al.[3] using TEM.

We measured the a.c. resistivities and d.c. susceptibilities of the samples. The resistive onsets occurred in excess of 90K in most samples. Slow cooling and/or annealing at about 500°C, in either air or oxygen, sharpens the transitions, in agreement with the results of others. Samples of stoichiometric 1:2:3 compositions and well defined orthorhombic distortions had onsets of 93 and R=0 at 91K. The same samples showed nearly complete flux expulsion. Samples containing the tetragonal phase show far broader transitions and smaller amounts of flux expulsion, 1-12% after correcting for the amounts of the 1:2:3 phase. The sample with the least amount of orthorhombic distortion, sample 194, had the broadest transition: T_{onset}=93K and R=0 at 53K. Samples with an orthorhombic distortion of about 1.4% but which were not slow cooled or held at a lower intermediary temperature, had high onsets but broad transitions. Thus having an orthorhombic structure does not necessarily mean a sharp transition. Only those samples that were slow cooled or held at a lower temperature had transition widths of a few degrees. We suggest that slow cooling allows more complete ordering of oxygen atoms on 0,1/2,0 sites.

To study the relationship between orthorhombic and tetragonal symmetry, we used a stoichiometric sample, number 223.3, with a well defined orthorhombic distortion of 1.017_3. After equilibration at 1000C, we quenched this sample in air. Quenching produced no measurable change in the b and c axial lengths, but about a 0.3% increase in the length of the a-axis; this corresponds to a

smaller orthorhombic distortion with b/a=1.013. The resistive transition degraded considerably. Prior to reheating, the superconducting properties of this sample were T_{onset}=93K and R=0 at 91K. After quenching, T_{onset}=85K and R=0 at 46K.

A set of nonstoichiometric samples were sintered at 1000°C in flowing oxygen for 24 to 96 hours assuring that the samples were in equilibrium. Specific samples were then removed every 24 hours by quenching in air. All samples had broad transitions of 30K. These samples all had tetragonal symmetry, suggesting that the tetragonal symmetry is the property of a high temperature phase and that the orthorhombic phase forms at a lower temperature.

The conversion from the orthorhombic to the tetragonal forms of the structure can be caused by a disordering of the oxygen atoms on the basal planes or by removing some of the oxygen atoms from the 0,1/2,0 positions. We believe both occur in samples heated at higher temperatures in air or oxygen. Alternately, the conversion can occur when samples are heated in a reducing atmosphere. In this case, the progression to a tetragonal structure was studied by neutron diffraction[12]. Oxygen atoms are removed preferentially from the 0,1/2,0 sites. This particular heat treatment produced a semiconducting sample.

We believe the orthorhombic distortion occurs on slow cooling or holding at some lower intermediary temperature when oxygen atoms diffuse from 1/2,0,0 sites to vacant 0,1/2,0 sites and by the addition of oxygen atoms from the ambient atmosphere. It is well established from earlier research that compounds with very closely related structures will incorporate an additional 10-15% more oxygen during a low temperature post anneal[13].

We therefore speculate that the superconductivity in this material is very strongly associated with the Cu-O chains in the basal plane and less influenced by the other atoms in the unit cell. Either disordering the chains or breaking them up by removing the oxygen is detrimental to superconductivity.

Engler et. al.[11] also found a possible association of the orthorhombic distortion and high T_c's. In their case they showed that most rare earth elements can be substituted for Y without a significant change in T_c, but that substitutions of La and Pr destroyed superconductivity even though the 1:2:3 stoichiometric phase was formed. For $PrBa_2Cu_3O_y$ they pointed out that the structure was tetragonal, not orthorhombic and therefore suggested the association between the orthorhombic distortion and superconductivity. Our findings on the La-Ba-Cu-O were slightly different. We found the stoichiometric composition not to be $LaBa_2Cu_3O_7$ but $La_{1.5}Ba_{1.5}Cu_3O_7$, in agreement with the original research on this phase by Er-Rakho et. al.[13] In samples slowly cooled in flowing oxygen or air, a procedure which should have produced the orthorhombic structure, the phase was instead tetragonal. We did not observe an orthorhombic structure in five samples of different compositions. The crystal structure was closely related to that for $YBa_2Cu_3O_7$, although there must be some substitution of La for Ba, and the ordering, if there is any, of oxygen atoms must be different. In our samples we saw no reason to use the larger lattice parameters $a=\sqrt{2}a_p$ as suggested by Er-Rakho et al. We find $a=3.925\pm.003$ and $c=11.784\pm.028$. The phase is not superconducting down to 4K. This result again strongly suggests that the ordered orthorhombic strucuture is associated with the very high T_c's.

We further speculate that the twinning that is prevalent in the

orthorhombic $YBa_2Cu_3O_7$ compound may be due to the tetragonal to orthorhombic transition associated with incorporating and ordering of oxygen atoms on the basal planes. The twinning may also be a result of relief of internal stresses built up due to the anisotropic linear expansion behavior of orthorhombic $YBa_2Cu_3O_7$ and may play a role in the anomalies reported in these materials at higher temperatures (240K). In what is possibly a related observation, Soviet scientists have seen a significant enhancement in T_c's in samples of heavily faulted tin[14].

On the basis of these observations we conclude the following:

1. A 1:2:3 phase with nearly tetragonal symmetry exists in addition to the phase with orthorhombic symmetry. The tetragonal phase is seen readily in samples off stoichiometry. Fast cooling from high temperatures favors its retention and suggests it may be a high temperature form of the 1:2:3. Its microstructure shows no striations. Its presence is associated with a broad transition and an incomplete Meissner effect.

2.The orthorhombic phase forms most easily in stoichiometric compositions. Very slow cooling and/or lower temperature post-anneals in oxygen or air promote a well formed orthorhombic distortion. Such samples exhibit striations in their microstructures, indicating the existence of extensive twinning. The presence of the ordered orthorhombic structure is associated with a sharp transition temperature and nearly complete flux expulsion.

3. Superconductivity is correlated with the ordering of the oxygen atoms on the basal plane producing one dimensional Cu-O chains.

4.Twinning-plane-superconductivity may be responsible for the anomalies observed at very high temperatures in these materials.

References:

1. S.B. Qadri, L.E.Toth, M. Osofsky, S. Lawrence, D.U. Gubser and S.A. Wolf, to be published , Rapid Communications

2. R.M. Hazen, L.W. Finger, R.J. Angel, C.T.Prewitt, N.L. Ross, H.K. Mao, C.G. Hadidiacos, P.H. Hor, R.L. Meng and C.W. Chu, to be published, Rapid Communications.

3. R. Beyers, G. Lim, E. M. Engler, R.J. Savoy, T.M.Shaw, T.R. Dinger, W. J. Gallagher, and R.L. Sandstrom, to be published

4. Y. Le Page, W.R. McKinnon, J.M. Tarascon, L.H. Greene, G.W. Hull and D.M. Hwang, to be published

5. Y. Syono, M. Kikuchi, K. Oh-ishi, K. Hiraga, H Arai, Y. Matsui, N. Kobayashi, T. Sasaoka and Y. Muto, to be published

6. R. J. Cava, B. Batlogg, R. B. VanDover, D. W. Murphy, s. Sunshine, T. Siegrist, J. P. Remeika, E. A. Rietman, S. Zahurak and G. P. Espinosa, to be published

7. M. Hirabayashi, H. Ihara, N. Terada, K. Senzaki, K. Hayashi, K. Murata, M. Tokumoto, S. Waki and Y. Kimura, to be published.

8. M. A. Beno, L. Soderholm, D. W. Capone II, D.G. Hinks, J.D. Jorgensen, I.K. Schuller, to be published.

9. F. Beech, S. Miraglia, A. Santoro and R. S. Roth, to be published

10. J. Rhyne, to be published.

11. E.M. Engler, V.Y. Lee, A.I. Nazzal, R.B. Beyers, G. Lim, P.M. Grant, S.S.P. Parkin, M.L. Ramirez, J.E. Vazquez and R.J. Savoy, submitted J. Amer. Chem. Soc.

12. L.H. Greene, Bell Communications Research, Private communication.

13. L. Er-Rakho, C. Michel, J. Provost and B. Raveau, J. Solid State Chem. 37, 151 (1981).

14. A.I. Buzdin and N.A. Khvorikov, Sov.Phys. JETP 62, 1071 (1985) and references therein.

Acknowledgements:

We acknowledge very useful discussions with T. Elam and the technical assistance of W. Lechter.

Note added:

At the completion of this manuscript we received a preprint from Schuller et. al. at Argonne reporting on an orthorhombic to tetragonal phase transition occuring at 750 C in $YBa_2Cu_3O_7$. This result strongly supports our conclusions.

Table I: COMPOSITION, HEAT TREATMENTS, LATTICE PARAMETERS, AND TRANSITION TEMPERATURES FOR Y-Ba-Cu-OXIDES

Sample No.	Nominal Composition	Heat Treatment*	Lattice Parameters a(A)	b(A)	c(A)	vol(A^3)	% Distortion	T_c(K)	ΔT_c**(K)
194	$Y_{0.1}Ba_{0.4}Cu_{0.5}O_y$	A	3.876±0.006	3.877±0.005	11.634±0.013	174.8	0.02	93	40
186B	$Y_{0.28}Ba_{0.32}Cu_{0.4}O_y$	B	3.867±0.013	3.872±0.012	11.633±0.030	174.2	0.14	85	30
193A	$Y_{0.2}Ba_{0.3}Cu_{0.5}O_y$	A	3.863±0.014	3.873±0.011	11.626±0.027	173.9	0.25	65	>30
223.3	$YBa_2Cu_3O_7$	C	3.834±0.007	3.884±0.007	11.70±0.02	174.2	1.3	85	40
177	$Y_{0.3}Ba_{0.3}Cu_{0.4}O_y$	D	3.835±0.007	3.890±0.008	11.680±0.019	174.3	1.4	93	33
183	$Y_{0.3}Ba_{0.2}Cu_{0.5}O_y$	D	3.826±0.013	3.879±0.011	11.739±0.031	174.2	1.4	80	25
223.3	$YBa_2Cu_3O_7$†	E	3.8220±0.0001	3.8855±0.0001	11.6797±0.0004	173.4	1.6	93	2
223.3	$YBa_2Cu_3O_7$	E	3.822±0.002	3.888±0.002	11.672±0.005	173.4	1.7	93	2
187	$Y_{0.24}Ba_{0.36}Cu_{0.4}O_y$	F	3.838±0.015	3.902±0.026	11.755±0.031	176.1	1.7	93	2
242	$Y_{0.15}Ba_{0.3}Cu_{0.55}O_y$	E	3.837±0.024	3.911±0.023	11.705±0.074	175.6	1.9	93	2

†Based on neutron diffraction measurements of J. Rhyne et al., to be published

*A = Sinter @ 900° C, air quench
B = Sinter @ 1000° C for 24-96 h, air quench
C = After E, reheat to 1000° C, air quench
D = Sinter @ 950° C, hold @ 700° C 1 hr
E = Sinter @ 937° C, cool 1°/min
F = Sinter @ 1000° C, hold at 450° C 24 hr

**ΔT_c ranges from R-onset to R=0

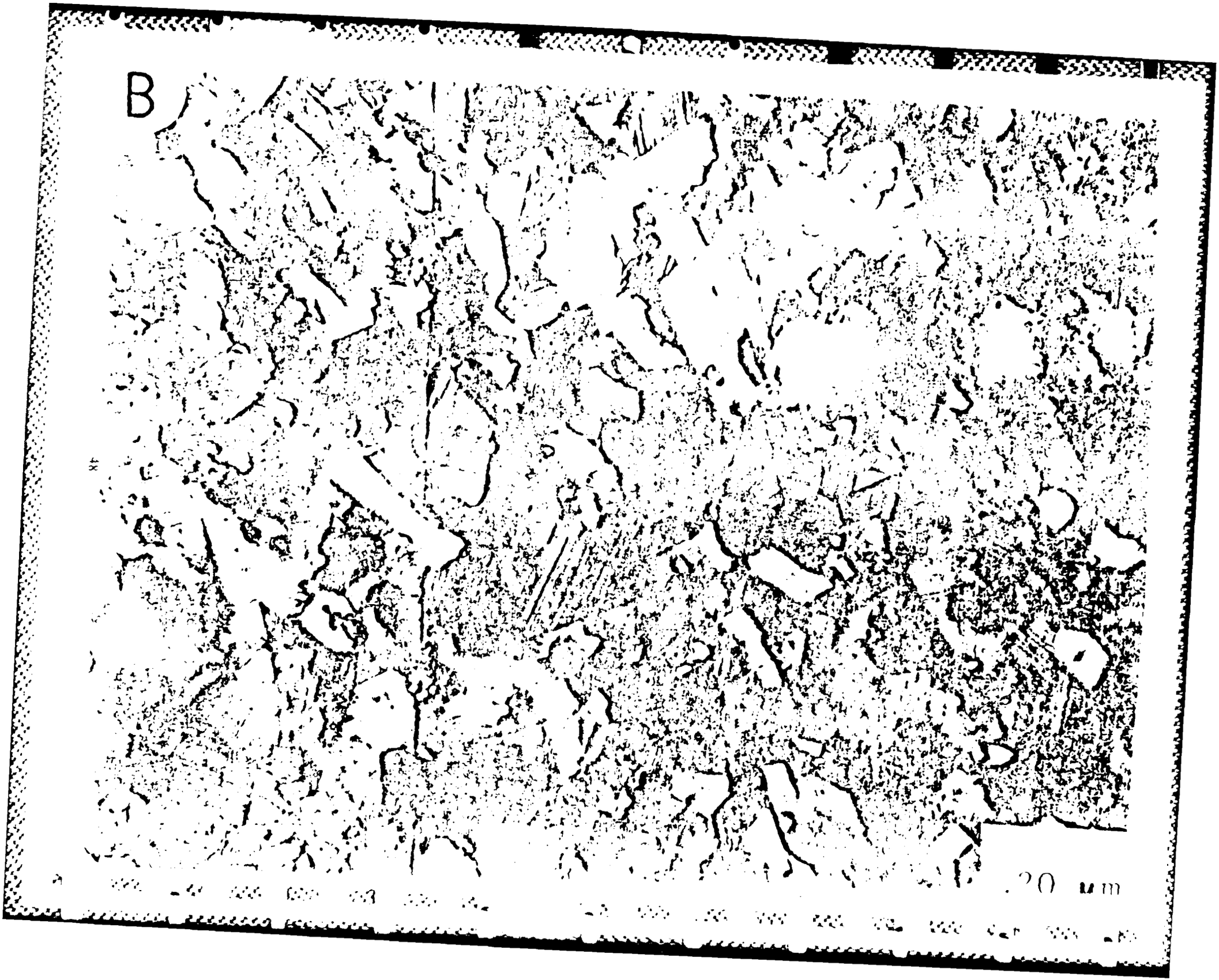
B
20 μm

Processing of High T_c Ceramic Superconductors: Structure and Properties

L. E. Toth[1], M. Osofsky[2], S.A. Wolf, E. F. Skelton, S. B.Qadri[3], W.W. Fuller, D.U. Gubser, J. Wallace, C.S. Pande, A.K. Singh[4], S. Lawrence[4], W.T. Elam, B. Bender, and J.R. Spann[4]

U.S. Naval Research Laboratory, Washington, DC 20375-5000

The processing of high T_c ceramic superconductors by traditional ceramic techniques is reviewed. All high T_c ceramic superconductors are layered Cu-O compounds that are closely related to each other. In each, Cu-O coordination polyhedra are typical of Cu^{+2} compounds. A critical step in processing these compounds is the intercalation of oxygen which changes the coordination polyhedra at a few atomic sites and causes a dramatic effect on the superconducting properties.

Introduction

Following Bednorz and Müller's publication (1) on high transition temperature, T_c, ceramic superconductors, there has been a deluge of papers on the subject. Momentum increased with the announcement by Wu et al.(2) of a T_c breakthrough in excess of 90K. Since then a great deal has been learned about superconducting properties, crystal structures and phase relationships in the Y-Ba-Cu-O system. Knowledge of processing these materials has improved but not to the same extent as some other areas. Each research group seems to report a different set of processing procedures. It is widely acknowledged that it is difficult to transfer processing procedures from one group to another and achieve comparable superconducting properties. In this paper we attempt to review some of the processing procedures. We pay particular attention to the underlying structure: crystal and microstructure. At this time, relationships between structure and superconducting properties are better defined than are relationships between processing and properties. Therefore, one can use the evolution of the desired structure as a guide to processing.

[1]On sabbatical leave from the National Science Foundation
[2]Office of Naval Technology Postdoctoral Fellow
[3]Sachs-Freeman Associates, Landover, MD
[4]Crystal Growth & Material Testing Assoc., Lanham, MD

Our group has been mainly concerned with traditional ceramic processing techniques involving solid state particulate reactions such as sintering and hot pressing. A number of other techniques, such as co-precipitation and organometallics, have been successfully used by others, but will not be discussed here. Regardless of the method of preparation, it is believed that all materials must end up with the same structural modifications to ensure good superconducting properties.

General

Structure: Some 14 different ceramic compounds are reported to superconduct with T_c's in excess of 35K. These are listed in Table I. There are 5 distinct classes of materials with 4 different lcrystal structures.

Table I. High Temperature Ceramic Superconductors

Formula	A	Reference
La_2CuO_4		(3)
$La_{2-x}A_xCuO_{4-x/2+\delta}$	Ba,Sr,Ca	(4-6)
$ABa_2Cu_3O_{6.5+\delta}$	Y,Lu,Nd,Sm,Eu,Gd Er,Ho,Yb	(2,7,8)
$La_3Ba_3Cu_6O_{14+\delta}$		(9)
$Y_2BaCu_2O_{6-x/2+\delta}$		(10)

There are several chemical and crystal structure similarities in the high T_c ceramic superconductors. A general feature in their crystal chemistry is the occurrence of a small number of Cu-O coordination polyhedra. As discussed by Wells(11), these are the same polyhedra that one finds in Cu-O compounds in which Cu has a +2 valence. Copper is located in one of three configurations: (1) at the center of a square array of coplanar oxygen atoms (square planar); (2) at the center of the square base of a pyramid with oxygen at the vertices, (pyramidal (4+1)); and (3) at the center of a distorted octahedra with oxygen at the vertices, (distorted octahedra (4+2)), (see Fig 1). In square planar, the Cu-O spacing is about 1.95A. In the pyramidal and distorted octahedra, there are 4 surrounding oxygen at short distances (1.95Å) comparable to those found in square planar, and 1 or 2 distances significantly longer (2.3Å). The notation (4+1) and (4+2) is used to denote the fact that 4 of the Cu-O distances are short and 1 or 2 are longer.

Table II lists the coordination of oxygen about the central copper atom in each of the high T_c ceramic superconductors and it lists typical Cu-O distances. In the crystal structures, the coordination polyhedra are arranged so that the square planar configurations are perpendicular to the c-axis of the unit cell and the long axis of the pyramids and octahedra are parallel to it. Within planes of Cu-O atoms, which are perpendicular to the unit

cell's c axis, the typical distance is 1.95A. Parallel to the c axis, the Cu-O distances are either shorter or longer. Thus all structures can be viewed as having parallel planes of Cu-O sheets in which the Cu-O spacing is 1.95A. The rare earth and oxygen atoms are also arranged in planes perpendicular to the c-axis. In $YBa_2Cu_3O_7$, there is a square planar ribbon at the basal planes of the unit cell which is parallel to the c axis and in which the Cu-O distance is only 1.85Å. The longest distance in this structure is also parallel to the c axis and is about 2.3Å, existing in both the distorted octahedra and 4+1 pyramidal structure. Figure 2 shows crystal structures of the four classes of superconducting materials, showing some elements of the Cu-O coordination polyhedra.

Table II. Comparison of Coordination Polyhedra for Cu-O in Superconducting Ceramic Oxide Phases

Compounds	Coordination	Distances Å		Refs
$La_{2-x}A_xCuO_{4-x/2+\delta}$	distorted octahedra (4+2)	$Cu-O_1$ (x4) $Cu-O_2$ (x2)	1.937 2.27	(12)
$La_3Ba_3Cu_6O_{14+\delta}$	square planar distorted octahedra (4+2) pyramidal(4+1)	Cu_2-O_1 (x4) Cu_2-O_1 (x4) Cu_2-O_3 (x1) Cu_4-O_2 (x4) Cu_4-O_3 (x1)	1.954 1.954 1.723 1.959 2.333	(13)
$La_{2-x}A_{1+x}Cu_2O_{6-x/2}$	pyramidal(4+1)	$Cu-O_1$ (x4) $Cu-O_2$ (x1)	1.94 2.27	(14)
$YBa_2Cu_3O_{6.5+\delta}$	square planar pyramidal(4+1)	Cu_1-O_1 (x4) Cu_1-O_4 (x4) Cu_2-O_2 (x2) Cu_3-O_3 (x2) Cu_3-O_1 (x2)	1.85 1.94 1.94 1.96 2.3	(15,16)

The superconducting and electronic transport properties of these materials are very sensitive to their oxygen content, thus it is important to understand where oxygen is added or subtracted in the unit cell. Table III lists positions where oxygen is added and its effect on T_c. For $YBa_2Cu_3O_x$, oxygen is added or subtracted from basal planes in the 0 1/2 0 and 1/2 0 0 positions. Also, oxygen can be ordered on the 0 1/2 0 sites leaving the 1/2 0 0 site vacant. This results in an orthorhomic distortion with $b/a \approx 1.7\%$, a unique one dimensional character to the structure and excellent superconducting properties (17). For $La_3Ba_3Cu_6O_{14}$ added oxygen fill the site 1/2 1/2 1/2 between two (4+1) pyramids, thus forming two distorted octahedra along the c axis. One octahedra is elongated and the other is compressed. Several groups (9,18) have found T_c onsets of 70K+ in $La_{3-x}Ba_{3+x}Cu_6O_{15}$ in samples annealed in a few atmospheres of oxygen.

If simple valences are considered, the addition of oxygen has the effect of raising a portion of the cations to a higher valence

state, or more likely, hybridizing Cu-O bonds producing metallic hole-type conduction. It is convenient, however, to refer to these materials as if they have some Cu^{+3}, even though in a formal sense this ion may not exist.

Table III. Location of δ Oxygen Atoms and Effects on Superconductivity

Compound	Location	Effect
$La_{2-x}A_xCu_{4-x/2+\delta}$	vacant octahedra corners	increases Cu^{+3}/Cu^{+2} ratio raises T_c
$La_3Ba_3Cu_6O_{14+\delta}$	vacant corner of octahedron at unit cell center	changes Cu coordination, pyramidal to octahedral increases $Cu^{+3/+2}$ ratio, semiconductor to 90K T_c
$YBa_2Cu_3O_{6.5+\delta}$	vacant site at 0 1/2 0	perfects square planar sites, increases $Cu^{+3/+2}$, orthorhombic distortion, raises T_c, 55 to 90K

Processing: All these materials can be processed in the same general manner. One starts with powders of the rare earth oxide (M_2O_3) or Y_2O_3, copper oxide CuO, and the carbonate of barium, strontium or calcium. The carbonates and rare earth oxides can be used in their as-received condition, but we have found that CuO requires additional milling to break up coarse particles. In addition, the powders should be predried to remove any adsorbed moisture prior to weighing. When drying, care should be taken to avoid agglomerate formation. The weighed powders are then thoroughly mixed in a mill or mortar and pestle. The powders are then calcined in open, flat crucibles. In the calcining step, carbonates are decomposed to the oxides and CO_2, and a multicomponent oxide is formed, i.e.

$$1/2\ Y_2O_3 + 2\ BaCO_3 + 3CuO \longrightarrow YBa_2Cu_3O_{6.5} + 2CO_2$$

The above formula assumes no addition or depletion of oxygen from the ambient during the calcining step, an assumption not always valid. The powders are not pelletized prior to calcining largely due to a large molar volume change (~30%) between reactants and products. One problem in calcining, is that the carbonates remain stable and do not always decompose. Furthermore, at the reaction temperatures particle sintering and grain growth occur. Thus, the calcined materials must be remilled. By monitoring the calcining step with x-ray diffraction, we have found that 3-4 hr at 925C is sufficient time for calcining, provided all starting powders are 10μ or less.

Once calcining is complete, the major molar volume changes have taken place and the milled powders can be pelletized for sintering. Here a multiple of traditional ceramic processing steps can be used

to form the material to its desired shape. The powders can be cold-pressed, with or without a binder, isostatically pressed, hot-pressed, mixed with binders and extruded into sheets, tubes, etc. Some members of our group, in collaboration with researchers at Brookhaven, have consolidated powders by plasma and flame spraying (19).

Once powders are consolidated and fired, the individual particles sinter together. This step is aided by a fine powder size (1-10μ) and a uniform dispersion of powders (no large voids). Typically 6-12 hours at 900-950C will sinter the particles to 80% density.

The final step in processing several of the high T_c ceramic superconductors is critical for good properties. The sintered samples are slowly cooled in flowing O_2 and held at some lower temperature to increase the oxygen content of the compound. For example,

$$ABa_2Cu_3O_{6.5} \text{ (from calcining)} + \delta/2\ O_2 \longrightarrow ABa_2Cu_3O_{6.5+\delta}$$

The effects of this step on superconductivity can be dramatic. For $YBa_2Cu_3O_7$, the fully oxygenated samples show a complete Meissner effect and R = 0 at temperatures in excess of 92K. Without the additional oxygen, the transitions are broad and the flux expulsion only partial (17). Table IV gives the composition ranges of intercalation of oxygen (20). The highest values of δ are obtained with long term anneals at about 500C under one atm of oxygen; lower values of δ are obtained with lower partial pressures. Table IV also shows the large effect intercalation has on the room temperature electrical conductivity, with samples becoming more metallic as oxygen is added.

Table IV. Known Ranges of Oxygen Intercalation in High T_c Ceramic Superconductors

Compound	Intercalation Range δ	Log Cond. Range (300K)
$La_{2-x}A_xCu_{4-x/2+\delta}$	0-0.3	1-1.8
$La_{2-x}A_{1+x}Cu_2O_{6-x/2+\delta}$	0-0.2	1-2.5
$La_3Ba_3Cu_6O_{14+\delta}$	0-0.4 0.4-1.0 (3 atm)	0.5-1.9
$YBa_2Cu_3O_{6.5+\delta}$	0-0.5	----

Individual Compounds

$YBa_2Cu_3O_x$: Processing this compound follows the general procedure outlined above. At temperatures above 700C, $YBa_2Cu_3O_x$ has a tetragonal structure (21). Its oxygen content is believed to be $YBa_2Cu_3O_{6.5}$. Below 700C, the unit cell is orthorhombic and the

composition adjusts towards $YBa_2Cu_3O_{7.0}$. The critical step in processing is to add this 0.5 oxygen atom per unit cell. This is critical because these oxygen atoms and their proper ordering on 0 1/2 0 sites dramatically improve superconducting properties. In such samples the T_c onsets are 93K, the transition widths 1K, and a full Meissner effect observed, i.e. the sample levitates in a strong magnetic field. The presence of the ordered intercalated oxygen atoms causes a distinct orthorhombic distortion in the unit cell of about 1.7% (17,21). Its presence can be readily observed from a splitting or shouldering the main X-ray diffraction peak at 32-33°. Normally the extra oxygen can enter during slow cooling (1°/min) from 900C in flowing oxygen. In some instances, furnace cooling is sufficient or alternatively one can anneal the sample at about 500-600C. We have observed, however, that some off-stoichiometric samples transform to the orthorhombic in a very sluggish manner. At this time, the reasons for this sluggishness in reaction are unclear. As another word of caution, we and others have observed that $YBa_2Cu_3O_{6.5}$ gradually decomposes when heated in air above 950C (22,23). By annealing a sample in air at 975C for 12 hours, we have nearly completely decomposed the phase into Y_2BaCuO_5, CuO and probably $BaCuO_2$. Reheating this same sample at 975C in flowing O_2, gradually reforms the $YBa_2Cu_3O_{6.5}$ phase.

The individual grains of samples with a pronounced orthorhombic distortion show striations or bands when viewed in an electron microscope (see figure 3). This is believed to be due to domain formation; in one band the "b" axis of the unit cell is oriented 90° to the "b" axis of the adjacent band. Electron microscopy also shows that small deviations from stoichiometry result in an amorphous second phase forming in the grain boundaries. Because most of the phases in equilibrium with $YBa_2Cu_3O_7$ are insulators, a grain boundary phase is probably an insulator.

Table V. Physcial and Superconducting Properties of $YBa_2Cu_3O_7$ (NRL Samples)

Lattice Parameters (A)	
a	3.822±0.002
b	3.888±0.002
c	11.672±0.005
Volume (A^3)	173.4
% Distortion	1.7
Oxygens per unit cell	6.94
T_c onset (K)	93
R=0 (K)	91
% flux expulsion	100
ρ (94K) ($\mu\Omega$-cm)	200
$(dH_c/dT)_{Tc}$ (kG/K)	22-36*
$H_{c2}(0)$ (kG)	1470-2370*
$H_{c1}(4.2K)$ (kG)	0.8
$H_c(0)$ (kG)	20-26*
$J_c(4K)$ (A/cm^2)	10^5+

*Calculated from critical field measurements
+Estimated from magnetization studies

We have measured a large number of superconducting properties on well characterized $YBa_2Cu_3O_7$ with a 1.7% orthorhombic distortion. These are listed in Table V.

$La_{3-x}Ba_{3+x}Cu_6O_{14+\delta}$: When processed by the general procedure, this sample is not superconducting. Mitzi et al. (9) showed that samples annealed for 24 hours at 450C in 3.5 atm of oxygen are superconductors, if $x > 0.75$, with T_c onsets of about 90K. We have verified these experiments (19). We find that the resistance behavior of $La_3Ba_3Cu_6O_{14+\delta}$ also becomes much more metallic after annealing in 3 atm of O_2. $La_2Ba_4Cu_6O_{14+\delta}$ becomes superconducting with T_c onset greater than 75K. The latter material shows a distinct second phase, however, so we cannot rule out the possibility that it is contributing to superconductivity. Also with x-ray analysis it is difficult to unambiguously decide if the crystal structure of this material is the Er-Rakho (13) or $YBa_2Cu_3O_7$ type. In both structures the cations have nearly identical positions, only the oxygen positions are significantly different. Both are very similar layered structures. The x-ray diffraction signatures, which are not sensitive to oxygen, are nearly identical. We see evidence for the very weak line at 2θ=16 as required for the (100) diffraction in the Er-Rakho tetragonal structure but also some evidence for peak shouldering which may indicate it is an orthorhombic structure and not tetragonal. It is also possible that both tetragonal and orthorombic phases exist as suggested by Lee et. al. (24). Because of the importance of this material in understanding superconductivity in high T_c ceramics, its structure should be refined by neutron diffraction.

$La_{2-x}A_xCuO_{4-x/2+\delta}$: A=Sr,Ba,Ca.

The optimum compositions for high T_c superconducting properties are for x=0.1 to 0.2. Samples are prepared according to the general procedure although processing temperatures of about 1100C are reported. The best samples are prepared in flowing O_2. Slow cooling and annealing at a lower temperature (500C) increase T_c by 1 to 2 degrees and also sharpen T_c. Likewise, annealing in vacuum destroys superconductivity. Reannealing in O_2 restores superconductivity. The degree of oxygen intercalation is small, δ=0 to 0.2 (20).

If x is small, less than 0.075, annealing in O_2 lowers T_c (25). If x=0, samples are not superconducting. Air-quenching samples annealed at 800-1000C causes a very small part of the sample to superconduct (27). This is probably grain boundary superconductivity because while R tends to zero, susceptibility measurements show only a trace of superconductivity. At very low temperatures, pure La_2CuO_4 transforms from an orthorhombic to an unknown structure (28). It has been speculated that this transformation may somehow inhibit superconductivity (29).

$Y_{2-x}Ba_{1+x}CuO_{6-x/2+\delta}$: It has been suggested that this phase is a high T_c superconductor (10). This observation has never been confirmed, and in fact, it is doubtful that this particular phase even exists. Nevertheless, the crystal structure of this family of

compounds, $La_{2-x}A_{1+x}Cu_2O_{6-x/2+\delta}$, is a layered one with coordination polyhedra like those found in the high T_c superconductors and the compounds' electrical conductivities show the same sensitivity to oxygen intercalation. Thus the compounds are obvious candidates for superconductivity.

Summary: High T_c ceramic superconductors have layered crystal structures with Cu-O coordination polyhedra typical of Cu+2. Intercalation of additional oxygen is critical to the superconducting properties. All these materials can be processed in a similar manner by traditional ceramic processing techniques.

Acknowledgments

The authors acknowledge the help of W. Lechter and R. Rayne in sample preparation and useful discussions with D. Schrodt, M. Kahn, D. Lewis and W. Lechter. B. Wood and R. Carpenter helped in manuscript preparation.

Literature Cited

1. J.G. Bednorz and K.A. Muller, Z. Phys. Rev. Lett, B 64, 189 (1986).
2. M.K. Wu, J.R. Ashburn, C.T. Torng, P.H. Hor, R.L. Meng, L. Gao, Z. Huang, Y.Q. Wang and C.W. Chu, Phys Rev Lett, 58, 908 (1987).
3. P.M. Grant, S.S.P. Parkin, V.Y. Lee, E.M. Engler, M.L. Ramirez, J.E. Vazquez, G. Lim, R.D. Jacowitz and R.L. Greene, Phys Rev Lett, June 1987 (to be published).
4. S. Uchida, H. Takagi, K. Kitazawa and S. Tanaka, Jpn J Appl Phys Lett 26,L1,(1987).
5. C.W. Chu, P.H. Hor, R.L. Meng, L. Gao, Z.J Huang, and Y.Q. Wang, Phys Rev Lett, 58, 405 (1987).
6. D.U. Gubser, R.A. Hein, S.H. Lawrence, M.S. Osofsky, D.J. Schrodt, L.E. Toth and S.A. Wolf, Phys Rev Lett, B 35, 5350 (1987) and references therein.
7. P.H. Hor, R.L. Meng, Y.Q. Wang, L. Gao, Z.J. Huang, J. Bechtold, K. Forster and C.W. Chu, Phys Rev Lett, 58, 1891 (1987)
8. D.W. Murphy, S. Sunshine, R.B. VanDover, R.J. Cava, B.Batlogg, S.M. Zahurak and L.F. Schneemeyer, Phys Rev Lett, 58, 1888 (1987).
9. D.B. Mitzi, A.F. Marshall, J.Z. Sun, D.J. Webb, M.R. Beasley, T.H. Geballe and A. Kapitulnik (submitted to Phys Rev).
10. Shiou-Jyh Hwu, S.M. Song, J. Thiel, K.R. Poeppelmeier, J.B. Ketterson and A.J. Freeman, Phys Rev Lett, B 35, 7119 (1987).
11. A. F. Wells, Structural Inorganic Chemistry 5th Ed. Claredon Press: Oxford, 1984.
12 R. J. Cava, A. Santoro and D.W. Johnson Jr., (to be published).
13. L. Er-Rakho, C. Michel, J. Provost and B. Raveau, J. Solid State Chem, 37, 151 (1981).
14. N. Nguyen, L. Er-Rakho, C. Michel, J. Choisnet and B. Raveau, Mate Res Bull, 15, 891 (1980).
15. M.A. Beno, L. Soderholm, D.W. Capone II, D.G. Hink, J.D. Jorgensen, Ivan K. Schuller C.U. Segre, K. Zhang and

J.D. Grace, Appl Phys Lett (to be published).
16. F. Beech, S. Miraglia, A. Santoro and R.S. Roth, (to be published).
17. L.E. Toth, E.F. Skelton, S.A. Wolf, S.B. Qadri, M.S. Osofsky, B.A. Bender, S.H. Lawrence and D.U. Gubser, (submitted for publication to Phys Rev) and also E.F. Skelton, S.B. Qadri, B.A. Bender, A.S. Edelstein, W.T. Elam, T.L. Francavilla, D.U. Gubser, R.L. Holtz, S.H. Lawrence, M.S. Osofsky, L.E. Toth and S.A. Wolf, MRS Proceedings, California 1987 (to be published).
18. Unpublished result, NRL.
19. J.P. Kirkland, R.A. Neiser, H. Herman and W.T. Elam, (unpublished).
20. C. Michel and B. Raveau, Rev Chim Minerals, 21, 407 (1987).
21. Ivan K. Schuller, D.G. Hinks, M.A. Beno, D.W.Capone II, L. Soderholm, J.-P. Locquet, Y. Bruynseraede, C.U.Segre, and K. Zhang, (submitted for publication, Solid State Commun.)
22. Unpublished result, NRL.
23. T.L. Aselage, B.C. Bunker, D.H. Doughty, M.O. Eatough, W.F. Hammetter, K.D. Keefer, R.E. Loehman, B. Morosin, E.L. Venturini and J.A. Voigt, MRS Proceedings, California 1987 (to be published).
24. Sung-Ik Lee, John P. Golben, Sang Y. Lee, Xuao-Dong Chen, Yi-Song, Tae W. Noh, R.D. McMichael, Yve Cao, Joe Testa, Fulin Zuo, J. R. Gaines, A.J. Epstein, D.L Cox, J.C. Garland, T.R. Lemberger, R. Sooryakumar, Bruce R. Patton and Rodney T. Tettenhorst, MRS Proceedings, California 1987 (to be published).
25. J.M. Tarascon, L.H. Greene, W.R. Mckinnon, G.W. Hull and T.H. Geballe, Science, 235, 1373 (1987).
26. P.M. Grant, S.S.P. Parkin, V.Y. Lee, E.M. Engler, M.L. Ramirez, J.E. Vazquez, G. Lim, R.D. Jacowitz and R.L. Greene, Phys. Rev. Lett. to be published.
27. E.F. Skelton, W.T. Elam, D.U. Gubser, V. Letourneau, M.S. Osofsky, S.B. Qadri, L.E. Toth and S.A. Wolf, submitted Phy. Rev. Lett.
28. R.V. Kasowski, W.Y. Hsu and F. Herman, Solid State Commun., to be published.

Figure 1. Coordination polyhedra of copper and oxygen atoms in high T_c superconductors: (a) square planar, (b) pyramidal (4+1) and (c) distorted octahedron (4+2). The distance x is about 1.95A and the distance y about 2.3A.

Figure 2. Crystal structures of ceramic high T_c superconductors. (a) K_2NiF_4 structure showing layers of distorted octahedra (4+2). (b) $YBa_2Cu_3O_7$ structure with nearly square planar and pyramidal (4+1) Cu-O coordination polyhedra, (c) Er-Rakho structure with square planar configurations perpendicular to, and distorted octahedra with the longer axis parallel to the c axis of the unit cell, (d) the $La_{2-x}Sr_{1+x}Cu_2O_{6-x/2+\delta}$ with (4+1) Cu-O pyramidal coordinations. The small solid circles are copper atoms, the large open circles are oxygen atoms, and the shaded circles are the rare earth, Y, Ba, or Sr atoms.

Figure 3. Transmission electron micrograph showing planar defects in $YBa_2Cu_3O_7$ uniformly spaced about 2000A and dispersed in the specimens. These have been identified as twins formed because of the slight difference in the a and b axes.

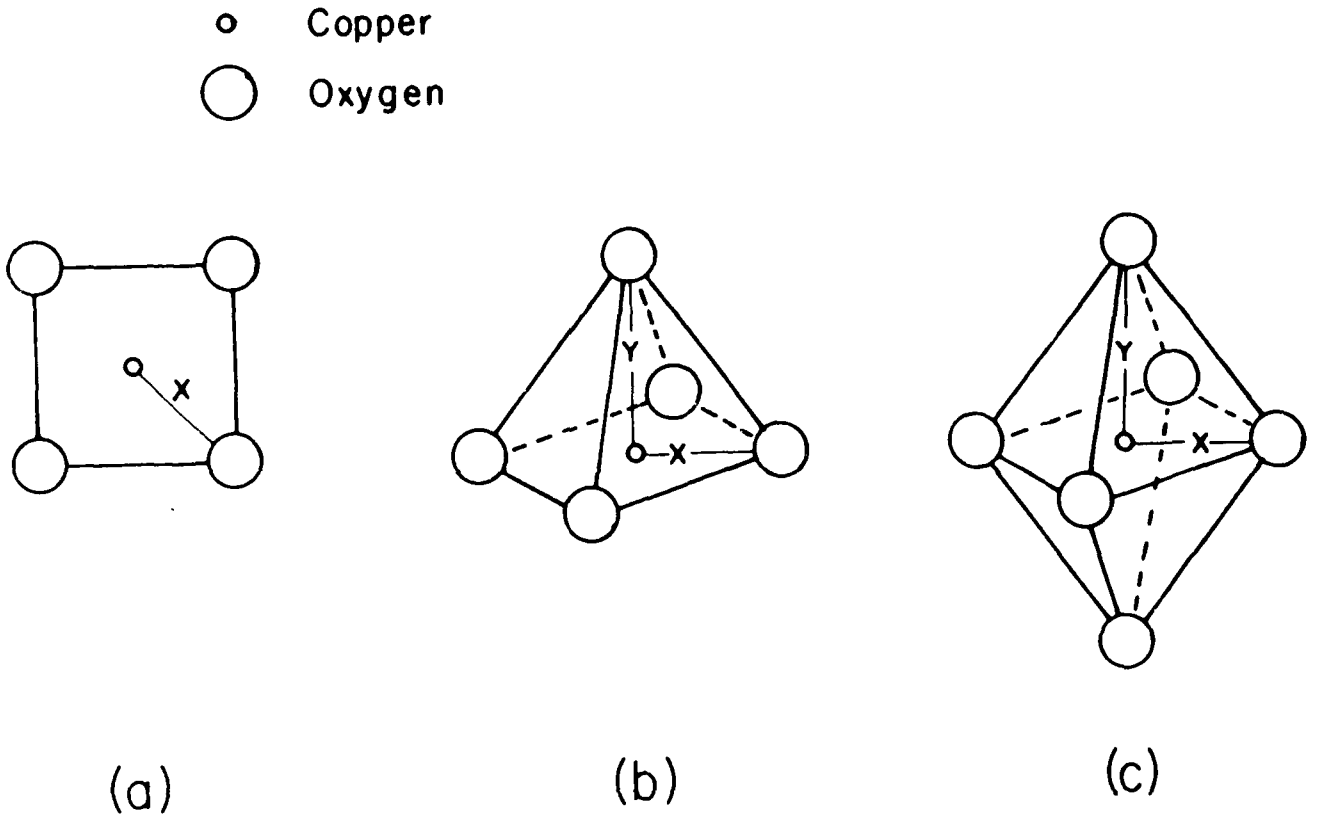
Copper
Oxygen
X
Y
X
Y
X
(a)
(b)
(c)

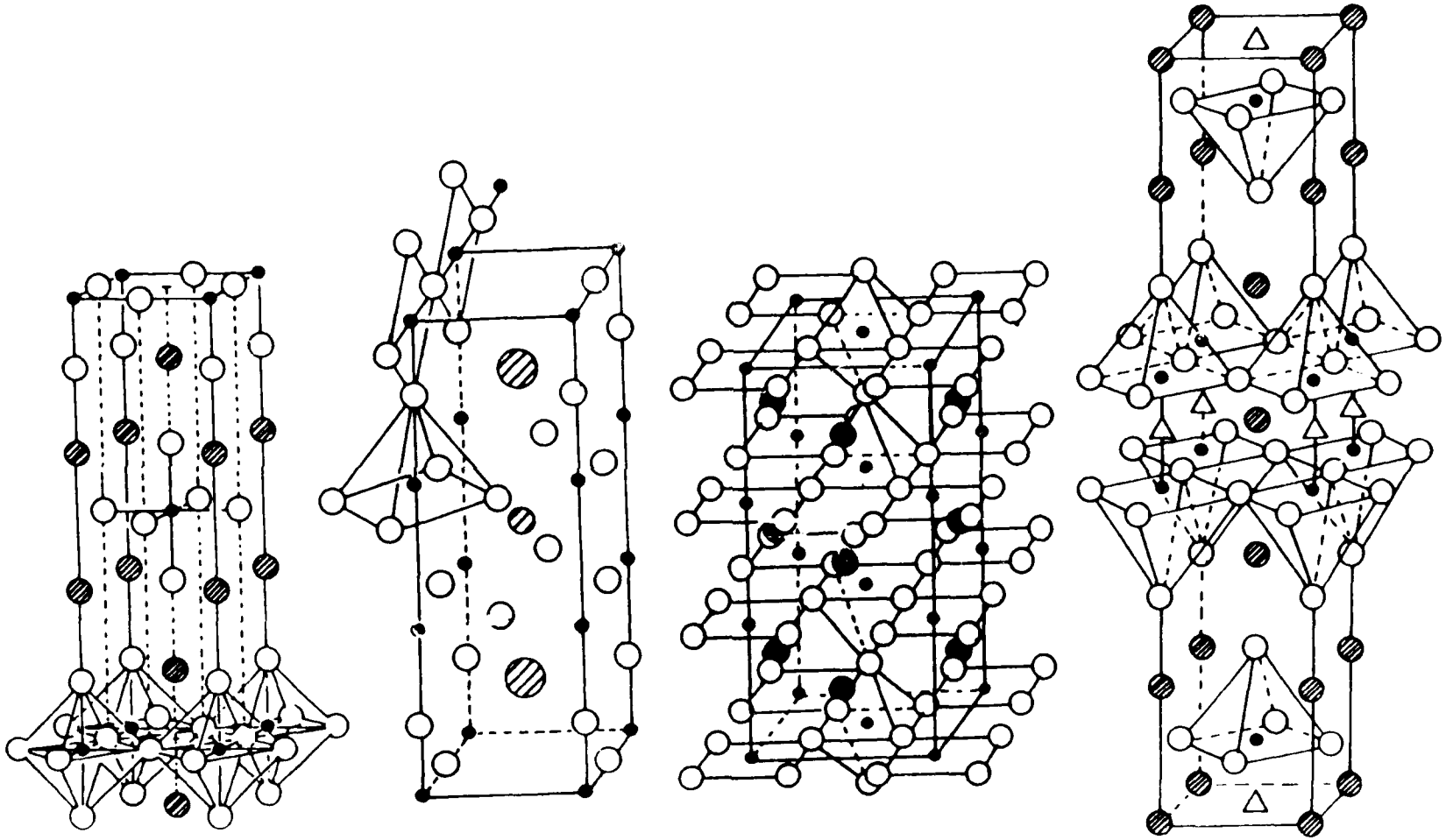
(a)
(b)
(c)
(d)

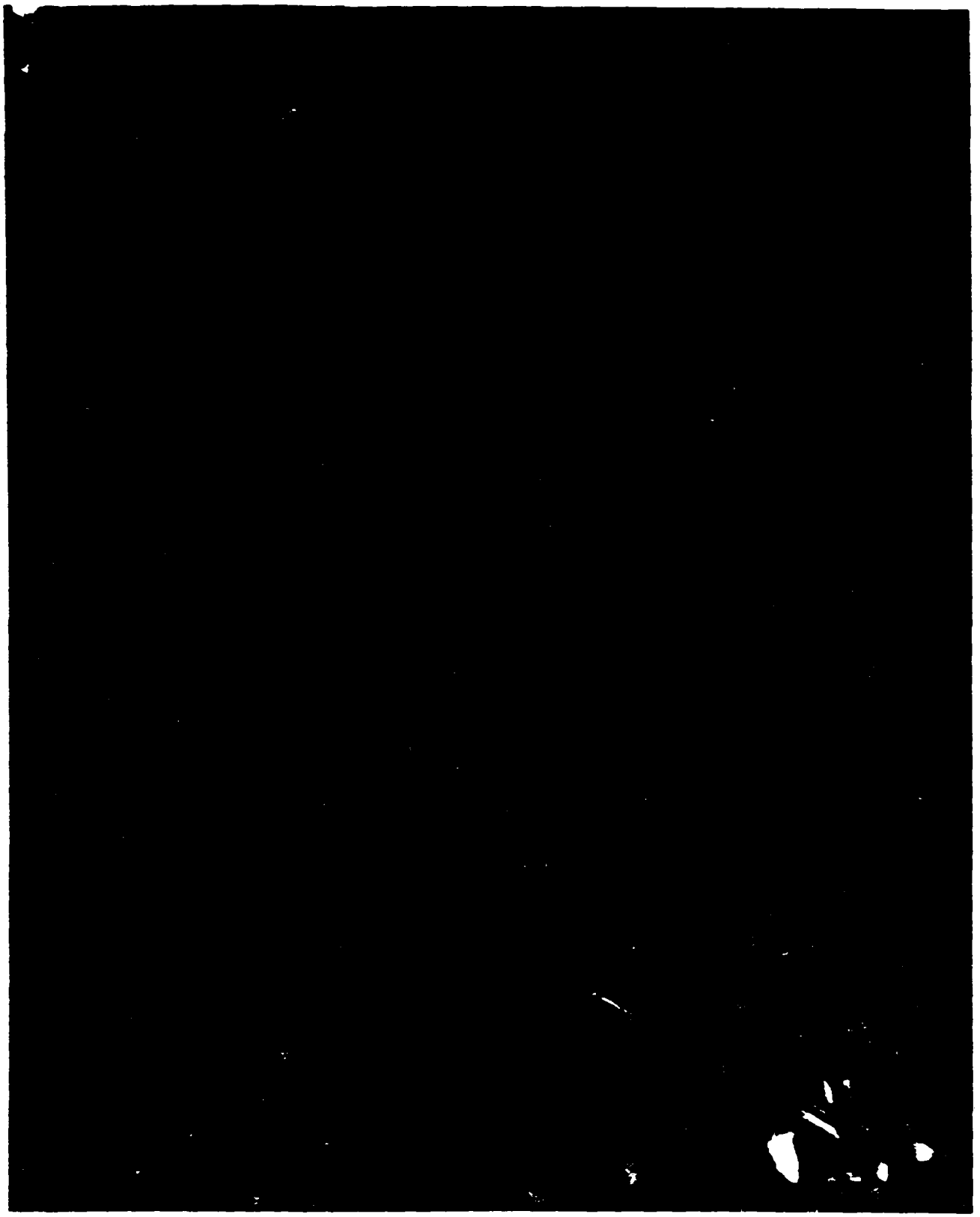

PROCESSING AND PROPERTIES OF THE HIGH T_c SUPERCONDUCTING OXIDE CERAMIC $YBa_2Cu_3O_7$

B. Bender*, L. Toth*†, J.R. Spann*††, S. Lawrence*††, J. Wallace*, D. Lewis*, M. Osofsky§, W. Fuller, E. Skelton, S. Wolf, S. Qadri§§, and D. Gubser
U.S. Naval Research Laboratory, Washington, DC 20375

The landmark discovery by Bednorz and Muller of a new class of superconducting materials in the lanthanum-barium (strontium)-copper oxide system,[1] with critical transition temperatures (T_c) above 30K, sparked unprecedented interest among a great many workers in a wide range of research areas. The ensuing efforts to find materials exhibiting superconductivity at even higher temperatures led to the report by Chu and coworkers of a two phase oxide ceramic system exhibiting onset of superconductivity above 90K.[2] Subsequent work which identified one of the phases, $YBa_2Cu_3O_7$ (YBC), as the oxide responsible for superconductivity provoked a tremendous amount of research on this compound (although the search for materials with even higher T_c's continues unabated). Our work, first with the Bednorz and Muller materials[3,4] and more recently with YBC,[5,6] has been directed primarily toward finding processing conditions leading to dense bulk and thick film materials while equaling or exceeding currently attainable superconducting properties. Toward this end we have sought to correlate processing parameters with microstructural and crystalline parameters and to provide high quality, well characterized samples suitable for detailed investigations of fundamental physical and superconducting properties.

Of the various methods available for the preparation of high T_c YBC, the one we usually employ is as follows: (a) mix and grind appropriate proportions of $BaCO_3$, CuO and Y_2O_3 predried powders; (b) calcine for 6-12 h at 900-950°C in air with intermediate grindings; (c) grind and cold press into pellets (or other shapes); (d) sinter in air or flowing oxygen at 925°C for about 12 h; (e) cool slowly in flowing oxygen at about 1°C/min or hold between 500-600°C for several hours.

Carried out properly, the aforementioned procedure produces a single phase YBC with a well defined orthorhombic distortion of 1.3-1.9% (from the tetragonal); concomitant with this are superior superconducting properties, as indicated by sharp transitions above 90K and complete flux expulsion. The procedure must be monitored carefully, however, to ensure that the formation of YBC is taking place at each step of the process. A number of steps are critical. First, we have found that heating YBC in air at temperatures above 950°C gradually decomposes the phase, with a green colored phase, Y_2BaCuO_x, and CuO being formed as a result. This reaction is reversible; heating below 950°C in air gradually reforms the superconducting phase. Heating in flowing oxygen raises the stability of YBC to at least 975°C. We have taken badly segregated samples containing little or no YBC and converted them into YBC by

---

* Member, the American Ceramic Society.
† On sabbatical leave from the National Science Foundation.
†† Crystal Growth and Material Testing Associates, Lanham, MD.
§ Office of Naval Technology Postdoctoral Fellow.
§§ Sachs-Freeman Associates, Landover, MD.

this treatment, thus confirming the reversibility of the process. Second, slow cooling in oxygen or air or holding at 500-600°C is necessary to form a phase with a well characterized orthorhombic distortion. Results suggest that the rate of cooling required is dependent in part on the extent of connected porosity, with greater porosity permitting a faster cooling rate (on the order of 1°C/min) than is advisable in samples with lower porosity; presumably such porosity facilitates the incorporation of oxygen necessary for the formation of the high T_c superconducting orthorhombic phase (vide infra).

Other means of processing have also been the subject of study. One effort has involved seeking an alternative to the use of $BaCO_3$ as the source of barium for YBC. In addition to its relatively high decomposition temperature (over 875°C), any undecomposed $BaCO_3$ present in a green body generates CO_2 during sintering, thus creating a gas phase barrier to the oxygen incorporation required to form the orthorhombic phase. Use of barium oxide, particularly in the finely powdered form required for dense samples, requires great care in avoiding exposure to humidity and CO_2, since the readily formed hydroxide and carbonate both decompose at relatively high temperatures. We also observed the earlier reported[7] poor stability toward hydrolysis of $Ba_4Y_2O_7$ while evaluating it as a starting material.

Another procedure involved vacuum hot pressing the prereacted materials prepared as above in place of sintering (step d), or reaction vacuum hot pressing with the appropriate portions of the predried powders (step a). In one variation of the latter, 2% by weight of the sample of BaF_2 was substituted for an equivalent amount of the $BaCO_3$ in an effort to achieve better densification.[8-10] The amount of BaF_2 used in this latter procedure is considerably less than the stoichiometric quantities used by other workers.[11] Prereacted powder produced a sample with a hot pressed density of about 73%. X-ray peaks were found for $BaCO_3$, CuO, and possibly YBa_2CuO, but none of those associated with either the reduced tetragonal or the more fully oxidized orthorhombic phase of YBC were present. However, reoxidation of the hot pressed sample at 975°C for over 36 h followed by slow cooling with a 2 h hold at 700°C produced a material with an orthorhombic structure (YBC) and a strong Meissner effect. When BaF_2 was used compaction was achieved at a lower temperature than with the prereacted powders as expected, but the reaction was incomplete even though the sample was hot pressed at 950°C for 15 min. $BaCO_3$, BaF_2, and CuO were found in the hot pressed disk by X-ray analysis, and densification was incomplete; the as-hot pressed density was only about 60% of the theoretical value, and upon reoxidation it decayed to approximately 50%. However, in spite of these difficulties the reoxidized samples were found to be YBC by X-ray diffraction and to have superconducting properties, as demonstrated by a strong Meissner effect and a sharp transition to near zero resistance between 90K and 92K.

Selected physical and superconducting properties of YBC samples prepared by sintering in air or oxygen are presented in Table 1, which also includes references to more detailed measurements, e.g. phonon spectra. Optical microscopy (figure 1) shows that nearly all grains of YBC have significant amounts of striations. It is believed these striations result from twinning associated with the orthorhombic distortion, as also seen by Beyers and coworkers using TEM.[16] We are using TEM to explore the nature of the twinning and to investigate the grain boundaries (figures 2 and 3). An important question in resistivity and critical current measurements is whether there are any grain boundary impurity phases. Our preliminary results suggest that most boundaries are free of these impurity phases; some, however, are separated by a thin impurity phase. This no doubt is the result of a small shift from the

stoichiometric composition.

In other work we have determined conditions for retaining at room temperature the high temperature tetragonal YBC phase. We index the x-ray diffraction data from the samples assuming that they all are orthorhombic, but when the distortion is less than 0.25% the phase is considered to be tetragonal. The composition of this phase is probably $YBa_2Cu_3O_{6.5}$, thus indicating that the phase is oxygen deficient relative to the orthorhombic phase. The tetragonal structure is found in samples that are rapidly cooled from 800-900°C and in which there is insufficient time for the sample to reach thermodynamic equilibrium with the ambient atmosphere. Conditions for retaining the phase vary from sample to sample and seem to depend on the extent of sintering. In several samples with well defined tetragonal structures the sintered density was 90% or better, making it difficult to achieve equilibrium with oxygen on cooling. The superconducting properties of tetragonal samples are inferior to those with orthorhombic distortions. We found $T_{c(onset)}$ values of 55K and R=0 at 35K. Other samples with tetragonal structures had higher $T_{c(onset)}$ values (90K) but very broad transitions (30-50K), possibly indicating a mixture of tetragonal and orthorhombic phases. These samples show very small Meissner effects (10%) compared to the complete expulsion of magnetic flux observed with the pure orthorhombic phase. These results strongly suggest the importance of the orthorhombic distortion in achieving high T_c values and the importance of the linear Cu-O chains which cause the distortion.

REFERENCES

1. J.G. Bednorz and K.A. Muller, Z. Phys. B, 64, 189 (1986).
2. M.K. Wu, J.R. Ashburn, C.J. Torng, P.H. Hor, R.L. Meng, L. Gao, Z.J. Huang, Y.O. Wang, and C.W. Chu, Phys. Rev. Lett., 58, 908 (1987).
3. D.U. Gubser, R.A. Hein, S.H. Lawrence, M.S. Osofsky, D.J. Schrodt, L. E. Toth, and S.A. Wolf, Phys. Rev. B, 35, 5350 (1987).
4. E.F. Skelton, W.T. Elam, D.U. Gubser, S.H. Lawrence, M.S. Osofsky, L. E. Toth, and S.A. Wolf, Phys. Rev. B, 35, 7140 (1987).
5. E.F. Skelton, S.B. Qadri, B.A. Bender, A.S. Edelstein, W.T. Elam, T. L. Francavilla, D.U. Gubser, R.L. Holtz, S.H. Lawrence, M.S. Osofsky, L.E. Toth, and S.A. Wolf, Extended Abstracts, Materials Research Society Conference on High T_c Superconductors, Anaheim, CA, April 1987.
6. M. Osofsky, L.E. Toth, S. Lawrence, S.B. Qadri, A. Shih, D. Mueller, R.A. Hein, W.W. Fuller, F.J. Rachford, E.F. Skelton, T. Elam, D.U. Gubser, and S.A. Wolf, Proceedings of the Materials Research Society Conference on High T_c Superconductors, Anaheim, CA, April 1987, submitted for publication.
7. W. Kwestroo, H.A.M. van Hal, and C. Langereis, Mat. Res. Bull., 9, 1631, (1974).
8. B.E. Walker, R.W. Rice, R.C. Pohanka, and J.R. Spann, Bull. Am. Ceram. Soc., 55, 274 (1976).
9. B.E. Walker, R.W. Rice, and J.R. Spann, U.S. Patent 3,753,911 (1973).
10. B.E. Walker, R.W. Rice, and J.R. Spann, U.S. Patent 3,862,046 (1975).
11. C. Politis, M.R. Dietrich, G.M. Friedman, J. Geerk, S.M. Green, R. Hu, S. Hufner, C. Jiang, W. Krauss, H. Kupfer, H. Leitz, G. Linker, H.L. Luo, Yu Mei, O. Meyer, B. Obst, P. Steiner, and H. Wuhl, Extended Abstracts, Materials Research Society Conference on High T_c Superconductors, Anaheim, CA, April 1987.

12. W.W Fuller, M.S. Osofsky, L.E. Toth, S.B. Qadri, S. Lawrence, R.A. Hein, T.L. Francavilla, D.U. Gubser, and S.A. Wolf, to be published in the Proceedings of the XVIII International Conference on Low Temperature Physics (LT18), Kyoto, Japan, August 1987.
13. R.L. Kurtz, R.L. Stockbauer, D. Mueller, A. Shih, L.E. Toth, M. Osofsky, and S.A. Wolf, Phys. Rev. B, accepted for publication.
14. J.J. Rhyne, D.A. Neumann, J.A. Gotaas, F. Beech, L. Toth, S. Lawrence, S. Wolf, M. Osofsky, and D.U. Gubser, Phys. Rev. Lett., accepted for publication.
15. R.A. Hein, M.S. Osofsky, L.E. Toth, D.U. Gubser, and S.A. Wolf, Phys. Rev. B, submitted for publication.
16. R. Beyers, G. Lim, E.M. Engler, R.J. Savoy, T.M. Shaw, T.R. Dinger, W.J. Gallagher, and R.L. Sandstrom, Appl. Phys. Lett., submitted for publication.

Table 1. Physical and Superconducting Properties of YBC

Lattice Parameters (Å)	
a	3.822±0.0002
b	3.888±0.0002
c	11.672±0.005
Volume ($Å^3$)	173.4
% Distortion	1.7
Oxygens per unit cell	6.94*
T_c(onset) (K)	93
R=0 (K)	91
% flux expulsion	100
ρ (94K) ($\mu\Omega$-cm)	200
$(dH_c/dT)\|_{T_c}$ (kG/K)	22-36†
$H_{c2}(0)$ (kG)	1470-2370†
H_{c1} (4.2K) (kG)	2.5†
$H_c(0)$ (kG)	20-26†
J_c (4K) (A/cm^2)	10^5†§
Photoemission	see Ref. 13#
Phonon Spectrum	see Ref. 14#
Magnetization	see Ref. 6 #
AC susceptibility	see Ref. 15#

*Determine by neutron diffraction refinement of the crystal structure, see Reference 14.
†See Reference 12.
§Determined from magnetization measurements.
#To be published.

Figure Captions

Fig. 1. Optical micrograph of $YBa_2Cu_3O_7$ showing striations in individual grains.

Fig. 2. Dark field (A) and (B) bright field TEM micrographs showing the twinning in orthorhombic $YBa_2Cu_3O_7$. The grain boundary in (B) is free of impurity phases.

Fig. 3. Impurity phase in grain boundary separating two YBC grains. Dark field TEM micrograph.

$YBa_2Cu_3O_7$. The grain boundary in (B) is free of an impurity phase

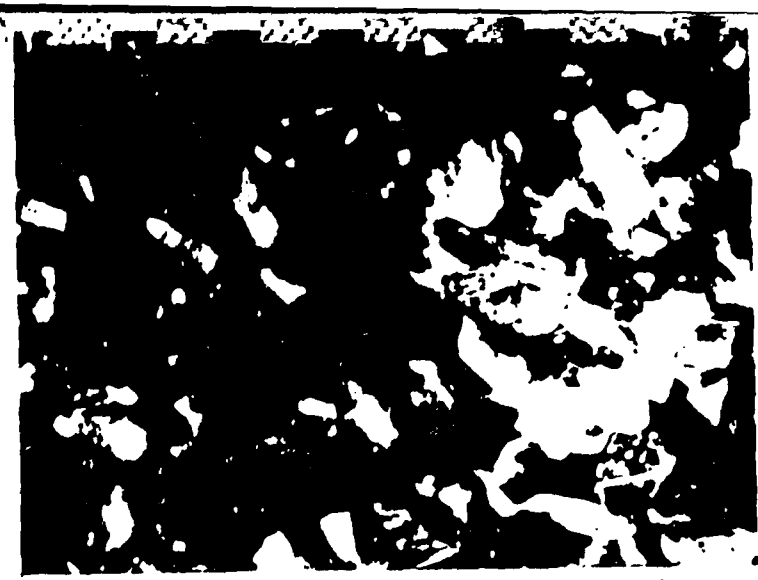

Optical Micrograph of $YBa_2Cu_3O_7$ showing striations in individual grains (xxx Mag)

Impurity phase in grain boundary separating two YBC grains. Dark field micrograph

Domain like defects observed in high temperature superconductor of Y-Ba-Cu-O system.

C. S. Pande* and A. K. Singh+, L. Toth**, D. U. Gubser**, and S. Wolf*

*Naval Research Laboratory
Washington, DC
+Crystal Growth Associates
Lanham, MD
**On Sabbatical leave from National
Science Foundation

Abstract

Extensive transmission electron microscopy of the high superconductivity transition temperature oxide Y Ba_2 Cu_3 O_x reveals the presence of planar defects along [110] direction uniformly more or less spaced (spacing ~ 2000A°) and dispersed throughout the specimens. These defects persisted on cooling upto the transition temperature (93°K), but disappeared on heating above 400°C in insitu experiments inside the electron microscope. Possible role of these 'domains' or interfaces in superconductivity is discussed.

The structure of the new (above 90K superconducting transition temperature) superconductor Y Ba_2 Cu_3 O_x has been found to be related to perovskites. [1] However the value of x is not 9, as expected for a typical perovskite, but has a value in most cases of about 7 ie about one quarter of the oxygen atoms are missing. In addition it appears that the high temperature superconducting phase is not tetragonal but orthorhombic, the a axis being about 1.6% longer than the 'b' axis. The orthorhombic structure may be a result of the way oxygen and vacancies occupy oxygen positions. In addition, several workers have reported planar defects in these materials, which have been variously identified as 'twins' [2] antiphase boundaries [3] and/or extrinsic planar faults. [4]. The aim of this note is to report the results a detailed transmission electron microscopy and electron diffraction study including insitu heating and cooling observations on thin foils of well characterization high Tc superconductors Y Ba_2 Cu_3 O_x with a T_c of 93°K and T_c width of about 2K. The bulk superconducting material was prepared by mixing and grinding appropriate portions of $BaCo_3$, CuO and Y_2O_3 predried powders, then calcined for 6-12 hours at 900-950°C in air, with intermediate graindings, ground and cold pressed into pellets, suited in flowing oxygen at 925°C for 12 hours and finally cooled slowley in flowing oxygen at about 1°C/minute. This produced almost a single phase compound with a well defined orthorhombic distortion (as determined from x-ray measurements) of 1.6% from tetragonal. The composition of the superconduting phase is probably very close to YBa_2 Cu_3 $O_{6.5}$ i.e. oxygen deficient.

The electron microscope specimens were prepared either (a) by finely grinding the bulk specimen and floating the powder in water and scooping the thin flakes on electron microscope copper grids coated with carbon or by ion milling with grazing Ar ions at an accelerating voltage of 5KV, till perforation. The planar defect as well as other lattice defects observed by

electron microscopy on the specimens obtained by the two methods were indistinguishable from each other indicating that the defects observed were not artifacts of our experimental procedure and that the defects are not due to radiation damage during ion milling. The transmission electron microscopy was done at an accelerating voltage of 200KV using JEOL 200CX transmission electron microscope.

Observing along the c axis [(001) orientation] invariably all the grains show the planar defects. Figure 1 is electron micrograph and Fig. 2 diffraction pattern from the same region. The direction of these faults are along [110]. Thin plates are twin related to each other and are shown edge on (ie. twin boundary is parallel to electron beam). The electron diffraction pattern (Fig. 2) shows the splitting of spots along only one of the diagonal and the separation increases in higher order reflections. This can be explained by twinning on [110] plane in these orthorhomic crystals. Due to slight difference in "a" and "b" parameters, and twinning the diffraction pattern will show the splitting of spots along one of the diagonal spots but not in other diagonal. Direction of splitting will be perpendicular to the diagonal. This is exactly what we are observing in the diffraction pattern. The angular value of the splitting assuming, a orthorhombic structure, and the fact that the splitting is due to twinning can be derived to be

$$\upsilon = 4 \tan^{-1}\left(\frac{a-b}{a+b}\right) \approx 4\left(\frac{a-b}{a+b}\right) \quad \text{if } a \approx b$$

where a, and b, values for the structure for the present compound was determined from x-ray measurement to be 3.86A° and 3.82A° respectively giving υ ≈ .03 radian in excellent agreement with the experimental value measured (0.3) from Fig. 2. A schematic arrangement of the interface is shown in Fig. 3. The difference between 'a' and 'b' axes is exaggerated. Very high contrast of boundaries should be noted, due probably to stress. After tilting, as

expected, these boundaries give the fringe contrast which is shown in Fig. 4. Figure 5 is another electron micrograph. Two orthogonal sets of domains are (sometimes but rarely) observed. Electron diffraction can again be well explained on the basis of [110] twinning.

In situ heating and cooling experiments were done inside the electron microscope. First the specimen was cooled gradually to liquid nitrogen temperature. No change in shape or size or electron diffraction pattern was observed; It appears that cooling had no effect on these domains upto a temperature close to the transition temperature of the material. The specimen was then gradually warmed from liquid nitrogen temperature upto a temperature of 150°C. Again no visible changes were observed. All the observations were made at a magnification of around x50K. The temperature was then suddenly raised to above 400°C. When the twin interfaces became sharper and then quickly disappeared throughout the specimen. On cooling many of the domains reappeared. The domains thus appear to be stable from about liquid nitrogen temperature to upto about 400°C.

Although is has not yet been determined from independent measurements that these oxide superconductors are ferroelectric, the planar interfaces observed by us, bear strong resemblance to 90° ferroelectric domains. Planar interface in these superconducting compounds have been observed by several workers, however, this is probably the first time that they have been definitely characterized as twins by extensive transmission electron microscopy and electron diffraction. Chen and coworkers, [37] for example identified these planar defects as antiphase boundaries. Our results are not in accord with this interpretation unless vacancy ordering is considered. However orthorhombic a and b axis do alternate across the boundary as pointed out by them. One interesting property of these interfaces is that they break the linear CuO chains. Schuller et al [5] have recently suggested that the main

diffraction between the tetragonal and orthorhombic phase is that in the former, the long range ordering of the oxygen vacancies in Cu-O planes is non-existent, i.e. one dimensional Cu-O chains are absent. Whereas in orthorhombic structure they are present. The ordering of oxygen and vacancies have recently been treated as an order disorder problem by de Fontain and Moss. [6] The other role of these interfaces could be in providing sites for semiconductor-metal transition, assuming the interfaces to behave like a semiconductor.

References

1. See for example
   L. E. Toth, E. F. Skelton, S. A. Wolf, S. B. Qadri, M. S. Osofsky, B. A. Bender, S. H. Lawrence and D. U. Gubser Phy Rev B (in press)

2. R. Beyers, G. Lim, E. M. Engler, and R. J. Savoy (to be published in App. Phys. Lett 29th June 1987)

3. C. H. Chen, D. J. Werder, S. H. Liuo, J. R. Kwo and M. Hong (to be published in Phys Rev B June 1, 1987)

4. A. Ourmazd, J. C. H. Spence, M. O'Keeffe, R. J. Graham, D. W. Johnson Jr., J. A. Rentschler, and W. W. Rhodes, Materials Research Society Proceedings to be published. Also Nature (In Press)

5. I. K. Schuller, D. G. Hinks, M. A. Beno, D. W. Capone II, L. Soderholm, J. P. Locquet, Y. Bruynseraede, C. U. Segre, and K. Zhang (submitted to Solid State Communication)

6. D. de Fontaine and S. C. Moss (submitted to Phys Rev Lett)

Legend of Figures

Fig. 1 Transmission electronmicrograph Y $Ba_2Cu_3O_x$ polycrystal. The parallel domains are on the average ~ 2000A° apart, and aligned along [110] direction. The interfaces are seen edge on. The orthorhombic a and b axes are found to alternate along these interfaces.

Fig. 2 Electron diffraction from the same region and orientation as in Fig. 1 Notice the splitting of spots along one direction.

Fig. 3 A schematic diagram of the interface. The difference between 'a' and 'b' axes is exaggerated.

Fig. 4 Transmission electron micrograph of the interfaces showing fringe contrast.

Fig. 5 Transmission electron micrograph showing two set of interfaces at approximately right angles to each other.

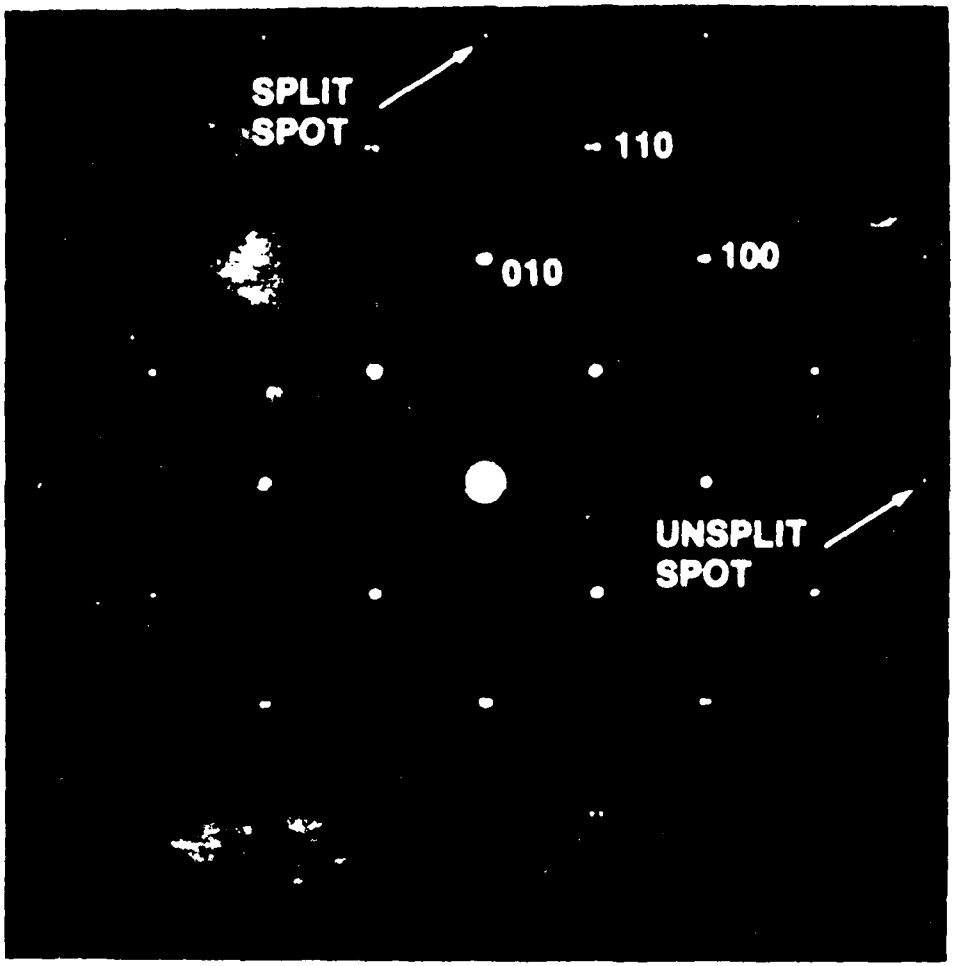
SPLIT
SPOT
110
010
100
UNSPLIT
SPOT

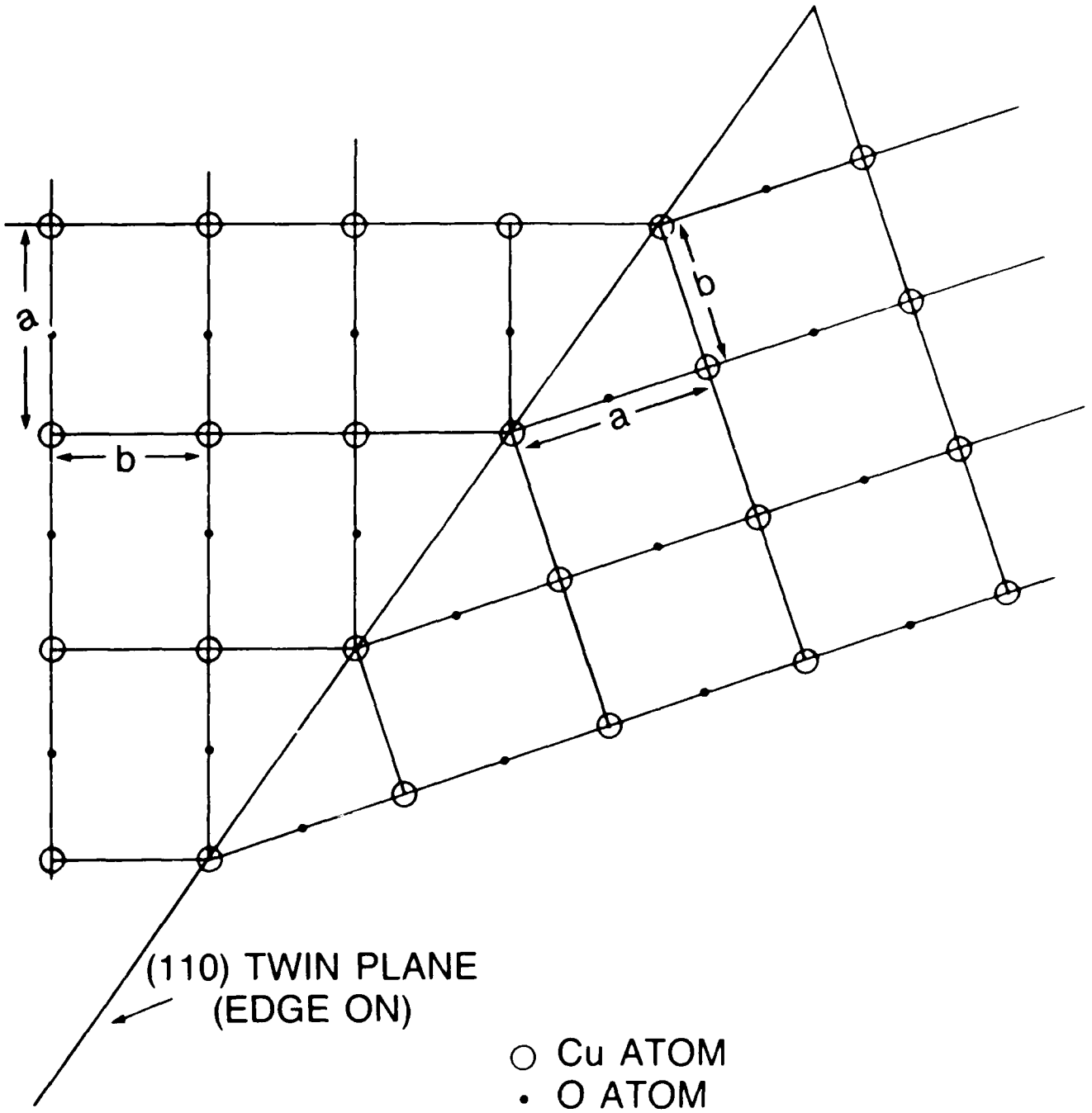
a
b
b
a
(110) TWIN PLANE
(EDGE ON)
Cu ATOM
O ATOM


0.2μm

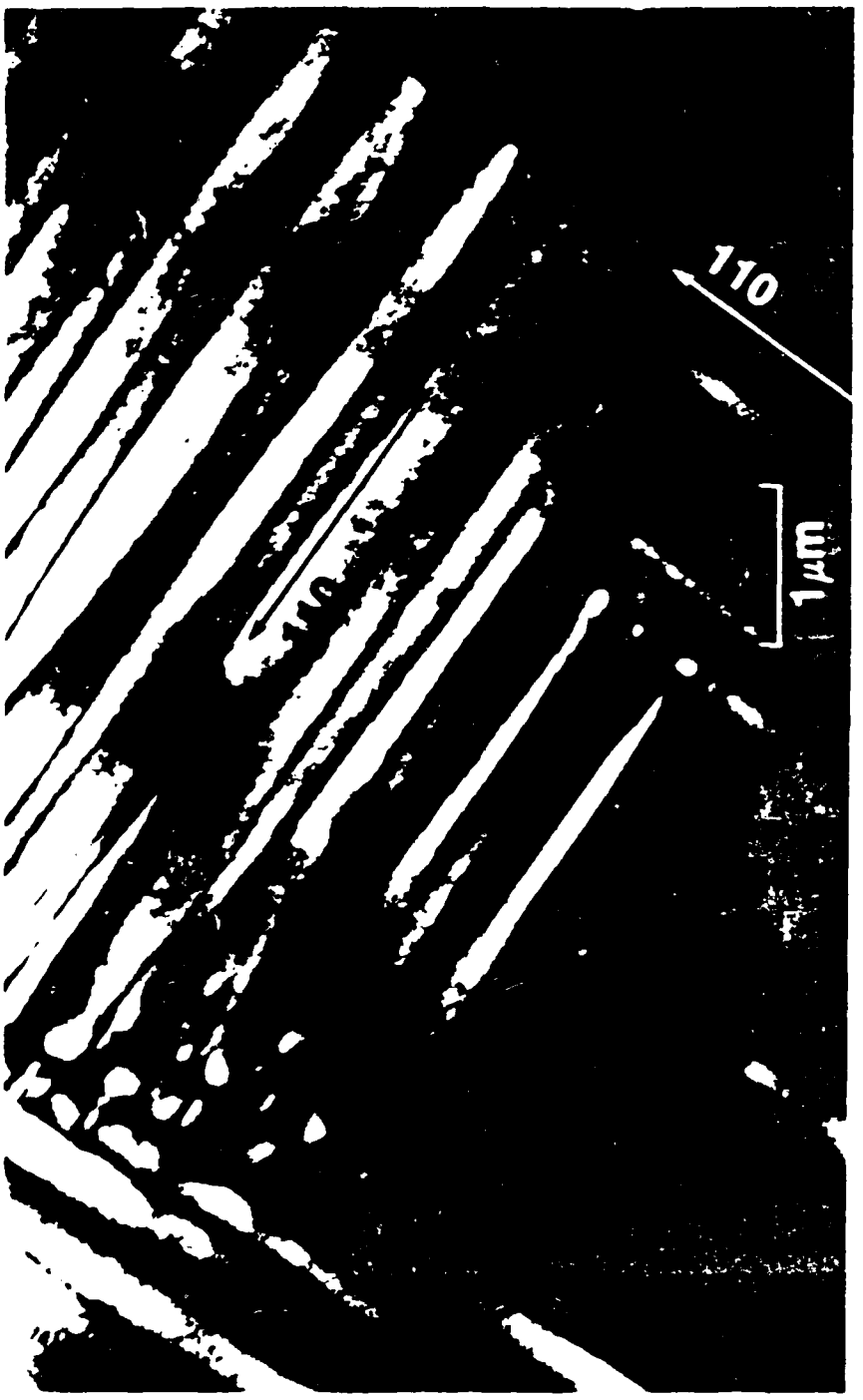
110
1μm

PHONON DENSITY OF STATES AND STRUCTURE OF THE SUPERCONDUCTOR $YBa_2Cu_3O_7$

J. J. Rhyne, D. A. Neumann, J. A. Gotaas, and F. Beech

Institute for Materials Science and Engineering

National Bureau of Standards

Gaithersburg, MD 20899

and

L. Toth, and S. Lawrence

Ceramics Branch

Naval Research Laboratory

Washington, DC 20375

and

S. Wolf, M. Osofsky, and D. B. Gubser

Metal Physics Branch

Naval Research Laboratory

Washington, DC 20375

ABSTRACT

Neutron scattering has been used to study the vibrational density of states and the atomic structure of the high temperature supercoductor $YBa_2Cu_3O_7$. The oxygen atoms were found to occupy four sites and to form chains along the b axis direction of the orthorhombic Pmmm cell. The density of states shows a strong double peak at about 20 meV and a second

major maximum near 70 meV with additional less-intense features present at intermediate energies.

INTRODUCTION

The discovery of superconductivity above 90 K by Wu et al.[1] in a polyphase sample of composition $Y_{1.2}Ba_{0.8}CuO_x$ and the subsequent identification of the superconducting phase[2] has prompted intense efforts in determining the properties of this and analogous compounds in the Y-Ba-Cu-O phase diagram.

Neutron scattering can provide unique information about these materials due to its strong sensitivity to the oxygen scattering. As will be shown later, this is represented in both the static (structural) information and in the dynamics (phonons).

The materials discussed here were prepared at the Naval Research Laboratory from 99.9% purity starting materials of Y_2O_3, CuO, and $BaCO_3$ and were of nominal composition $YBa_2Cu_3O_x$. The powders were predried to remove adsorbed H_2O and then premixed carefully to break up agglomerates. The premixed powders were calcined at temperatures of 900 - 950°C for a period of six hours with hourly intermediate regrindings. The degree of chemical reaction was monitored by x-rays. The calcined powders were then ground and cold-pressed into pellets of 1-2 gm size and sintered for 12 hours at 937 °C. The samples were finally annealed under oxygen at 900 °C for three hours and then furnace cooled at 1° per minute to 300 °C before removal from the furnace. Individual pellets were characterized with x-ray diffraction and found to be identical.

The samples were examined for superconductivity by four probe resistance measurements and by dc susceptibility. The resistance data (see Fig. 1) showed the first deviation from a linear temperature dependence at temperatures in excess of 115 K. Between 115 K and 93 K the sample resistance drops by about 10% from a straight line extrapolation of the high T data. At 93 K the resistance drops sharply and the sample is fully superconducting at 91 K. The magnetic moment measured in a dc field of 100 gauss is shown in Fig. 2 and shows an onset of diamagnetic behavior at 92 K. The transition is complete around 30 K and corresponds to a flux expulsion of greater than 60%. Geometric considerations limit the precision of the flux expulsion fraction.

STRUCTURE OF THE COMPOUND

Unlike x-ray diffraction, neutron diffraction is strongly sensitive to the oxygen atoms and thus a rather precise determination can be made of both position and occupation of the oxygen sites in these compounds. The technique of total profile refinement was applied to the powder diffraction data taken on the five-detector powder instrument at the National Bureau of Standards Reactor. From this refinement it was determined that the compound has orthorhombic symmetry of space group Pmmm, and that the stoichometry of the compound was $YBa_2Cu_3O_{6.95}$ with an uncertainty of 0.01 in the oxygen composition. The lattice parameters (a_o = 3.8220 Å, b_o = 3.8855 Å, and c_o = 11.6797 Å) and atomic positions determined from the refinement were essentially identical to those found by Beech etal.[3] from a sample prepared by a similar procedure and having nearly identical superconducting properties. The structure of this compound is shown in Figure 3. The

essential features are that the copper atom Cu(1) is located at the center of a distorted rectangle formed by two O(4) atoms and two O(1) atoms. This forms oxygen chains along the b axis, alternated with Cu (1) atoms. This b-axis atom configuation is presumably responsible for the orthorhombic distortion versus the a axis direction which does not have the oxygen chains. The second Cu site Cu(2) is also surrounded by four oxygen atoms in sites O(2) and O(3) which are almost co-planar and form a tetrahedron with the O(1) site. The Cu(2) atom is slightly displaced from the oxygen plane. The O(1), O(2), and O(3) sites are fully occupied in this compound, while the O(4) site contains a small deficiency of 0.05 atom (total oxygen concentration is 6.95 atoms/formula unit).

It should be noted that the thermal factors refined from the neutron data are of comparable magnitude for the O(2) and O(3) sites ($2W \approx 0.6$), and is somewhat larger for the O(1) site ($2W \approx 0.92$) and anomalously large for the O(4) site ($2W \approx 2.02$). This suggests that considerable dynamic fluctuations may occur for atoms in the O(4) site of the b axis chain.

PHONON DENSITY OF STATES

The question of an electron-phonon driven superconducting transition in these compounds makes a determination of the vibrational modes important. Unfortunately due to the absence of large single crystals, a phonon dispersion measurement can not perfomed. Instead a measurement has been made of the wave vector (q) averaged vibrational density of states.

The vibrational density of states was obtained from the inelastic neutron scattering data using the incoherent approximation; that is we have

assumed that the dynamic coherent scattering function can be replaced by its incoherent counterpart[4,5]. Within this formalism, the scattering function is given by[6]

$$\frac{d^2\sigma}{d\Omega d\omega} \propto \frac{k'}{k} \frac{n(\omega)+1}{\omega} \left[\sum x_i I_i(\omega) g_i(\omega)\right] \qquad (1)$$

where $I_i(\omega)$ is defined by

$$I_i(\omega) = \frac{\sigma_i}{m_i} \langle (\vec{Q}\cdot\vec{\epsilon}_i)^2 e^{-2W_i} \rangle \ . \qquad (2)$$

Here k and k' are the magnitudes of the incident and final neutron wavevectors, $\vec{Q}$ is the scattering vector, $n(\omega)$ is the Bose occupation factor for a vibrational state of energy ω, and x_i, m_i, σ_i, and $\vec{\epsilon}_i$ are the atomic concentration, nuclear mass, total scattering cross section, and displacement vector of the ith atomic species respectively, W_i is the Debye-Waller factor, which was assummed to be negligble the sample temperatures in this study, and the brackets indicate that an average has been taken over all sites of type i and over all modes of energy ω. Finally, $g_i(\omega)$ represents the density of states for the ith constituent, which is defined by

$$g_i(\omega) = \sum_{\beta} \delta(\omega-\omega_{i,\beta}) \qquad (3)$$

where the sum is taken over all normal modes. Therefore the scattering does reflect the phonon density of states, however the contributions from the different species are weighted by the values of $I_i(\omega)$. From equation 2 one

sees that the important quantity in determining this weighting is the total scattering cross section divided by the mass. For O, Cu, Ba, and Y these values are 0.26, 0.12, 0.043, and 0.08 (barns/amu) respectively. It is then evident that our results will over-emphasize those modes in which the oxygen atoms play a predominant role.

The inelastic neutron scattering data were collected using a triple-axis instrument located at the NBS reactor. The low energy portion ($\omega \leq 25$ meV) of the density of states was obtained using the constant Q mode with a fixed final energy of 13.8 meV. Pyrolytic graphite ((002) reflection) was used for both the monochromator and analyzer and a graphite filter was placed in the scattered beam to remove harmonic contamination. The collimation was 40'-40'-40'-80' yielding a resolution of about 1-3 meV in the range of energy transfers probed with the triple-axis configuration. Data were taken at several values of the scattering vector between 3.3 and 5.0 $\AA^{-1}$ and then averaged in order to assure that the incoherent approximation was indeed satisfied.

This spectrometer is also equipped with a Be-graphite-Be filter analyzer assembly. In this case, the analyzer was fixed at a scattering angle of 90° allowing Q to vary as a function of energy. Data were collected between 20 and 40 meV with a graphite monochromator and collimation of 40'-20' yielding energy resolutions between 2 and 3 meV. At larger energy transfers (33 meV $\leq \omega \leq$ 130 meV), a Cu monochromator ((220) reflection) was used with a collimation of 60'-40' therby giving a resolution of 2-6 meV. No collimation was placed after the sample thus yielding some averaging over the scattering vector, despite the fact that data were collected at only one average scattering angle. In addition, the scattering vector was relatively large, thereby minimizing the effects due

to coherent scattering. Considering these factors and the results of previous neutron scattering studies concerning the density of states of coherent scatterers[6,7,8], we conclude that any effects due to coherent scattering will only be manifested in the relative intensities of the various features and that they will affect the relative intensities by at most 25%, or approximately the size of the error bars.

The contribution to the scattering from the fast neutron background was measured and subtracted directly. The scattering from the sample can was measured and found to be negligble. Multiphonon and multiple scattering corrections were obtained by extrapolation from energies where one phonon scattering is absent. The data were also corrected for all of the energy dependent factors given in equation 1. Then, using the overlapping energy regions as a guide, the density of states obtained in the three different energy ranges was scaled to obtain a single density of states.

The neutron weighted phonon density of states, $\bar{g}(\omega)$, of $YBaCu_3O_7$ at 120 K is shown in figure 4. Below 9 meV $\bar{g}(\omega)$ displays the typical ω^2 dependence characteristic of three dimensional systems. At an energy of about 12 meV, there is a small peak most probably due to a zone boundary interlayer shear mode. The density of states then further increases, reaching a large maximum at 19-20 meV, after which it falls to shoulder at roughly 25 meV before dropping precipitously to a minimum at 28-30 meV. There is then a broad feature centered at about 34 meV where the data displays a great deal of scatter which made the scaling difficult introducing some uncertainty in the relative heights of the low and high energy portions of the density of states. Close inspection of this region shows that there is more than one point at several of the energies. These points correspond to data taken in different data collection modes and indicate that the scaling which we have

chosen is certainly reasonable. At an energy of 44 meV, the data displays another small maximum which is somewhat narrower than the feature at 34 meV. Then above 50 meV $\bar{g}(\omega)$ increases, diplaying a shoulder at about 60 meV and then a peak at 70 meV before dropping to zero at about 90 meV. The data which is omitted around 53 meV corresponds to a region of anomalous transmission of the filter analyzer making it impossible to determine the density of states for these points. We also note that the high energy modes certainly involve the O atoms therby increasing their relative weight in the scattering. Thus the rather unusual relative height of the low energy and the high energy density of states peaks is probably due to the the degree of O atom participation in the modes in these energy regions.

We have also measured the density of states in the superconducting state at at a temperature of 12 K. The only difference which we were able to clearly discern was a slight shift (roughly $\frac{1}{2}$ - 1 meV) in the energy range of 10-20 meV which can be accounted for by rather typical anharmonic effects. All other differences were so slight that they may easily have been due to slight differences in the corrections applied to the data.

ACKNOWLEDGEMENTS

The authors have benefitted extensively from discussions with J. J. Rush on the density of states measurements and with A. Santoro, and S. Miraglia on the structure determination and also appreciate their help in the crystal structure refinement and the use of their results prior to publication.

REFERENCES

1. M. K. Wu, J. R. Ashburn, C. J. Torng, P. H. Hor, R. L. Meng, L. Gao, Z. J. Huang, Y. Q. Wang, and C. W. Chu, Phys. Rev. Lett. 58, 908 (1987).
2. R. J. Cava, B. Batlogg, R. B. van Dover, D. W. Murphy, S. Sunshine, T. Siegrist, J. P. Remeika, E. A. Rietman, S. Zuhurah, and G. P. Espinosa, (to be published).
3. F. Beech, S. Miraglia, A. Santoro, and R. S. Roth (to be published).
4. M. M. Bredov, B. A. Kotov, N. M. Okuneva, V. S. Oskotskii, and A. L. Shakh-Bugadov, Sov. Phys. Solid State 9, 214 (1967).
5. V. S. Oskotskii, Sov. Phys. Solid State 9, 420 (1967).
6. N. Lustig, J. S. Lannin, J. M. Carpenter, and R. Hasegawa, Phys. Rev. B 32, 2778 (1985).
7. N. Maley, J. S. Lannin, and D. L. Price, Phys. Rev. Lett. 56, 1720 (1986).
8. P. F. Miceli, S. E. Youngquist, D. A. Neumann, H. Zabel, J. J. Rush, and J. M. Rowe, Phys. Rev. B 34, 8977 (1986).

FIGURE CAPTIONS

Figure 1. Temperature dependence of the resistance of a sample of $YBa_2Cu_3O_{6.95}$ showing that the sample is fully superconducting at 91 K.

Figure 2. Temperature variation of the magnetization in an applied field of 100 gauss. The Meissner effect is complete around 30 K.

Figure 3. Structure of the compound as determined from neutron diffraction showing location of the four O sites, 2 Cu sites and single Ba and Y sites (from Ref. 3).

Figure 4. Vibrational density of states as measured with inelastic neutron scattering. The largest spectral weight is contained in peaks involving oxygen vibrations (see text).

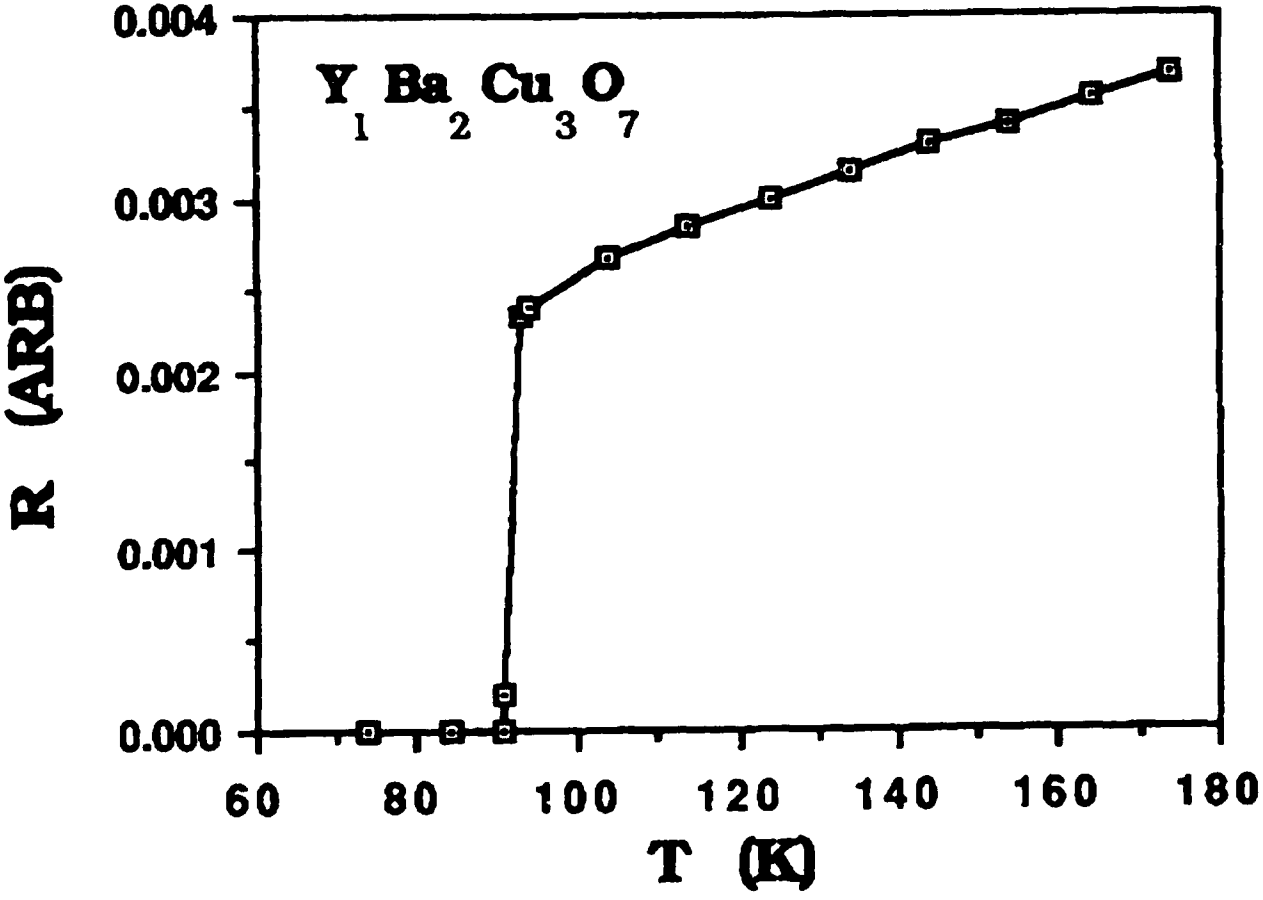
Y Ba Cu O
1 2 3 7
0.004
0.003
0.002
0.001
0.000
R (ARB)
60
80
100
120
140
160
180
T (K)

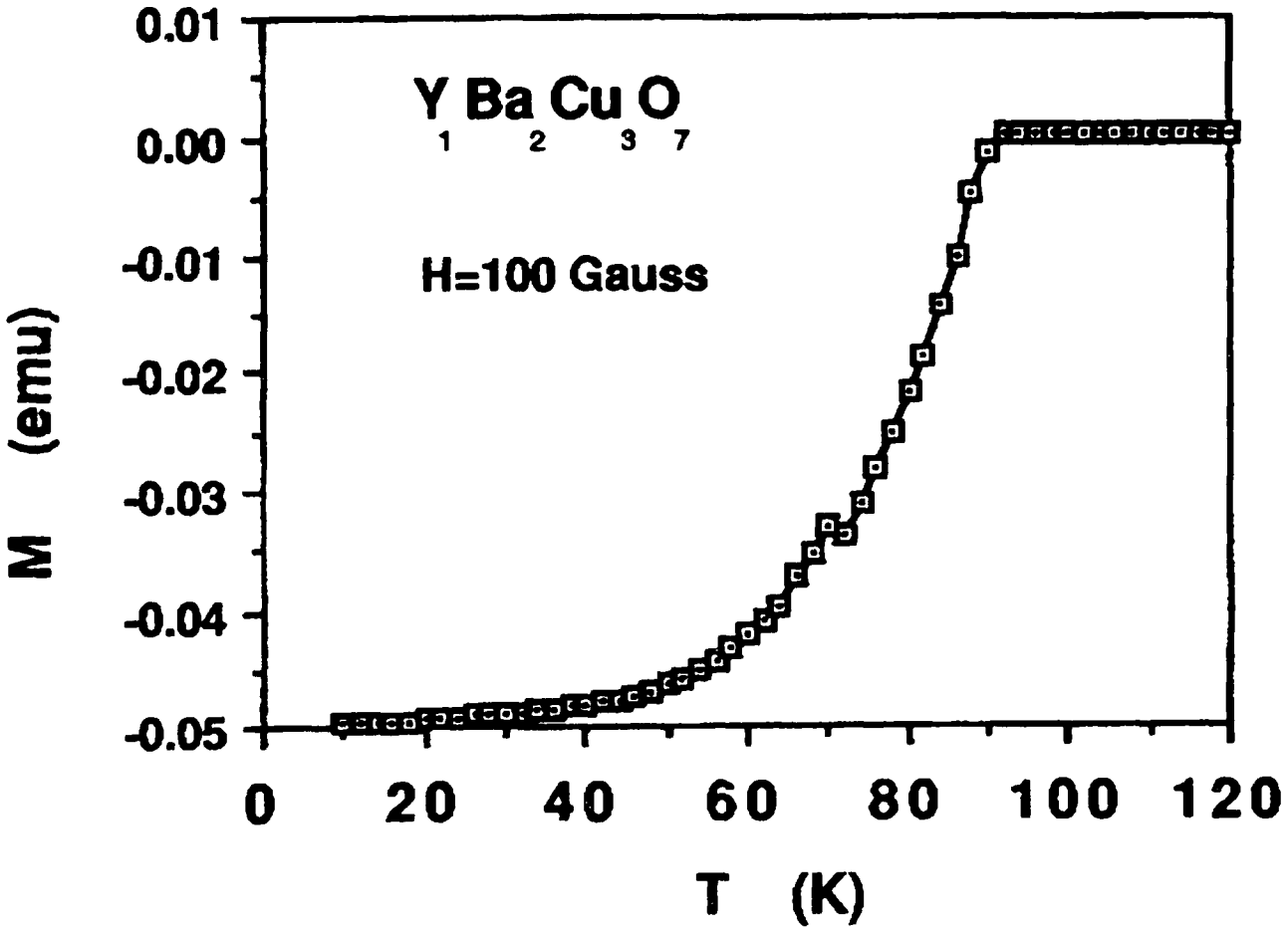
Y Ba Cu O
1 2 3 7
H=100 Gauss
M (emu)
0.01
0.00
-0.01
-0.02
-0.03
-0.04
-0.05
0
20
40
60
80
100
120
T (K)

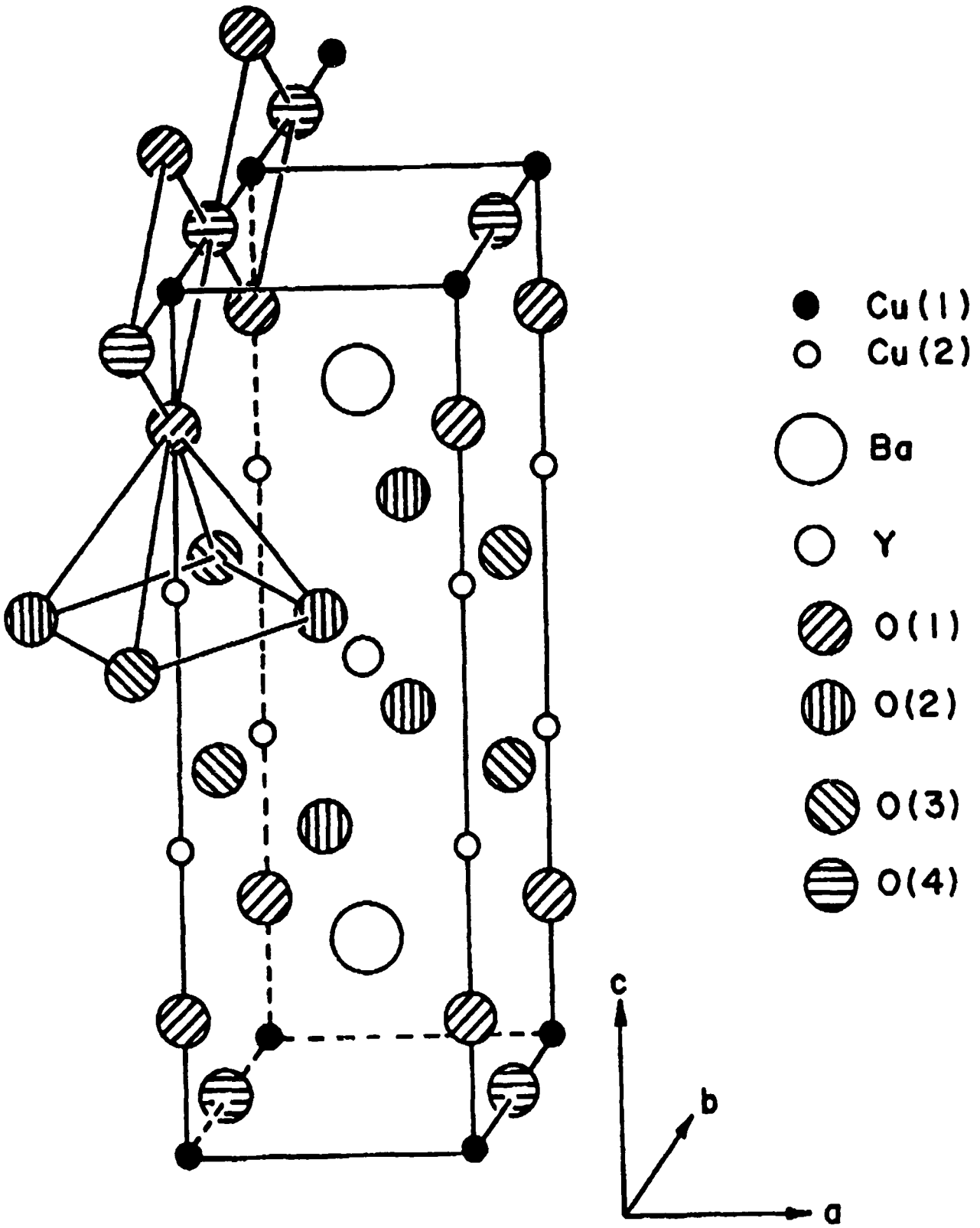
Cu(1)
Cu(2)
Ba
Y
O(1)
O(2)
O(3)
O(4)
c
b
a

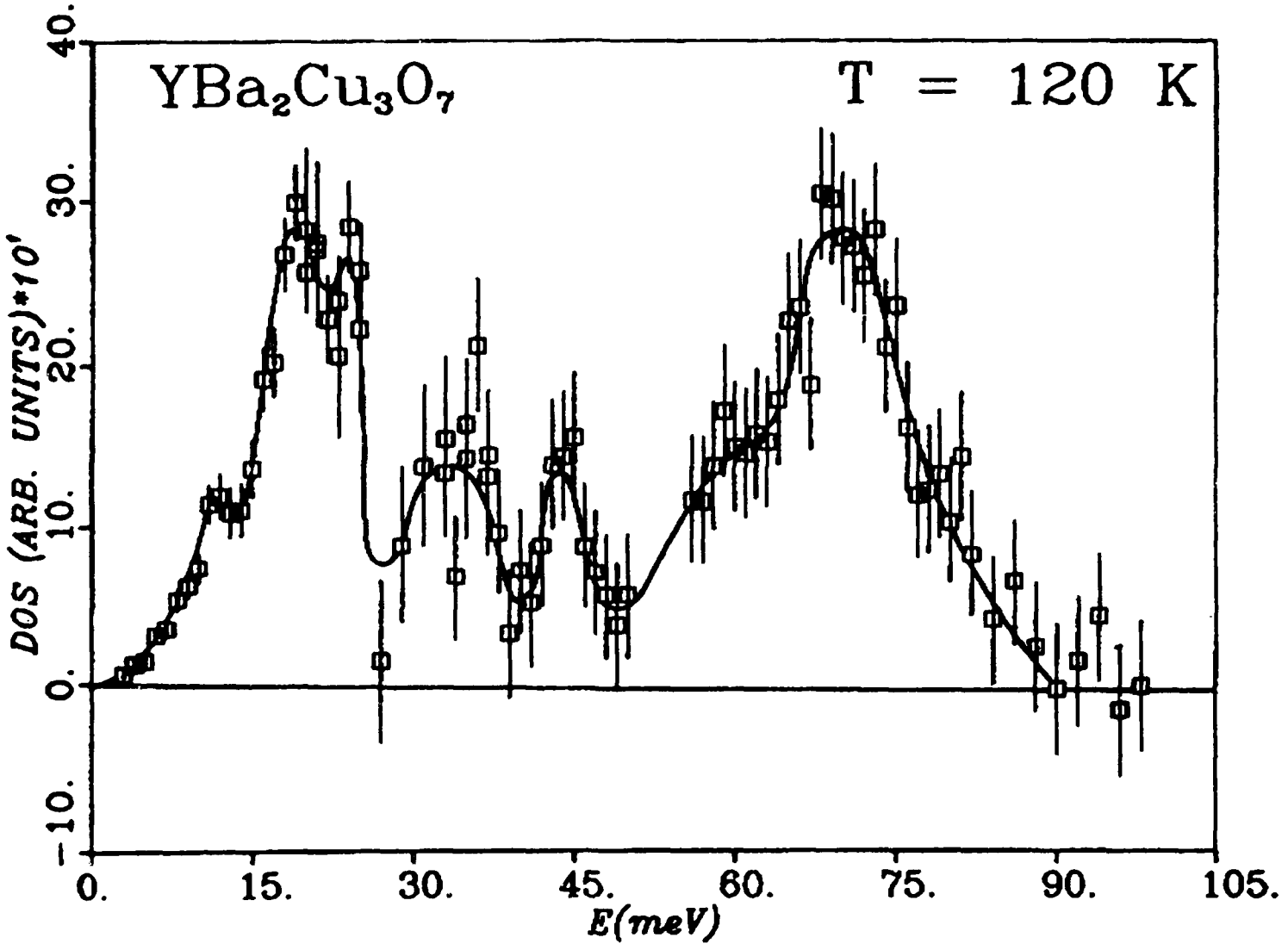
YBa2Cu3O7
T = 120 K
DOS (ARB. UNITS)*10'
40.
30.
20.
10.
0.
-10.
0.
15.
30.
45.
60.
75.
90.
105.
E(meV)

AD-A189 137 COMPILATION OF NRL PUBLICATIONS ON HIGH TEMPERATURE SUPERCONDUCTIVITY(U) NAVAL RESEARCH LAB WASHINGTON DC D U GUBSER 1987 2/3

UNCLASSIFIED F/G 20/3 NL

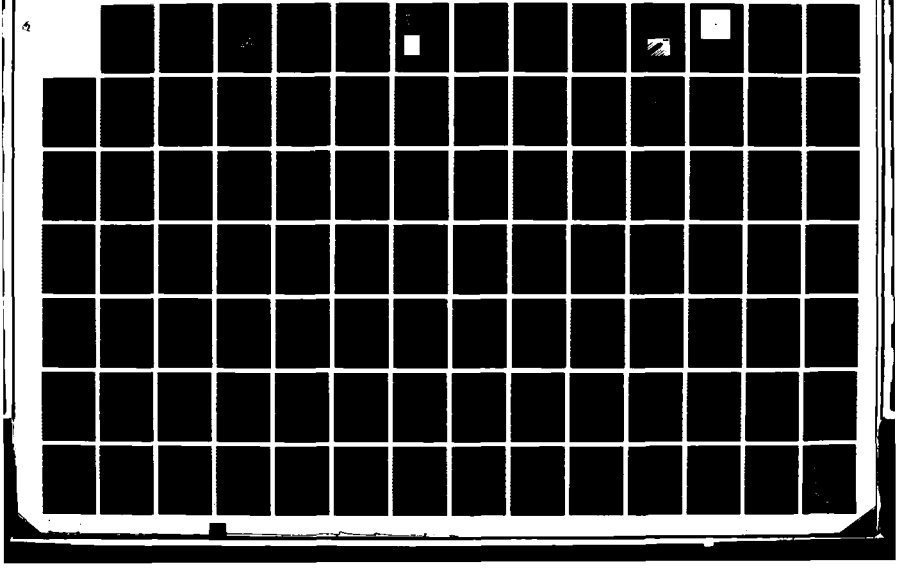

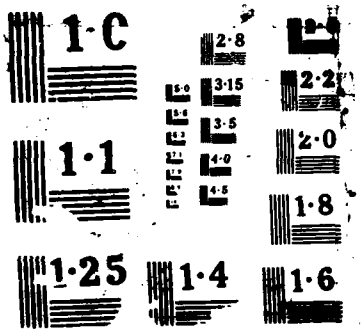
1·C
1·1
1·25
1·4
1·6
2·8
3·15
3·5
2·2
2·0
1·8

EXPERIMENTAL PROGRAM ON HIGH T_c OXIDE SUPERCONDUCTORS AT THE NAVAL RESEARCH LABORATORY

M. OSOFSKY*, L.E. TOTH**, S. LAWRENCE†, S.B. QADRI††, A. SHIH, D. MUELLER***, R.A. HEIN, W.W. FULLER, F.J. RACHFORD, E.F. SKELTON, T. ELAM, D.U. GUBSER, AND S.A. WOLF
Naval Research Laboratory, Washington, DC 20375-5000
J.A. GOTAAS, J.J. RHYNE, R. KURTZ, AND R. STOCKBAUER
National Bureau of Standards, Gaithersburg, MD 20899

ABSTRACT

Since the middle of December 1987, the Naval Research Laboratory (and its collaborators) has had a program to study the very exciting new class of very high superconducting transition temperature copper oxides based on the perovskite structure. We have attempted to assemble a synergistic combination of physicists, ceramists, chemists, and metallurgists in order to synthesize, and characterize these materials as well as to begin the process of evaluating them for specific applications of interest both to the DoD and the more general community. We have studied both the 40K superconductors based on the K_2NiF_4 structure consisting of $La_{2-x}M_xCuO_4$ where M=Ba, Sr and Ca and the 95K superconductor based on the $YBa_2Cu_3O_7$ structure.

The bulk samples were prepared using conventional powder ceramic processing technique from powders of the metallic oxides or carbonates and calcined in air at temperatures ranging from 850-1000 C. The samples were cold pressed into pellets and sintered in air and annealed in oxygen.

Film samples are being prepared by sputtering, electron beam evaporation and chemical vapor deposition.

The samples were characterized electrically by a large number of techniques including resistance, dc and ac susceptibility, magnetoresistance and microwave impedance. The structure and microstructure were studied by electron and neutron diffraction, scanning electron microscopy, transmission electron microscopy, electron microprobe, x-ray and ultraviolet photoemission spectroscopy and electron spin resonance.

Highlights of the more significant result of our program are discussed below.

Structure and Microstructure

X-ray diffraction studies in the Y-Ba-Cu-O system enabled us to isolate and identify the phase responsible for superconductivity and to locate the sites for all the atoms in the structure as well as the space group. A neutron diffraction study completely determined the precise atomic positions and occupancy of all the sites in the unit cell. We associated the superconductivity with Cu-O chains in the Cu-O plane between the Ba ions. By correlating the orthorhombic to tetragonal conversion in the structure as the oxygen order or occupancy was changed. Microstructural work showed that the fully stoiciometric compound was strongly twinned and orthorhombic whereas the tetragonal phase of the structure forms well developed elongated crystallites that are not at all twinned.

*ONT Post Doc
**On Sabbatical Leave from NSF
***NRC Post Doc
†Crystal Growth & Mater. Test. Assoc.
††Sachs/Freeman Assoc.

Electrical Measurements

The superconducting transition was determined by a combination of four lead resistivity and ac and dc susceptibility measurements. The critical magnetic fields and critical currents were determined by a combination of SQUID magnetization measurements to 9T and magnetoresistance measurements to 13T. The best 40K material had an extrapolated upper critical field of about 90T and a low field critical current density well in excess of 1000 A/cm^2 at 4K. The 90K superconductor had an extrapolated critical field in excess of 200T. The ac susceptibility showed a peak in the loss component only below 70 Hz indicating that the material was a very good superconductor with a resistivity of approximately 200$\mu\Omega$-cm. The microwave surface impedance measurements showed that the bulk samples had a sharp onset at 10Ghz with a very large penetration of the fields.

Inelastic Neutron Scattering

The phonon density of states was measured in both the 40K and the 90K superconductors. The most significant results on $La_{1.8}Sr_{.2}CuO_4$ were that there was a very sharp peak at 2.5 meV and a very large peak at 10 meV in addition to a number of peaks at higher energy. Neutron diffraction on this sample at 10K clearly showed that this sample had an orthorhombic distortion of about 0.2%. Results on $YBa_2Cu_3O_7$ are shown in Fig. 1.

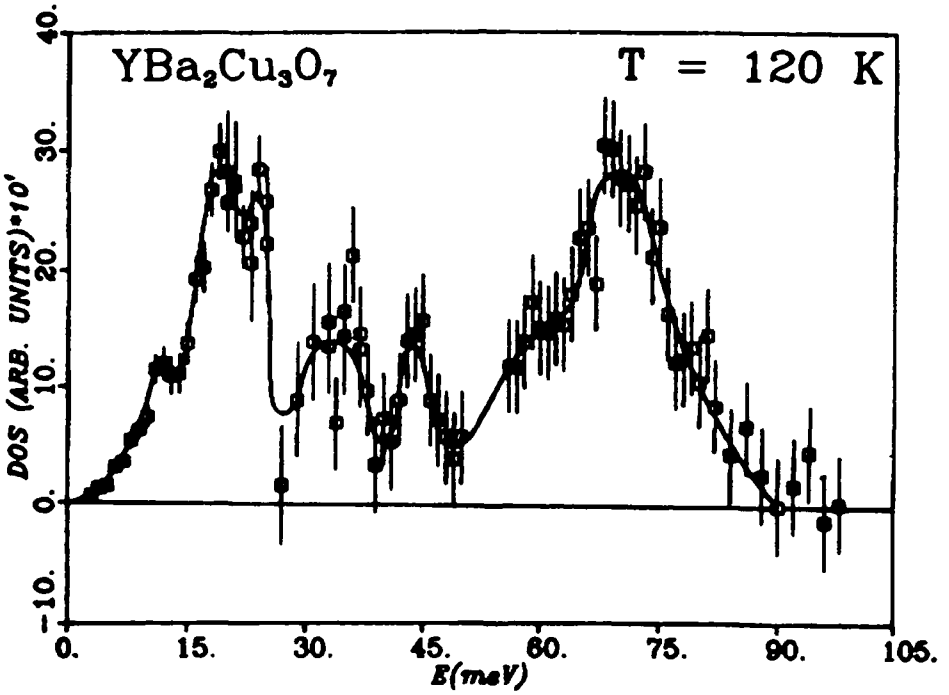

Fig. 1. Vibrational Density of states as measured with inelastic neutron scattering

Ultraviolet Photoemission Spectroscopy

These measurements represent the first experimental investigation of the electronic structure of $YBa_2Cu_3O_7$. Resonant photoemission was used to assist in determining the chemical origin of the various features in the electronic structure. No sharp Fermi edge was observed and the density of states at the Fermi level is relatively small. The binding energies and widths of the various peaks are as follows:

Level	Energy	FWHM
Cu3d/O2p	2.3	2.0
Cu3d/O2D	4.5	3.0
Y/Cu satellite	9.4	1.9
Cu satellite	12.4	2.5
Ba 5p	15.0	2.9
O 2S	20.1	3.3
Y 4P	24.0	3.1
Ba 5S	28.8	3.6

Spectra was taken at room temperature as well as just above and below the transition temperature. No change in the valence band electronic structure was observed within this temperature range.

HIGH TEMPERATURE SUPERCONDUCTORS

by

D.U. Gubser, S.A. Wolf, M.S. Osofsky,
B.A. Bender, S.H. Lawrence,
E.F. Skelton, and S.B. Qadri
Naval Research Laboratory
Washington, DC 20375-5000

High temperature superconducting materials have recently been found in a class of metallic oxide ceramics[1]. Superconducting transition temperatures T_c as high as 95K has been observed in $M_1 Ba_{0.2} Cu_3 O_7$ samples where M is Y or any of the 4f rare earth metals except Ce and Pr[2,3]. Superconductivity has also been observed in $La_{1.8} M_{0.2} Cu_1 O_4$ where M is Ba, Sr, or Ca with T_c up to 40K[4]. These materials form oxygen defect, perovskite crystal structures with some unusual features.

The crystal structures of these ceramic superconductors is shown in figure 1. The notable feature on the $La_{1.8} Sr_{0.2} Cu_1 O_4$ system is the Cu - O planes perpendicular to the c axis. These planes have two dimensional nature as evidenced both from the arrangement of the atoms and detailed electronic band structure calculations. The $Y_1 Ba_2 Cu_3 O_7$ compound has a different atomic structure with two prominent features[5]. The first feature is that the Cu atoms have two nonequivalent sites, one having a 5 fold coordination number, while the other has a 4 fold planar coordination number. The Cu - O bonding with four fold coordination form linear chains, or ribbons along the b axis which leads to a slight orthorhombic elongation along this axis. Enhanced superconductivity has been correlated with the integrity of these Cu - O chains.

These ceramic superconductors are easily prepared by mixing CuO, BaCO, and Y O together in the proper ratio and calcining for several hours at temperatures near 950K. The resultant powders and then ground and pressed into pellets for sintering at 900K followed by lower temperature oxygen anneals to obtain the proper oxygen stoichiometry. Figure 2 shows the microstructure of a $Y_1 Ba_2 Cu_3 O_7$ sample which has been prepared in the above manner. Polycrystalline samples with a large number of twinning plane defects are evident in the photograph. These twinning planes are easily formed in the high T_c orthorhombic material because and oxygen defect can easily disrupt the 1-dimension Cu O chains and start growth of the chains in another direction[6]. By quenching the material from high temperatures a metastable tetragonal structure can be formed. These materials have the oxygen atoms in the 4 fold coordination site randomly occupying the a and b directional sites, show little evidence of twinning plane faults, and have degraded superconducting temperatures

The superconducting transition temperature of the $Y_1 Ba_2 Cu_3 O_7$ material is shown in figure 3. It has a sharp transition to the superconducting state at 92K with a precursor to the transition beginning over 100K. The corresponding dc magnetic transition is shown in figure 4. This transition has an onset of 90K and is broader than the resistive transition, presumeably do to the granualarity of the sample itself. The total change in magnetic moment represents a 90 - 10 % total flux expulsion from the sample.

In addition to the resistance and magnetic transitions, we have measured the magnetization curves as a function of temperature, critical magnetic fields, critical currents, and microwave losses. We have made careful X-ray structure measurements as a function of temperture to determine the temperature dependent structure variations. Thin film materials have also been made and their superconducting properties will be reported. In addition we have measured the phonon spectra in a collaborative effort with the National Bureau of Standards. These and other properties will be discussed in the talk.[7]

References

1. J. G. Bednorz and K.A. Mueller, Z Phys. B64, 189 (1986)

2. M.K. Wu, J.R. Ashburn, C.J. Torng, P.H. Hor, R.L. Meng, L. Gao, Z.J. Huang, Y.Q. Wang, and C.W. Chu, Phys. Rev. Lett. 58, 908 (1987)

3. E. M. Engler, V.Y. Lee, A.I. Nazzal, R.B. Beyers, G. Lim, P.M. Grant, S.S.P. Parkin, M.L. Ramirez, J.E. Vazquez and R.J. Savoy, submitted J. Amer. Chem Soc.

4. D.U. Gubser, R A. Hein, S.H. Lawrence, M.S. Osofsky, D.J. Schrodt, L.E. Toth, and S.A. Wolf, Phys. Rev B (1987)

5. F. Beech, S. Miraglia, A Santoro, and R.S. Roth to be published and J. Rhyne to be published

6. L. E. Toth, E.F. Skelton, S.A. Wolf, S.B. Qadri, M.S. Osofsky, B.A. Bender, S.H. Lawrence, and D.U. Gubser to be published

7. For a good review of the subject, see the proceedings of the MRS meeting, Spring 1987 edited by D. Gubser and M. Schluter.

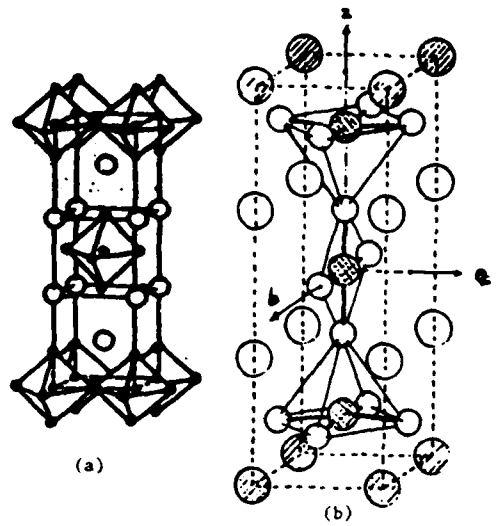

Figure 1. Crystal structure unit cells the the $La_{1.8}Sr_{0.2}Cu_1O_4$ superconductor (a) and the $Y_1Ba_2Cu_3O_7$ superconductor (b).

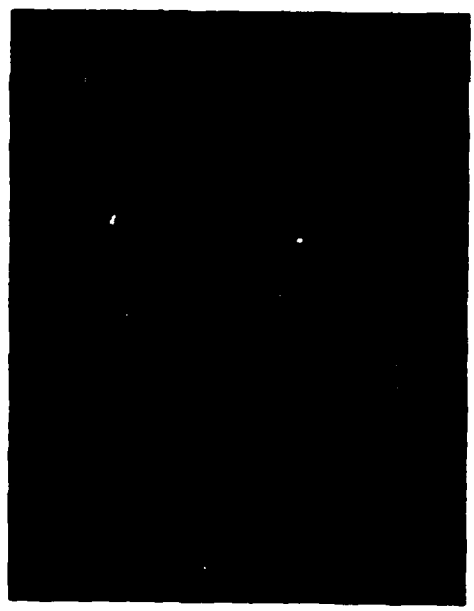

Figure 2. Photomicrograph of the $Y_1Ba_2Cu_3O_7$ ceramic sample.

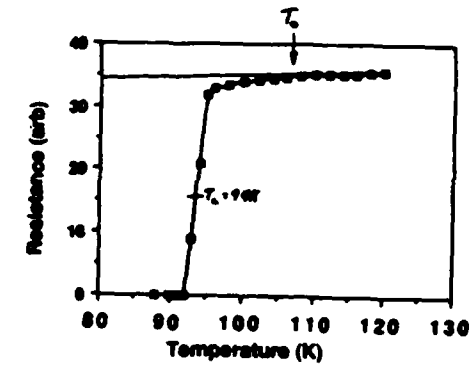

Figure 3. Resistive transition of the $Y_1Ba_2Cu_3O_7$ superconductor

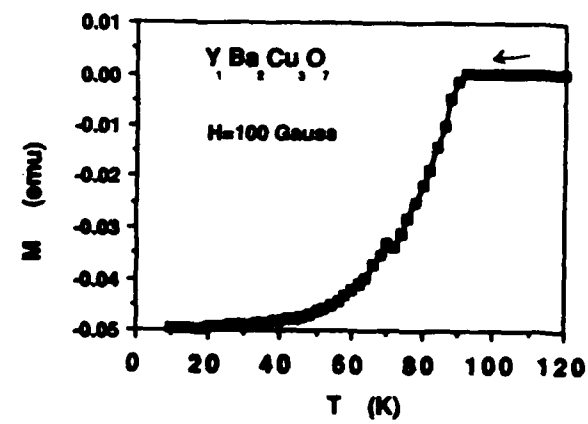

Figure 4. DC magnetic transition of the $Y_1Ba_2Cu_3O_7$ superconductor

Magnetic Field Studies of the $La_{2-x}M_xCuO_4$ and $Ba_2Y_1Cu_3O_7$ High T_c Superconductors

W.W. FULLER, M.S. OSOFSKY*, L.E. TOTH**, S.B. QADRI, S.H. LAWRENCE, R.A. HEIN, D.U. GUBSER
T.L. FRANCAVILLA, and S.A. WOLF

Naval Research Laboratory, Washington, DC 20375-5000, USA

We have prepared and characterized high T_c single phase samples of $La_{2-x}M_xCuO_4$ (where M = Sr, Ba, or Ca and x = 0.1, 0.2, or 0.3) and $Ba_2Y_1Cu_3O_7$. We report on the dc susceptibility, magnetization, and magnetoresistance. We have extracted many of the critical superconducting and normal state parameters from the data.

1. INTRODUCTION

Superconductivity in La-Ba-Cu-O at 30 K was reported by Bednorz and Muller [1] Since then other compounds with a transition temperature, T_c, near 40 K have been reported [2], [3]. In the Y-Ba-Cu-O compound a T_c above 90 K was reported by Wu et al. [4]. We have prepared a variety of these materials, $La_{2-x}M_xCuO_4$ (M = Sr, Ba, and Ca) and $Ba_2Y_1Cu_3O_7$, to undertake magnetic field studies of these new high T_c superconductors.

2. EXPERIMENTAL TECHNIQUES AND RESULTS

The $La_{1.8}Sr_{0.2}CuO_4$, $La_{1.9}Ba_{0.1}CuO_4$, and $La_{1.7}Ca_{0.3}CuO_4$ samples were prepared as described in an earlier paper [5]. This procedure produced nearly single phase samples with the K_2NiF_4 structure as determined by x-ray diffraction. The $Ba_2Y_1Cu_3O_7$ samples were prepared under processing conditions which produced an orthorhombic structure (as determined by neutron and x-ray diffraction) with two one-dimensional Cu-O-Cu chains on the basal plane of the unit cell [6].

The samples were first cooled in a SQUID susceptometer in a small (typically 100 G) magnetic field. The magnetization data (see Table I) for the $La_{2-x}M_xCuO_4$ (M = Ba and Ca) showed diamagnetic onsets at 20 K and 31 K with 10% and 20% flux expulsion at 10 K (the lowest temperature measured) respectively. The curves were not flat at 10 K indicating that the samples were still expelling flux. The presence of these broad transitions with small flux expulsion along with the x-ray data indicating nearly single phase materials is a manifestation of the oxygen's importance in the superconductivity (x-rays do not couple strongly to oxygen). The M = Sr sample had an onset at 36 K with 40% flux expulsion at 10 K and the $Ba_2Y_1Cu_3O_7$ sample showed the onset at 93 K with 90 - 100% flux expulsion by 40 K.

The samples were next warmed above their transition temperatures, cooled in zero field and magnetization, M, versus field, H, measurements were made with fields up to 80 kG. All of the samples have hysteretic M vs. H curves characteristic of type II superconductors with flux pinning centers. The lower critical fields, H_{c1}, for the $La_{2-x}M_xCuO_7$ materials are 100 - 300 G at 10 K, Table I. The critical currents, estimated from the hysteresis in the M vs. H curve [7], are rather low at 10 K. A series of measurements on $La_{1.8}Sr_{0.2}CuO_4$ at several temperatures shows a critical current of 4000 A/cm^2 at 4.2 K which degrades dramatically at higher temperatures.

The 4.2 K magnetization data for the BaYCuO sample was highly hysteretic, Fig. 1. The lower critical field was -2.5 kG (see insert on Fig. 1) and the critical current was 10^5 A/cm^2 consistent with the results reported by IBM [8].

The upper critical fields for these materials were measured by monitoring the samples' 4-probe resistance as the temperature was swept in a constant magnetic field. The magnetoresistance of the carbon glass thermometer was taken into account in determining the temperature. The critical temperature in a given field was taken as that temperature where the sample resistance was 50% of the normal value.

The magnetic field significantly broadened the transition for the lower T_c materials. This is perhaps due to inhomogeneities in these samples. A field of 100 kG has a negligable effect on the onset temperature.

In Fig. 2 the critical field is plotted as a function of temperature for the $La_{1.8}Sr_{0.2}CuO_4$ and $Ba_2Y_1Cu_3O_7$ samples. From the slope, $dH_{c2}/dT|_{T_c}$, one is able to calculate a variety of the material parameters [9]. Table I presents the results of these calculations. The ranges given represent the uncertainty in determining $dH_{c2}/dT|_{T_c}$ For the $La_{2-x}M_xCuO_4$ samples the H_{c1} obtained from $dH_{c2}/dT|_{T_c}$ and the resistivity, ρ, agree within a factor of two with the value obtained from the magnetization data. However, in $Ba_2Y_1Cu_3O_7$ the agreement is only to within a factor of three. This is not too surprizing since the calculations assume an isotropic, 3D Fermi surface. These materials are known to be anisotropic, with the superconductivity believed to be 2D for $La_{2-x}M_xCuO_4$ and 1D for $Ba_2Y_1Cu_3O_7$ [6].

Our value for γ, the density of states at the Fermi level, is in the range 2500 - 4030 (ergs/cc -K^2) for $Ba_2Y_1Cu_3O_7$. This is to be compared with 2150 (ergs/cc - K^2) as obtained from the jump in the specific heat [10]. The agreement is quite

---

* Office of Naval Technology postdoctoral fellow
** On sabbatical leave from the National Science Foundation, Washington, DC, USA

good considering the imprecision in determining $dH_{c2}/dT|_{T_c}$ and ρ for this material.

3. CONCLUSION

We have performed a variety of magnetic field measurements on the new superconductors. The $La_{2-x}M_xCuO_4$ (M = Ba, Sr, Ca) materials show incomplete flux expulsion and very broad transitions, both magnetic and resistive, in magnetic fields. The samples of $Ba_2Y_1Cu_3O_7$ show negligible broadening of the transition at 130 kG. This result, along with processing [6] and neutron studies, shows that good superconducting behavior strongly depends upon the Cu-O-Cu chains in the basal plane of the structure. The lower dimensional nature of the superconductivity in these materials manifests itself in the descrepency between H_{c1} calculated from $dH_{c2}/dT|_{T_c}$ and that measured by the magnetization. The fact that the descrepency is less for the La samples than for the Y samples could be related to the 2D behavior of the former and the 1D behavior for the latter.

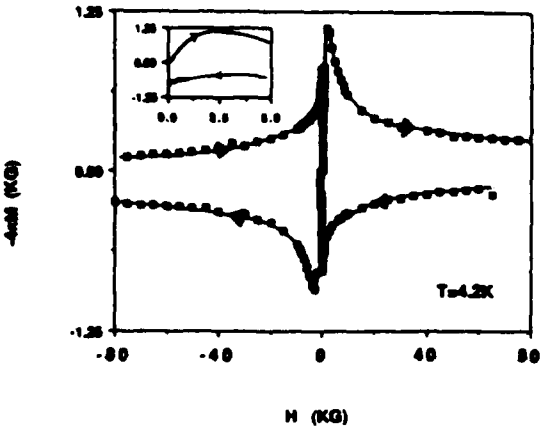

Fig. 1. Magnetization versus magnetic field hysteresis loop of $Ba_2Y_1Cu_3O_7$ at 4.2 K. The sample was cooled in zero field. The lower critical field, H_{c1}, is 2.5 kG (inset).

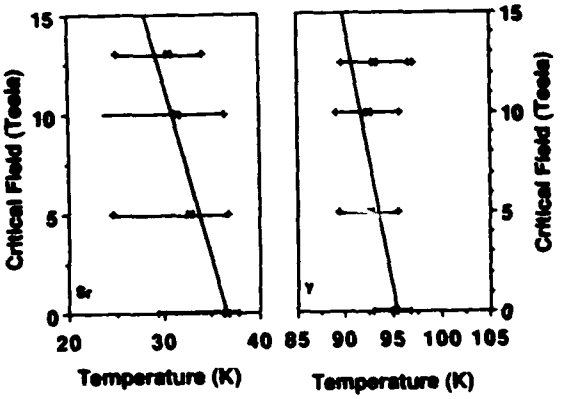

Fig. 2. The upper critical field as a function of temperature for $La_{1.8}Sr_{0.2}CuO_4$ (left) and $Ba_2Y_1Cu_3O_7$ (right). The extent of the 10% - 90% points of the transitions are shown. The lines through the data points are guides to the eye.

REFERENCES

1) J.G. Bednorz and K.A. Muller: Z. Phys. B64(1986) 189.
2) R.J. Cava, R.B. van Dover, B. Battlogg, and E.A. Reitman: Phys. Rev. Lett. 58(1987) 408.
3) K. Kishio, K. Kitazawa, S. Kanbe, I. Yamada, N. Sugii: Jpn. J. Appl. Phys. (to be published).
4) M.K. Wu, J.R. Ashburn, C.J.Torng, P.H. Hor, R.L. Meng, L. Gao, Z.J. Huang, Y.O. Wang, and C.W. Chu: Phys. Rev. Lett. 58(1987) 908.
5) D.U. Gubser, R.A. Hein, S.H. Lawrence, M.S. Osofsky, D.J. Schrodt, L.E. Toth, and S.A. Wolf: Phys. Rev. B35(1987) 5350.
6) L.E.Toth, E.F. Skelton, S.A. Wolf, S.B. Qadri, M.S. Osofsky, B.A. Bender, S.H. Lawrence, and D.U. Gubser: (submitted to Phys. Rev B)
7) W.A. Fietz and W.W. Webb: Phys. Rev. 178(1969) 657.
8) private communication
9) T.P. Orlando, E.J. McNiff, Jr., S. Foner, and M.R. Beasley: Phys. Rev 19(1979) 4545.
10) A. Junod, A. Bezinge, T. Graf, J.L. Jorda, J. Muller, L. Antognazza, D. Cattani, J. Cors, M. Decroux, O. Fischer, M. Banovski, P. Genoud, L. Hoffmann, A.A. Manuel, M. Peter, E. Walker, M. Francois, and K. Yvon: (submitted Europhysics Lett.)

Table I. Parameters calculated from the data

Material	ρ ($\mu\Omega$ - cm)	T_c(50%) (K)	$dH_c/dT\|_{T_c}$ (kG/K)	$H_{c2}(0)$ (kG)	ξ_{GL} (Å)	γ (ergs/cc - K^2)	κ_{GL}	$H_{c1}(0)$ kG calculated	H_{c1}:T kG:T measured	J_c(4K) A/cm^2
$Sr_{0.2}$	350	34	-13 - -40	330 - 930	19 - 31	840 - 2500	76 - 132	0.180 - 0.190	0.35:4.2	4000
$Ba_{0.1}$	350	27	-9.6 - -15.6	190 - 280	34 - 42	600 - 1000	65 - 83	0.134 - 0.136	0.2:10	-
$Ca_{0.3}$	350	15	-22 - -26	230 - 270	35 - 38	1370 - 1630	97 - 106	0.079 - 0.081	0.1:10	-
Y	200	95	-22 - -36	1470 - 2370	12 - 15	2500 - 4030	75 - 95	0.820 - 0.870	~2.5:4.2	10^5

Preparation, Structure, and Magnetic Field Studies of High T_c Superconductors.

M.S. Osofsky*, W.W. Fuller, L.E. Toth**, S.B. Qadri+, S.H. Lawrence++, R.A. Hein+++, D.U. Gubser, S.A. Wolf, C.S. Pande, A.K. Singh++, E.F. Skelton and B.A. Bender

Naval Research Laboratory, Washington, DC 20375-5000

We have prepared and characterized high T_c single phase samples of $La_{2-x}M_xCuO_4$ (where M=Sr, Ba, and Ca and x=0.1, 0.2 or 0.3) and $Ba_2YCu_3O_7$. Transmission electron microscopy of the $Ba_2YCu_3O_7$ samples reveals twinning defects in the [110] direction which disappear when the sample is heated above 400°C. We report on the dc susceptibility, magnetization, and magnetoresistance. We have extracted many of the critical superconducting and normal state parameters from the data.

INTRODUCTION

Superconductivity in La-Ba-Cu-O at 30°K was reported by Bednorz and Muller [1] Since then other compounds with a transition temperature, T_c, near 40°K have been reported [2], [3]. In the Y-Ba-Cu-O compound a T_c above 90°K was reported by Wu et al. [4]. We have prepared $La_{2-x}M_xCuO_4$ (M = Sr, Ba, and Ca) and $Ba_2Y_1Cu_3O_7$, for magnetic field studies of their superconducting transitions.

SAMPLE PREPARATION AND CHARACTERIZATION

The $La_{1.8}Sr_{0.2}CuO_4$, $La_{1.9}Ba_{0.1}CuO_4$, and $La_{1.7}Ca_{0.3}CuO_4$ samples were prepared as described in an earlier paper [5]. This procedure produced nearly single phase samples with the K_2NiF_4 structure as determined by x-ray diffraction.

The $Ba_2Y_1Cu_3O_7$ samples were prepared under processing conditions which produced an orthorhombic structure (as determined by neutron and x-ray diffraction) with two one-dimensional Cu-O-Cu chains on the basal plane of the unit cell [6]. The procedures were: (a) Premix powders of $BaCO_3$, CuO

and Y_2O_3. (b) immerse mixture in alchohol and pulverize loose agglomerates in an ultrasonic mixer, (c) calcine for 6 hours at 925-950°C with intermediary grindings, (d) grind and cold press into pellets and sinter in air at 925-950°C for 12 hours, and (e) move into an oxygen furnace , heat to 950C for several hours and slow cool (1°/min). Alternatively, step (e) could be equilibrate in oxygen, reduce the temperature to 500-700°C, hold for several hours and cool at a moderately slow rate.

Samples made with these procedures consist of 10-20 micron single phase grains surrounded by trace amounts of amorphous Y-Ba-Cu-O compounds. Extensive transmission electron microscopy of the individual grains reveal parallel 'domains' with an average width of 2000Å (Figure 1). Electron diffraction shows that the boundaries between these regions are in the [110] direction. The electron diffraction pattern (Figure 2) shows the splitting of spots along only one diagonal with increasing separation in higher order reflections. This can be explained by twinning on the [110] plane in the orthorhombic crystals confirming earlier work [7]. In situ heating and cooling experiments showed no changes in the diffraction pattern down to liquid nitrogen temperatures. The domains disappeared when the specimen was heated above 400°C. Many of the domains reappeared when the sample was re-cooled. This behavior is consistent with the many reports of a tetragonal to orthorhombic transformation above 400°C in these materials.

Fig. 1. Transmission Electron Micrograph of a region of a grain of $Ba_2YCu_3O_7$. The parallel domains average 2000Å in width.

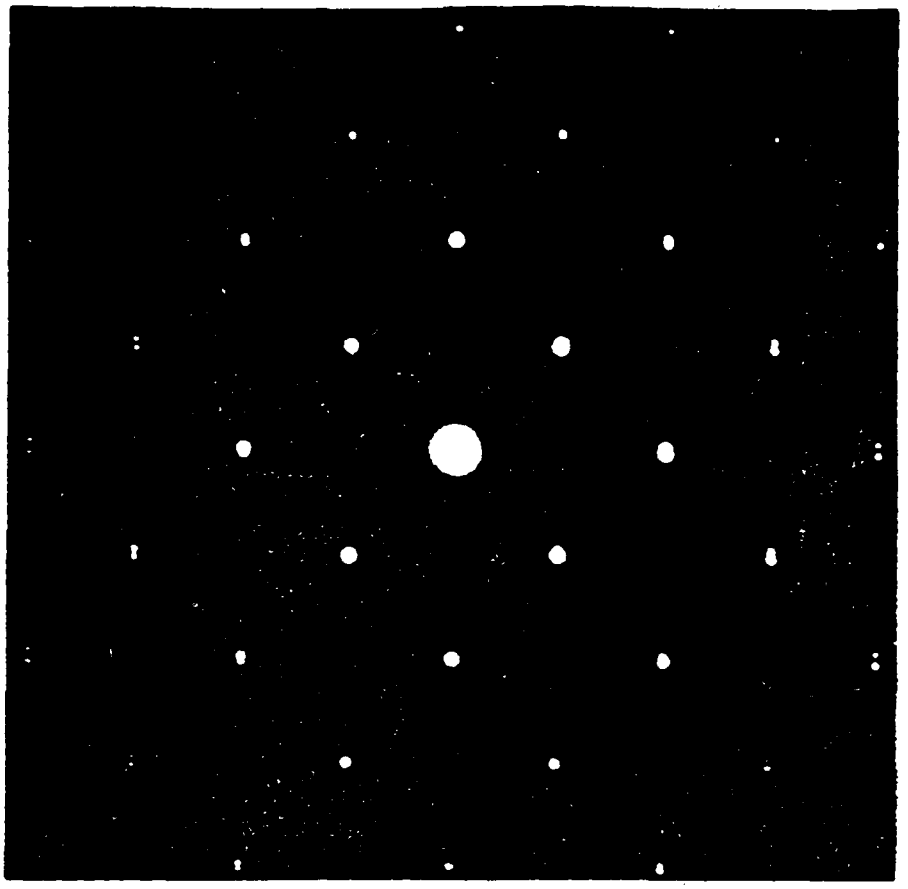

Fig. 2. Electron diffraction pattern of $Ba_2YCu_3O_7$. Spots split in one diagonal direction with increasing separation in higher order reflections indicating twinning in the [110] direction.

EXPERIMENTAL TECHNIQUES AND RESULTS

The samples were first cooled in a SQUID susceptometer in a small (typically 100 G) magnetic field. The magnetization data (see Table I) for the $La_{2-x}M_xCuO_4$ (M = Ba and Ca) showed diamagnetic onsets at 20°K and 31°K with 10% and 20% flux expulsion at 10°K (the lowest temperature measured) respectively. The curves were not flat at 10°K indicating that the samples were still expelling flux. The presence of these broad transitions with small flux expulsion along with the x-ray data indicating nearly single phase materials is a manifestation of the oxygen's importance in the superconductivity (x-rays do not couple strongly to oxygen). The M = Sr sample had an onset at 36°K with 40% flux expulsion at 10°K and the $Ba_2Y_1Cu_3O_7$ sample showed the onset at 93°K with 90 - 100% flux expulsion by 40°K (Figure 3).

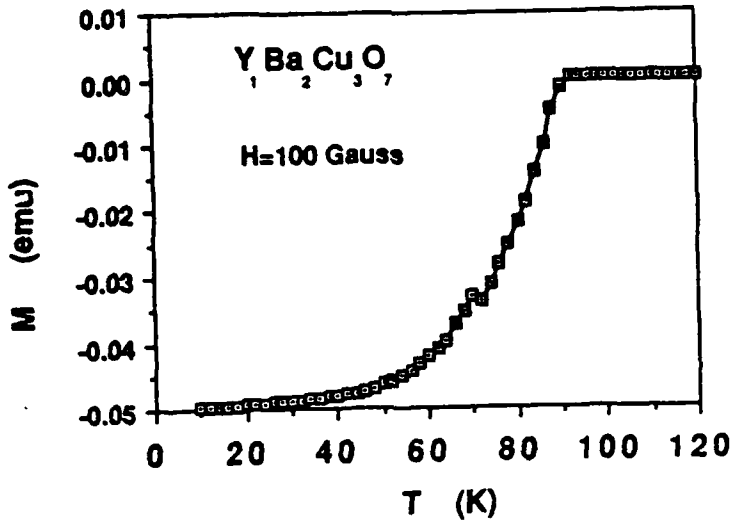

Fig. 3. Magnetization versus temperature for $Ba_2YCu_3O_7$. The low temperature diamagnetic signal shows nearly complete flux expulsion.

The samples were next warmed above their transition temperatures, cooled in zero field and magnetization, M, versus field, H, measurements were made with fields up to 80 kG. All of the samples have hysteretic M vs. H curves characteristic of type II superconductors with flux pinning centers. The lower critical fields, H_{c1}, for the $La_{2-x}M_xCuO_7$ materials are 100 - 300 G at 10°K (Table I). The critical currents, estimated from the hysteresis in the M vs. H curve [8], are rather low at 10°K. A series of measurements on $La_{1.8}Sr_{0.2}CuO_4$ at several temperatures shows a critical current of 12000 A/cm^2 at 4.2°K which degrades dramatically at higher temperatures. Figure 4 shows J_c versus H for this sample. This curve is typical of a superconductor with strong pinning centers (insert).

The 4.2°K magnetization data for the BaYCuO sample was highly hysteretic (Figure 5). The lower critical field was ~0.6 kG (Figure 6). Figure 7 shows critical current versus field for this sample. At H_{c1} the critical current is 2×10^5 A/cm^2 consistent with the results reported by IBM [9]. The shape of the low field region (insert) is typical of a weak pinning superconductor.

The upper critical fields for these materials were measured by monitoring the samples' 4-probe resistance as the temperature was swept in a constant magnetic field. The magnetoresistance of the carbon glass thermometer was taken into account in determining the temperature. The critical temperature in a given field was taken as that temperature where the sample resistance was 50% of the normal value.

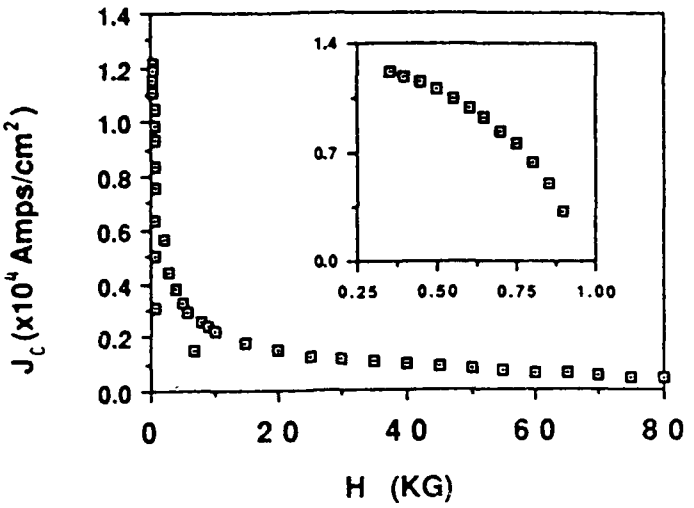

Fig. 4. Critical current versus magnetic field for $La_{1.8}Sr_{0.2}CuO_4$ (estimated from the hysteresis in the M vs. H curve). The low field data is typical of a superconductor with strong pinning centers (insert).

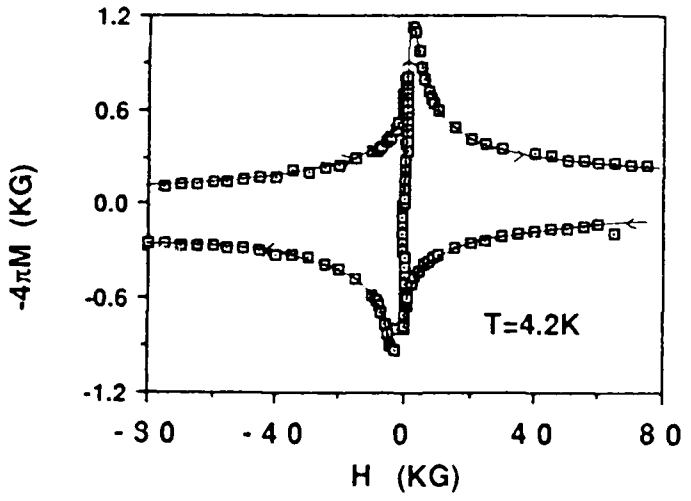

Fig. 5. Magnetization versus magnetic field hysteresis loop of $Ba_2Y_1Cu_3O_7$ at 4.2°K. The sample was cooled in zero field.

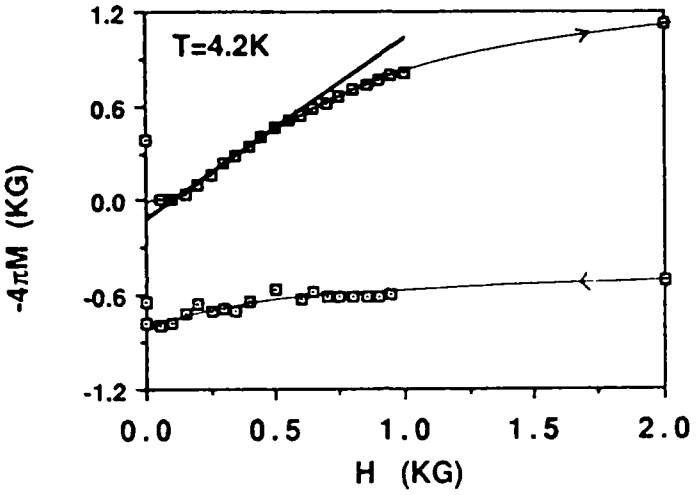

Fig. 6. Low field data from Figure 5. The lower critical field, H_{c1}, is 0.6 kG.

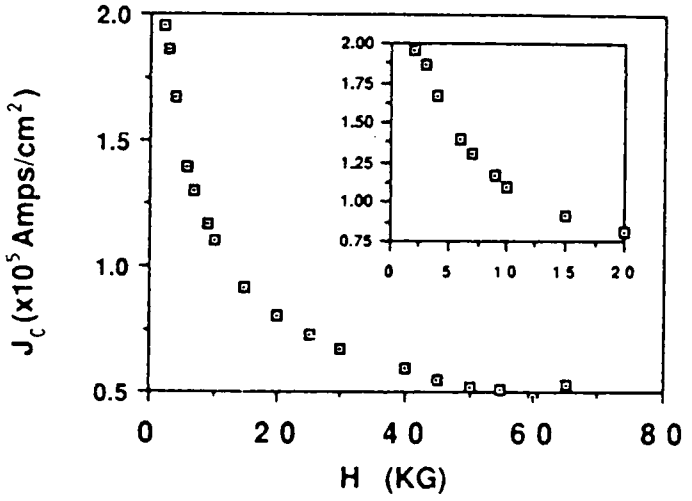

Fig. 7. Critical current versus magnetic field for $Ba_2Y_1Cu_3O_7$ (estimated from the hysteresis in the M vs. H curve). The low field data is typical of a superconductor with weak pinning centers (insert).

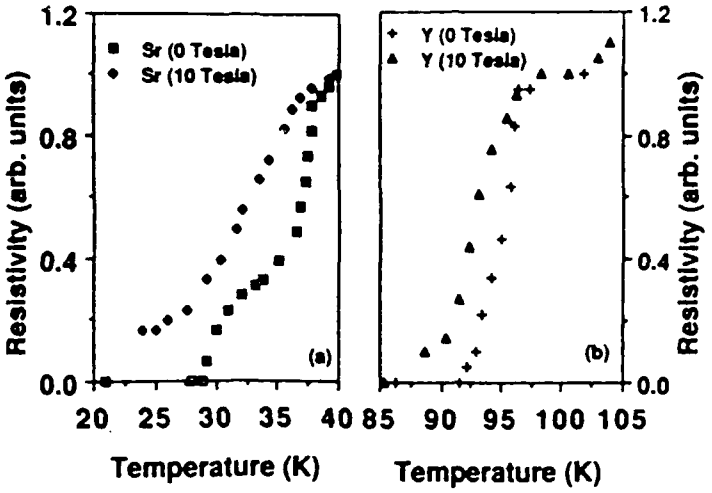

Fig. 8. Resistance versus temperature of (a)$La_{1.8}Sr_{0.2}CuO_4$ and (b)$Ba_2Y_1Cu_3O_7$ in 0 and 10 Tesla magnetic fields.

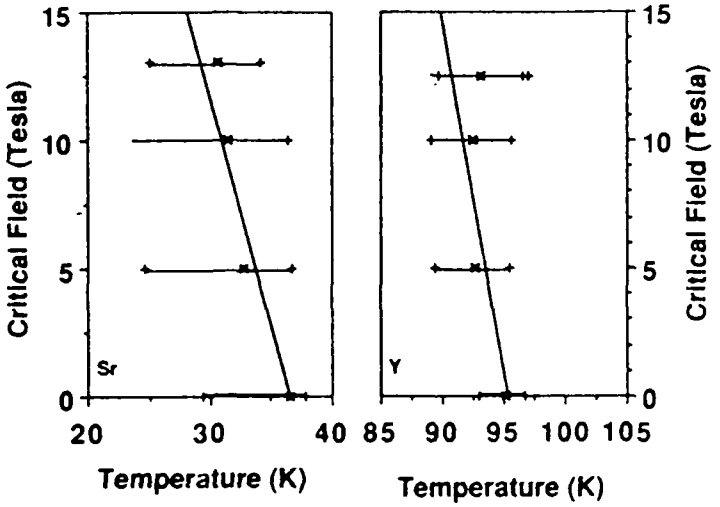

Fig. 9. The upper critical field as a function of temperature for $La_{1.8}Sr_{0.2}CuO_4$ (left) and $Ba_2Y_1Cu_3O_7$ (right). The extent of the 10% - 90% points of the transitions are shown. The lines through the data points are guides to the eye.

The magnetic field significantly broadened the transition for the lower T_c materials (Figure 8). This is perhaps due to inhomogeneities in these samples. A field of 100 kG has a negligable effect on the onset temperature. The magnetic field only slightly broadened the transition of

Table I. Parameters calculated from the dc magnetization and critical field data.

Material	T_c(50G) (K)	$dH_{c_2}/dT\|_{T_c}$ (kG/K)	$H_{c2}(0)$ (kG)	ξ_{GL} (Å)	γ (ergs/cc - K^2)	$H_c(0)$ (kG)	κ_{GL}	$H_{c1}(0)$ kG calculated	H_{c1}:T kG:K measured	J_c(4K) A/cm^2	T_c onset (K) magnetic	% flux expelled at 10K
$Sr_{0.2}$	34	-13 - -40	330 - 930	19 - 31	840 - 2500	4.5 - 7	76 - 132	0.180 - 0.190	0.35:4.2	1.2×10^4 800* 1.1×10^8 1.7×10^8	36	40
$Ba_{0.1}$	27	-9.6 - -15.6	190 - 280	34 - 42	600 - 1000	3.0 - 3.6	65 - 83	0.134 - 0.136	0.2:10	- 57* 6.4×10^7 7.6×10^7	31	20
$Ca_{0.3}$	15	-22 - -28	230 - 270	35 - 38	1370 - 1630	2.4 - 2.6	97 - 106	0.079 - 0.081	0.1:10	- 12.8* 3.8×10^7 4.2×10^7	20	16
Y	95	-22 - -35	1470 - 2370	13 - 16	2500 - 4030	20. - 26.	75 - 95	0.820 - 0.870	~0.6:4.2	2×10^5 1.1×10^9 1.4×10^9	93	100

Note: For the resistivity we used ρ=350 $\mu\Omega$-cm for the Sr, Ba, and Ca compounds and 200 $\mu\Omega$-cm for the Y. This was measured for the Sr and compounds and assumed for the Ba and Ca.

bracketed values are theoretical values for J_c at 0°K.

*J_c measured at 10°K.

the higher T_c material. In Fig. 9 the critical field is plotted as a function of temperature for the $La_{1.8}Sr_{0.2}CuO_4$ and $Ba_2Y_1Cu_3O_7$ samples. From the slope, $dH_{c2}/dT|_{T_c}$, one is able to calculate a variety of the material parameters [10]. Table I presents the results of these calculations. The ranges given represent the uncertainty in determining $dH_{c2}/dT|_{T_c}$. For the $La_{2-x}M_xCuO_4$ samples the H_{c1} obtained from $dH_{c2}/dT|_{T_c}$ and the resistivity, ρ, agree within a factor of two with the value obtained from the magnetization data. In $Ba_2Y_1Cu_3O_7$ the agreement is quite good which is surprising since the calculations assume an isotropic, 3D Fermi surface and these materials are known to be anisotropic, with the superconductivity believed to be quasi-2D for $La_{2-x}M_xCuO_4$ and possibly quasi-1D for $Ba_2Y_1Cu_3O_7$ [6].

Our value for γ, the density of states at the Fermi level, is in the range 2500 - 4030 (ergs/cc -K^2) for $Ba_2Y_1Cu_3O_7$. This is to be compared

with 2150 (ergs/cc - K^2) as obtained from the jump in the specific heat [11]. The agreement is quite good considering the imprecision in determining $dH_{c2}/dT|_{T_c}$ and ρ for this material.

CONCLUSION

We have prepared, characterized and performed a variety of magnetic field measurements on the new superconductors. The $La_{2-x}M_xCuO_4$ (M = Ba, Sr, Ca) materials show incomplete flux expulsion and very broad transitions, both magnetic and resistive, in magnetic fields. The samples of $Ba_2Y_1Cu_3O_7$, which have extensive twinning domains due to the crystal's orthorhombic structure, show negligible broadening of the resistive transition at 130 kG. This result, along with processing [6] and neutron studies, shows that good superconducting behavior strongly depends upon the Cu-O-Cu chains in the basal plane of the structure.

REFERENCES

* Office of Naval Technology Postdoctoral Fellow
** On sabbatical leave from the National Science Foundation, Washington, DC, USA
+ Sachs-Freeman Associates, Landover, MD.
++ Crystal Growth and Material Testing Associates, Lanham, MD.
+++ Catholic University of America, Washington, DC

1) J.G. Bednorz and K.A. Muller: Z. Phys. B64(1986) 189.
2) R.J. Cava, R.B. van Dover, B. Battlogg, and E.A. Reitman: Phys. Rev. Lett. 58(1987) 408.
3) K. Kishio, K. Kitazawa, S. Kanbe, I. Yamada, N. Sugii: Jpn. J. Appl. Phys. (to be published).
4) M.K. Wu, J.R. Ashburn, C.J.Torng, P.H. Hor, R.L. Meng, L. Gao, Z.J. Huang, Y.O. Wang, and C.W. Chu: Phys. Rev. Lett. 58(1987) 908.
5) D.U. Gubser, R.A. Hein, S.H. Lawrence, M.S. Osofsky, D.J. Schrodt, L.E. Toth, and S.A. Wolf: Phys. Rev. B35(1987) 5350.
6) L.E.Toth, E.F. Skelton, S.A. Wolf, S.B. Qadri, M.S. Osofsky, B.A. Bender, S.H. Lawrence, and D.U. Gubser: (submitted to Phys. Rev B)
7) r.Beyers, G.Lim, E.M.Engler, and R.J.Savoy:(to be published in Appl. Phys. Lett., 29 June 1987)
8) W.A. Fietz and W.W. Webb: Phys. Rev. 178(1969) 657.
9) private communication
10) T.P. Orlando, E.J. McNiff, Jr., S. Foner, and M.R. Beasley: Phys. Rev 19(1979) 4545.
11) A. Junod, A. Bezinge, T. Graf, J.L. Jorda, J. Muller, L. Antognazza, D. Cattani, J. Cors, M. Decroux, O. Fischer, M. Banovski, P. Genoud, L. Hoffmann, A.A. Manuel, M. Peter, E. Walker, M. Francois, and K. Yvon: (submitted Europhysics Lett.)

Evidence of conventional superconductivity in La-Ba-Cu-O compounds

W. E. Pickett
Naval Research Laboratory, Washington, D.C. 20375-5000

H. Krakauer
Department of Physics, College of William and Mary, Williamsburg, Virginia 23185

D. A. Papaconstantopoulos and L. L. Boyer
Naval Research Laboratory, Washington, D.C. 20375-5000

(Received 5 March 1987)

First-principles methods are applied to investigate the electronic structure and electron-phonon coupling in the end-point members ($x=0$ and $x=1$) of the new high-transition-temperature (T_c) superconductor $La_{2-x}Ba_xCuO_4$ and their counterpart cubic perovskites $La_{1-x}Ba_xCuO_3$. Alloying with Ba ($x=1$) induces non-rigid-band changes in the Cu and O density of states, but the Cu charge state changes rather little. The calculated McMillan-Hopfield parameter η coupled with soft phonon modes provides a strong electron-phonon interaction $\lambda \sim 2.5$ that can account for the high T_c of ~ 30–40 K in these systems.

LC3674BR 1987 PACS numbers 74.10.+v 63.20.Kr 74.70.Ya

Within the last few months a new class of superconductors has been discovered. Bednorz and Müller[1] first reported the occurrence of an apparent superconducting transition at 30 K in the oxide material $La_{2-x}Ba_xCuO_4$, with $x=0.15$ and $y>0$ (probably small) which has the tetragonal layer-perovskite K_2NiF_4 structure. This result has since been reproduced and improved by alloying with Sr instead of Ba.[2-6] In this paper we report results of first-principles band-structure calculations which assess the relative contributions of the oxygen, copper, and other metal atoms to the states which drive the superconductivity as well as identifying changes in ionicity and other effects of alloying. We also investigate the importance of the perovskite substructure in these materials, especially on the electron-phonon coupling strength. It is found that T_c in these layer perovskites can be explained by conventional phonon-mediated superconductivity in which soft phonon modes due to the vibrations of the light O atoms play the main role.

Our primary interest in these materials is in understanding what interaction between electrons is responsible for producing the superconducting state. Conventional superconductors utilize the electron-phonon interaction (EPI), which is normally enhanced by a large electronic density of states (DOS) at the Fermi level and by a strong electron-ion scattering.[7] These new alloys, however, are oxides and not at all usual metals, with resistivities above T_c which are more than an order of magnitude larger than the resistivities of conventional superconductors, i.e., they might be semimetals. Since they are not good metals in the usual sense, the pairing interaction may be different from the conventional one. Suggestions include electrons coupled by two-dimensional plasmons, polarons, or bipolarons, although a novel kind of EPI is also a reasonable guess. In this paper we provide an accurate description of the electronic structure of pure La_2CuO_4 and $LaBaCuO_4$ (i.e., replacement of one of the La atoms in the unit cell by a Ba atom) in order to elucidate the effects of alloying. We also investigate the role of the perovskite-type layers by performing parallel calculations for the perovskite compounds $LaCuO_3$ and $BaCuO_3$. For purposes of comparison, the lattice parameter for the perovskites was chosen by taking a weighted average of the in-plane short Cu—O bond and the long Cu—O bond along the normal direction.

The calculations for La_2CuO_4 and $LaBaCuO_4$ were carried out with the self-consistent linearized-augmented-plane-wave (LAPW) method[8] within the framework of the local-density-functional approximation using the Hedin-Lundqvist exchange-correlation potential. This method employs shape-unrestricted charge densities and potentials and basis sets of 500–600 LAPW's. Two "energy windows"[8] were used so that the "semicore" O($2s$) and La,Ba($5p$) states could also be treated variationally. Similar calculations were performed using the APW method (in the muffin-tin approximation) for the perovskite $LaCuO_3$ and $BaCuO_3$ compounds with the same treatment of semicore levels and exchange correlation as in the LAPW calculations. Self-consistency in the LAPW calculations was achieved using a mesh of 16 special k points in the $\frac{1}{16}$th irreducible Brillouin zone (IBZ), and three special k points for the semicore states. In the final iteration, energies and wave functions were calculated at 135 equally spaced k points in the IBZ for further analysis. A Fourier-series spline fit,[9] which is constrained to pass smoothly through all 135 points, was then used to generate 542 points in the IBZ to calculate the density of states (DOS) using the linear analytic tetrahedron method. The APW DOS was calculated in a similar manner using another scheme[10] to generate energy bands at 165 k points from 35 first-principles APW points in the $\frac{1}{48}$ zone. For the layer perovskites, the lattice parameters were taken to be $a=7.1622$ and $c=24.964$ a.u. The out-of-plane O distance was taken as $z=4.543$ a.u. and that of the La (Ba) atom was taken as $z=3.445$ a.u. The muffin-tin sphere radii are given in Table I. The cubic-perovskite

TABLE I. Sphere radii (a.u.) and valence-electron charge inside the various spheres. The $5p$ semicore electron charge is also given for the La and Ba spheres.

	R_S	La_2CuO_4	$LaBaCuO_4$
La	2.90	1.263	1.240
La($5p$)	2.90	5.599	5.616
Ba	2.90	· · ·	1.208
Ba($5p$)	2.90	· · ·	5.058
Cu	1.95	9.180	9.058
O_{xy}	1.55	3.460	3.378
$O_{z,La}$	1.55	3.349	3.272
$O_{z,Ba}$	1.55	3.349	3.267

lattice parameter was set equal to $a = 7.8234$ a.u. and the sphere radii were 3.576 a.u. for La and 1.956 a.u. for Cu and O.

An overview of the electronic structure can be seen in the DOS. The DOS of the layer-perovskite compounds are shown in Fig. 1 and that of the cubic perovskites in Fig. 2. In both Figs. 1 and 2 the Fermi energy (E_F) moves to lower energy upon replacement of La by Ba, and as seen in Table II the DOS at E_F, $N(E_F)$, increases. Matheiss[11] and Yu and Freeman[12] have also obtained the La_2CuO_4 band structure with the LAPW method. The DOS in Fig. 1(a) is very similar to that given by Mattheiss.[11] It is immediately apparent that while one might have expected simple rigid-band behavior in going to the 50% Ba compound, this is not at all the case *in general*. One prominent change is the shift in spectral weight on the Cu atom from higher to lower energy. This is also seen in the perovskite compounds in Fig. 2, and represents primarily a rearrangement of t_{2g} spectral weight. It is also interesting that the Cu t_{2g} contribution to the DOS at E_F is zero. In both structures Cu-O $dp\sigma$-type bands cross E_F.

While the in-plane O_{xy} DOS in the layer compound is changed relatively little by the addition of Ba, there is a significant change in the O_z DOS. The 50% Ba compound

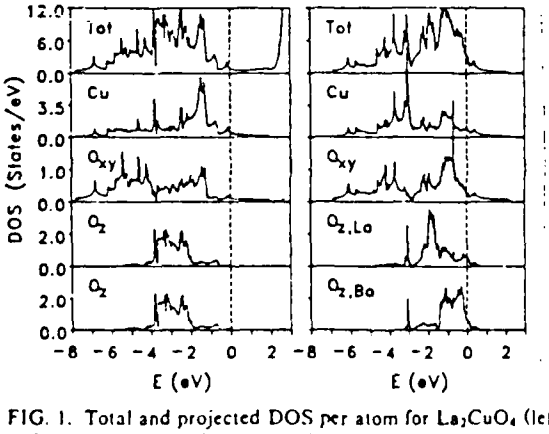

FIG. 1. Total and projected DOS per atom for La_2CuO_4 (left panel) and $LaBaCuO_4$ (right panel). The dashed line indicates E_F.

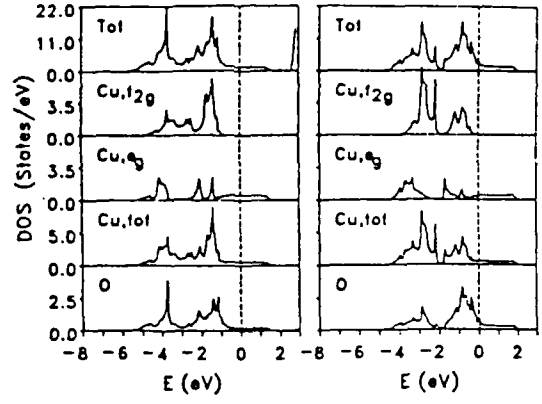

FIG. 2. Total and projected DOS (per atom) for $LaCuO_3$ (left panel) and $BaCuO_3$ (right panel).

has two inequivalent O_z atoms, one which is nearly coplanar with the La atoms while the other lies in a Ba layer. Although La (Ba) may not be fully trivalent (divalent), nevertheless the La sphere is essentially one unit more ionic than Ba. [Since the La and (especially) Ba $5p$ core states are quite extended, we have used rather large spheres and treated the $5p$ states variationally in a separate window. As a result of the large sphere radius, the valence charge (see Table I) in the sphere is 1.24 for La and 1.21 for Ba, approximately one electron of which can be attributed to overlapping oxygen states.] Due to the unit difference in ionic charge between Ba and La the $O_{z,Ba}$ atoms experience a less attractive electrostatic potential than do the $O_{z,La}$ atoms, which accounts for the $O_{z,Ba}$ DOS being nearer E_F than the $O_{z,La}$ DOS. For the $O_{z,Ba}$ atom, $N(E_F)$ is also about 10% larger than for the $O_{z,La}$ atom. In addition, there is more spectral weight above E_F on both O_z atoms compared to Fig. 1(a), i.e., adding Ba causes the originally $2-O_z$ ions to become partially metallic.

Rigid-band behavior does appear to hold near E_F, however, where only the broad $d_{x^2-y^2}$-$p_{x(y)}$ band contributes to $N(E)$. From Figs. 1(a) and 1(b) it is evident that there is similar structure in $N(E)$ in the region of $E_F(La_2CuO_4)$, with the prominent feature being the van Hove peak 0.1 eV below E_F in Fig. 1(a) which occurs at a concentration $x = x_{cr} \approx 0.14$ of Ba. This peak is of similar height in the two calculations, and x_{cr}, defined from the La_2CuO_4 DOS, lies within about 0.03 eV of the peak in $LaBaCuO_4$. Thus using the rigid-band model for $x \lesssim 0.2$ should be realistic.

The van Hove peak, which defines x_{cr}, occurs very near the concentration of Ba (and Sr) where T_c is highest. The peak results from a saddle point in the $d_{x^2-y^2}$-$P_{x(y)}$ band slightly beyond the zone boundary along the x (and y) axis, which lies midway between the nearly touching corners of the La_2CuO_4 Fermi surface (see Fig. 3 of Mattheiss[11]). At $x = x_{cr}$ the Fermi surface transforms from distorted holelike cylinders along the z axis centered at the X ("corner") point to distorted electron cylinders centered at Γ. Many transport and thermodynamic prop-

TABLE II. Total DOS at E_F (states/eV) and the McMillan-Hopfield parameter η *per atom* (eV/Å^2).

	La_2CuO_4	$LaBaCuO_4$	$LaCuO_3$	$BaCuO_3$
$N(E_F)$	1.24	3.69	1.42	2.70
η_{La}	0.00	0.08	0.00	...
η_{Ba}	...	0.16	...	0.012
η_{Cu}	0.62	1.08	0.89	1.65
η_{O_z}	0.72	0.32	0.48	0.60
$\eta_{O_{z,La}}$	0.04	0.15		
$\eta_{O_{z,Ba}}$	0.04	0.33		

erties can be extremely x dependent[13] near $x \simeq x_{cr}$.

Whether T_c in these compounds arises from EPI is a question of fundamental interest. To investigate this question, the Fermi-surface-averaged electron-ion matrix elements were evaluated using the rigid muffin-tin approximation (RMTA) of Gaspari and Gyorffy.[14] Quantities entering the calculation of the McMillan-Hopfield constant η are presented in Table II. The main features of the calculations of η are the following. The La and Ba atoms always have very small η's within RMTA. The Cu atoms have moderately sized values of η which are enhanced by the replacement of La by Ba. The O_z atoms have very small η's in La_2CuO_4 but are moderate in size in $LaBaCuO_4$. The O_{xy} η is larger than for O_z but is reduced in $LaBaCuO_4$. The contributions to η come predominantly from the Cu(d)-O(p) interaction. While replacement of La by Ba triples $N(E_F)$, the η's do not increase proportionally. It is interesting to note the approximate transferability of the η values, that is, those in La_2CuO_4 are comparable to those of $LaCuO_3$: $\eta_{Cu}=0.62$ (respectively 0.89), $\eta_{O,total}=1.52$ (respectively 1.44) eV/Å^2. This suggests that the cubic-perovskite structure, if stable, might also provide high-T_c materials. Because the η's are significantly smaller than those of typical high-temperature superconductors (e.g., $A15$ compounds, NbN) it appears likely that the layered perovskites possess soft phonon modes as found by Weber.[15]

The quantity which characterizes the contribution to the electron-phonon interaction strength λ from a given type of atom is[7]

$$\lambda_i = \eta_i/(M_i \Omega^2) , \qquad (1)$$

where Ω is an rms vibrational frequency. We propose an EPI mechanism for superconductivity with the transition temperature given by the Allen-Dynes equation[16] $T_c = T_c^{AD}(\eta_i, \mu^*, \Omega)$, where $\mu^* = 0.1$ is the Coulomb pseudopotential.

In the absence of experimental information on the phonon spectrum, we use for the spectral function $\alpha^2 F$ a two-peak Einstein model with frequencies Ω_{Cu} and Ω_O. Since the important vibrations are expected to involve Cu-O bond stretching[15] and since each Cu-O force constant contributes equally to $M\Omega^2$ projected onto each of the atoms, we assume $M_{Cu}\Omega_{Cu}^2 = M_O\Omega_O^2$ and study the effect on T_c of varying Ω_O. Using the rigid-band model discussed above for $La_{2-x}Ba_xCuO_4$ for $x = x_{cr} = 0.14$, we find $\eta_{Cu} = 0.74$ and $\eta_{O,total} = 2.2$ eV/Å^2. In Fig. 3 we show

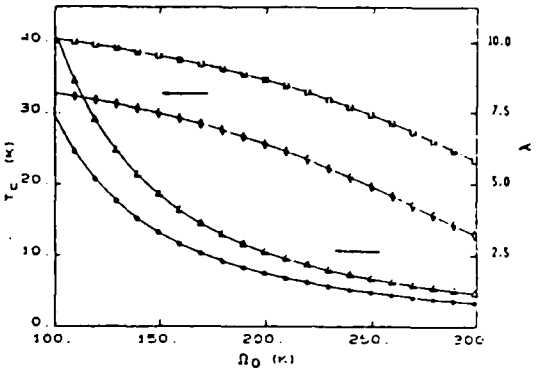

FIG. 3. Values of λ and T_c (from the Allen-Dynes equation) as a function of Ω_O. The bottom curve in each case corresponds to La_2CuO_4 (stars and diamonds), while the top curves (triangles and squares) correspond to $La_{2-x}Ba_xCuO_4$, $x = 0.14$, in the rigid-band picture.

T_c and λ as a function of Ω_O for both $x = 0.0$ and $x = x_{cr}$. These results indicate that for mean oxygen frequencies of about 200 K, λ is about 2.6 and T_c exceeds 34 K in the case $x = x_{cr}$. Experimental values of T_c are sample dependent but lie in the range 30–40 K and peak near $x = x_{cr}$. (Note that for $\lambda > 2$ it is important to include the prefactors f_1, f_2 in the Allen-Dynes equation[16] for T_c.) These conclusions are in agreement with those of Weber.[15] Our results also indicate that, were it not for the electronically driven structural transition[11,12] for $x = 0.0$, the pure compound would also be a superconductor with a somewhat lower T_c, within the same frequency range for Ω_O. On the other hand, Weber expects additional softening as x is decreased from 0.15 which would raise T_c, contrary to experimental evidence. Both analyses give strong support to the assertion that soft phonon modes due to the vibrations of the light O atoms are the main cause of superconductivity in these compounds. This is reminiscent of the situation[17] in PdH, where the hydrogen optic-phonon modes play a key role in the occurrence of superconductivity.

To summarize, we have shown that replacement of La by Ba in La-Cu-O compounds leads to large changes in the Cu and O spectral density without inducing large changes in their charge state. Although these compounds display an unusual mixture of ionic and metallic character not seen in other high-T_c superconductors, calculation of the EPI strength indicates that it may be of the magnitude necessary to account for the high-T_c values in these systems.

This work was supported in part by National Science Foundation (NSF) Grant No. DMR-84-16046 and by Office of Naval Research Contract No. N00014-83-WR-30007. The computations were carried out under the auspices of the NSF on CRAY X-MP's at the University of Illinois and at the University of Pittsburgh. We thank L. F. Mattheiss, A. J. Freeman, and W. Weber for copies of their papers prior to publication. We are pleased to thank P. B. Allen, R. E. Cohen, D. U. Gubser, B. M. Klein, and S. A. Wolf for helpful discussions.

[1]J. G. Bednorz and K. A. Müller, Z. Phys. B 64, 189 (1986).
[2]H. Takagi, S. Uchida, K. Kitazawa, and S. Tanaka, Jpn. J. Appl. Phys. Lett. (to be published).
[3]R. J. Cava, R. B. van Dover, B. Batlogg, and E. A. Rietman, Phys. Rev. Lett. 58, 408 (1987).
[4]C. W. Chu, P. H. Hor, R. L. Meng, L. Gao, Z. J. Huang, and Y. Q. Wang, Phys. Rev. Lett. 58, 405 (1987).
[5]F. S. Razavi, F. P. Koffyberg, and B. Mitrovic (unpublished).
[6]D. U. Gubser, R. A. Hein, S. H. Lawrence, M. S. Osofsky, D. J. Schrodt, L. E. Toth, and S. A. Wolf (unpublished).
[7]B. M. Klein and W. E. Pickett, in *Superconductivity in d- and f-Band Metals*, edited by W. Buckel and W. Weber (Kernforschungszentrum, Karlsruhe, 1982), p. 97, and references therein.
[8]S.-H. Wei and H. Krakauer, Phys. Rev. Lett. 55, 1200 (1985), and references therein.
[9]D. D. Koelling and J. H. Wood, J. Comput. Phys. 67, 253 (1986).
[10]L. L. Boyer, Phys. Rev. B 19, 2824 (1979).
[11]L. F. Mattheiss, Phys. Rev. Lett. 58, 1028 (1987).
[12]J. Yu and A. J. Freeman, Phys. Rev. Lett. 58, 1035 (1987).
[13]I. M. Lifshitz, Zh. Eksp. Teor. Fiz. 38, 1569 (1960) [Sov. Phys. JETP 11, 1130 (1960)].
[14]G. D. Gaspari and B. L. Gyorffy, Phys. Rev. Lett. 28, 801 (1972).
[15]W. Weber, Phys. Rev. Lett. 58, 1371 (1987).
[16]P. B. Allen and R. C. Dynes, Phys. Rev. B 12, 905 (1975).
[17]D. A. Papaconstantopoulos, B. M. Klein, E. N. Economou, and L. L. Boyer, Phys. Rev. B 17, 141 (1978).

ELECTRONIC STRUCTURE, BONDING AND ELECTRON-PHONON INTERACTION IN La-Ba-Cu-O SUPERCONDUCTORS

W.E. PICKETT*, H. KRAKAUER†, D. A. PAPACONSTANTOPOULOS*, L.L. BOYER* AND R.E. COHEN*
* Naval Research Laboratory, Washington D.C. 20375-5000
† College of William and Mary, Williamsburg, VA 23185

The discovery of superconductivity above 30 K by Bednorz and Müller [1] in the La-Ba-Cu-O system was a breakthrough in the field of superconductivity. The superconductivity has since been established to be associated with the layer perovskite K_2NiF_4-type structure, with the peak transition temperature T_c above 40 K occurring in $La_{2-x}M_xCuO_4$ at an alkaline earth (M=Ba,Sr) concentration x=0.15 [2]. Central questions to consider then are: what is the interaction responsible for such high temperature superconductivity, in what way is the crystal structure responsible for this interaction, and what apparently crucial role is the alkaline earth substitution playing?

To address these questions we have begun a study of the electronic structure of the layer perovskite La-Ba-Cu-O compounds and their cubic perovskite counterparts $MCuO_3$, M=La,Ba,Sr. We use the local density approximation within the (both linearized and unlinearized) augmented plane wave method, and details of the application to these systems has been presented elsewhere [3]. Here we summarize results of studies of La_2CuO_4 and $LaBaCuO_4$ in the layer perovskite structure and the cubic perovskites mentioned above. Differences between these layer perovskites focus attention on the effect of alloying La with Ba, while comparison of the layer structures with their cubic counterparts may illuminate important structurally related similarities or differences.

As reported previously [3-5], the Fermi level E_F in both the layer and cubic compounds lies in a region crossed by a single O-Cu pdσ band, and near E_F a rigid band model appears to be reasonable. Within this picture a van Hove peak occurs in the density of states below E_F in the layer perovskites corresponding to a concentration x=0.14 of Ba or Sr, i.e. just where T_c is found to peak, and it seems clear that this van Hove singularity is intimately related to the enhanced superconductivity. Well below E_F, however, strongly non-rigid band behavior occurs in the local density of states of the Cu and O atoms neighboring the dopant, reflecting the change in crystal field when La^{3+} is replaced by Ba^{2+}.

Investigation of the electron-phonon interaction (EPI) strength λ is important; in fact, Bednorz and Müller were studying these systems in anticipation of observing very large EPI. We have evaluated the Fermi surface averaged electron-ion scattering constant η for $La_{2-x}Ba_xCuO_4$, x=0.0, 0.14 and 1.0, and for $LaCuO_3$ and $BaCuO_3$ [3]. In all cases the contributions come primarily from the Cu and O atoms, and compared to transition metal superconductors are rather low. However, this can be compensated considerably by the small O mass and low frequency lattice vibrations. Assuming $(M\omega^2)_{Cu}=(M\omega^2)_O$ [3] and using a McMillan mean oxygen frequency of ω_O=200 K, which appears to be consistent with what neutron scattering information is available, we find T_c=35 K for x=0.14, with $\lambda\approx 2.5$. The pure La compound (x=0.0), if it were to remain in the tetrahedral structure, would have a T_c 10 K lower. More details of these studies are given in Ref. 3.

Phonon frequencies and eigenvectors are particularly important in determining whether pairing results from the EPI. Since these are extraordinarily difficult to obtain from first principles (e.g. from frozen phonon studies) we are investigating the predictions of the Potential Induced Breathing (PIB) model [6], which is an overlapping ion,

Gordon-Kim type ab initio approach developed for ionic oxides. For both the layer perovskite structure and the experimentally observed orthorhombic structure, the lowest phonon branch along Γ-X is unstable. For the tetragonal structure, this branch is the oxygen breathing mode discussed by Weber [7] at X, but changes continuously into a mode at the zone center which involves only sliding motions in the x-y plane of the La and O_z atoms.

These compounds display an unusual combination of ionic and metallic characteristics, especially for high T_c materials. The PIB model provides a reference ionic charge density that allows us to see the bonding and density distortions more clearly. Figure 1 shows the difference (LAPW minus PIB) in total charge densities, with contour interval of 0.005 el/bohr^3. The very small differences around the O_z atom verify that it is fully ionic. The small differences near La are due to orthogonalization of O_z states to the La core and/or small amounts of La *f* character. The major differences are in the Cu-$O_{x,y}$ plane. Figure 1 shows that, compared to the overlapping ion reference, charge moves away from the Cu-O line except for a small bonding increase at the midpoint. The result is to produce non-spherical Cu and $O_{x,y}$ ions. This illustrates the usefullness of comparing with overlapping spherical ions, because these distortions are not discernible in crystal density plots alone.

Since the Cu d and $O_{x,y}$ p shells are not completely filled, one expects non-rigid charge rearrangements to be dominated by charge fluctuations on these atoms. We have studied the charge density rearrangements due to small atomic motions. When the O_z atoms are moved directly toward the Cu from above and below, the primary non-rigid charge shift, shown in Figure 2, is <u>from</u> the $O_{x,y}$ atoms <u>to</u> the Cu d(x^2-y^2). It is somewhat surprising that this movement causes charge to move **onto** the Cu, and it is more unexpected that the change on the $O_{x,y}$ atoms appears to be **isotropic** rather than purely p(x,y)-like. Further studies may be necessary to provide an understanding of this mixing of ionic-metallic character.

This work was supported by NSF Grant No. DMR-84-16064 and by ONR Contract No. N00014-84-WR-24005. Computations were carried out under the auspices of the NSF on CRAY X/MP's at the University of Pittsburgh and the University of Illinois. We have benefitted from discussions with a number of colleagues.

1. J. G. Bednorz and K. A. Müller, Z. Physik B <u>64</u>, 189 (1986).
2. B. Batlogg, A. P. Ramirez, R. J. Cava, R. B. van Dover and E. A. Rietman, Phys. Rev. B <u>35</u>, 5340 (1987).
3. W. E. Pickett, H. Krakauer, D. A. Papaconstopoulos and L. L. Boyer, Phys. Rev. B <u>35</u>, xxxx (1987).
4. L. F. Mattheiss, Phys. Rev. Lett. <u>58</u>, 1024 (1987).
5. J. Yu, A. J. Freeman and J. H. Yu, Phys. Rev. Lett. <u>58</u>, 1028 (1987).
6. L. L. Boyer, et al., Phys. Rev. Lett. <u>54</u>, 1940 (1985); <u>57</u>, 2331 (1986); R. E. Cohen, Geophys. Res. Lett. <u>14</u>, 37 (1987).
7. W. Weber, Phys. Rev. Lett. <u>58</u>, 1371 (1987).

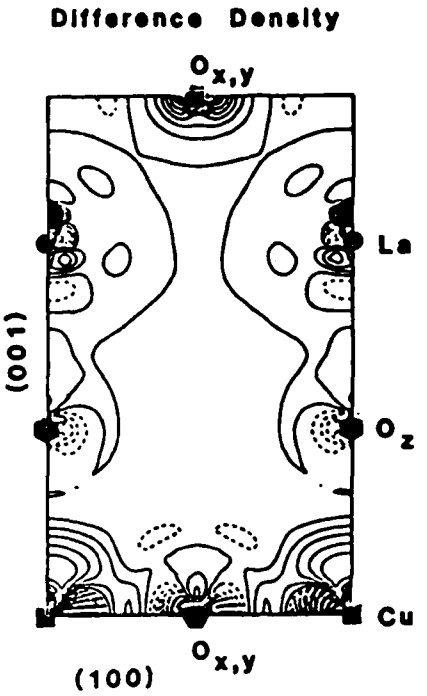

Figure 1. Charge density difference between the self-consistent crystal (LAPW) density and the overlapping ion (PIB) density, in the (100) plane. Contour interval is 0.005 el/bohr^3. Solid (dashed) lines denote a positive (negative) difference.

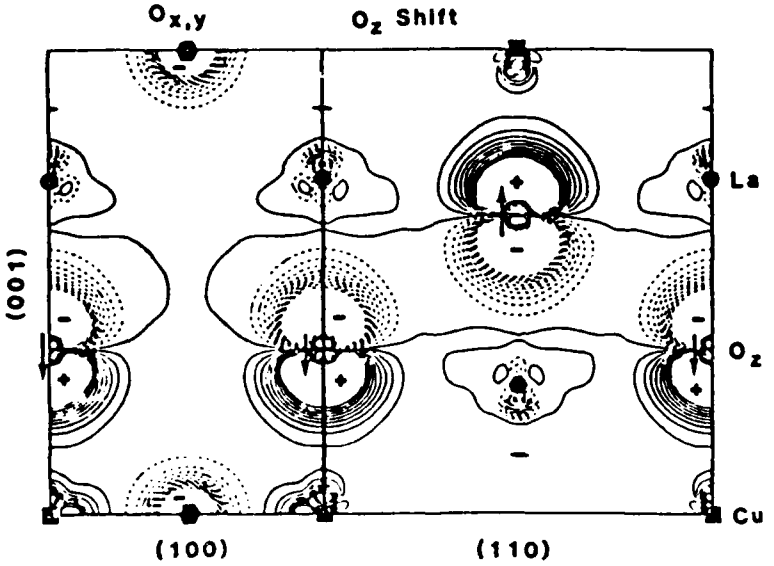

Figure 2. Charge rearrangement (from self-consistent LAPW calculations) due to displacement of the O_z atoms toward the nearest Cu (arrows) by 0.05 Å, shown in the (100) and (110) planes. Solid (dashed) lines denote increases (decreases) in density and +(-) signs denote regions where large positive (negative) contours have been truncated.

BAND STRUCTURE AND ELECTRON-PHONON INTERACTION CALCULATIONS FOR PROPOSED HIGH-T_C SUPERCONDUCTING OXIDES: $MCuO_3$ (M = LA, BA, CS, Y) IN THE PEROVSKITE STRUCTURE.

D. A. Papaconstantopoulos and L. L. Boyer*

Metal Physics Branch and *Condensed Matter Physics Branch
Naval Research Laboratory
Washington, DC 20375-5000

The crystal structures reported for the recently discovered high-T_c superconductors containing copper and oxygen have one thing in common; structural similarity to ideal perovskite. The systems which superconduct with T_c ~ 35 K, e.g., $La_{2-x}Ba_xCuO_4$ with x ~ 0.1 - 0.2, either have the tetragonal K_2NiF_4 structure or small orthorhombic distortions therefrom.[1-4] The K_2NiF_4 structure can be described qualitatively as alternating layers of perovskite ($KNiF_3$) and rock salt (KF) structures. The structures reported for the Y-Ba-Cu-O systems, which have T_c ~ 90 K, are described approximately as an ordered superlattice of oxygen deficient perovskite cells.[5-7] The common elements in all the superconductors discovered so far with T_c > 30 K are copper and oxygen. These results suggest that the local environment of the copper and oxygens in the perovskite structure is somehow conducive to high temperature superconductivity.

In an effort to explore these ideas theoretically we have carried out electronic band structure calculations for $MCuO_3$ (M = Cs, Ba, La and Y) in the ideal perovskite structure. Band structure quantities were calculated using the self-consistent APW method in the muffin-tin approximation with a local density approximation[8] for exchange and correlation. From these quantities we determine values for the McMillan-Hopfield parameter η (total and site decomposed), using the rigid muffin-tin approximation,[9] to provide some indication of the strength of the electron-phonon interaction in these idealized systems.

The calculations for M = La, Ba, and Cs were carried out for a lattice constant a = 7.8234 a.u., which is two times the average copper-oxygen separation in the La_2CuO_4 compound. A smaller value, a = 7.2943 a.u., was selected for the M = Y compound to correspond approximately to the difference between the ionic radii of Y and La. The muffin-tin radii used in the calculation were chosen to minimize the interstitial volume: R_M = 3.5761 a.u. and $R_{Cu} = R_O$ = 1.9558 a.u. for M = La, Ba, and Cs; R_Y = 3.3343 a.u. and $R_{Cu} = R_O$ = 1.8236 a.u. for the yttrium compound. States falling within ~ 1.5 Ry of the Fermi energy (E_F) were treated as bands in a semirelativistic approximation[10]. These include, of course, the valence bands, which are predominantly Cu-3d and O-2p, and O-2s, La-5p, Ba-5p, Cs-5p and Y-4p states as well. Deeper core levels were allowed to relax self consistently using a fully relativistic atomic code.

The band structures and total densities of states N(E) are shown in Figs. 1-4 along with selected contributions to N(E), N(Cu-t_g), N(Cu-e_g) and N(O-p), which reveal the predominant character of the valence bands. The La-f decomposed density of states (DOS) is also shown since this is a prominent feature in the conduction bands for the La compound. For the La, Ba and Y compounds, N(E_F) is composed mainly of Cu-3d states with e_g symmetry and O-2p states, while for $CsCuO_3$, there is a large contribution from the t_g symmetry copper states as well. This can be understood as a nearly rigid band shift of the Fermi level into the Cu-t_g bands, which are fully occupied for the La, Ba and Y compounds. The additional contribution from the Cu-t_g bands approximately triples the total DOS at E_F for $CsCuO_3$. The band structure of $CsCuO_3$ differs from the La and Ba compounds in another respect: the M-5p states (not shown for M = La and Ba) shift from ~-0.5 for La to ~-0.35 for Ba to ~-0.1 for Cs, where for Cs they hybridize with the valence bands.

The electron-phonon interaction parameter λ, which governs T_c in the conventional theory of superconductivity, is given by $\lambda = N(E_F)\langle I^2\rangle/F$, where F is a force constant which gives an average stiffness of the crystal against phonon modes, and $\langle I^2\rangle$ is an average electron-phonon matrix element. We have calculated values for $\eta_s = N(E_F)\langle I^2\rangle_s$ using the rigid muffin-tin approximation to evaluate the average electron-phonon matrix elements $\langle I^2\rangle_s$ for each site s. These results are listed in Table 1 along with the total and decomposed DOS at E_F, which enter the calculation of η_s.

The calculated values of η_s for the Y compound are qualitatively similar to those for La and Ba compounds, the latter of which were reported and discussed in a previous paper[11]. In Ref. 11 it was argued that T_c could be calculated as a function of a single parameter representing an average Cu-O force constant. The argument was based on the result that η_M was nearly zero for these materials. Calculations of T_c as a function of this parameter showed that T_c's of 30 to 40 K could be achieved with a modest amount of phonon softening. The same conclusion is probably true for the Cs compound, although a similar quantitative analysis would not be valid owing to the substantial contribution of η_{Cs}. In spite of the large increase in N(E_F) for $CsCuO_3$, η is about the same as for the Y, La, and Ba compounds. Unfortunately, the large increase in N(E_F) is approximately cancelled by a corresponding decrease in the size of the matrix elements for the Cu and O sites.

Our calculations suggest that the ideal perovskite analogs of the high-T_c oxide superconductors would themselves be high-T_c materials if they were to form in the ideal (no defects) perovskite structure. It seems unlikely that this conclusion would change if the calculations were carried out using more reliable estimates of the lattice constants. We plan to carry out total energy calculations on these idealized materials in the future to answer conclusively this question and to investigate the stability of the perovskite structure.

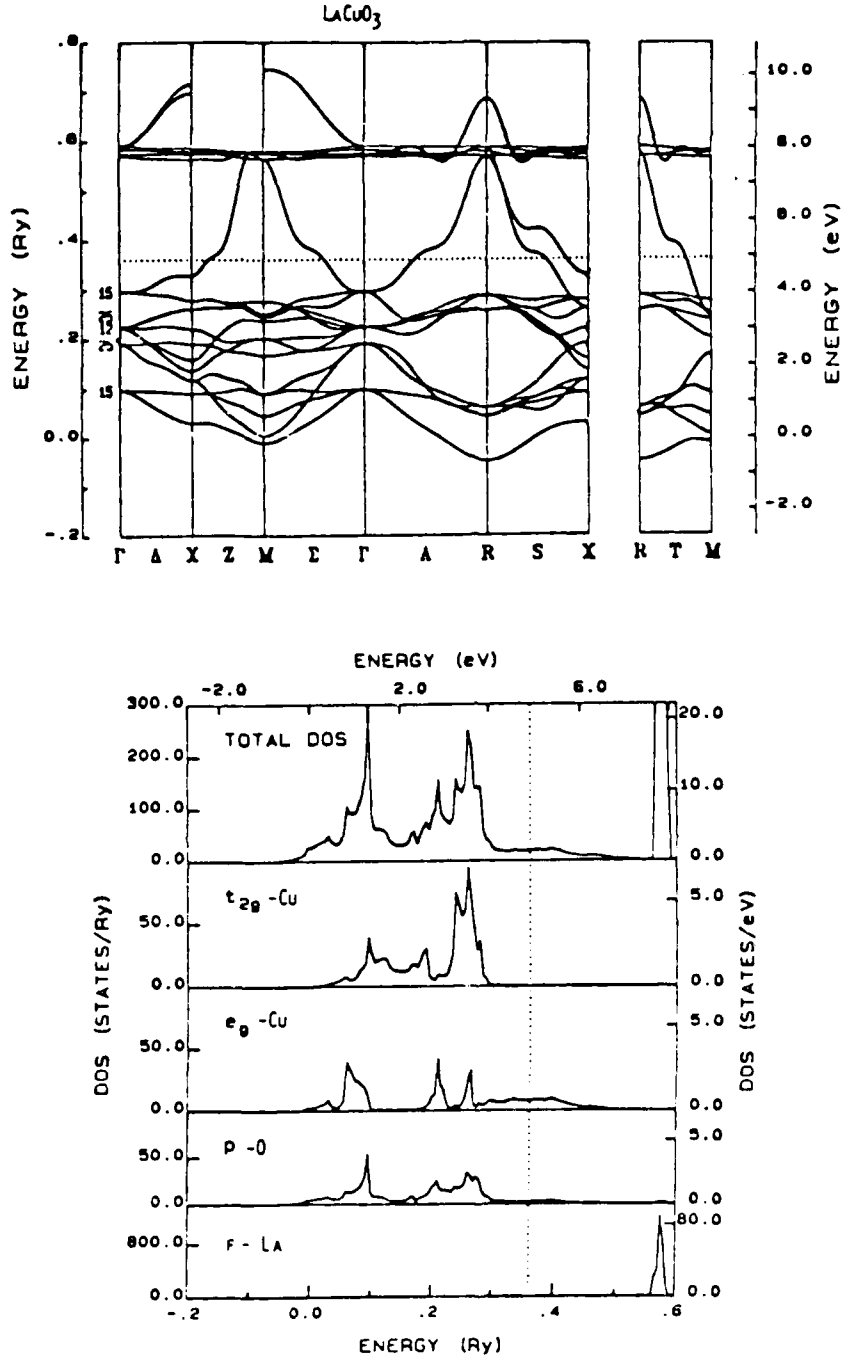

Figure 1. Band structure, density of states (DOS) and selected decomposed DOS for $LaCuO_3$.

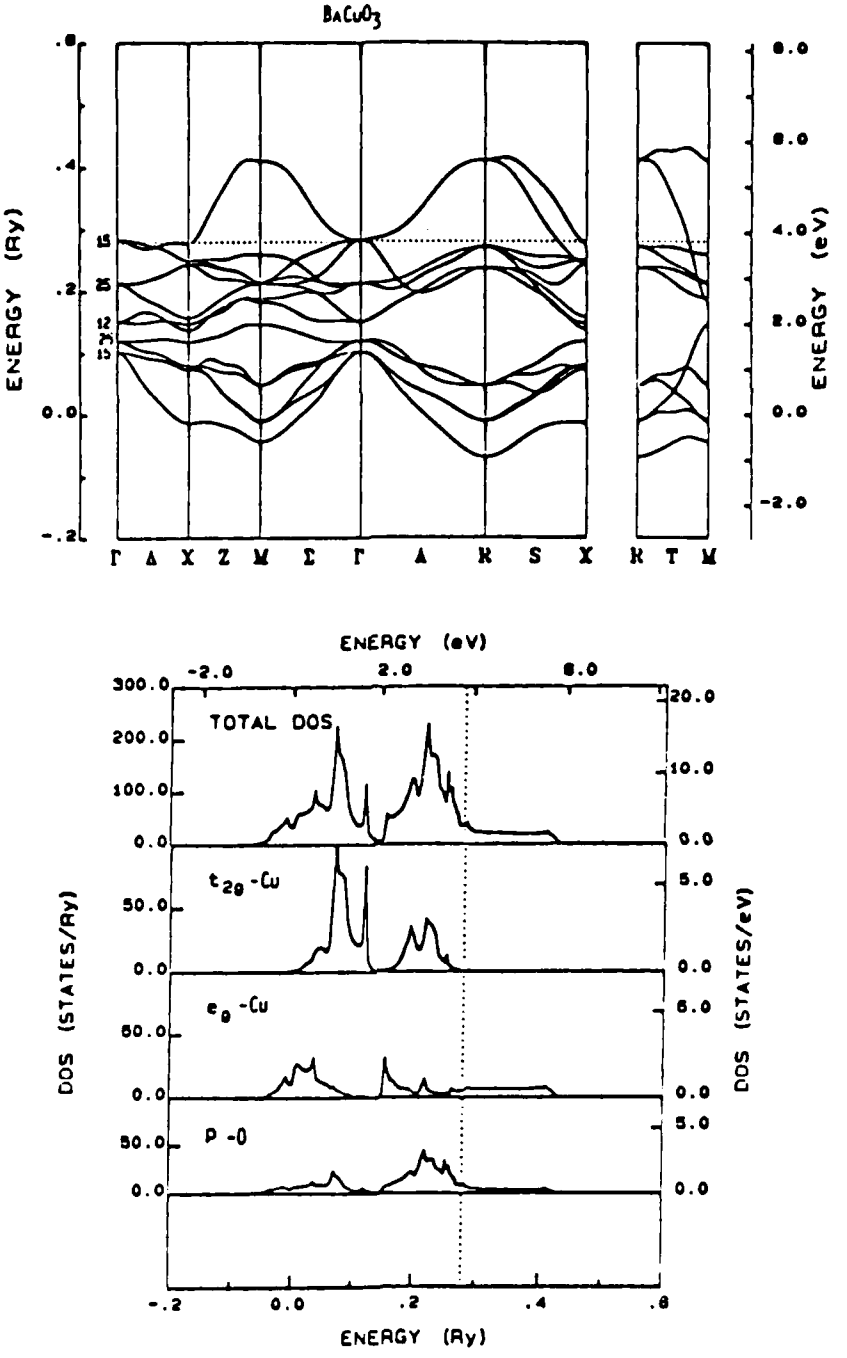

Figure 2. Band structure, density of states (DOS) and selected decomposed DOS for $BaCuO_3$.

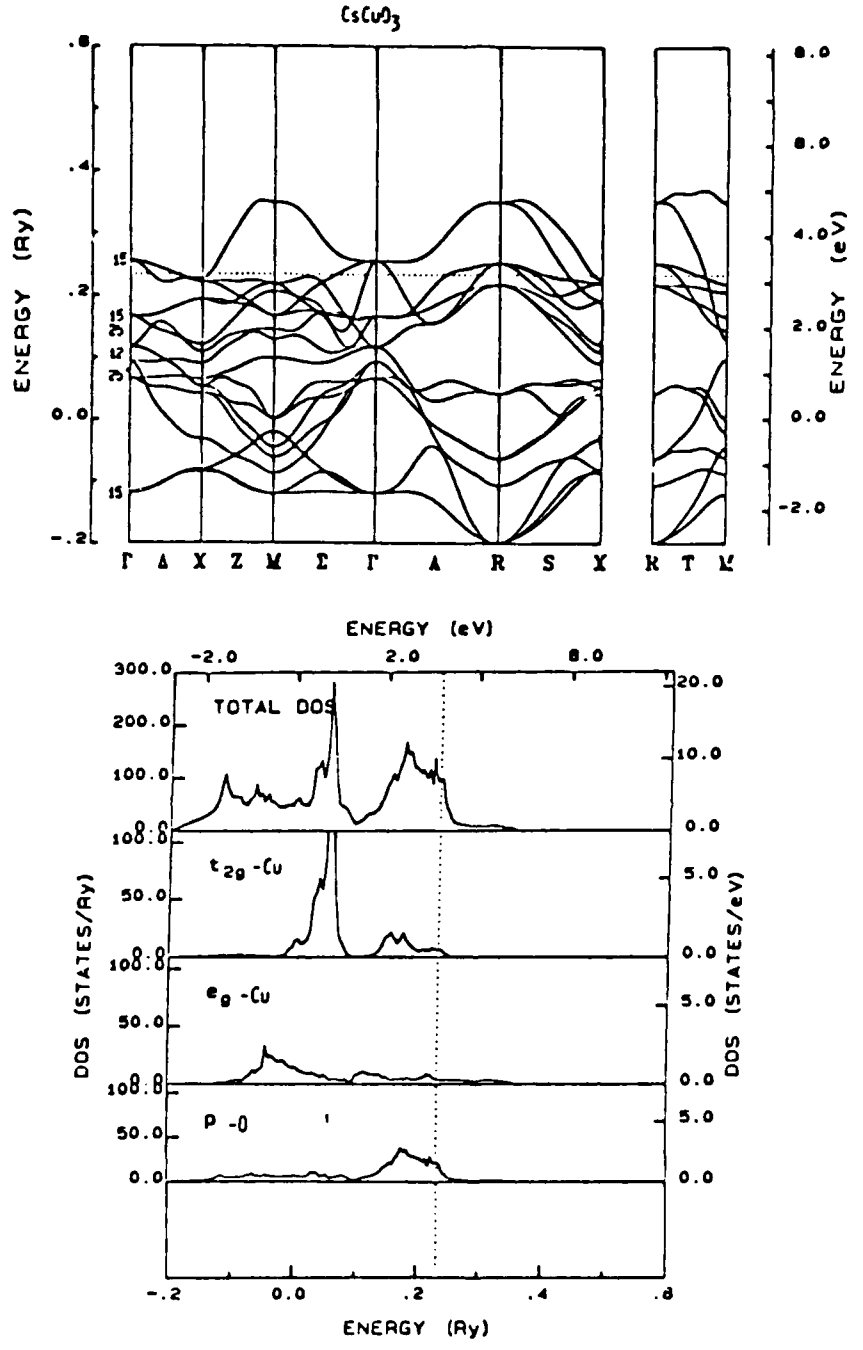

Figure 3. Band structure, density of states (DOS) and selected decomposed DOS for $CsCuO_3$.

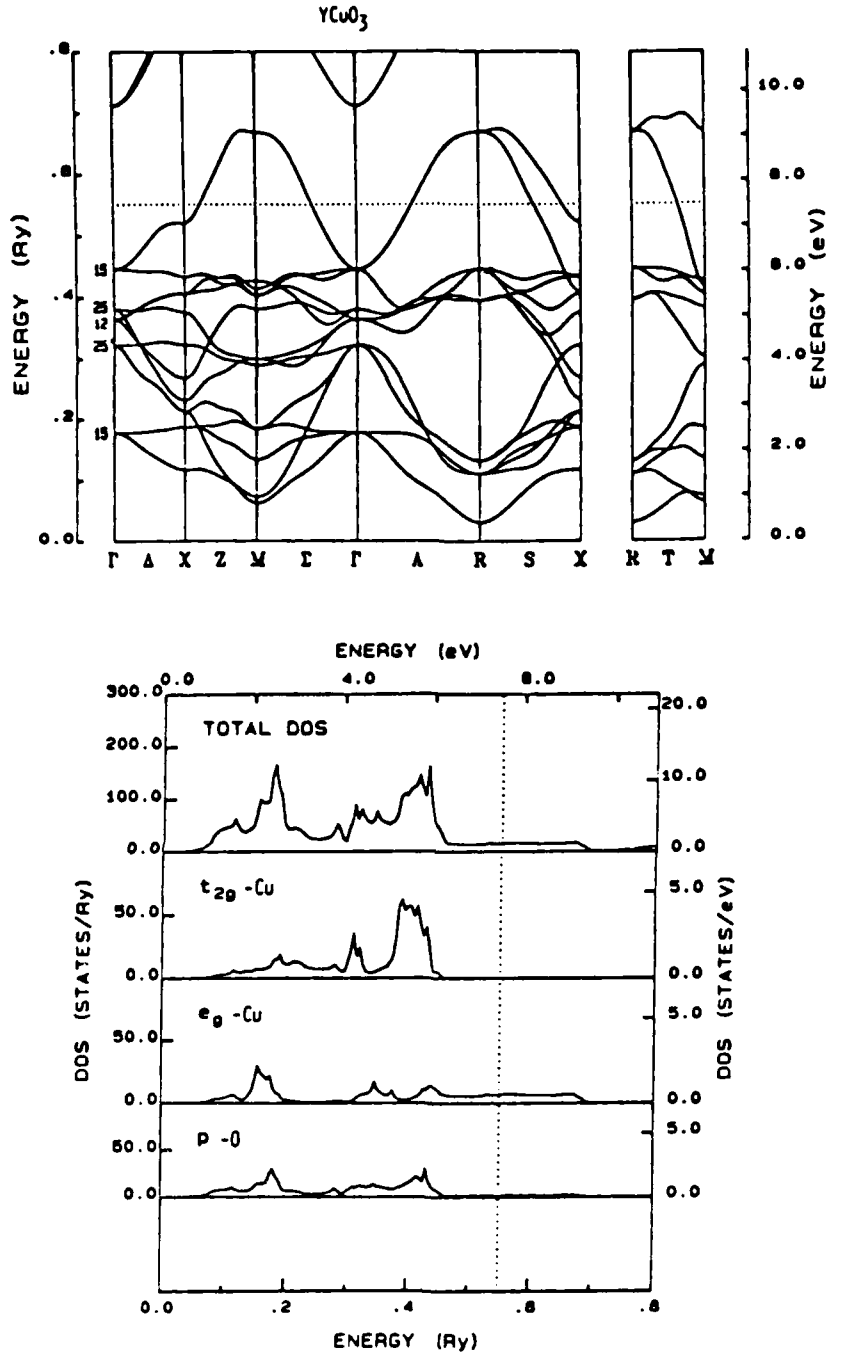

Figure 4. Band structure, density of states (DOS) and selected decomposed DOS for $YCuO_3$.

Table 1. Fermi energy E_F (Ry), decomposed and total densities of states (states/Ry) at E_F and contributions to η (eV/A^2) from the M, Cu, and O sites in $MCuO_3$.

	M-La	M-Ba	M-Cs	M-Y
E_F	0.382	0.280	0.233	0.551
N(M-s)	0.0042	0.0071	0.0645	0.0050
N(M-p)	0.0189	0.4968	15.7506	0.0095
N(M-t_{2g})	0.0442	0.1601	0.3147	0.0307
N(M-e_g)	0.0034	0.0013	0.1767	0.0060
N(M-f)	0.0956	0.0899	0.4303	0.0244
N(Cu-s)	0.1219	0.1205	0.0743	0.1205
N(Cu-p)	0.2607	0.4087	0.2578	0.1923
N(Cu-t_{2g})	0.0754	0.7294	6.6017	0.0156
N(Cu-e_g)	7.3835	4.9116	3.6857	7.0666
N(Cu-f)	0.0181	0.0890	0.0628	0.0119
N(O-s)	0.2175	0.1614	0.1058	0.2733
N(O-p)	9.6388	26.4336	61.3162	6.8178
N(O-t_{2g})	0.0144	0.0135	0.0238	0.0136
N(O-e_g)	0.0868	0.0765	0.0581	0.0982
N(O-f)	0.0229	0.0099	0.0190	0.0277
N(E_F)	19.3697	36.7274	94.9097	15.8271
ηM	0.000	0.012	0.485	0.000
ηCu	0.894	1.650	0.815	1.127
ηO	1.433	1.810	1.528	2.139

REFERENCES

1. E. F. Skelton, W. T. Elam, D. U. Gubser, S. H. Lawrence, M. S. *Osofsky, L. E. Toth, and S. A. Wolf, Phys Rev.* B 35:7140 (1987).
2. J. D. Jorgensen, H.-B. Schuttler, D. G. Hinks, D. W. Capone II, K. Zhang, M. B. Brodsky, and D. J. Scalapino, Phys. Rev. Lett. 58:1024 (1987).
3. R. M. Fleming, B. Batlogg, R. J. Cava, and E. A. Rietman, Phys. Rev. B 35:7191 (1987).
4. D. McK. Paul, G. Balakrishnan, N. R. Bernhoeft, W. I. F. David, and W. T. A. Harrison, Phys. Rev. Lett. 58:1976 (1987).
5. R. M. Hazen, L. W. Finger, R. J. Angel, C. T. Prewitt, N. L. Ross, H. K. Mao, C. G. Hadidiacos, P. H. Hor, R. L. Meng, and C. W. Chu, Phys. Rev. B 35:7238 (1987).
6. Y. LePage, W. R. McKinnon, J. M. Tarascon, L. H. Green, G. W. Hull, and D. M. Hwang, Phys. Rev. B 35:7245 (1987).
7. T. Siegrist, S. Sunshine, D. W. Murphy, R. J. Cava, and S. M. Zahurak, Phys. Rev. B 35:7137 (1987).
8. L. Hedin and B. I. Lundqvist, J. Phys. C 4:2064 (1971).
9. G. D. Gaspari and B. L. Gyorffy, Phys. Rev. Lett. 28:801 (1972).
10. D. D. Koelling and B. N. Harmon, J. Phys. C 10:3107 (1977).
11. W. E. Pickett, H. Krakauer, D. A. Papaconstantopoulos, and L. L. Boyer, Phys. Rev. B 35:7252 (1987).

BAND THEORY ANALYSIS OF ANISOTROPIC TRANSPORT IN La_2CuO_4 - BASED SUPERCONDUCTORS

by

Philip B. Allen,* Warren E. Pickett
Condensed Matter Physics Branch
Naval Research Laboratory
Washington, DC 20375-5000

and

Henry Krakauer
Department of Physics
College of William and Mary
Williamsburg, VA 23185

Abstract

The anisotropic resistivity $\rho_{\alpha\alpha}$ and Hall coefficient $R_{\alpha\beta\gamma}$ of $La_{2-x}M_xCuO_4$ are analyzed as a function of x using a rigid band treatment of the previously given LAPW bands of tetragonal La_2CuO_4. The experimental $\rho_{xx}(T)$ is used to extract λ_{tr}~3.8, which permits a conventional electron-phonon interpretation of the high T_c. The Hall coefficients are qualitatively explained, including sign discrepancies in published measurements.

*Department of Physics, State University of New York, Stony Brook, NY 11794-3800

PACS numbers: 74.70.-b, 72.15.Eb, 72.15.Gd

In cubic metals, band theoretic analysis of transport properties has given insight into electron-phonon interactions and superconducting properties.[1,2] Here we present a similar analysis for the new superconducting materials based on La_2CuO_4, with T_c~40K. A new feature of this analysis is that, unlike materials studied previously, these have highly anisotropic transport behavior. Our conclusion is that a consistent picture of both transport and superconductivity can be based on the standard electron-phonon model, using available density-functional band structures.[3,4] This conclusion agrees with the calculation of Weber,[5] and Pickett *et al.*,[4] and is not directly contradicted by any experimental evidence (the zero isotope effect[6] has only been reported in $YBa_2Cu_3O_7$).

The Bloch-Boltzmann theory of transport properties,[7] like the BCS-Eliashberg theory of superconductivity,[8] rests on the Migdal approximation[8,9] and is believed to be quantitatively reliable provided three circumstances hold: (1) the dominance of electron-phonon (as opposed to Coulomb) interactions, (2) the availability of the correct quasiparticle band structure, and (3) the smallness of the parameters $N(\epsilon_F)\hbar\omega_D$ and $N(\epsilon_F)\hbar/\tau$ where $N(\epsilon_F)$ is the Fermi-level density-of-states, ω_D is a characteristic phonon frequency, and $1/\tau$ the electronic scattering rate. The degree of success of our calculation serves as a test of the conjecture that circumstances (1) and (2) hold; circumstance (3) is directly checked later in the paper.

The free-electron formulas $\sigma=ne^2\tau/m$ and $R_H=-1/ne$ are meaningless except in cases where bands are parabolic, which does not apply here. On the other hand, a complete treatment using Bloch-Boltzmann theory is impossible until more is known about the phonon spectrum. Therefore we use an intermediate level of theory, where the collision term in the Boltzmann equation is repre-

sented by $-(F_k-f_k)/\tau$, F_k and f_k being the non-equilibrium and equilibrium (Fermi-Dirac) distribution functions. This model does not adequately describe effects due to inelastic or anisotropic scattering, but such effects are quite unimportant[1] except below $T=\theta_D/2$. The correct semiclassical dynamics is used, giving the results:[10]

$$j_\alpha = \sigma_{\alpha\beta}E_\beta + \sigma_{\alpha\beta\gamma}E_\beta B_\gamma \quad + \ldots \tag{1}$$

$$\sigma_{\alpha\beta} = e^2\tau(n/m)_{\alpha\beta} = (e^2\tau/\Omega)\sum_k v_{k\alpha}v_{k\beta}\,\delta(\epsilon_k-\epsilon_F) \tag{2}$$

$$\sigma_{\alpha\beta\gamma} = -(e^3\tau^2/\hbar c\Omega)\sum_k v_{k\alpha}\left[(\underline{v}_k\times\underline{p}_k)_\gamma v_{k\beta}\right]\delta(\epsilon_k-\epsilon_F) \tag{3}$$

where $\hbar v_{k\alpha}=\partial\epsilon_k/\partial k_\alpha$ and Ω is the volume of the crystal. We use the body-centered tetragonal (K_2NiF_4) unit cell with $a=3.79$ Å and $c=13.21$ Å. The tetragonal symmetry makes $\sigma_{\alpha\beta}$ diagonal with $\sigma_{xx}=\sigma_{yy}\neq\sigma_{zz}$, and $\sigma_{\alpha\beta\gamma}$ vanishes unless the tetragonal axes α,β,γ are all different. The Onsager antisymmetry $\sigma_{\beta\alpha\gamma}=-\sigma_{\alpha\beta\gamma}$ combined with tetragonal symmetry shows that there are only two independent components, σ_{xyz} (when $\underline{B}$ is parallel to the c axis, $\hat{z}$) and $\sigma_{yzx}=\sigma_{zxy}$ (when $\underline{B}$ is in the basal plane). The corresponding elements of the Hall coefficient tensor are

$$R_{xyz} = E_y/j_xB_z = \sigma_{xyz}/\sigma_{xx}\sigma_{yy} \tag{4}$$

with $R_{yzx}=R_{zxy}$ given by cyclic permutation. The formula for τ is in general[11] quite complicated, but at temperatures of order $0.7\theta_D$ or higher, a good[1,11] approximation is

$$\hbar/\tau = 2\pi\lambda_{tr}k_BT/F_{th} \tag{5}$$

$$F_{th} \cong (1-0.038\theta_D^2/T^2)^{-1} \tag{6}$$

Here λ_{tr} is a close approximation to the coupling constant[12] λ which fixes T_c, and F_{th} is a thermal correction factor. The value of λ_{tr} can be deduced by

comparing Eqs. (2) and (5) with the experiment. In the approximation used here, τ cancels from Eq. (4) for R_H.

Energy bands ϵ_k were taken from Ref. (4). The effect of alloying with divalent atoms (Sr, Ba) in place of La was treated in rigid band approximation by lowering the Fermi level appropriately, to accommodate x holes per primitive cell according to the formula $La_{2-x}M_xCuO_4$. For small x an orthorhombic distortion occurs which opens a gap, converting pure La_2CuO_4 into a semiconductor. The calculation was for the hypothetical tetragonal metal which presumably closely approximates the actual structure of the superconducting phase. For purposes of performing the Brillouin-zone sums in Eqs. (2,3), the tetrahedron method was used on a dense mesh of ~1000 inequivalent k-points. The values of ϵ_k on this mesh came from a careful Fourier interpolation based on LAPW calculations at 135 inequivalent k-points.

Numerical results are shown in Fig. 1 and Table I. There is inevitable noise in Brillouin zone sums which stems from the finite number of k points at which the bands ϵ_k are actually computed. Fourier interpolation can also introduce unphysical oscillations, but we minimized these using variations of the scheme of Koelling and Wood.[13] Nevertheless, mild unphysical oscillations exist, which are magnified in second derivatives of ϵ_k, especially in the z direction where dispersion is small and sampling was sparse. Therefore the Hall tensor (which involves second derivatives) is especially noisy, and this shows up in Fig. 1 as a discrepancy between R_{yzx} and R_{zxy}, which are supposed to be equal by symmetry. The computed R_{yzx} is quite smooth, whereas R_{zxy} (which alone involves $\partial^2\epsilon/\partial k_z^2$) has kinks and oscillations. The magnitudes are always in quite good agreement, especially in the range near x=0.15 of optimum T_c. The small kinks seen in $N(\epsilon)$ in Fig. 1 line up with the large

kinks in R_{zxy}, showing that these are also numerical noise.

A convenient formula which follows from Eq. (2) and (5) is

$$\lambda_{tr}/F_{th} = 0.842\times10^{-3}(\rho_{aa}(295K)-\rho_{aa}(0))\Omega_{paa}^2 \qquad (7)$$

where ρ is measured in $\mu\Omega$ cm, $\rho(0)$ is the residual resistance and the Drude plasma frequency (in eV) is defined by

$$\Omega_{pa\beta}^2 = 4\pi e^2(n/m)_{a\beta} = 4\pi e^2 N(\epsilon_F)\langle v_{ka}v_{k\beta}\rangle/\Omega_{cell} \qquad (8)$$

where Ω_{cell} is the volume of a unit cell and the average over the Fermi surface denoted by $\langle\ \rangle$ is defined by comparing Eq. (8) with Eq. (2). Figure 1 shows that whereas the density of states $N(\epsilon_F)$ is rapidly varying as x varies (this is a 2-d logarithmic saddle point feature, broadened into a bump by the weak z-direction dispersion of the band) the Drude plasma energy is smoothly varying and thus presumably insensitive to the minor discrepancies between the various energy band calculations of Refs. (3,4). Since Ω_p is the only theoretical input needed in Eq. (7) to obtain λ from ρ, this method is especially reliable, provided single-crystal resistivity measurements are used. A large single crystal was measured by Hidaka *et al.*[14] Unfortunately the superconducting and transport properties are not perfect enough for our purposes. Very beautiful measurements were obtained by Suzuki and Murakami[15] on a thin film single crystal of $La_{2-x}Sr_xCuO_4$ with x=.06 and a superconducting transition between 15 and 23K. The film was grown epitaxially on $SrTiO_3$ (100) and has the c axis perpendicular to the film. The measured value of $\rho_{xx}(0)$ was extrapolated to be ~250 $\mu\Omega$ cm, and $\rho_{xx}(295K)-\rho_{xx}(0)$ is ~450 $\mu\Omega$ cm. Taking Ω_p=2.9 eV from Table I, Eq. (7) yields λ_{tr}/F_{th}=3.2. The thermal factor F_{th} is greater than 1 and probably less than 1.2 yielding λ_{tr}~3.2-3.8 which can easily give T_c~40K or higher. This conclusion is consistent with estimates made in Refs. 4 and 5. Gurvitch reported[16] a preliminary estimate of λ_{tr}

using an isotropic average Ω_p^2 from Mattheiss[4] and polycrystalline data for $\rho(T)$. His estimate of λ_{tr} was similar in magnitude.

An important question is whether the measured temperature-dependent resistivity is actually caused by electron-phonon interactions and can be analyzed using Bloch-Boltzmann theory. The data of Ref. 15 give very strongly the expected appearance of an electron-phonon mechanism, except that the value of ρ is larger by 10 than in other good electron-phonon metals. This magnitude is accounted for in our model by the smallness of $(n/m)_{eff}$ and the strength of the scattering as measured by λ. A test of the validity of the analysis is to compute the dimensionless ratios $N(\epsilon_F)\hbar/\tau$ and a/ℓ. Both are about 1 at 295K in our analysis. This is common in good superconductors such as Nb_3Sn.[2] However, in the past whenever these ratios became as large as 1, a strong "saturation" effect[17] occurred in $\rho(T)$, indicating a failure of Bloch-Boltzmann theory, whereas no sign of saturation appears in the data of Ref. 15. A difference between La_2CuO_4 and Nb_3Sn is that in Nb_3Sn there are for almost all $\underset{\sim}{k}$ at the Fermi surface, other bands within $\hbar/\tau$~0.3 eV of ϵ_F, which mix with the band at ϵ_F at higher T due to virtual phonon scattering. In La_2CuO_4, with an even larger $\hbar/\tau$~0.6 eV, there are no other bands this close for most $\underset{\sim}{k}$. Allen and Chakraborty[18] have shown how the virtual interband scattering effect provides a plausible mechanism for the saturation effect, and the present data add weight to the argument.

A prediction of the present calculations is the anisotropy ratio $\rho_{zz}/\rho_{xx}=(\Omega_{pxx}^2/\Omega_{pzz}^2)$ which is 28 at x=0.15. This anisotropy has not yet been measured in crystals with good (Bloch-Boltzmann-like) conductivity. However, Shamoto *et al.*[19] have reported "preliminary measurements" of the critical field (H_{c2}) anisotropy for T close to T_c, obtaining $(H_{c2\parallel}/H_{c2\perp})^2$~170 and 40

for crystals doped with Ba and Sr respectively. This ratio should approximately equal ρ_{zz}/ρ_{xx}.

The Drude plasma frequency is in principle accessible to optical measurement, from the formula[20]

$$\sigma_{\alpha\beta}(\omega) = \frac{\Omega_{p\alpha\beta}^2/4\pi i}{\omega(1+\lambda(\omega)) + i/\tau(\omega)} + \sigma_{\alpha\beta}^{\text{interband}}(\omega).$$

For $\omega>\omega_D$, the phonon part of $\lambda(\omega)$ decays to zero and the phonon part of $1/\tau$ becomes a constant. A non-phonon (e.g. ordinary Coulomb) contribution to λ may remain at $\omega=\Omega_p$ however, which will affect the apparent measured value of Ω_p, as will structure in the interband part. Single crystal infrared data have not yet been reported, but would be very useful. On polycrystalline samples, Tajima *et al.*[21] have reported a plasma edge at wavelength 1.5 μm or $\hbar\Omega_p$=0.83 eV, which can be compared with our values of 2.9 eV and ~0.5 eV for light polarized $\perp$ or to the c axis.

Finally we discuss the Hall coefficient. The only single crystal measurement reported so far is R_{xyz}, with the $\underline{B}$ field perpendicular to the same film[15] on which $\rho_{xx}(T)$ was measured. The result has an interesting T dependence not contained in the simple theory of Eqs. (2,3). However, the accuracy of Eqs. (2,3) is expected to be less for R_H than for ρ. The reason is that these equations are equivalent to an <u>ansatz</u> that the distribution function F is displaced rigidly in reciprocal space by an amount proportional to $\underline{E}$ (when $\underline{B}$=0) and by an additional amount proportional to $\underline{E}x\underline{B}$ when $\underline{B}\neq 0$. The variational principle[7] (which holds for ρ but <u>not</u> for R_H) ensures that an error of order ϵ in F translates only into an error of order ϵ^2 in ρ, but remains on error of order ϵ in R_H. In Nb and Cu,[10] Eqs. (2,3) do quite well for R_H at T=300K, while in Pd,[22] large curvature anistropy caused an error of

a factor of 2. At lower T, significant T-dependence occurs in R_H of Cu, which has been explained[23] semiquantitatively by including corrections in F due to inelasticity and anisotropy. The temperature dependence of R_{xyz} reported in Ref. 15 is not entirely unlike that seen in Cu, and may be explainable as an electron-phonon effect when a more complete calculation is possible. The measured magnitude of R_{xyz} at 300K is $+92 \times 10^{-11} m^3/C$, larger by a factor 2.6 than our calculated value of $36 \times 10^{-11} m^3/C$ at x=0.06. This discrepancy is not much outside our previous experience in better understood metals, and the sign is correct (hole-like). It is interesting that R_{xyz} is predicted to switch to electron-like at x>0.24. This result underlines the fallacy in interpreting R_H as -1/ne. Such a picture would require a diverging number of holes as x increased toward 0.24, which converts instantly to a diverging number of electrons as x increases further. It is also interesting that when the $\underline{B}$ field is oriented parallel to the metallic xy layers, the Hall coefficient is predicted to be electron-like. This helps explain why measurements on polycrystalline samples[24] by different groups have yielded differing signs of R_H.

In summary, our results show that the biggest puzzle, the origin of the high T_c, is compatible with $\rho(T)$ and band theory in a conventional electron-phonon interpretation in La_2CuO_4-based superconductors. This makes the zero isotope shift of $YBa_2Cu_3O_7$ all the more puzzling. A new puzzle is exposed, the absence of saturation in $\rho(T)$ when $a/\ell \sim 1$, and a possible resolution is offered.

Acknowledgments

We thank B. Chakraborty for helpful discussions. P. B. Allen acknowledges a sabbatical stay at the Naval Research Laboratory, with support under the Intergovernmental Personnel Act. This work was supported by the Office of Naval Research Contract No. N00014-84-WR-24055 and National Science Foundation (NSF) Grant No. DMR-84-16046. Computations were done with NSF support on CRAY X-MP's at the University of Pittsburgh and the University of Illinois.

References

1. For cubic elements, see: P.B. Allen, T.P. Beaulac, F.S. Khan, W.H. Butler, F.J. Pinski, and J.C. Swihart, Phys. Rev. B34, 4331 (1986); P.B. Allen Phys. Rev. B (Rapid Commun. in press).

2. For A15 structure materials, see P.B. Allen, W.E. Pickett, K.M. Ho, and M.L. Cohen, Phys. Rev. Lett. 40, 1532 (1978).

3. L.F. Mattheiss, Phys. Rev. Lett. 58, 1028 (1987); J. Yu, A.J. Freeman, and J.-H. Xu, Phys. Rev. Lett. 58, 1035 (1987); T. Oguchi, Japanese J. Appl. Phys. 26, L417 (1987); K. Takegahara, H. Harima, and A. Yanase, Japanese J. Appl. Phys. 26, L352 (1987).

4. W.E. Pickett, H. Krakauer, D.A. Papaconstantopoulos, and L.L. Boyer, Phys. Rev. B 35, 7252 (1987).

5. W. Weber, Phys. Rev. Lett. 58, 1371 (1987).

6. B. Batlogg, R.J. Cava, A. Jayaraman, R.B. van Dover, G.A. Kourouklis, S. Sunshine, D.W. Murphy, L.W. Rupp, H.S. Chen, A. White, A.M. Mujsce, and E.A. Rietman, preprint.

7. For example J.M. Ziman, Electrons and Phonons (Oxford Univ. Press, 1960).

8. For example, D.J. Scalapino, in Superconductivity, edited by R.D. Parks (M. Dekker, NY, 1969) p 449.

9. A.B. Migdal, Zh. Eksperim i Teor. Fiz. 32, 399 (1957); Sov. Phys. JETP 5, 333 (1957).

10. T.P. Beaulac, F.J. Pinski, and P.B. Allen, Phys. Rev. B23, 3617 (1981).

11. P.B. Allen, Phys. Rev. B17, 3725 (1978).

12. W.L. McMillan, Phys. Rev. 167, 331 (1968); P.B. Allen and R.C. Dynes, Phys. Rev. B12, 905 (1975).

13. D.D. Koelling and J.H. Wood, J. Comp. Phys. 67, 253 (1986).

14. Y. Hidaka, Y. Enomoto, M. Suzuki, M. Oda, and T. Murakami, Japanese J. Appl. Phys. 26, L377 (1987).

15. M. Suzuki and T. Murakami, Japanese J. Appl. Phys. 26, L524 (1987).

16. M. Gurvitch, Bull. Am. Phys. Soc. 32, 905 (1987).

17. P.B. Allen, in Superconductivity in d- and f-band Metals, H. Suhl and M.B. Maple, eds. (Academic Press, NY, 1980) p 215.

18. P.B. Allen and B. Chakraborty, Phys. Rev. B23, 4815 (1981).

19. S. Shamoto, M. Onoda, and M. Sato, Sol. State Commun. 62, 479 (1987).

20. P.B. Allen, Phys. Rev. B3, 305 (1971).

21. S. Tajima, S. Uchida, S. Tanaka, S. Kanbe, K. Kitazawa, and K. Fueki, Japanese J. Appl. Phys. 26, L432 (1987).

22. T.P. Beaulac and P.B. Allen, J. Phys. F13, 383 (1983).

23. T.P. Beaulac and P.B. Allen, Phys. Rev. B28, 5439 (1983).

24. M. Tonouchi, Y. Fujiwara, S. Kita, T. Kobayashi, M. Takata, and T. Yamashita, Japanese J. Appl. Phys. 26, L519 (1987); S. Uchida, H. Takaji, H. Ishii, H. Eisaki, T. Yabe, S. Tajima, and S. Tanaka, ibid., L440.

Figure Caption

Figure 1. Rigid band calculations of density of states $N(\epsilon_F)$, Hall coefficients, and Drude plasma energies of $La_{2-x}M_xCuO_4$ versus x, the concentration of the divalent atom M. Negative x could be achieved by doping with a quadrivalent atom.

Table Caption

Table I. Rigid band calculations as in Fig. 1 at various concentrations x of divalent atoms.

x	0.00	0.05	0.10	0.15	0.20	unit
$N(\epsilon_F)$	16.0	19.2	25.3	28.4	26.6	(state/Ry cell)
$\sqrt{\langle v_x^2 \rangle}$	3.0	2.7	2.3	2.2	2.2	(10^7cm/s)
$\sqrt{\langle v_z^2 \rangle}$	0.32	0.36	0.37	0.41	0.46	(10^7cm/s)
Ω_{pxx}	3.0	2.9	2.9	2.9	2.8	(eV)
Ω_{pzz}	0.32	0.38	0.47	0.55	0.58	(eV)
R_{xyz}	46.7	37.8	28.3	18.4	8.4	($10^{-11}m^3$/C)
R_{yzx}	-151.	-122.	-107.	-94.	-96.	($10^{-11}m^3$/C)

La(2)CuO(4)

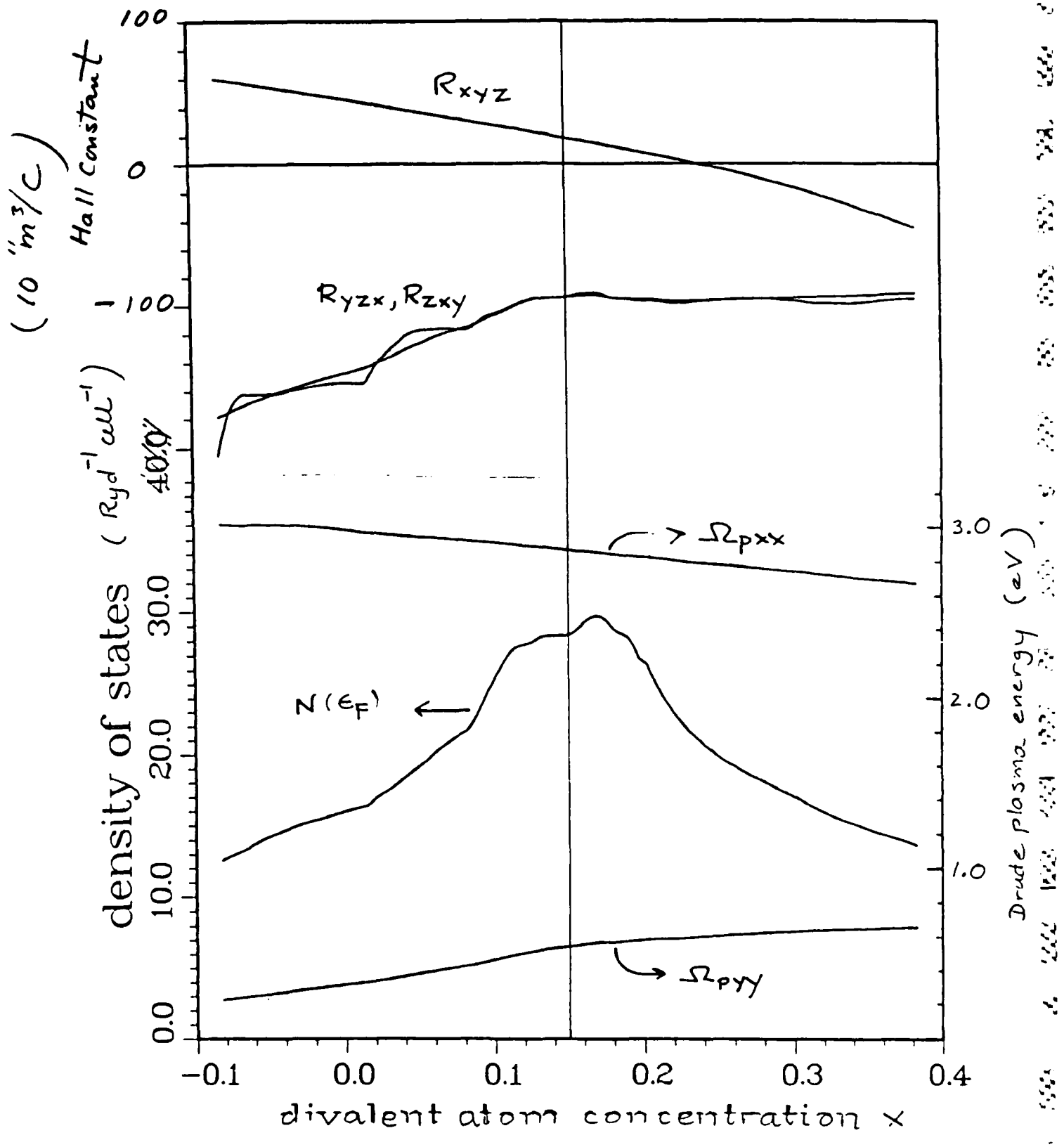
100
0
-100
Hall constant
(10 $^{-3}$ m^3/C)
R_{xyz}
R_{yzx}, R_{zxy}
Ω_{pxx}
Ω_{pyy}
$N(\epsilon_F)$
density of states (Ryd^{-1} cell^{-1})
40.0
30.0
20.0
10.0
0.0
3.0
2.0
1.0
Drude plasma energy (eV)
-0.1
0.0
0.1
0.2
0.3
0.4
divalent atom concentration x

High Temperature Superconductors: Electronic Structure Changes due to Replacement of La with Ba and Sr in the Cu-O - based Systems

H. KRAKAUER,* W. E. PICKETT, D. A. PAPACONSTANTOPOULOS, AND L. L. BOYER

*College of William and Mary, Williamsburg, VA 23185
Naval Research Laboratory, Washington, DC 20375-5000

The replacement of some La in La_2CuO_4 with divalent atoms has been found to lead to high temperature superconductivity with T_c=30-40 K. These superconductors have a bct layer perovskite structure with large anisotropies in their electronic band structure. Using first principles local density methods applied to both layer perovskite and the related cubic perovskite structures, we find that alloying on the La site leads to large changes in the chemical bonding of both structures, except near the Fermi level where a rigid band picture is reasonable. Large changes in the spectral density near the "dopant" atom occurs on both the nearby O and Cu atoms, and is not simply described by a Cu(2+)-Cu(3+) valence change. These results are consistent with recent x-ray absorption studies by Tranquada et al.

1. INTRODUCTION

The discovery of high temperature superconductivity in rare-earth copper oxides by Bednorz and Muller [1] and the subsequent extension of the critical temperature (T_c) to the 90-100 K range by a large number of laboratories has raised intriguing questions regarding the origin of the coupling mechanism in these materials. The important questions are more fundamental even than the origin of the pairing interaction, however, since these copper oxides are qualitatively different from previous high T_c superconductors. These copper oxides are ceramics which in spite of being metallic possess a large degree of ionic character. As a result, the electronic structure and response, the effects of alloying and the character of the electron-phonon interaction may be qualitatively different from conventional superconductors.

2. DESCRIPTION OF THE CALCULATIONS

We have used the Linearized Augmented Plane Wave (LAPW) method [2] to investigate the electronic structure of La_2CuO_4 and $LaBaCuO_4$. Since the layer perovskite structure is a relatively low symmetry bct structure and displays an unusual mixture of ionic and metallic characteristics, it is preferable to use the fully general form for the density and potential which we have implemented in our LAPW. For the cubic perovskites $MCuO_3$, M=La,Ba, we have used the Augmented Plane Wave method in the muffin-tin approximation. In both sets of calculations the Hedin-Lundqvist form of local density exchange-correlation potential was used. A more complete description of the methods has been presented elsewhere [3].

3. DISCUSSION

A synopsis of the phenomenology of the La-Cu-O system is this. The pure La compound, which probably contains a few percent O vacancies, appears from the rise in resistivity at low temperature to be semiconducting. Investigation of its crystal structure revealed a unit cell-doubling distortion to an orthorhombic structure [4]. When Sr or Ba is substituted for La, however, the orthorhombic distortion is inhibited (or very nearly so), the material shows metallic resistance behavior, and it becomes superconducting at 30-40 K [1,5,6]. A central question then is the role of the alkaline earth alloying. Does this replacement simply "dope" the semiconducting orthorhombic phase, thereby causing it to become metallic, and therefore superconducting? Does addition of Ba or Sr move the system away from an electronic instability, and therefore restore a crystal structure which is superconducting? This point of view has been taken by Mattheiss [7] and by Weber [8], who find a strong coupling between the in-plane Cu-O breathing mode and electronic states near the Fermi level. Finally, there is even the possibility that the divalent cation is essential to the pairing of electrons, such as might result from a Cu(2+) to Cu(3+) valence change or fluctuation.

It is such questions as these which have led us to study the influence of Ba on the electronic structure of La_2CuO_4. The question of the valence change is clear in our calculations: the electron which is lost when one La atom per unit cell is replaced with a Ba atom comes more or less equally from the Cu and the four O(x,y) atoms, that is, it simply comes from the O-Cu band crossing the Fermi level. Thus we find no support for the widely discussed Cu(2+)-Cu(3+) valence change, and this is in agreement with the x-ray absorption studies of Tranquada et al. [9]

By comparing the density of states N(E) of La_2CuO_4 and $LaBaCuO_4$ near the number of electrons for x=0.0-0.2, we can ascertain whether a rigid band model is reasonable for describing the bands near E_F in $La_{2-x}Ba_xCuO_4$. The rigid band picture has been invoked without explicit justification by several workers, based on its success (for small alloy concentrations) in many metallic systems. In the present materials, which have a high degree of ionic character and for which the alloying involves replacing the La^{3+} ion with a Ba^{2+} ion, the rigid band picture must be suspect. Our results show, however, that near E_F this picture should give a reasonable description of N(E), and therefore apply about equally well to both Ba and Sr additions. Well below E_F, on the other hand, the spectral density on both the Cu and O(z) atoms near the Ba atom is rearranged substantially. These shifts may produce changes in the polarizability of the material which will affect the electronic response, which could in turn be important in either phononic or electronic pairing mechanisms.

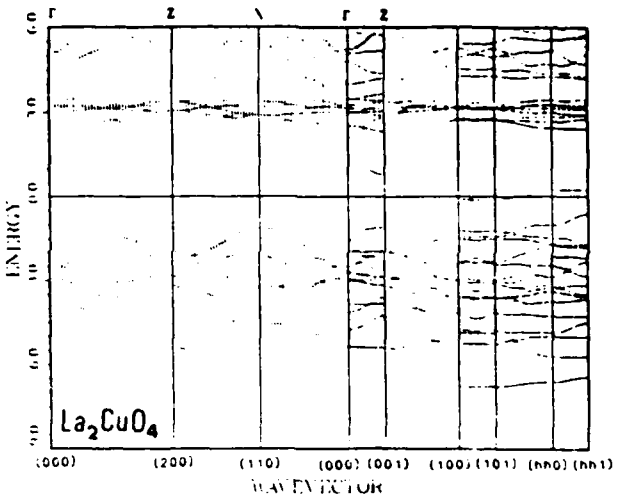

Figure 1. Band structure of La_2CuO_4 along several directions, given in units of (π/a, π/a, 2π/c), h=1/2. High symmetry points are labelled at the top.

Using the rigid band picture, then, we can give the band theory prediction of the effects of varying the Ba (or Sr) concentration x. A van Hove singularity occurs in the density of states (published previously [3]) at x=0.14, which is also very near the concentration at which the measured T_c is found to be a maximum. The band structure along several directions is shown in Fig. 1, where the position of the van Hove singularity along the $(k_x,0,0)$ direction is reflected in the band which comes within 0.1 eV of E_F. We find $N(E_F,x=0.14)=29$ states/Ry-cell, compared to $N(E_F,x=0.0)=16$ states/Ry-cell, which leads to an increase in the McMillan-Hopfield parameter (one component of the electron-phonon interaction strength) by 20% for the Cu atom and nearly 50% for the in-plane O atom. The studies of the electron-phonon coupling strength and resulting values of T_c are presented elsewhere in these proceedings.

4. ACKNOWLEDGMENTS

This work was supported by National Science Foundation (NSF) Grant No. DMR-84-16046 and by Office of Naval Research Contract Nos. N00014-84-WR-24055 and N00014-87-WX-24226. Computations were carried out under the auspices of the NSF on CRAY X-MP's at the University of Pittsburgh and the University of Illinois. We acknowledge assistance of P. B. Allen in preparing Figure 1.

REFERENCES

[1] J. G. Bednorz and K. A. Müller: Z. Phys. B64, (1986)189.
[2] S.-H. Wei and H. Krakauer: Phys. Rev. Lett. 55, (1985)1200, and references therein.
[3] W. E. Pickett, H. Krakauer, D. A. Papaconstantopoulos and L. L. Boyer: Phys. Rev. B35, (1987)xxxx.
[4] J. D. Jorgensen et al.: Phys. Rev. Lett. 58, (1987)1024.
[1] J. G. Bednorz and K. A. Müller: Z. Phys. B64, (1986)189.
[5] R. J. Cava, R. B. van Dover, B. Batlogg, and E. A. Rietman: Phys. Rev. Lett. 58, (1987)408.
[6] C. W. Chu, P. H. Hor, R. L. Meng, L. Gao, Z. J. Huang, and Y. Q. Wang: Phys. Rev. Lett. 58, (1987)405.
[7] L. F. Mattheiss: Phys. Rev. Lett. 58, (1987)1028.
[8] W. Weber: Phys. Rev. Lett. 58, (1987)1371.
[9] J. M. Tranquada, S. M. Heald, A. Moodenbaugh and M. Suenaga: Phys. Rev. B35, (1987)xxxx.

Calculations of the Superconducting Properties of Cu-O Based Perovskite-Like Structures

D. A. PAPACONSTANTOPOULOS, W. E. PICKETT, H. KRAKAUER,* AND L. L. BOYER

Naval Research Laboratory, Washington, DC 20375-5000
*College of William and Mary, Williamsburg, VA 23185

We have used the results of first principles local density band structure calculations to calculate the McMillan-Hopfield parameter η in a series of ordered cubic perovskite and layered perovskite structures of the form $M_xN_yCuO_z$, where M and N are La, Ba, and Cs. We find relatively low values of η compared to those of transition metal superconductors, but within a range of soft oxygen phonon modes the resulting electron-phonon coupling strength λ is large ($\lambda \sim 2.5$). This strength appears to be sufficient to explain the high transition temperatures T_c=30-40 K in these materials within the usual electron-phonon mechanism.

1. INTRODUCTION

The recent remarkable discoveries [1-4] of superconducting transition temperatures T_c in the range of 40-100 K in perovskite-like compounds, has raised the question as to whether the traditional electron-phonon mechanism is valid in these systems. We investigate this question using a method which has been highly successful in evaluating the superconducting properties of the previously known superconductors.

2. CALCULATIONS AND DISCUSSION

We have performed band structure calculations [5] for the system $La_{2-x}Ba_xCuO_{4-y}$ with x=0,1 and y=0. This alloy is a high temperature superconductor for small values of x and y, with a maximum T_c=40 K at x=0.15. We have used the results of the band calculations and the theory of Gaspari and Gyorffy [6] to calculate the McMillan-Hopfield parameter $\eta = N(E_F)\langle I^2\rangle$. The values of η together with the average electron-ion matrix elements $\langle I^2\rangle$ are given in Table I for each component of the layered compounds La_2CuO_4 and $LaBaCuO_4$ and for the x=0.14 material in the rigid band approximation. For comparison we have also performed similar calculations for the cubic perovskites $LaCuO_3$, $BaCuO_3$ and $CsCuO_3$ and the results are included in Table I. From Table I we note that $N(E_F)$ is significantly larger for the Ba than for the La compounds. However, in the Ba compounds the matrix elements $\langle I^2\rangle$ decrease moderately for the Cu site and substantially for the O sites.

As a result η, which is the product of $N(E_F)$ and $\langle I^2\rangle$, doesn't increase proportionally to $N(E_F)$. In fact η_O decreases from La_2CuO_4 to $LaBaCuO_4$ in spite of the factor of three increase in $N(E_F)$. An interesting point is that the values of η_{Cu} and $\eta_{O_{tot}}$ are fairly close between La_2CuO_4 and $LaCuO_3$ which suggests that the cubic-perovskite structure, if stable, might also provide high temperature superconductors.

If we consider the per atom value of both $N(E_F)$ and η in these materials it becomes clear that they both are significantly smaller than those of previously referred to as high temperature superconductors (A15 compounds, NbN, etc.). On the other hand an analogy can be drawn with PdH which has $N(E_F)$=0.48 states/eV, η_{Pd}=0.86 $\frac{eV}{\text{Å}^2}$, η_H=0.39 $\frac{eV}{\text{Å}^2}$ and $T_c \approx 10$ K. In PdH soft phonon modes associated with hydrogen vibrations have been shown to be responsible for the electron-phonon coupling [7].

In an attempt to raise the value of η in this class of materials we performed the same calculation for $CsCuO_3$. This calculation brings E_F into a high DOS region ($N(E_F)$=3.48 states/eV/spin) but due to a decrease in $\langle I^2\rangle$ the values of η, with the exception of η_{Cs}, remain close to those of the other compounds.

In this spirit we calculate the electron-phonon coupling λ as follows. We first write λ as a sum of contributions for the different atomic sites, i.e.

$$\lambda = \left(\frac{\eta_{La}}{M_{La}} + \frac{\eta_{Cu}}{M_{Cu}} + \frac{\eta_O}{M_O} \right) \frac{1}{\langle \omega^2 \rangle} \qquad (1)$$

where $\langle \omega^2 \rangle$ is an rms vibrational frequency. Because we find that $\eta_{La} \approx 0$ and because $M_{Cu} \gg M_O$ we can write,

$$\lambda = \frac{\eta_{Cu}}{M_{Cu}\omega_{Cu}^2} + \frac{\eta_O}{M_O \omega_O^2} . \qquad (2)$$

The average phonon frequencies ω_{Cu} and ω_O may be obtainable from Born-von Karman fits to neutron scattering measurements. However, since such analysis is not available at present we have made the simplifying assumption that

$$M_{Cu}\omega_{Cu}^2 = M_O \omega_O^2 \qquad (3),$$

which follows if Cu-O modes dominate the coupling to Fermi surface electrons. Treating ω_O as a variable parameter, we have calculated λ as a function of ω_O. Subsequently we calculate T_c using the Allen-Dynes equation [8]:

$$T_c = f_1 f_2 \frac{\omega_{log}}{1.2} \exp_2 \left[- \frac{1.04(1+\lambda)}{\lambda - \mu^* - 0.62\,\lambda\mu^*} \right] \qquad (4)$$

where μ^*=0.1 is the Coulomb pseudopotential the inclusion of the prefactors f_1 and f_2 are important for large values of λ as discussed by Allen and Dynes.

Our results for both λ and T_c as a function of ω_O are shown in Fig. 1 for x=0.0 and for x=0.14 based on a rigid band model evaluation (justified elsewhere) of $N(E_F)$ and η.

Figure 1 shows that for values ω_0 close to 200 K λ is about 2.6 and T_c is about 35 K. This result indicates that as long as the average phonon frequency is in the above frequency range at least the 40 K superconductors can be understood within the conventional electron-phonon mechanism.

3. ACKNOWLEDGMENTS

This work was supported by National Science Foundation (NSF) Grant No. DMR-84-16046 and by Office of Naval Research Contract Nos. N00014-84-K-24055 and N00014-87-K-24226. Computations were carried out under the auspices of the NSF on CRAY X-MP's at the University of Pittsburgh and the University of Illinois.

REFERENCES

[1] J. G. Bednorz and K. A. Müller: Z. Phys. B 64, (1986)189.
[2] H. Takagi, S. Uchida, K. Kitazawa, and S. Tanaka: Jpn. J. Appl. Phys. Lett. 26, (1987)L123.
[3] R. J. Cava, R. B. van Dover, B. Batlogg, and E. A. Rietman: Phys. Rev. Lett. 58, (1987)408.
[4] C. W. Chu, P. H. Hor, R. L. Meng, L. Gao, Z. J. Huang, and Y. Q. Wang: Phys. Rev. Lett. 58, (1987)405.
[5] W. E. Pickett, H. Krakauer, D. A. Papaconstantopoulos, and L. L. Boyer: Phys. Rev. B35, (1 May 1987, in press).
[6] G. D. Gaspari and B. L. Gyorffy: Phys. Rev. Lett. 28, (1972)801.
[7] D. A. Papaconstantopoulos, B. M. Klein, E. N. Economou, and L. L. Boyer: Phys. Rev. B17, (1978)141.
[8] P. B. Allen and R. C. Dynes: Phys. Rev. B12, (1975)905.

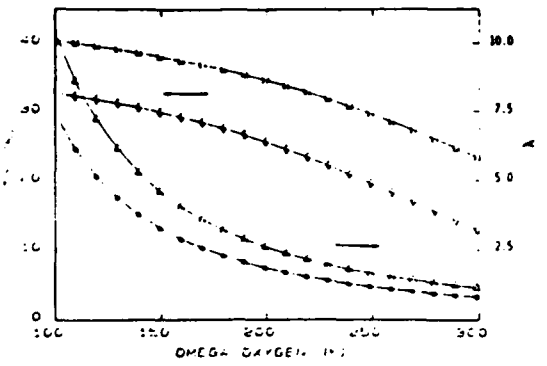

Figure 1. Calculated values of λ (right hand scale) and T_c (left hand scale). In each case the lower curves refer to La_2CuO_4 (i.e. stars and diamonds) and the upper curves (triangles and squares) refer to $La_{1.86}(Ba,Sr)_{0.14}CuO_4$.

Table I. Densities of states at E_F (states/eV/spin), electron-ion matrix element $\langle I^2 \rangle$ (eV/A)^2 and McMillan-Hopfield parameter η (eV/A^2) per atom, and the total η for all O atoms in the cell. For the $LaBaCuO_4$ compound, the La and Ba quantities have been averaged.

	La_2CuO_4	$La_{1.86}Ba_{0.14}CuO_4$	$LaBaCuO_4$	$LaCuO_3$	$BaCuO_3$	$CsCuO_3$
$N(E_F)$	0.62	1.08	1.85	0.71	1.35	3.48
$\langle I^2 \rangle_{La,Ba,Cs}$	0.0	0.006	0.07	0.0	0.009	0.14
$\langle I^2 \rangle_{Cu}$	1.00	0.69	0.59	1.25	1.22	0.24
$\langle I^2 \rangle_{O_{xy}}$	1.16	0.94	0.17	0.68	0.44	0.15
$\langle I^2 \rangle_{O_z}$	0.06	0.10	0.13	-	-	-
$\eta_{La,Ba,Cs}$	0.0	0.006	0.12	0.0	0.012	0.49
η_{Cu}	0.62	0.74	1.08	0.89	1.65	0.82
$\eta_{O_{xy}}$	0.72	1.00	0.32	0.48	0.60	0.51
η_{O_z}	0.04	0.10	0.24	-	-	-
$\eta_{O_{tot}}$	1.52	2.20	1.12	1.44	1.80	1.53

PREDICTION OF ANISOTROPIC THERMOPOWER OF $La_{2-x}M_xCuO_4$

Philip B. Allen,* Warren E. Pickett, and Henry Krakauer**

Condensed Matter Physics Branch, Naval Research Laboratory, Washington, DC 20375-5000, *Department of Physics, State University of New York, Stony Brook, NY 11794-3800, **Department of Physics, College of William and Mary, Williamsburg, VA 23185

INTRODUCTION

The thermopower tensor $S_{\alpha\beta}(T)$ of a tetragonal or orthorhombic crystal is diagonal in the crystallographic axes and equals, according to Boltzmann theory[1]

$$S_{\alpha\alpha}(T) = -\frac{k_B}{e}\int d\epsilon\left(\frac{\epsilon-\mu}{k_BT}\right)\sigma_{\alpha\alpha}(\epsilon)\left(-\frac{\partial f}{\partial\epsilon}\right)/\int d\epsilon\,\sigma_{\alpha\alpha}(\epsilon)\left(-\frac{\partial f}{\partial\epsilon}\right) \tag{1}$$

$$\sigma_{\alpha\alpha}(\epsilon) = e^2N(\epsilon)\,v_\alpha^2(\epsilon)\tau(\epsilon) \tag{2}$$

where $N(\epsilon)$, $v_\alpha^2(\epsilon)$, and $\tau(\epsilon)$ are the density of states, mean square velocity (α-component) and scattering lifetime, averaged for states with energy ϵ. If a Sommerfeld expansion of $\sigma_{\alpha\alpha}(\epsilon)$ is valid, the integrals in Eq. (1) yield a result linear in T and proportional to $\sigma'_{\alpha\alpha}(\mu)/\sigma_{\alpha\alpha}(\mu)$. However, the integrands in Eq. (1) do not become vanishingly small until $\pm 10k_BT \sim .02$Ry (at 300K) above and below ϵ_F, so the Sommerfeld expansion fails and S is not linear.

We have used the band structure of Pickett *et al.*[2] and the rigid band approximation to calculate $S_{xx}(T)$ and $S_{zz}(T)$ for $La_{2-x}M_xCuO_4$ where M is Ca, Sr, or Ba. The values of $N(\epsilon)$ and $v_\alpha^2(\epsilon)$ come directly from the calculated eigenvalue spectrum, whereas $\tau(\epsilon)$ requires an additional calculation. If electron-phonon scattering dominates (which provides a reasonable and conservative explanation[3] for the measured $\rho_{\alpha\alpha}(T)$ in samples with linear T-dependence and rrr≥4) then $\tau(\epsilon)$ is given by

$$1/\tau(\epsilon) = 2\pi\lambda(\epsilon)k_BT/\hbar \tag{3}$$

and $\lambda(\epsilon)$ can be approximated by $\sum_a \eta_a(\epsilon)/M_a\langle\omega^2\rangle$ where $\eta_a(\epsilon)$ has already been calculated[2] in the rigid muffin tin model. Alternately, if impurity scattering dominates, one might assume $1/\tau(\epsilon) \propto N(\epsilon)$, or possibly $1/\tau(\epsilon) =$ const. The results for $\sigma_{\alpha\alpha}(\epsilon)$ and $S_{\alpha\alpha}(T)$ for all three models are shown in Figs. 1 and 2. All three models predict moderately large positive ("hole-like") behavior of S_{zz} and smaller, negative ("electron-like") behavior of S_{xx}. In polycrystalline samples, Maeno *et al.*[4] have reported

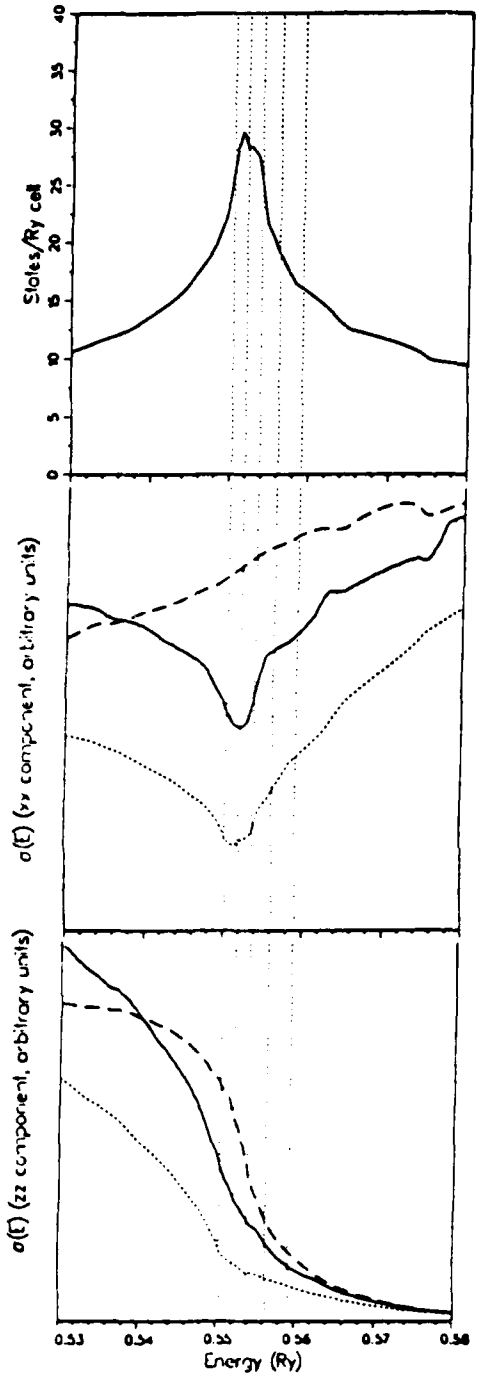

Figure 1. Upper panel: $N(\epsilon)$ vs ϵ; middle and lower panels: $\sigma_{xx}(\epsilon)$ and $\sigma_{zz}(\epsilon)$ assuming: (solid line: $1/\tau \propto \sum_i \eta_a/M_a$); (dotted line: $1/\tau \propto N(\epsilon)$); (dashed line: $1/\tau$ = const.) The vertical dotted lines denote $\epsilon_F(x)$ for concentrations x of divalent atoms equal to 0.2, 0.15, 0.1, 0.05, and 0 in order of increasing ϵ_F.

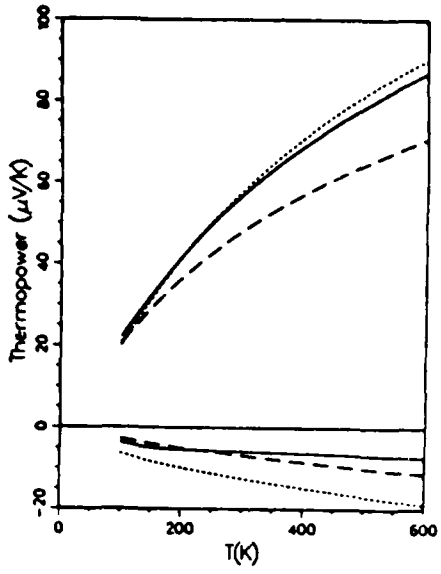

Figure 2. $S_{zz}(T)$ (positive values) and $S_{xx}(T)$ (negative values) versus T for concentration x=0.15. The solid, dotted, and dashed lines follow the code of Fig. 1.

a positive and nearly T-independent $S(T) \approx 25\mu V/K$ at x=0.15 and T=300 K. We find a fairly weak x-dependence of S, as shown in Table I. It is amusing that the "sign of the carriers" predicted in our thermopower calculation switches depending on crystallographic orientation, just as our prediction of the Hall tensor,[3] but in an opposite way: the Hall coefficient is "hole-like" if the orbits are in the xy plane, whereas $S_{xx} - S_{yy}$ is "electron-like".

ACKNOWLEDGMENTS

P. B. Allen acknowledges a sabbatical stay at the Naval Research Laboratory, with support under the Intergovernmental Personnel Act. This work was supported by the Office of Naval Research Contract No. N00014-84-WR-24055 and the National Science Foundation (NSF) Grant No. DMR-84-16046. Computations were done with NSF support on CRAY X-MP's at the University of Pittsburgh and the University of Illinois.

Table I. Thermopower (in $\mu V/K$) at 300 and 600 K for various concentrations x (the crystal structure is assumed tetragonal K_2NiF_4-type; the scattering rate $1/\tau$ is taken proportional to $\sum_a \eta_a/M_a$).

x	S_{xx}(300K)	S_{xx}(600K)	S_{zz}(300K)	S_{zz}(600K)
0.00	-15.	-20.	59.	111.
0.05	-17.	-19.	61.	105.
0.10	-15.	-14.	60.	97.
0.15	- 6.	- 7.	57.	87.
0.20	6.	1.	50.	76.

REFERENCES

1. N.W. Ashcroft and N.D. Mermin, Solid State Physics, (Holt, Rinehart, and Winston, New York, 1976, pp 250-8.
2. W.E. Pickett, H. Krakauer, D.A. Papaconstantopoulos, and L.L. Boyer, Phys. Rev. B35, 7252 (1987).
3. P.B. Allen, W.E. Pickett, and H. Krakauer, to be published.
4. Y. Maeno, Y. Aoki, H. Kamimura, J. Sakurai, and T. Fujita, Japan. J. Appl. Phys. 26, L402 (1987).

CHARACTER OF STATES NEAR THE FERMI LEVEL IN $YBa_2Cu_3O_7$

H. Krakauer* and W. E. Pickett**

*College of William and Mary, Williamsburg, VA 23185
**Condensed Matter Physics Branch, Naval Research Laboratory, Washington, DC 20375-5000

INTRODUCTION

The discovery of very high temperature superconductivity in copper oxide materials[1,2] raises a number of fundamental questions. Many of these are related to the fact that these oxides are qualitatively different than nearly all other high temperature superconductors (they are similar in some ways to the Ba-(Pb-Bi)-O system). Preparation requires techniques which are used in the preparation of ceramics, and their properties are similar to many ceramics - brittle rather than malleable, strongly tending to crack rather than bend. Yet, at high temperature they show conductivity characteristic of low density of states metals, and become superconducting in the range T_c = 30-100 K.

Band structure calculations[3-5] indicate these materials are metals with bands crossing the Fermi level which have Cu-O d-p character. They are relatively broad bands, nearly 10 eV wide, which arise from the strong Cu-O overlap due to their small separation. In the La-Ba-Cu-O system the bands at E_F are dpσ antibonding bands, and several studies[3,5,6] have shown that these states are strongly modulated by the relative motion of the atoms, that is, there is a strong electron-phonon interaction (EPI). These studies and others[7] indicate that the EPI is strong enough to account for the observed T_c = 30-45 K in this system.

In the $YBa_2Cu_3O_7$ system (including materials obtained by the replacement of Y by a number of rare earth elements), there are several indications that the EPI may not be responsible for the superconductivity. The high values of T_c, in the 90-100 K range[2], alone are enough to suggest that a novel mechanism is responsible, and recently two laboratories[8,9] have found no detectable dependence of T_c on the mass of oxygen. The replacement of Y by a number of rare earth elements which have masses up to twice as large and T_c over 90 K also suggests that superconductivity is independent of the mass of the trivalent atom in this structure. Preliminary studies[10] of the calculated EPI in this material (using the rigid atom approximation) also suggests it is no larger than that in the La-(Ba,Sr)-Cu-O system.

Whatever the mechanism giving rise to superconductivity in $YBa_2Cu_3O_7$, there seems to be little doubt that it is due to pairing of electron states at the Fermi level E_F. Therefore it is of central interest to investigate the character of the states at and near E_F and their energy- and real-space distribution. In this paper we present results of detailed Linearized Augmented Plane Wave calculations of these properties.

CALCULATIONAL RESULTS

The atomic geometry of $YBa_2Cu_3O_7$ has been determined by several groups.[11] The unit cell is orthorhombic with space group Pmmm, containing one formula unit per unit cell. The structure can be pictured as a defect perovskite structure, with a superlattice-like ordering of the Y and two Ba atoms along the c direction serving to define the unit cell. In addition, the oxygen atom is missing from the Y layer, and in the Cu-O layer sandwiched between the Ba planes one of the two oxygen atoms is missing. The structure then consists of the Y and two symmetry-related Ba atoms, Cu(1) and O(1) atoms in the Cu-O chain with O(4) oxygen atoms above and below the Cu(1) atom, and two Cu-O corrugated planes with Cu(2), O(2) and O(3) atoms in each. We find that, although the interactions between the two planes and between the planes and the chains are small, they are larger than the interactions between the Cu-O planes in the La_2CuO_4 system.

The details of the calculations will be given elsewhere. We note here only that although this material has a very large unit cell with low symmetry, we have carried out very well converged calculations. The charge density and potential were expanded in the interstitial region in 14600 planes waves and inside the inscribed spheres around each atom in lattice harmonics through l=12. The secular equation dimension was about 850. The densities of states and band structure plots given below were obtained from disciplined Fourier series representations based on 165 first-principles points in the irreducible zone. The present calculations are much more highly converged than those of Mattheiss and Hamann[12] (who used a geometry which has since been shown to be incorrect) and are also more extensive than those of Massidda *et al.*[13]

The density of states (DOS) of $YBa_2Cu_3O_7$ is shown in Fig. 1. The same DOS is also shown on an expanded scale in Fig. 2 for energies within 0.4 eV of the Fermi energy. The values of the projected DOS at E_F are summarized in Table I and compared to those of $La_{2-x}(Ba,Sr)_xCuO_4$. Among the notable features seen in Figs. 1 and 2 is the nearly identical character of the O(2) and O(3) DOS, reflecting the nearly identical chemical environment of these two atoms due to the small size of the orthorhombic distortion. By contrast, the spectral weight of the O(1) and O(4) atoms is shifted to higher energies, and at E_F, the DOS of the O(1) and O(4) atoms is more than twice as large as that of the O(2) and O(3) atoms and comparable to that of the Cu atoms. The linear chain Cu(1) atom is four-fold planar coordinated with the O(1) (along the b axis) and O(4) (along the c-axis) atoms, and this accounts for the overall similarity of the spectral densities of the O(1) and O(4) atoms. There is a sharp peak 0.1 eV below E_F on the O(1) atom and, slightly reduced, also on the O(4) atom. E_F itself falls on a rather smooth region of spectral density.

The DOS at the Fermi energy $N(E_F)$ of the O(1) and O(4) atoms is much larger than that of the O atoms in the La-Ba-Cu-O compounds. For the ideal compounds (δ=0 and x=0 in Table I), the DOS of the O(1) and O(4) atoms is more than four times larger than on the O(x,y) atom in La_2CuO_4. Highest T_c's have been achieved in Y-Ba-Cu-O compounds with oxygen vacancies as low as δ=0.03,[14] while x=0.15 seems to yield the highest T_c

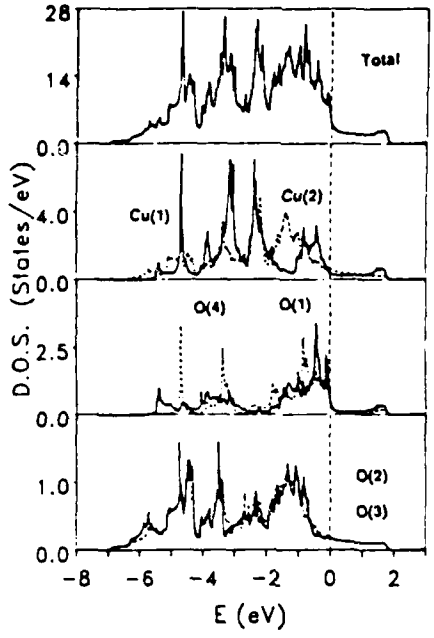

Figure 1. Density of states for $YBa_2Cu_3O_7$. The total DOS is shown in the top panel and muffin-tin projected DOS per atom are shown in the other panels (see text for atom identification). Note the change of scale from panel to panel.

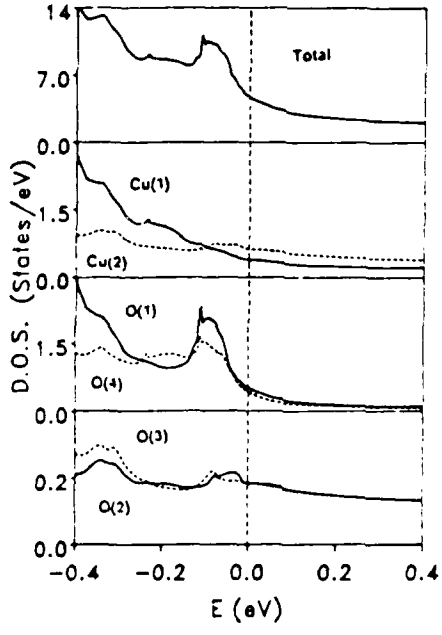

Figure 2. Same as Fig. 1, but for an expanded energy scale near E_F. Note the change of scale from panel to panel.

in the La-Sr based systems. For these compounds, the rigid band values in Table I still give O(1) and O(4) $N(E_F)$'s which are more than twice as large as that on that on the La-(Ba,Sr)-Cu-O compound. Furthermore, $N(E_F)$ on the Cu, O(1) and O(4) atoms are more nearly comparable to each other than are those in the La-based compounds.

The "rigid band" values presented in Table I have been determined using the standard procedure whereby the oxygen is assigned the nominal O^{2-} character, and the creation of an oxygen vacancy implies the loss of 6 O p states below E_F while the removal of the neutral O atom subtracts only 4 p electrons. Thus the creation of δ O vacancies provides 2δ extra electrons for the band states above E_F. This picture is certainly not strictly correct when O-related bands cross E_F, both because the O^{2-} designation is not correct and because the O p states which are removed in forming the vacancy do not lie entirely below E_F. Other problems with the rigid band model for oxygen vacancies are discussed in the next section. On the other hand, the rigid band model should be more appropriate for substitutional fluorine in place of oxygen.[15] For the T_c=150 K compound in Ref. 15, $YBa_2Cu_3F_2O_y$ (assuming the same structure and y=5) this would increase E_F by about 1 eV into a region of <u>reduced</u> $N(E_F)$.

The band structures near E_F are shown in Figs. 3 and 4. Since it is essential to identify the contributions of the chains and the planes separately, the bands which are strongly associated with the chains, that is, the Cu(1), O(1) and O(4) atoms, are emphasized in Fig. 3. In Fig. 4 the bands associated with the layers, comprised of the Cu(2), O(2) and O(3) atoms, are emphasized. There are four bands which cross E_F (numbers 33 to 36, to accommodate the 68 electrons per unit cell). The layers give rise to two of the bands crossing E_F, corresponding to one band for each layer. These bands are similar to those crossing E_F in La_2CuO_4, but differ here in that they are not precisely half filled. The Cu-O chain gives rise to one steep band crossing E_F, which is strongly dispersing only in the chain direction, that is, along X-S and Γ-Y. In addition there is a <u>flat chain-related band just at E_F along the Y-S direction</u>. Here we show the bands only in the k_z=0 plane, but there is some small but important dispersion along the c direction which will be discussed elsewhere.

From Fig. 2 the peak in $N(E_F)$ 0.1 eV below E_F is seen to be associated solely with the chain-related O(1) and O(4) atoms, and does not show up at all on the Cu(1) chain atom. Therefore this peak arises from states which lie along the chain but <u>avoid</u> the Cu(1) atom, and apparently relating primarily to O(1)-O(4) ppσ interactions. Figures 3 and 4 show there are mostly chain derived states, rather than layer-derived, within 0.5 eV below E_F, and the peak is associated with the flat portion of the uppermost filled band midway between Γ and S.

DISCUSSION

The presence of a more complex unit cell here than in the La_2CuO_4 compound leads to bands which are not half filled and have more complex Fermi surfaces. The chain-related bands crossing E_F may lead to qualitatively new processes related to its strong one-dimensional character, and due to the two dimensional planes and one dimensional chains the electronic properties have strongly anisotropic character in all three directions.

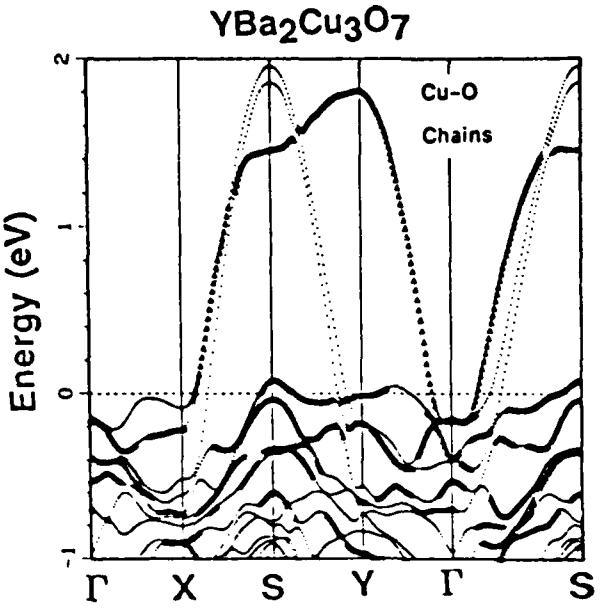

Figure 3. Band structure of $YBa_2Cu_3O_7$ in the k_z=0 plane of the orthorhombic zone, near the Fermi level E_F=0. States with more than 60% of their charge on the Cu(1)-O(1)-O(4) chains are emphasized with the large symbols.

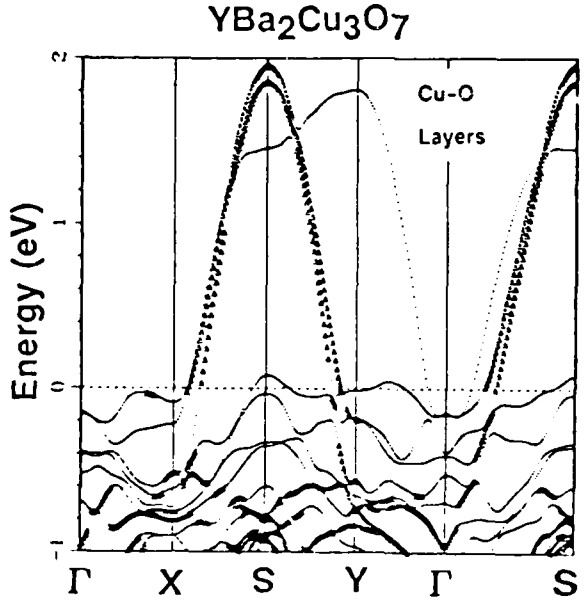

Figure 4. As in Fig. 4, except the emphasized states are those with more than 80% charge on the two Cu(2)-O(2)-O(3) layers.

In the La-(Ba,Sr)-Cu-O system we have shown that a rigid band model should be realistic for moderate (15-20%) substitutions of La. In the present system one would expect because of the similarity of the materials that a rigid band model should also work for substitution of Y on Ba sites, and vice versa. The results given in Table I should be applicable for this case, although substantial variation away from the Y:Ba ratio of 1:2 leads to the formation of other phases.[2] One is tempted to apply a rigid band model to the case of oxygen vacancies (which occur on the O(1) sites along the Cu-O chains under non-optimum conditions), but caution is necessary in this situation. The change in the on-site potential due to the removal of an oxygen atom is drastic, and several possibilities arise. The extra electrons originally on the O ion when the neutral O atom is removed may go equally into the bands crossing E_F, but they may also perhaps remain in part on the empty site, stabilized by the Madelung potential as in the F-center in ionic oxides. Not only is the on-site change in potential large, which will alter the band structure, but the coordination of the neighboring copper atoms decreases from 4 to 3. As a result, oxygen vacancies will result in both a change in the Cu(1) states as well as a disruption of the one-dimensional chain structure.

It is evident that the disruption of the chain, such as by the removal or displacement of an O(1) atom, can have serious consequences for transport properties if the one dimensionality is strong, because an electron cannot avoid a defect in one dimension. If, as seems to be the case in La_2CuO_4, that the Cu has a tendency to become magnetic, the lowering of its coordination will suppress the banding of the d-states and enhance magnetic tendencies. [Vacancies are a necessary precondition of the antiferromagnetic state in La_2CuO_4.] Although there have been studies in $YBa_2Cu_3O_{7-\delta}$ of the effects of oxygen vacancies, from near δ=o to δ=1 per formula unit, no magnetic transitions have been reported. It has been found, however, that superconductivity is strongly depressed as δ is increased, and a metal-to-insulator transition occurs at δ=0.5. Such a transition is not predicted by the rigid band model, again suggesting it is not applicable in describing oxygen defect compounds.

This work has been supported by the National Science Foundation (NSF) Grant No. DMR-84-16046 and the Office of Naval Research Contract No. N00014-84-WR-24055. Computing was done under the auspices of the NSF at the supercomputing centers at Cornell University and at the University of Pittsburgh, as well as the Naval Research Laboratory.

TABLE I. Comparison of Fermi level densities of states $N(E_F)$(in states /eV-atom). Also shown are rigid band values of $N(E_F)$ corresponding to oxygen vacancies in Y-Ba-Cu-O and alloying with Sr or Ba in La-Cu-O.

$YBa_2Cu_3O_{7-\delta}$

E_F(Ry)	E_F(eV)	δ	holes	N(E)	Cu(1)	Cu(2)	Cu-avg	O(1)	O(4)	O(2)	O(3)
.4412	.000	.00	.00	4.78	.352	.602	.519	.518	.452	.175	.175
.4446	.047	.10	-.20	3.77	.316	.571	.486	.319	.246	.171	.168
.4490	.107	.20	-.40	3.02	.257	.501	.420	.195	.155	.155	.152
.4542	.177	.30	-.60	2.62	.229	.451	.377	.143	.117	.143	.141

$La_{2-x}Sr_xCuO_4$

E_F(Ry)	E_F(eV)	x	elect	N(E)	Cu	O(z)	O(x,y)
.5590	.000	.00	.00	1.24	.540	.039	.113
.5530	-.082	.14	-.14	2.03	1.045	.108	.181

REFERENCES

1. J.G. Bednorz and K.A. Muller, Z. Pys. B64, 189 (1986).
2. M.K. Wu *et al.*, Phys. Rev. Lett. 58, 908 (1987).
3. L.F. Mattheiss, Phys. Rev. Lett. 58, 1028 (1987).
4. J. Yu and A.J. Freeman, Phys. Rev. Lett. 58, 1035 (1987).
5. W.E. Pickett, H. Krakauer, D.A. Papaconstantopoulos, and L.L. Boyer, Phys. Rev. B35, 7252 (1987).
6. W.Weber, Phys. Rev. Lett. 58, 1371 (1987).
7. P.B. Allen, W.E. Pickett, and H. Krakauer, preprint.
8. B. Batlogg *et al.* Phys. Rev. Lett. 58, 2333 (1987).
9. L.C. Bourne *et al.*, Phys. Rev. Lett. 58, 2337 (1987).
10. H. Krakauer and W.E. Pickett, unpublished.
11. S.B. Qadri, L.E. Toth, M. Osofsky, S. Lawrence, D.U. Gubser, and S.A. Wolf, Phys. Rev. B35, 7235 (1987); T. Siegrist, S. Sunshine, D.W. Murphy, R.J. Cava, and S.M. Zahurak, Phys. Rev. B35, 7137 (1987); P.M. Grant *et al.*, Phys Rev. B35, 7242 (1987); R.M. Hazen *et al.*, Phys. Rev. B35, 7238 (1987); Y. LePage, W.R. McKinnon, J.M. Tarascon, L.H. Greene, G.W. Hull, and D.M. Hwang, Phys. Rev. B35, 7245 (1987).
12. L.F. Mattheiss and D.R. Hamann, preprint.
13. S. Massidda, J. Yu, A.J. Freeman, and D.D. Koelling, preprint.
14. J.J. Rhyne, D.A. Neuman, J.A. Gotaas, F. Beech, L.E. Toth, S. Lawrence, S. Wolf, M. Osofsky, and D.U. Gubser, preprint; L.E. Toth, private communication.
15. S.R. Ovshinsky, R.T. Young, D.D. Allred, G. DeMaggio, and G.A. Van der Leeder, Phys. Rev. Lett. 58, 2579 (1987).

EFFECT OF LOW DIMENSIONALITY ON THE PARAMETERS OF HIGH T_c SUPERCONDCUTORS

V.Z. Kresin

Materials and Chemical Sciences Division, Lawrence Berkeley Laboratory, University of California, Berkeley, CA 94720, U.S.A.

S.A. Wolf
Naval Research Laboratory Washington, DC [redacted]

A method of determining the values of main parameters such as the effective mass, the Fermi energy, and the coherence length for the new high T_c superconductors is developed. The method is based on specific heat data. The new T_c materials are low dimensional systems and this feature plays a crucial role in the analysis. The parameters are calculated for $La_{2-x}Sr_xCuO_4$, $x \simeq 0.2$. Particularly interesting is the small value of the Fermi energy.

1. INTRODUCTION

Since the recent discovery of very high transition temperature superconducting ceramics [1] there has been great activity associated with characterizing these materials. In order to carry this analysis forward one must be sure to take into account the dimensionality of the carriers that are a consequence of the constraints of the structure. In the course of determining the structure and affects of the structure on superconductivity it has been concluded that these superconducting oxides are lower dimensional systems. In fact, the superconductors based on the K_2NiF_4 structure such as $La_{2-x}Sr_xCuO_4$ ($x \simeq 2$) are highly two dimensional[2] while those based on the $YBa_2Cu_3O_7$ structure contain one dimensional chains.[3,4] This paper is therefore concerned with the determination of the materials parameters when the dimensionality is reduced. Expressions for effective mass, Fermi energy, Fermi velocity and coherence length will be derived for both one and two dimensional systems.

We will attempt to evaluate many of the materials parameters based on some recent experimental data.[5-7] Since many of the important parameters can be estimated using only structural information and knowledge of the Sommerfeld constant γ, the most reliable source for this constant is electronic heat capacity measurements. For isotropic superconductors, γ can be estimated from the slope of the upper critical field H_{c2} at T_c.[8] However for polycrystalline samples containing anisotropic crystals this is not very reliable. In this paper we focus on the determination of the main parameters from the experimental data on heat capacity.

The paper consists of two parts. In Sec. 2 the expressions allowing us to determine the parameters directly from heat capacity measurements will be derived. We considered both the 2D and 1D cases. It will be shown that the parameters are very sensitive to the dimensionality, and the analysis should be carried out in a consistent way. A set of parameters for the La-Sr-Cu-O system is obtained (Sec. 3).

2. THEORY

2.1. *2D case*

Consider a model containing 2D sheets. Each of them contains a 2D Fermi gas of carriers. There are a small number of interlayer transitions which are important if we are concerned with 2D fluctuations. But for our present purpose we can consider isolated 2D subsystems. Superconducting pairing occurs between two electrons (or holes) belonging to the same sheet. The energy in the normal state is equal to:

$$E = \sum_i \int \phi_i f_i \, d\epsilon_i , \tag{1}$$

where $\phi_i = \epsilon_i \nu_i^{2D}$, $\nu_i^{2D} = 2(dp_x \, dp_y/d\epsilon_i)S_i (2\pi\hbar)^{-2}$ is the 2D density of states (DOS). S_i is the area, $f_i = [\exp(-(\epsilon_i - \epsilon_{Fi})/T + 1)]^{-1}$, ϵ_{Fi} is the Fermi level for the i-th sheet; the summation in (1) is taken over all 2D sheets. The DOS in the 2D case can be written in the form

$$\nu_i^{2D} = m_i (2\pi\hbar^2)^{-1} , \tag{2}$$

where m_i is the effective mass defined by the relation: $m_i = \int d l v_i^{-1}$; here $v_i = \partial\epsilon_i/\partial p_i$ and the integration is over the Fermi curve. For a simple quadratic dispersion relation $m_i = p_i/v_i$. Calculating the energy with the use of the expression $E = E_o + \sum_i (\partial\phi/\partial\epsilon_i)_F (k_B T)^2$, we arrive at the following expression for the specific heat: $C = \gamma T$, where

$$\gamma = (\pi/3\hbar^2) k_B^2 \sum_{i=1}^{k} S_i m_i . \tag{3}$$

Consider the case when all the 2D sheets are equivalent and equidistant. Then we obtain

$$\gamma = (\pi^2/3\hbar^2) m^* k_B^2 a^{-1} \text{ erg K}^{-2}\text{ cm}^{-3} \tag{4}$$

Here a is the interlayer distance, $m^* \equiv m_i$, k_B is the Boltzmann's constant. It is essential that in the 2D case γ does not depend on the electron concentration. The situation is entirely different in the 1D (see below) and 3D cases.

The quantity γ can be measured experimentally; then the effective mass can be determined directly from the equation

$$m^* = (3\hbar^2/\pi)\, k_B^{-2}\, a\, \gamma . \qquad (5)$$

We will use this expression in order to evaluate m^* for the La-Sr-Cu-O system (see Sec. 3).

We have noted that γ for a 2D system does not depend on the carrier concentration. The latter affects noticeably the Fermi momentum which is equal to (see e.g., ref. [9]):

$$p_F = (2\pi N_s)^{1/2} \hbar , \qquad (6)$$

where N_s is the surface concentration. In our case $N_s = na$, where n is the usual volume concentration. The values of the Fermi energy $\epsilon_F = p_F^2/2m^*$ and the Fermi velocity can be evaluated with the use of Eqs. (5), (6). Then the coherence length $\xi_o = (\hbar\, v_F/2\pi kT_c)$ can be also calculated (see below, Sec. 3).

2.2. *1D case*

Consider the model which is a set of 1D channels (lines). The energy can be described by Eq. (1) with the substitution $\nu^{2D} \rightarrow \nu^{1D}$, where ν^{1D} is DOS in the 1D case. As a result we obtain the following expression for γ:

$$\gamma = (\pi/12\hbar)\, k_B^2 \sum_i^k l_i\, v_i^{-1} ; \qquad (7)$$

where l_i is the length of the i-th line. If all lines are equivalent, we obtain:

$$\gamma = (\pi/12\hbar)\, k_B^2\, \sigma^{-2}\, v_F^{-1} . \qquad (8)$$

Here σ^{-2} is the number of lines per unit area. Note that in the 1D case the Fermi momentum is equal to (see e.g. Ref. 9) $p_F = 2\pi\hbar N_L$, where N_L is the linear carrier concentration.

Consider the special case when the system is a combination of 2D and 1D structures (probably, it is related to $Y_1 Ba_2 Cu_3 O_7$ structures, see Ref. 3,4). Namely, the system is layered, similar to the case studied in p.1, but each layer consist of a set of 1D parallel chains. In this case,

$$p_F = 2\pi\hbar nab \qquad (9)$$

where b is the distance between neighboring chains (within one layer). The effective mass is described by the expression

$$m^* = 12(\hbar\, k_B^{-1}\, ab)^2 n\, \gamma . \qquad (10)$$

3. THE PARAMETERS OF THE La-Sr-Cu-O SYSTEM

Eqs. (5) and (6) can be used in order to calculate the main parameters of high T_c 2D superconductors. In this section we apply the method described in Sec. 2 for a calculation of the parameters for $La_{2-x}Sr_xCuO_4$, $x \simeq 0.2$. Our method is based on the heat capacity measurements. These measurements are difficult because of a large lattice contribution. The experiments have been carried out by several groups[5-7] by various methods. Different values of γ have been reported. For example, according to refs. 5,6 $\gamma \simeq 7.5$ mJ/mole K^2. The value $\gamma \simeq 12$ mJ/mole K^2 was obtained in 7. The value n depends on the quality of the sample, on the concentration x; according to experimental data[10,11] n is within the interval 10^{21} cm^{-3} < n < 5×10^{21} cm^{-3}. For the purpose of an estimate, we can put $\gamma \simeq 10$ mJ/mole K^2, $n \simeq 5 \times 10^{21}$ cm^{-3}.

The effective mass m^* can be calculated with the use of Eq. (5); a = 6.6 Å [2]. Then we obtain $m^* \simeq 5.5\, m_e$. The value of p_F can be calculated with the use of Eq. (6), and we obtain $p_F = 5 \times 10^{-20}$ g-cm/sec. It is interesting to note that despite the relatively small value of n, the value of p_F is close to that in some metals. This is due to the 2D structure of the material. The Fermi energy is small ~ 0.15 eV, because of the large value of m^*.

Superconductivity in materials with such a small Fermi energy is quite unusual. The fact that E_F and the energy gap are comparible is unprecedented. The small value of E_F might have a strong impact on lattice instability. This problem will be discussed in detail elsewhere.

The Fermi velocity is equal to $v_F \simeq 8 \times 10^6$ cm/sec, and the coherence length $\xi_o = \hbar\, v_F/2\pi kT_c$ appears to be about 25 Å.

We have estimated the parameters by putting $\gamma \simeq 10$ mJ/mole K^2, $n \simeq 5 \times 10^{21}$ cm^{-3}. It is important to stress that the exact values of the parameters can be obtained from Eq. (5); their accuracy can be improved with more precise measurements of γ and n.

A detailed analysis has been carried out in [5]; the magnetic field dependence of the specific heat was studied. According to [5], the value of γ is within the interval 6.5 mJ/mole $K^2 < \gamma <$ 8.5 mJ/mole K^2 (the spread is due to the uncertainty in the value of H_{c2} which determines the amount of the normal phase present). A close value of γ was obtained in [6] by a different method. The parameter values obtained from Eq. (5) with $\gamma = 7.5$ mJ/mole K^2 and $n = 3 \times 10^{21}$ cm^{-3} are given in the table.

Recently, heat capacity measurements for $Y_1 Ba_2 Cu_3 O_7$ were carried out in [12]. If superconductivity in this material is confined to 1D chains only (this problem is still unresolved), then one can show with the use of Eqs. (9) and (10) that one is also dealing with a very unusual system with a large m^* and small ϵ_F. This problem will be discussed in detail elsewhere.

4. CONCLUSION

The values of the parameters depend strongly on the dimensionality of the system. The new high T_c superconductors are low dimensional materials and the evaluation of the parameters should be carried out with considerable care. In many instances, 3D expressions have already been used, leading to incorrect results. In this paper we derived the expressions for such parameters as m^*, p_F, v_F, ϵ_F and ξ_o based on specific heat data. We calculated the values of the parameters for $La_{2-x}Sr_xCuO_4$, $x \simeq 0.2$. In particular, we would like to stress the small value of the Fermi energy. The low dimensionality plays a crucial role in this analysis.

Acknowledgments -- The authors are grateful to Prof. A. Stacy for a valuable discussion. This work was supported in part by the Office of U.S. Naval Research under Contract No. N00014-86-F0015 and carried out at the Lawrence Berkeley Laboratory under contract No. DE-AC03-76SF00098.

Table

Parameters for $La_{2-x}Sr_xCuO_4$ ($x \simeq 0.2$)

m^*	p_F	ϵ_F	v_F	ξ_o
$4\ m_e$	3.7×10^{-20} gm × cm/sec	0.12 eV	9.25×10^6 cm/sec	23.5 Å

REFERENCES

1. J. Bednorz and K. Müller. Z. Phys. B66, 189 (1986).
2. M. Tahagi et al. Jpn. J. Appl. Phys. *26*, L123 (1987).
3. F. Beech et al. (preprint).
4. L. Toth et al. Phys. Rev. Lett. (submitted).
5. N. Phillips et al. (preprint).
6. B. Batlogg et al. Phys. Rev. B*35*, 5340 (1987).
7. S. Tanaka et al. Proc. of MRS meeting (Anaheim, 1987; in press).
8. T. Orlando et al. Phys. Rev. B*35*, 5347 (1987).
9. V. Kresin, Phys. Rev. B*25*, 157 (1982); B34, 7587 (1986).
10. A. Panson et al. Appl. Phys. Lett. *50*, 1104 (1987); M. Tonouchi et al. Jpn. J. of Appl. Phys. *26* L519 (1987); N. Ong et al. (preprint).
11. W. Kwok et al. Phys. Rev. B*35*, 5343 (1987); S. Uchida et al. Jpn. J. of Appl. Phys. *26*, L443 (1987).
12. H. Junod et al. (preprint).

PARAMETERS AND EXOTIC PROPERTIES OF HIGH T_c SUPERCONDCUTORS

V.Z. Kresin

Materials and Chemical Sciences Division
Lawrence Berkeley Laboratory
University of California
Berkeley, CA 94720, U.S.A.

S.A. Wolf

Naval Research Laboratory
Washington, DC 20375

ABSTRACT

A method of determining the values of main parameters such as the effective mass, the Fermi energy, and the coherence length for the new high T_c superconductors is developed. The method is based on specific heat data. The new T_c materials are low dimensional systems and this feature plays a crucial role in the analysis. Particularly interesting is the small value of the Fermi energy. The result of the analysis shows that we are dealing with unusual systems. Energy gap appears to be comparable with E_F, and the coherence length is small. Contrary to the usual case, the large fraction of carriers is paired.

INTRODUCTION

Since the recent discovery of very high transition temperature superconducting ceramics[1] there has been great activity associated with characterizing these materials. In order to carry this analysis forward one must be sure to take into account the dimensionality of the carriers that are a consequence of the constraints of the structure. In the course of determining the structure and affects of the structure on superconductivity it has been concluded that these superconducting oxides are lower dimensional systems. In fact, the superconductors based on the K_2NiF_4 structure such as $La_{2-x}Sr_xCuO_4$ ($x \simeq 2$) are highly two dimensional[2] while those based on the $Y_1Ba_2Cu_3O_7$ structure contain one dimensional chains.[3,4] This paper is therefore concerned with the determination of the materials parameters when the dimensionality is reduced. Expressions for effective mass, Fermi energy, Fermi velocity and coherence length will be derived for both one and two dimensional systems.

We will attempt to evaluate many of the materials parameters based on some recent experimental data.[5-7] Since many of the important parameters can be estimated using only structural information and knowledge of the Sommerfeld constant γ, the most reliable source for this constant is

electronic heat capacity measurements. For isotropic superconductors, γ can be estimated from the slope of the upper critical field H_{c2} at T_c.[8] However for polycrystalline samples containing anisotropic crystals this is not very reliable. In this paper we focus on the determination of the main parameters from the experimental data on heat capacity. It will be shown that we are dealing with an exotic system with unusual properties.

The paper consists of two parts. In Sec. 2 the expressions allowing us to determine the parameters directly from heat capacity measurements will be derived. We considered both the 2D and 1D cases. It will be shown that the parameters are very sensitive to the dimensionality, and the analysis should be carried out in a consistent way. A set of parameters for the La-Sr-Cu-O and Y-Ba-Cu-O systems is obtained (Sec. 3).

THEORY

2D Case

Consider a model containing 2D sheets. Each of them contains a 2D Fermi gas of carriers. There are a small number of interlayer transitions which are important if we are concerned with 2D fluctuations. But for our present purpose we can consider isolated 2D subsystems. Superconducting pairing occurs between two electrons (or holes) belonging to the same sheet. The energy in the normal state is equal to:

$$E = \sum_i \int \phi_i \, f_i \, d\epsilon_i \, , \tag{1}$$

where $\phi_i = \epsilon_i \, \nu_i^{2D}$, $\nu_i^{2D} = 2(dp_x \, dp_y/d\epsilon_i)S_i \, (2\pi \hbar)^{-2}$ is the 2D density of states (DOS), S_i is the area, $f_i = [\exp(-(\epsilon_i - \epsilon_{Fi})/T + 1)]^{-1}$, ϵ_{Fi} is the Fermi level for the i-th sheet; the summation in (1) is taken over all 2D sheets. The DOS in the 2D case can be written in the form

$$\nu_i^{2D} = m_i \, (2\pi \hbar^2)^{-1} \, , \tag{2}$$

where m_i is the effective mass defined by the relation: $m_i = \int dl v_i^{-1}$; here $v_i = \partial\epsilon_i/\partial p_i$ and the integration is over the Fermi curve. For a simple quadratic dispersion relation $m_i = p_i/v_i$. Calculating the energy with the use of the expression $E = E_o + \sum_i (\partial\phi/\partial\epsilon_i)_F \, (k_B T)^2$, we arrive at the following expression for the specific heat: $C = \gamma T$, where

$$\gamma = (\pi/3 \, \hbar^2) \, k_B^2 \sum_{i=1}^{k} S_i \, m_i \, . \tag{3}$$

Consider the case when all the 2D sheets are equivalent and equidistant. Then we obtain

$$\gamma = (\pi/3 \, \hbar^2) \, m^* \, k_B^2 \, a^{-1} \text{ erg/K cm}^3 \, . \tag{4}$$

Here a is the interlayer distance, $m^* = m_i$, k_B is the Boltzmann's constant. It is essential that in the 2D case γ does not depend on the electron concentration. The situation is entirely different in the 1D (see below) and 3D cases.

The quantity γ can be measured experimentally; then the effective mass can be determined directly from the equation

$$m^* = (3\hbar^2/\pi)\, k_B^{-2}\, a\, \gamma \ . \qquad (5)$$

We will use this expression in order to evaluate m^* for the La-Sr-Cu-O system (see Sec. 3).

We have noted that γ for a 2D system does not depend on the carrier concentration. The latter affects noticeably the Fermi momentum which is equal to (see e.g., ref. [9]):

$$p_F = (2\pi N_s)^{1/2}\, \hbar \ , \qquad (6)$$

where N_s is the surface concentration. In our case $N_s = na$, where n is the usual volume concentration. The values of the Fermi energy $\epsilon_F = p_F^2/2m^*$ and the Fermi velocity can be evaluated with the use of Eqs. (5), (6). Then the coherence length $\xi_o = (\hbar\, v_F/2\pi kT_c)$ can be also calculated (see below, Sec. 3).

1D Case

Consider the model which is a set of 1D channels (lines). The energy can be described by Eq. (1) with the substitution $\nu^{2D} \to \nu^{1D}$, where ν^{1D} is DOS in the 1D case. As a result we obtain the following expression for γ:

$$\gamma = (\pi/12\,\hbar)\, k_B^2 \sum_i^k l_i\, v_i^{-1} \ ; \qquad (7)$$

where l_i is the length of the i-th line. If all lines are equivalent, we obtain:

$$\gamma = (\pi/12\,\hbar)\, k_B^2\, \sigma^{-2}\, v_F^{-1} \ . \qquad (8)$$

Here σ^{-2} is the number of lines per unit area. Note that in the 1D case the Fermi momentum is equal to (see e.g. Ref. 9) $p_F = 2\pi\hbar N_L$, where N_L is the linear carrier concentration.

Consider the special case when the system is a combination of 2D and 1D structures (probably, it is related to $Y_1\, Ba_2\, Cu_3\, O_7$ structures, see Ref. 3,4). Namely, the system is layered, similar to the case studied in p.1, but each layer consist of a set of 1D parallel chains. In this case,

$$p_F = 2\pi\hbar nab \qquad (9)$$

where b is the distance between neighboring chains (within one layer). The effective mass is described by the expression

$$m^* = 12(\hbar\, k_B^{-1}\, ab)^2 n\, \gamma \ . \qquad (10)$$

THE PARAMETERS OF THE La-Sr-Cu-O AND Y-Ba-Cu-O SYSTEM

Eqs. (5) and (6) can be used in order to calculate the main parameters of high T_c 2D superconductors. In this section we apply the method described in Sec. 2 for a calculation of the parameters for $La_{2-x}Sr_xCuO_4$, $x \approx 0.2$. Our method is based on the heat capacity measurements. These measurements are difficult because of a large lattice contribution. The experiments have been carried out by several groups[5-7] by various methods. Different values of γ have been reported. For example, according to refs. [5,6] $\gamma \approx 7.5$ mJ/mole K^2. The value $\gamma \approx 12$ mJ/mole K^2 was

obtained in [7]. The value n depends on the quality of the sample, on the concentration x; according to experimental data[10,11] n is within the interval 10^{21} cm^{-3} < n < 5 × 10^{21} cm^{-3}. For the purpose of an estimate, we can put γ = 10 mJ/mole K^2, n = 5 × 10^{21} cm^{-3}.

The effective mass m^* can be calculated with the use of Eq. (5); a = 6.6 Å [2]. Then we obtain $m^* = 5.5\ m_e$. The value of p_F can be calculated with the use of Eq. (6), and we obtain $p_F = 5 \times 10^{-20}$ g-cm/sec. It is interesting to note that despite the relatively small value of n, the value of p_F is close to that in some metals. This is due to the 2D structure of the material. The Fermi energy is small ~ 0.15 eV, because of the large value of m^*.

Superconductivity in materials with such a small Fermi energy is quite unusual. The fact that E_F and the energy gap Δ are comparible is unprecedented. The small value of E_F might have a strong impact on lattice instability. This problem will be discussed in detail elsewhere.

The Fermi velocity is equal to $v_F \approx 8 \times 10^6$ cm/sec, and the coherence length $\xi_o = \hbar\, v_F/2\pi kT_c$ appears to be about 25 Å.

We have estimated the parameters by putting $\gamma \approx 10$ mJ/mole K^2, n ≈ 5 × 10^{21} cm^{-3}. It is important to stress that the exact values of the parameters can be obtained from Eq. (5); their accuracy can be improved with more precise measurements of γ and n.

A detailed analysis has been carried out in [5]; the magnetic field dependence of the specific heat was studied. According to [5], the value of γ is within the interval 6.5 mJ/mole K^2 < γ < 8.5 mJ/mole K^2 (the spread is due to the uncertainty in the value of H_{c2} which determines the amount of the normal phase present). A close value of γ was obtained in [6] by a different method. The parameter values obtained from Eq. (5) with γ = 7.5 mJ/mole K^2 and n = 3 × 10^{21} cm^{-3} are given in the table.

The measurements of heat capacity for $Y_1\ Ba_2\ Cu_3\ O_7$ have been performed [13,14]. Our analysis in this case is based on Eqs. (9), (10). We use the values $\gamma \approx 20$ mJ/mole K^2 [13], n ≈ 5 × 10^{21} cm^{-3}. The obtained values of parameters are presented in the table.

CONCLUSION

The values of the parameters depend strongly on the dimensionality of the system. The new high T_c superconductors are low dimensional materials and the evaluation of the parameters should be carried out with considerable care. In many instances, 3D expressions have already been used, leading to incorrect results. In this paper we derived the expressions for such parameters as m^*, p_F, v_F, ϵ_F and ξ_o based on specific heat data. We calculated the values of the parameters. In particular, we would like to stress the small value of the Fermi energy. The low dimensionality plays a crucial role in this analysis.

We would like to stress two important results. First of all, the ratio Δ/T_c is much larger than for conventional superconductors. It means that a large fraction of carriers in the new materials are paired. Note that the expression $\xi_o = \hbar\, v_F(2\pi T_c)^{-1}$ is valid, if $\Delta \ll \epsilon_F$ (see, e.g. [15]). The smallness of the coherence length also makes the systems unique.

Table

	m^*	p_F	ϵ_F	v_F	ξ_o
$La_{1.8}Sr_{0.2}CuO_4$	$4\ m_e$	3.7×10^{-20} gm x cm/sec	0.12 eV	9.25×10^6 cm/sec	23.5 Å
$Y_1Ba_2Cu_3O_7$	$\sim 10^2\ m_e$	1.5×10^{-19} gm x cm/sec	0.07 eV	1.2×10^6 cm/sec	*

*Expression $\xi_o = \hbar v_F (2\pi k T_c)^{-1}$ is not applicable for this case for such small ϵ_F and such large T_c.

Acknowledgments

The authors are grateful to K. Müller and A. Stacy for valuable and interesting discussions. This work was supported in part by the Office of U.S. Naval Research under Contract No. N00014-86-F0015 and carried out at the Lawrence Berkeley Laboratory under contract No. DE-AC03-76SF00098.

REFERENCES

1. J. Bednorz and K. Müller. Z. Phys. B66, 189 (1986).
2. M. Tahagi et al. Jpn. J. Appl. Phys. 26, L123 (1987).
3. F. Beech et al. (preprint).
4. L. Toth et al. Phys. Rev. Lett. (submitted).
5. N. Phillips et al. (preprint).
6. B. Batlogg et al. Phys. Rev. B35, 5340 (1987).
7. S. Tanaka et al. Proc. of MRS meeting (Anaheim, 1987; in press).
8. T. Orlando et al. Phys. Rev. B35, 5347 (1987).
9. V. Kresin, Phys. Rev. B25, 157 (1982); B34, 7587 (1986).
10. A. Panson et al. Appl. Phys. Lett. 50, 1104 (1987); M. Tonouchi et al. Jpn. J. of Appl. Phys. 26 L519 (1987); N. Ong et al. (preprint).
11. W. Kwok et al. Phys. Rev. B35, 5343 (1987); S. Uchida et al. Jpn. J. of Appl. Phys. 26, L443 (1987).
12. H. Junod et al. (preprint).
13. N. Phillips et al. (preprint).
14. O. Fisher et al. (preprint).
15. P. G. DeGennes, "Superconductivity of Metals and Alloys," W. A. Benjamin, Inc., New York (1966).

COMPLEX HAMILTONIANS: COMMON FEATURES OF MECHANISMS FOR HIGH-T_c AND SLOW RELAXATION

K.L. Ngai, R.W. Rendell and A.K. Rajagopal

Naval Research Laboratory
Washington, D.C. 20375-5000, USA

INTRODUCTION

The discoveries of the new ceramic superconductors $La_{2-x}A_xCuO_{4-z}$ [1] and $YBa_2Cu_3O_{7-x}$ [2] with T_c of about 40K and 90K respectively have given new impetus to the discussions of high-T_c mechanisms. The specific mechanism by which electrons lower their energy by pairing in these superconducting ceramics is at issue. Conventional lattice vibration mechanisms may be inappropriate in view of experimental evidence of the absence of an isotope effect[3], and inadequate on theoretical grounds for the high transition temperature. For these reasons, alternative models have been seriously considered. By now, a number of mechanisms for high-T_c superconductivity have either been proposed specifically for these new materials or suggest themselves to be possible candidates. These include the resonating valence bond (RVB)[4], the negative-U models[5-7], the Bose condensation of bipolarons models[8,9], the d-wave pairing near a spin-density-wave instability of a positive-U Hubbard model[10], the surface or two-dimensional plasmon models[11,12], acoustic plasmon models[13], the excitonic models[14,15], the dynamic instability model[16], and many others that possibly we are not aware of. The answer to which one of these many theoretical ideas is ultimately responsible for the superconductivity in these ceramics will have to wait for further experimental investigations of both the normal and superconducting states. Arguments have been given that existing experimental data including the linear specific heats at low temperatures seems to eliminate even some unconventional versions of BCS theory of coupling between electron pairs and phonons, and indicates some models are favored.[17] The possibility should also be considered that the linear specific heat observed[36,37] at low temperatures in these new high-T_c materials may contain contributions from excess modes such as two-level-systems.

It has been recognized that in these high-T_c oxides, defects are present. Some of the defects are definitely related to vacancies caused by deficiency in oxygen. Studies of $La_{2-y}Sr_yCuO_{4-x}$ perovskite have shown that T_c is dramatically affected by subtle changes in oxygen content. Similarly, changes in oxygen content in the 90K series $REBa_2Cu_3O_{7-x}$ also drastically affect their physical properties and T_c[18]. Even in undoped La_2CuO_{4-y}, the occurrence of trace and filamentary superconductivity is extremely process dependent[19]. It can be reversibly removed or restored by heating the material in argon or oxygen. Moreover, the antiferromagnetism found[20] in La_2CuO_{4-y} is quite sensitive to the oxygen concentration parameter y. The

antiferromagnetic ordering temperature determined from neutron scattering rose from 50K to 150K with annealing in a vacuum to remove oxygen. The existence of a small oxygen vacancy concentration (y>0) appears to be crucial for promoting antiferromagnetism. Changes in the oxygen content may affect the average copper valence via corresponding changes in the oxidation states of copper atoms. The average valence of copper increases with the oxygen content. For example[18], it was found in $YBa_2Cu_3O_7$ that the oxygen content can change from 6.7 to 6.2 resulting in a change in the average valence of copper from 2.2 to 1.8. The valence implies the formation of Cu^{+1}. This change of the oxidation state has a number of implications including the possible charge fluctuations between $Cu^{++}O^{--}$ and $Cu^{+}O^{-}$ in the CuO_{1+x} planes[21], the spawning of negative-U centers[5], and the possible modification of the suggested Cu^{3+} - Cu^{4+} - like charge fluctuations which induce attractive interactions (-U centers) both in the chains and to the 2-dimensional (Cu2) bands.[7] Oxygen vacancies may also modify the RVB or spin-liquid model in the present form. The occurrence of "unsynchronized" resonance in the RVB model due to oxygen vacancies has also been pointed out[22].

The discussions in the previous paragraph serve the purpose of emphasizing that the real high-T_c materials are more complicated than the representations given by the model Hamiltonians of the proposed mechanisms. Some interactions are neglected and provisos are missing in the description of the realistic superconducting ceramics in the context of any one of these proposed models. In writing down the Hamiltonian for any of these models with a specific mechanism, a simplified form of it is usually adopted. The actual Hamiltonian may be more complex. For example, the negative-U Hamiltonian of a double-valence fluctuating molecule hybridized with the conduction-electron band is often drastically simplified to have the manageable form as given in References 5 & 6 for calculations of enhancement of T_c by use of perturbative techniques and Monte Carlo simulation techniques. A negative-U term $Un_{j\uparrow}n_{j\downarrow}$ is used to describe the attractive interaction when conduction electrons are transferred by hybridization onto the negative-U centers. The actual picture may be more truthfully described by orbitals, potentials, lattice distortions and kinetic degrees of freedom of both the conduction electron and the impurity electron. For the purpose of addressing the problem of enhancement of superconductivity, the simplification is not a problem and the approach adequate. However, a full representation of all the details and complicated aspects of the physics corresponding to any of these mechanisms would require a Hamiltonian more complex than is given. A large class of complex Hamiltonians possesses the generic feature of low-lying near degenerate states. The latter are particularly prominent if electron-electron correlations are important which appears from experimental inference[20] to be the case in La_2CuO_{4-y}. Low-lying near degenerate states are characteristics of metastability and the glassy state. However the existence of these near degenerate states does not necessarily imply metastability. In either case, a subset of these near degenerate states are responsible for the slowing down of long time relaxation processes resulting in slow nonexponential relaxations of the type commonly observed in equilibrium viscous liquids as well as in nonequilibrium glasses[23]. The existence of these near-degenerate states for quantum Hamiltonians in which there are strong correlations between different degrees of freedom has been documented to be a generic property. We will refer to systems with this property as complex Hamiltonians. In the corresponding classical limit, Hamiltonians are generally nonintegrable and possess a characteristic structure of regular and chaotic orbits in phase space. In either the quantum or the classical

context, we have provided a framework to show how the respective generic property manifests itself in slowing down of the primary relaxation rate W_o to have the self-similar time-dependent form of $W(t) = W_o(\omega_c t)^{-n}$, $0<n<1$, for $\omega_c t>1$. From this, the fractional exponential relaxation (Kohlrausch) function $\phi(t) = \exp[-(t/\tau^*)^{1-n}]$ along with additional predictions follow.[24] Another approach based on classical mechanics with time-dependent Dirac constraints and statistical mechanics of irreversible processes has also led to the same conclusions.[25]

From the previous discussions, it is clear that slow relaxation may naturally arise from the complex and non-integrable (in the classical mechanics sense) nature of the total unabridged Hamiltonian for many of the proposed high-T_c mechanisms if realistic interactions, conditions such as the existence of clusters and their different phase coherences, and imperfections in material are taken into account. If any of these proposed mechanisms turn out to be correct, then both high-T_c superconductivity and slow relaxation are two accompanying consequences of the same complex Hamiltonian. We are led to expect that in some of the high-T_c superconducting ceramics we may be able to observe experimentally a slow relaxation phenomenon. This turns out to be indeed the case and will be discussed in the next section. By contrast, the conventional BCS phonon mechanism for superconductivity in simple metals does not involve a complex Hamiltonian and slow relaxation is not expected there. Slow relaxation will provide, in addition to superconductive and magnetic properties, another handle on the physics of the high-T_c materials. A parallel study of superconductivity and slow relaxations and a comparison of their variations with conceivable modification of sample structure and defect concentrations by various means including heat treatment and sample preparation method, etc. may reveal correlations of their variations. The result may be able to provide some guidance in the search for the origin of high-T_c in these ceramic materials.

INFERENCES FROM EXPERIMENTS

In the previous section, we discussed that any alternative models to the BCS theory of phonon mediated superconductivity to account for the high-T_c superconductivity in the ceramics are likely to involve a complex Hamiltonian. Whichever it and the mechanism it represents may be, slow relaxation will be an accompanying feature as expected from our general considerations of relaxations in complex systems. In fact, Müller, Takashige and Bednorz[26] have found signatures for both a glass state and slow nonexponential decays from susceptibility and magnetic moment measurements in powder samples of La_2CuO_{4-y}:Ba. The experimental data and the sample properties suggest the picture of coupled superconducting clusters or grains each with size small compared with the London penetration depth and are weakly coupled into closed loops. The picture[27] is similar to a spin glass. This state in La_2CuO_{4-y} has been called the superconductive-glass state[26]. An estimate of the single phase area and the grain size has led to the conclusion that the superconductive-glass state is present in the La_2CuO_{4-y}:Ba grains. The Hamiltonian describing the entire array of weakly coupled grains[27] involves the sum over all distinct pairs of grains of terms $J_{ij}\cos(\phi_i-\phi_j-A_{ij})$ where ϕ_i and ϕ_j are phases of the complex energy gaps and A_{ij} is a magnetic field phase factor. Slow relaxation is attributed to correlation, cooperativity and coupling between grains. It is argued that "the phase coherence for a certain cluster has to become

close enough to neighboring ones that it can relax. This becomes less probable when the system evolves in time, and large volumes with different phase coherences are present". This qualitative argument for slow relaxation is consistent with our view of the slowing down of the relaxation rate by the coupling between clusters with Hamiltonian $\sum J_{ij}\cos(\phi_i-\phi_j-A_{ij})$.

Measurements of the real and imaginary parts of the ac susceptibility of the Y-Ba-Cu-O system have been made over a frequency range of a few decades[28]. The susceptibility exhibits frequency dependence at temperatures below 70K. The complicated temperature and frequency dependences of the susceptibility are attributed to inter-grain boundary effects. In the future, we can expect more investigations of relaxation properties in the high-T_c ceramics to be reported. The results will be useful for correlation with the superconductivity properties and their relation to the microstructure and chemical constituents of these materials.

COMPLEX HAMILTONIANS

In addition to the complex Hamiltonian discussed in the previous section that arises from coupled superconducting clusters that are present in some though perhaps not all of the high-T_c oxides, another source of complex Hamiltonian comes from the electron correlation effects that are important in any of the mechanisms for high-T_c superconductivity. Again let us consider the negative-U models or bipolaron models. The interaction for zero and double occupancies at the negative-U center usually involves significant lattice distortions and hence nonlinear potentials in the dynamical trapping of the pair of electrons. There are examples of such nonlinear Hamiltonians which in the classical context gives rise to chaos in phase space, and in the quantum context to near degenerate levels with a distribution conforming to so-called Gaussian Orthogonal Ensemble (GOE) of random matrix theory. These include several Hamiltonians with two degrees of freedom coupled by nonlinear potentials in the coordinates.

$$H = \sum(p_i^2/2m_i) + \alpha V(q_1,q_2) \qquad (1)$$

For a large class of potentials V, the quantum energy levels are found to exhibit level repulsion and their fluctuation properties conform to well-defined statistical distributions as α increases and the correlations between degrees of freedom become important. An example is the Morse potential, $V = [1-\exp[-a(q_2 - q_1)]]^2$, which is often used to represent molecular bonds. This is also equivalent via canonical transformation to a Hamiltonian with coupling in the kinetic energy. The quantized energy spectra of the Morse potential system has been studied numerically.[29] In particular, the nearest-neighbor level-spacing distributions were constructed for different values of the Hamiltonian parameters. In the limit of strong coupling, where the Hamiltonian is expected to be complex, the calculated distributions are closely described by $P(S/\bar{S}) = (\pi S/2\bar{S}^2)\exp(-\pi S^2/4\bar{S}^2)$, where S is the nearest-neighbor level spacing and $\bar{S}$ is the mean spacing. This is the Wigner distribution which also closely describes the GOE of random matrix theory. The same limit of strong coupling in this system corresponds to classical motion which is nonintegrable and predominantly chaotic as exhibited by trajectories in Poincare sections of the Hamiltonian. As α decreases and the interparticle correlations become less important, $P(S/\bar{S})$ tends instead to a simple Poisson distribution and the corresponding classical motion becomes dominated by regular trajectories. These quantum and classical results are borne out by explicit solutions of many other nonlinear potentials.

In addition to these explicit numerical solutions, arguments have been proposed by Pechukas, and improved upon by Berry and Yukawa, to understand the spectral properties of Hamiltonians in a more general context as α varies in strength.[30] These are based on the observation that for complex Hamiltonians, there are no strong selection rules and the off-diagonal matrix elements of V between nearby states are large and of the same average strength. These matrix elements also fluctuate rapidly with α. However, for simple Hamiltonians, with strong selection rules, off-diagonal matrix elements are small compared to the mean level spacing. Within this context, an explicit analytical construction of the level spacing distribution functions were developed by supplementing the Hamiltonian $H = H_o + \alpha V$ with statistical mechanical arguments. For Hamiltonians representing quantum systems with time-reversal symmetry, the results (in arbitrary number of dimensions) are again in accord with GOE when the Hamiltonian is complex and α is large and makes a transition to the Poisson distribution as α decreases. More recently, Nakamura and Lakshmanan[30] have proposed a rigorous basis for these developments based on Lax forms and their solutions. Berry[31] has also discussed the generic occurrence of level repulsion in connection with the Wigner-von Neumann theorem for energy level degeneracies. Thus there is increasing understanding of how specific features of complex Hamiltonians influence the generic features of level spectra. Others have suggested the use of Lanczos-Haydock-Heine tridiagonalization methods to study the spectra of electronic bands in imperfect solids. A simple example of this was actually studied previously by Berry[31] for motion in a 2-d lattice of hard scatterers (i.e. quantum billiard). Solution of the KKR determinant of this system revealed a GOE spectrum. The corresponding classical behavior is strongly chaotic.

Consider next the RVB model with inclusion of possible oxygen vacancies and frustrations. The RVB or spin singlet liquid state has been suggested as being the appropriate ground state for $S = \frac{1}{2}$ Heisenberg antiferromagnets. The characterization of quantum and classical generic features in lattice spin systems has recently been addressed by Muller.[32] Spin systems containing N spins can be studied in the limit of N finite, $S \to \infty$ (classical limit) as well as in the limit of S finite, $N \to \infty$ (thermodynamic limit). The classical limit was examined by Nakamura and Bishop[33] by explicit calculations on a three-spin triangular lattice with antiferromagnetic coupling:

$$H = J\sum(\vec{S}_i \cdot \vec{S}_{i+1} + \sigma S_i^z S_{i+1}^z) \qquad (2)$$

where $J>0, -1\leq\sigma<0$ and $i = 1,2,3$. Boundary conditions are periodic. The triangular lattice with antiferromagnetic coupling is frustrated in the sense that there are competing interactions, especially for small values of S. For $S = \frac{1}{2}$, the presence of frustration will enhance the formation of the RVB. For $S>\frac{1}{2}$, the classical dynamics of this system appear to be nonintegrable (excluding the isotropic limit $\sigma = 0$) and the semiclassical quantum spectra exhibits level repulsion. A sufficient number of levels to explore the statistical properties of the spectrum were available even for the three-spin cluster by using spin values as large as $S = 36\frac{1}{2}$. From these results, the authors expect studies with even larger S will reveal a Poisson distribution for $\sigma = 0$ and a Wigner distribution for $\sigma<0$. Muller expects this situation to be generic for the classical limit of spin systems. He also discusses the work of Frahm and Mikeska on a driven one-spin system who found both a Wigner distribution and nonintegrable classical dynamics in the $S>>1$ regime. Thus the behavior of spin systems in the classical and semiclassical regimes is accessible by study of small spin clusters of large but finite S. Here the generic level spacing structure

is a precursor of classical dynamical chaos. For the situation representative of the high-T_c ceramics, the Hamiltonian is far more complicated than the simple Heisenberg system in Eq. (2). Of more immediate interest is the study of the appropriate Hamiltonian in the complementary limit of small S (e.g. S = ½) and a large spin cluster, i.e. the thermodynamic limit. This is more difficult to analyze theoretically but Muller[32] has suggested that the spectrum of quantum spin systems is generically irregular in this limit with strong level repulsion due to the lack of a sufficient number of conservation laws (i.e. selection rules). He discusses and presents evidence for the emergence in this limit of an irregular spectrum which is not constrained by a piece-wise smooth energy density with isolated van Hove singularities. Muller presents the $N\to\infty$ limit of quantum spin systems as a regime of quantum chaos for which the long time dynamical behavior will be modified. Although the corresponding spectrum has not yet been completely studied, it can be expected that large numbers of quantum spins with complicated and frustrated interactions will introduce some type of generic complexity into the Hamiltonian.

Let us finally return to the other class of complex Hamiltonians describing the coupling between superconducting clusters in some samples of the high-T_c ceramics. The diamagnetic response of weakly linked superconducting clusters was modeled by Ebner and Stroud[27] in terms of coupling between the host material and the grains according to the Hamiltonian

$$H = \sum J_{ij}\cos(\phi_i-\phi_i-A_{ij}) \qquad (3)$$

where J_{ij} is the coupling energy between grains i and j, and the phase factors A_{ij} are due to the presence of a static external magnetic field. This "Josephson tunneling" model is characterized by frustration in that any cluster of grains has numerous competing ground states with nearly equal energy. Such frustration is familiar from previously studied systems such as spin glass models. Randomness can enter through the Josephson coupling energy J_{ij} and also through the grain sizes. The existence of many local energy minima in classical XY systems and planar spin models with random J_{ij} similar to Eq. (3) are known from numerical studies. For the purpose of relaxation, this situation leads to a picture in which some clusters must wait to relax until the phase coherence becomes close encugh to neighboring ones. Such cooperativity due to correlations between degrees of freedom has many of the ingredients present in our discussion of relaxation of complex Hamiltonians. It is possible that a system described by a Hamiltonian such as Eq. (3), supplemented by other additional interactions and randomness which will inevitably be present in a realistic representation of the ceramics, may constitute a complex Hamiltonian in this sense. Efetov[34] has given an example of an electron in which the presence of a random distribution of impurities induces a complex level spectra described by the GOE distribution. Simple driven spin systems in the regime in which the driving force acts as a random interaction also exhibit the generic GOE level spectra. The more complicated granular superconductor system must then be seriously considered as a possible complex Hamiltonian.

SLOWING DOWN OF RELAXATION RATE

We have seen that it is likely that the complex Hamiltonians proposed for high-T_c will give rise to low-lying degenerate levels. A possible source of the latter is the strong electron correlation effects common to a number of these complex Hamiltonians. If we pick out a dynamical variable

(say the spin) and consider its relaxation, then the electron correlation effects present would make the relaxation process difficult to describe. Basically, we have to deal with a many-body problem in an irreversible process for which there is no standard method of solution. We have recognized the possibility that the dynamical variable is being coupled to others and its relaxation rate is slowing down with time by the constraints imposed by the others. The idea that the relaxation rate that enters into a master equation can be a time-dependent function is a central idea of our models and this is physically reasonable for relaxation in complex systems with correlations. Rates for kinetic equations are known to be generally time-dependent and constant relaxation rates have been derived only for simple integrable Hamiltonians under some simplifying assumptions of the heat bath such as the weak-coupling limit. Intuitively, a time-dependent relaxation rate W(t) can be motivated by cooperativity which entails dynamics of other variables sequential to the initial relaxation of a primary variable. It is also consistent with general properties of relaxation functions. Remarkably, the only time-dependence of W(t) which guarantees that a change of temperature will change only the timescale but not the functional form of the relaxation function of a relaxation process (i.e. thermorheological simplicity)[25] has the monomial form of

$$W(t) = W_o(\omega_c t)^{-n} \tag{4}$$

where W_o is the primary relaxation rate, ω_c is a characteristic frequency and n is a fraction of unity. We can arrive at the same result by another requirement for the stability of the relaxation spectrum in forming the macroscopic relaxation spectrum by superposition of microscopic relaxation spectra. In addition to these general considerations, W(t) can be derived on the basis of Hamiltonian dynamics where the generic properties of complex Hamiltonians are taken into account. We have modeled the sequential dynamics of the other variables by the transitions among the low-lying near degenerate levels of the complex Hamiltonian. If the initial (at short times) relaxation rate of the primary variable is W_o, then the accompanying transitions modify it to have the time-dependent form of Eq. (4). This can also be derived[35] directly in terms of the corresponding classical generic property, classical chaos. The current understanding of the relation between kinetic equations for the approach to thermodynamic equilibrium and microscopic equations of motion are based on the methods developed by van Hove, Prigogine, and others. A Hamiltonian H_S interacting with a heat bath will systematically produce irreversible kinetic equations with constant relaxation rates W_o. Previous workers have only derived kinetic equations corresponding to integrable Hamiltonians H_S, whereas it has become known that Hamiltonians are generically nonintegrable. We have recently derived[35] kinetic equations directly from the equations of motion for classical nonintegrable H_S's interacting with a heat bath. In the weak-coupling limit, we find that the effect of nonintegrability for a large class of systems is generally to modify the constant relaxation rates by a multiplicative time-dependent factor: $W_o f(t)$. The form of f(t) has been investigated both analytically and numerically and its origins can be traced to the mechanism of classical chaos. The results are again consistent with: $f(t) = 1$, $\omega_c t<1$ and $f(t) = (\omega_c t)^{-n}$, $\omega_c t>1$ where $0<n<1$. This leads directly to nonexponential relaxation $\exp[-(t/\tau^*)^{1-n}]$ along with the modified relaxation time $\tau^* = [(1-n)\omega_c^n/W_o]^{1/(1-n)}$ as has been experimentally documented for glasses and polymers. These are examples of our continuing effort to improve our understanding of relaxations in complex systems which may include some of the high-T_c materials.

This work is supported in part (K. L. Ngai and R. W. Rendell) by ONR Contract No. N0001487WX24039.

REFERENCES

1. J. G. Bednorz and K. A. Müller, Z. Phys. B64:189 (1986).
2. M. K. Wu, J. R. Ashburn, C. T. Torng, P. H. Hor, R. L. Meng, L. Gao, Z. J. Huang, Y. Q. Wang, and C. W. Chiu, Phys. Rev. Lett. 58:908 (1987).
3. B. Batlogg, R. J. Cava, A. Jayaraman, R. B. van Dover, G. A. Kourouklis, S. Sunshine, D. W. Murphy, L. W. Rupp, H. S. Chen, A. White, K. T. Short, A. M. Mujsie, and E. A. Rietman, to be published (1987).
4. P. W. Anderson, Science 235:1196 (1987).
5. C. S. Ting, D. N. Talwar and K. L. Ngai, Phys. Rev. Lett. 45:1213 (1980); C. S. Ting, K. L. Ngai, and C. T. White, Phys. Rev. B22:2318 (1980).
6. H. B. Schuttler, M. Jarrell, and D. J. Scalapino, Phys. Rev. Lett. 58:1147 (1987).
7. J. Tu, S. Massidda, A. J. Freeman, and D. D. Koelling, to be published.
8. A. S. Alexandrov, J. Ranninger, and S. Robaszkiewicz, Phys. Rev. B33:4526 (1986); L-Y. Zhang, Solid State Comm. 62:491 (1987).
9. N. Mott, Nature 327:185 (1987).
10. D. J. Scalapino, E. Loh, and J. E. Hirsch, Phys. Rev. B34:8190 (1986).
11. E. N. Economou and K. L. Ngai, Solid State Comm. 17:1155 (1975).
12. V. Kresin, to be published.
13. J. Ruvalds, to be published.
14. J. Bardeen, in: Superconductivity in d- and f-Band Metals, D. Douglas, ed., Plenum, NY (1976).
15. C. M. Varma, S. Schmitt-Rink, and E. Abrahams, to be published.
16. K. L. Ngai and T. L. Reinecke, Phys. Rev. B16:1077 (1977).
17. P. W. Anderson and E. Abrahams, Nature 327:363 (1987).
18. J. M. Tarascon, W. R. McKinnon, L. H. Greene, G. W. Hull and E. M. Vogel, to be published.
19. P. M. Grant, S. S. P. Parkin, V. Y. Lee, E. M. Engler, M. L. Ramirez, J. E. Vazquez, G. Lim, R. D. Jacowitz, and R. L. Greene, Phys. Rev. Lett. 58:2482 (1987).
20. D. Vaknin, S. K. Sinha, D. E. Moncton, D. C. Johnston, J. Newsam, C. R. Safinya, and H. E. King, Jr., to be published, Science 236:780 (1987).
21. P. H. Hor, R. L. Meng, Y. Q. Wang, L. Gao, Z. J. Huang, J. Bechtold, K. Forster, and C. W. Chu, Phys. Rev. Lett. 58:1891 (1987).
22. L. Pauling (preprint).
23. Dynamic Aspects of Structural Change in Liquids and Glasses, C. A. Angell and M. Goldstein, eds., Annals, New York Acad. Sci. 484 (1986).
24. For a review, see K. L. Ngai, R. W. Rendell, A. K. Rajagopal, and S. Teitler, in Ref. 23, pp. 150-184; pp. 321-323.
25. K. L. Ngai, A. K. Rajagopal, and S. Teitler, to be published.
26. K. A. Müller, M. Takashige and J. G. Bednorz, Phys. Rev. Lett. 58:1143 (1987).
27. C. Ebner and D. Stroud, Phys. Rev. B31:165 (1985).
28. K. V. Rao, D. X. Chen, J. Nogues, C. Politis, C. Gallo, and J. A. Gerber, to be published.
29. T. Terasaka and T. Matsushita, Phys. Rev. A32:538 (1985).

30. K. Nakamura and M. Lakshmanan, Phys. Rev. Lett. 57:1661 (1986) and references therein.
31. M. V. Berry, Ann. Phys. 131:163 (1981).
32. G. Muller, Phys. Rev. A34:3345 (1986).
33. K. Nakamura and A. R. Bishop, Phys. Rev. B33:1963 (1986).
34. K. B. Efetov, Adv. Phys. 32:53 (1983).
35. R. W. Rendell and K. L. Ngai, to be published.
36. M. Decroux, A. Junod, A. Bezinge, D. Cattani, J. Cors, J. L. Jorda, A. Stettler, M. Francois, K. Yvon, O. Fischer and J. Muller, Europhys. Lett. 3:1035 (1987).
37. M. E. Reeves, T. A. Friedmann and D. M. Ginsberg, Phys. Rev. B35:7207 (1987).

LOW TEMPERATURE STRUCTURAL PHASE TRANSITION IN La_2CuO_4

E. F. Skelton, W. T. Elam, D. U. Gubser, V. Letourneau,

M. S. Osofsky, S. B. Qadri, L. E. Toth[†], and S. A. Wolf

Condensed Matter and Radiation Sciences Division

Naval Research Laboatory
Washington, DC 20375-5000

Abstract

Electrical reistance and x-ray diffraction measurements have been made on several samples of La_2CuO_4. The electrical data on one sample show the presence of a semiconductive to metallic transition on cooling near 35 K; this could be evidence of superconductivity. The x-ray data reveal the presence of one (possibly two) structural phase transition(s) at 32-34 K and below 15 K. The lower transition is reversible and seen in all samples, along with remanents of the orthorhombically distorted K_2NiF_4-structure of the parent phase. The observed peaks in the low temperature phase can be indexed to a monoclinic lattice. It is believed that the orthorhombic phase is responsible for the recently discovered superconductivity in some La_2CuO_4 samples and that the monoclinic polymorph reported here is responsible for the low temperature semiconductive behavior of most La_2CuO_4 samples. These conclusions are in agreement with recent theoretical predictions.

[†]Permanent address: National Science Foundation, Washington, DC, 20550.

M.S.O. was partially supported by the Office of Naval Technology.

Recently, there has been a tremendous interest and excitment generated by the new class of oxygen defect, perovskite related, copper oxide superconductors. All of this was initiated by the discovery of superconductivity at temperatures in excess of 30 K in La-Ba-Cu-oxides [1] and the subsequent discovery of superconductivity in excess of 90 K in Y-Ba-Cu-oxides.[2] The prototypical compound for the lower transition temperature materials is La_2CuO_4 in the orthorhombically distorted K_2NiF_4-structure. It has recently been shown that the superconducting compounds $La_{2-x}M_xCuO_4$, where M = Sr, Ba, or Ca, are also orthorhombic above T_c.[3,4] Based on first-principles calculations, Pickett et al. predicted that tetragonal La_2CuO_4 should be superconducting.[5] Very recent band structure calculations and group theoretical analyses of Kasowski, Hsu, and Herman [6] indicate also that orthorhombic La_2CuO_4 should also be metallic and superconducting. Indeed, recent experiments performed here and elsewhere on La_2CuO_4-samples quenched from high temperatures (> 800° C) show evidence that portions of the sample are superconducting.[7]. Thus, it has been a mystery why single phase samples of La_2CuO_4 show a semiconducting-like behavour at low temperatures. Kasowski et al.[6] suggest that there is an additional phase transition occuring at low temperatures from the orthorhombically distorted K_2NiF_4-structure to a lower symmetry structure, possibly monoclinic. Detailed temperature dependent x-ray diffraction data reported here show unambiguously that indeed a structural transition (or possibly two transitions) does occur at low temperatures. We believe that the orthorhombic phase is responsible for the recently discovered superconductivity in some La_2CuO_4 samples and that the low temperature polymorph is responsible for the low temperature semiconductive behavior of most La_2CuO_4 samples. These conclusions are in agreement with recent theoretical predictions.

Test specimens were prepared by mixing appropriate proportions of reagent grade powders of La_2O_3 and CuO to yield a product of La_2CuO_4. The La_2O_3 was 99.99% pure and contained 1 ppm of Ca, with no Sr or Ba detected; the CuO contained 1 ppm Ba and less than 1 ppm Sr. The powders were reacted in air at 950° C for 6 h, with one grinding after 3 h. The powders were again ground and pressed at 20 kpsi into 1/2-in. diameter pellets, sintered at 950° C in air for 15 h, and then slowly cooled

(~2°C/min). These samples gradually fell apart in a matter of days when left exposed to air at room temperature due to the absorption of water. The crumbled pellets were again resintered at 940° C in air and furnace cooled to 400° C. At this point the samples were transferred to a dessicator where they remained stable. One sample (referred to below as "quenched") was reheated to 900° C in air overnight and then rapidly cooled in air.

Resistance measurements were made using standard ac, four-probe method with currents of 5 and 50 μA. Results of these measurements are shown in Fig. 1. The sample which was slowly cooled showed no evidence of metallic behavior between 295 and 5 K, in contrast to this, the sample which was quenched, exhibited an maximum in resistance on cooling at about 36 K, below which it did behave as a metal. It is possible that this indicates that portions of the material are superconducting. We note that Grant et al. recently reported evidence of superconductivity in these materials, but found it to be trace-like, filamentary, and very sensitive to stoichiometry.[7]

Portions of the two La_2CuO_4 samples were separately ground, mixed in a dilute solution of celvacene and acetone, and evaporated onto a conductive sample mount. The samples were mounted in an x-ray cryostat and studied in a manner similar to that recently discussed for $La_{1.9}Ba_{0.1}CuO_4$.[8] A diffraction spectrum taken of the slowly cooled sample at 295 K is shown in Fig. 2a. All of the major peaks can be indexed on the basis of the orthorhombic lattice initially reported by Longo and Raccah.[8] Unit cell parameters determined from this spectrum are: a = 5.363±0.010; b = 5.400±0.012; c = 13.16±0.02 Å; these are in agreement with those reported by Longo and Raccah.[9] Similar results were obtained for the quenched sample.

On cooling, there was no evidence of of any structural change above about 15 K. Below this however, there was a major change in the diffraction spectrum. Fig 2b is a spectrum of the quenched sample recorded at 11.5±0.5 K. There is a small fraction of the sample which is still in the orthorhombic phase; diffraction peaks marked by the arrows correspond to this. However, the major portion of the sample has undergone a phase transformation as indicated by the other peaks in the pattern. Although attempts were made to index the low temperature pattern to higher symmetry lattices, the best fit was found for a monoclinic lattice with the following parameters: a = 6.495±0.005 Å; b = 4.163±0.002 Å; c = 5.522±0.002 Å; β = 96.15±0.05°.

It is our presumption that this new phase is responsible for the semiconductive behavior at low temperatures, as predicted by Kasowski et al.[6] However, the fact that this semiconducting behavior can be seen at higher temperatures, suggests that there also may be other, more subtle, mechanisms involved, such as the charge-density wave distortion predicted by Mattheiss [10] and possibly seen by Stavola et al.[11]

In an attempt to identify the structural transition temperature, the x-ray detector was centered with a wide angle window on the prominent diffraction peak in the low temperature phase at 27.5° 2θ. The intensity of this peak was monitored as the sample was slowly warmed; see Fig. 3. At approximately 27 K, the intensity began to decrease; background level was attained at about 37 K. On cooling, the reverse transition, as determined by the growth of this peak, was not observed at temperatures above 15 K, however below this a steady growth took place. If a portion of the sample had already partially transformed, a substantial increase in the magnitude of this peak could be produced by repetitive cycling between 27 and 10 K.

In a few cases, on warming through the transition near 35 K, the declining intensity would pass through a small local maximum before dropping to the background level. We suspect that this may be indicative of a possible second, intermediate phase encountered on warming and we have provisional x-ray data to support this. Further investigation of this is underway. It is unclear to us why other reported low temperature structural investigations of this material have not seen this transition.[12-14] A possible explanation could be the sluggish nature of the transition on cooling, especially if cooled quickly and held at very low temperatures.

The point that we are making in this letter is that there exists a heretofore unknown low temperature phase in La_2CuO_4. It is presumed that this is the phase predicted by Kasowski et al.[5] and that responsible for the low temperature semiconductive properties of most La_2CuO_4-samples. All samples that we studied also exhibited evidence of residual elements of the orthorhombic phase at the lowest temperatures; the amounts of this phase varied from sample to sample. We believe that it is this phase which is responsible for the superconductivity seen in some La_2CuO_4-samples. These results are consistent with the recent discovery by Grant et al. [7]

Acknowledgments

We thank Dr. Warren E. Pickett for helpful discussions, Mr. William Lichter for assistance in preparation of some of the samples, and Dr. Larry W. Finger of the Carnegie Institution of Washington for assistance with the indexing program.

References

1. J. G. Bednorz and K. A. Muller, Z. Phys. **B64**, 189 (1986).

2. M. K. Wu, J. R. Ashburn, C. J. Torng, P. H. Hor, R. L. Meng, L. Gao, Z. J. Huang, Y. Q. Wang, and C. W. Chu, Phys. Rev. Lett. **58**, 908 (1987).

3. U. Geiser, M. A. Beno, A. J. Schultz, H. H. Wang, T. J. Allen, M. R. Monaghan, and J. M. Williams, Phys. Rev.-B **35**, 6721 (1987).

4. M. Onoda, S. Shamoto, M. Sato, and S. Hosoya, Jpn. J. Appl. Phys. **26**, l363 (1987).

5. W. E. Pickett, H. Krakauer, D. A. Papaconstantopoulos, and L. L. Boyer, Phys. Rev.-B **35**, 7252 (1987).

6. R. V. Kasowski, W. Y. Hsu, and F. Herman, Solid State Commun., -in press.

7. P. M. Grant, S. S. P. Parkin, V. Y. Lee, E. M. Engler, M. L. Ramirez, J. E. Vazquez, G. Lim, R. D. Jacowitz, and R. L. Greene, Phys. Rev. Lett.,-to appear 8 June 1987.

8. E. F. Skelton, W. T. Elam, D. U. Gubser, S. H. Lawrence, M. S. Osofsky,

L. E. Toth, and S. A. Wolf, Phys. Rev. B **35**, 7140 (1987).

9. J. M. Longo and P. M. Raccah, J. Solid State Chem. **6**, 526 (1973).

10. L. F. Mattheiss, Phys. Rev. Lett. **58**, 1028 (1987).

11. M. Stavola, R. J. Cava, and E. A. Rietman, Phys. Rev. Lett. **58**, 1571 (1987).

12. J. D. Jorgensen, H. -B. Schuttler, D. G. Hinks, D. W. Capone, II, K. Zhang, M. B. Brodsky, and D. J. Scalapino, Phys. Rev. Lett. **58**, 1024 (1987).

13. T. Freltoft, J. P. Remeika, D. E. Moncton, A. S. Cooper, J. E. Fischer, D. Harshman, G. Shirane, S. K. Sinha, and D. Vaknin, -in press.

14. S. Mitsuda, G. Shirane, S. K. Sinha, D. C. Johnston, M. S. Alvarez, D. Vaknin, and D. E. Moncton, -in press.

Figure Captions

Fig. 1: Temperature dependence of the ac resistance of quenched and slowly cooled samples of La_2CuO_4.

Fig. 2a: X-ray diffraction spectrum of La_2CuO_4 recorded at 295K.

Fig. 2b: X-ray diffraction spectrum of La_2CuO_4 recorded at 11.5±0.5 K; the upper curve is the same spectrum with the scale factor of the ordinate multiplied by 10. The arrows indicate peaks believed to be associated with the high temperature, orthorhombic phase.

Fig. 3: Temperature dependence of the diffracted intensity near 27.5° 2θ recorded on cooling (lower curve) and warming (upper curves).

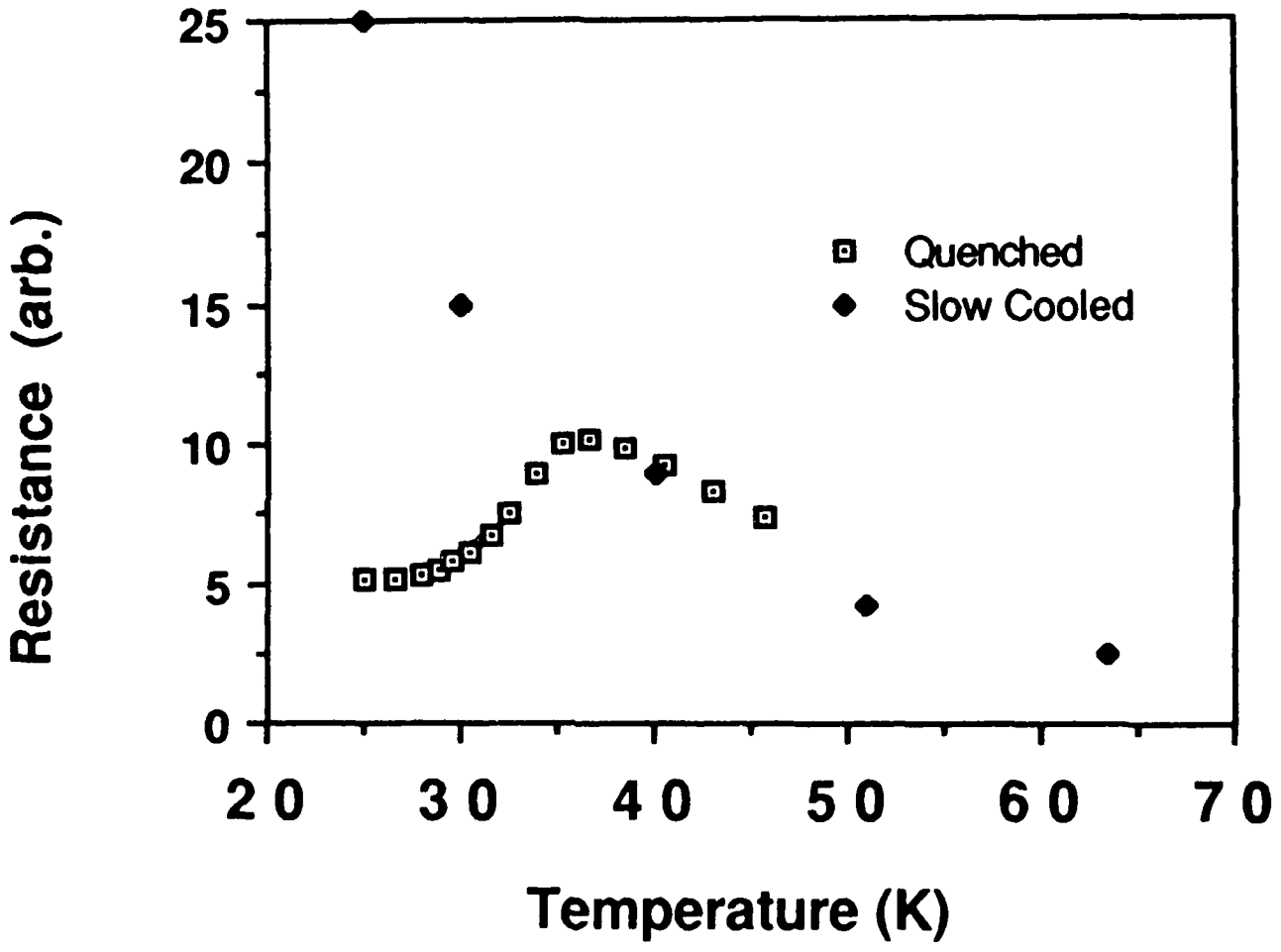
25
20
15
10
5
0
Resistance (arb.)
Quenched
Slow Cooled
20
30
40
50
60
70
Temperature (K)

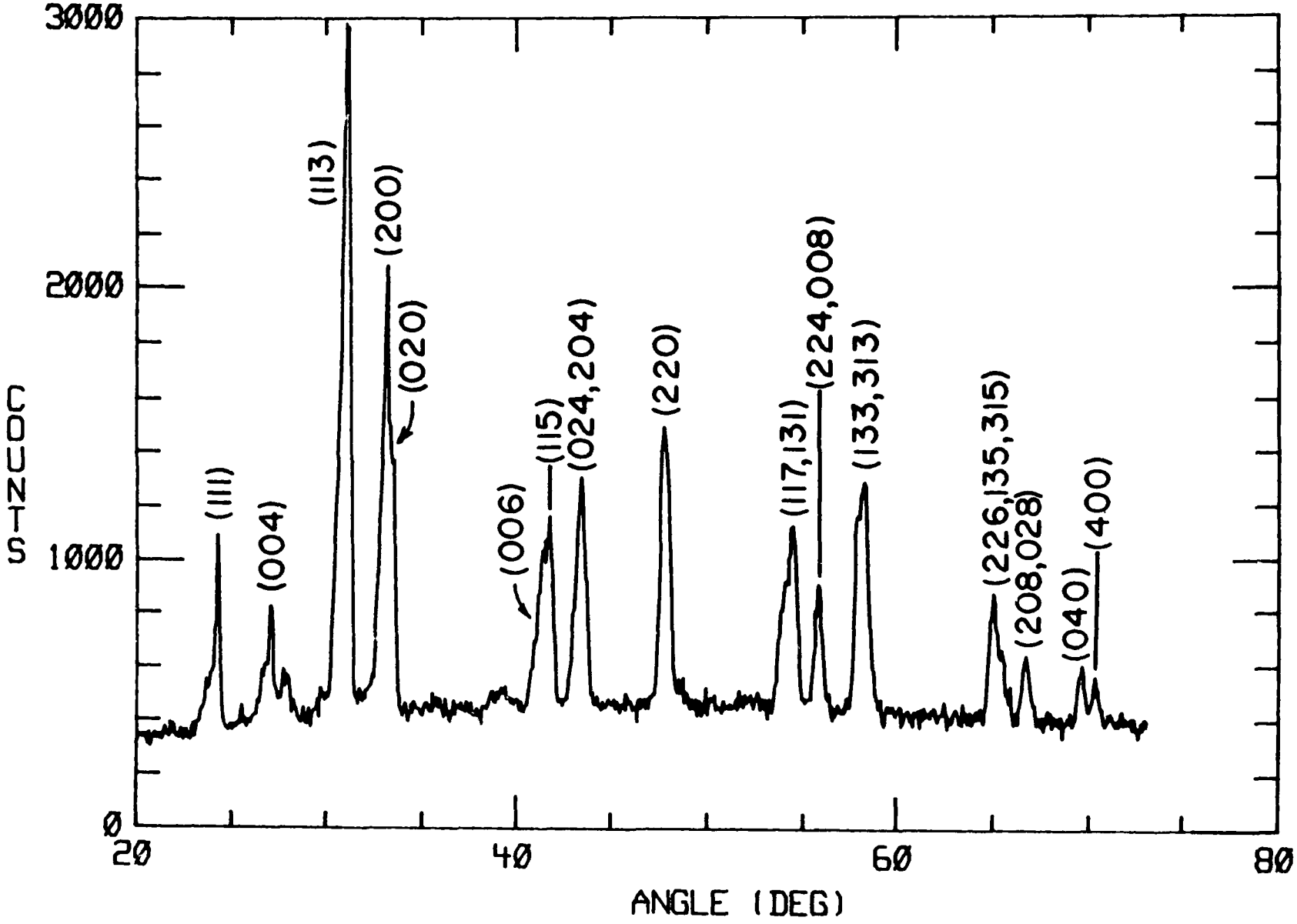
3000
2000
1000
0
COUNTS
20
40
60
80
ANGLE (DEG)
(111)
(004)
(113)
(200)
(020)
(006)
(115)
(024,204)
(220)
(117,131)
(224,008)
(133,313)
(226,135,315)
(208,028)
(040)
(400)

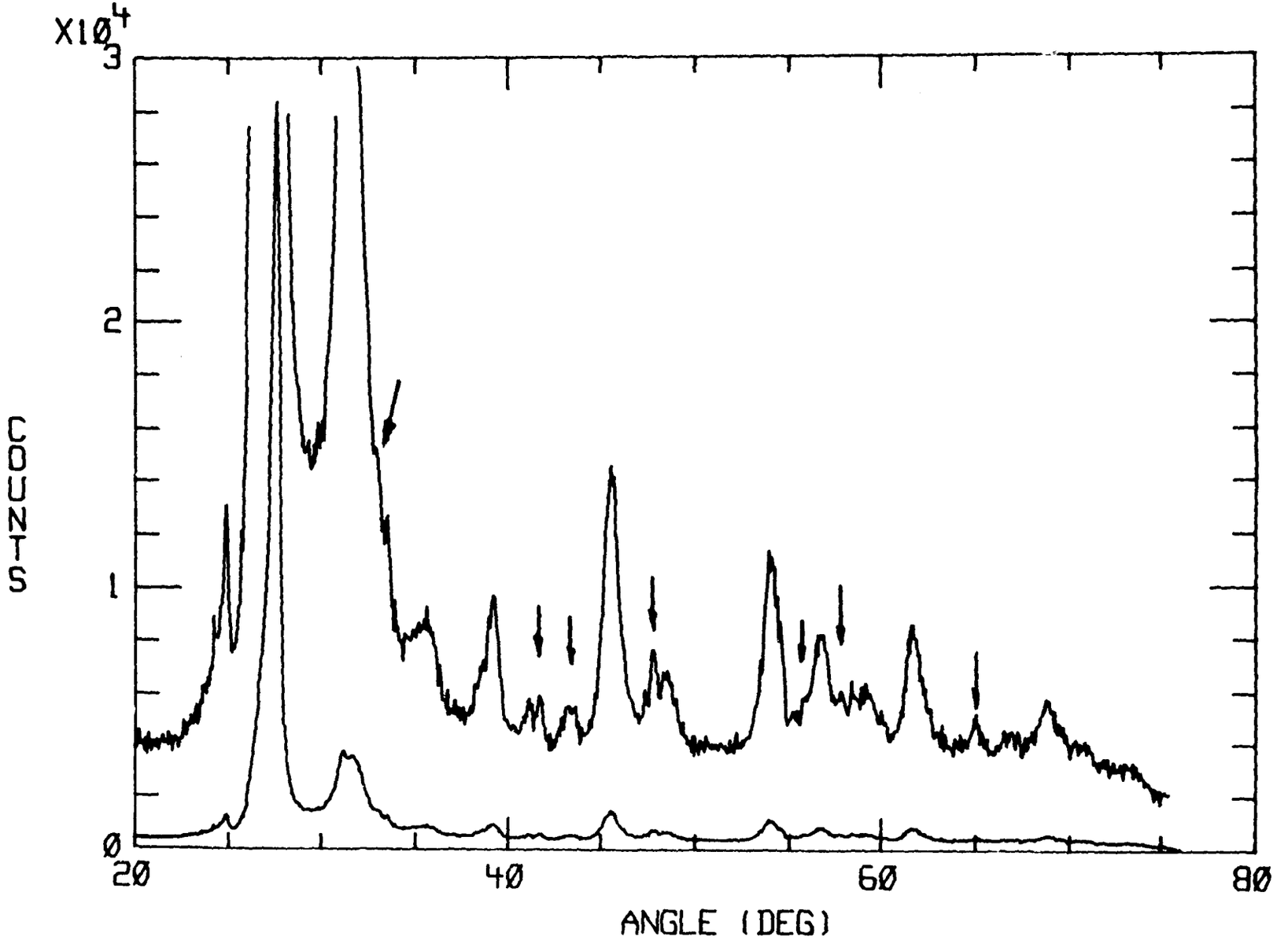
X10^4
3
2
1
0
COUNTS
20
40
60
80
ANGLE (DEG)

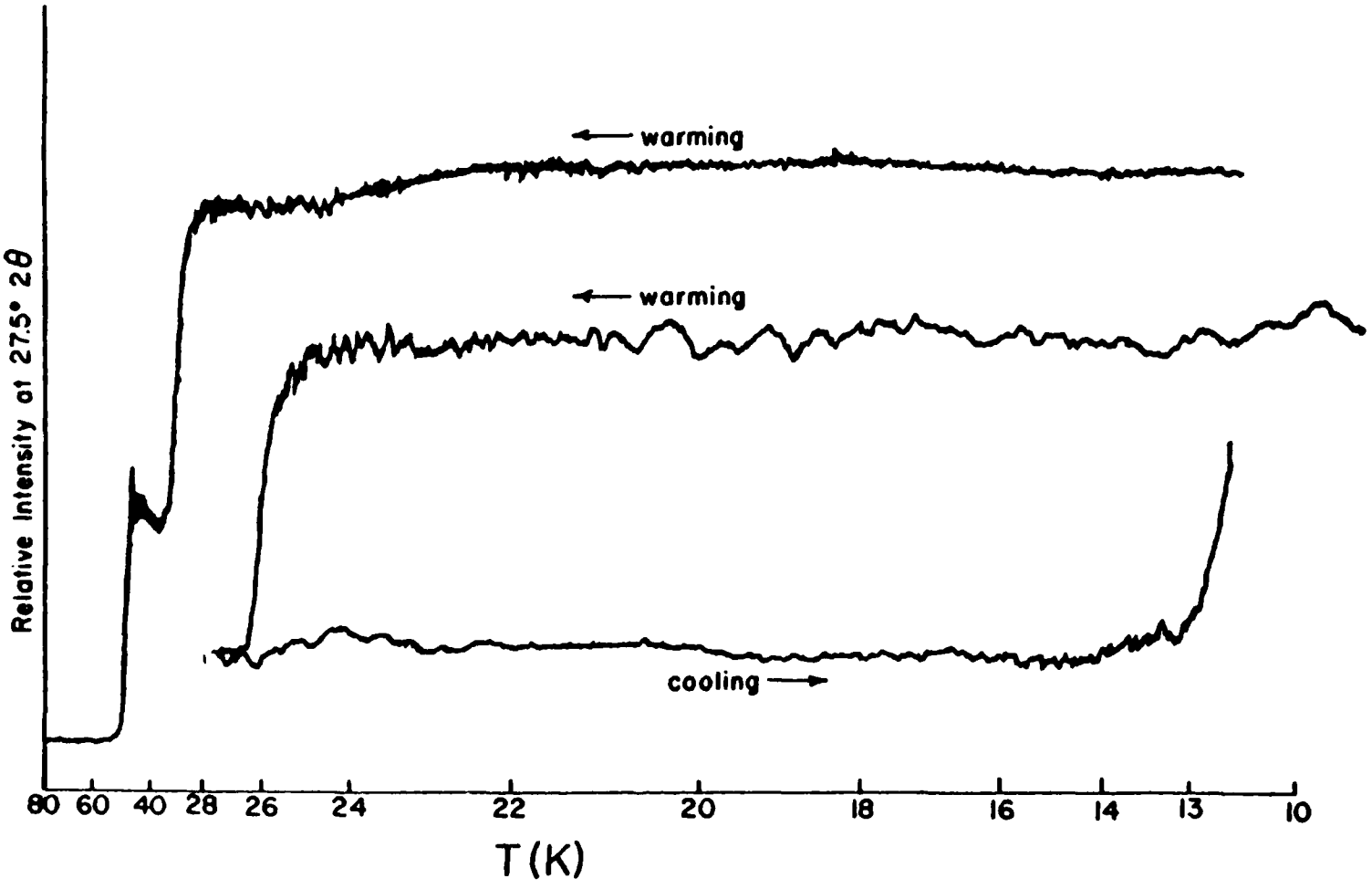
warming
warming
cooling
Relative Intensity at 27.5° 2θ
80 60 40 28 26 24 22 20 18 16 14 13 10
T(K)

A COUPLED STRUCTURAL AND ELECTRICAL TRANSITION IN La_2CuO_4 NEAR 30 K

E. F. Skelton, W. T. Elam, D. U. Gubser, R. A. Hein, V. Letourneau, M. S. Osofsky[†], S. B. Qadri, L. E. Toth[††], and S. A. Wolf

Condensed Matter and Radiation Sciences Division,
Naval Research Laboratory, Washington, DC 20375-5000

[†]Supported by the Office of Naval Technology
[††]Permanent address: National Science Foundation,
Washington, DC 20550

INTRODUCTION

Recently there has been an explosion of activity focused on the new class of oxygen defect, perovskite related, copper oxide superconductors. All of this was initiated by the discovery of superconductivity at temperatures in excess of 30 K in La-Ba-Cu-oxides[1] and the subsequent discovery of superconductivity in excess of 90 K in Y-Ba-Cu-oxides.[2] The prototypical compound for the lower transition temperature materials is La_2CuO_4 which, at room temperature, crystallizes in an orthorhombic distortion of the K_2NiF_4-structure.[3,4] It has recently been shown that the superconducting compounds $La_{2-x}M_xCuO_4$, where M = Ba, Ca, or Sr, are also orthorhombic above T_c.[5,6]

Based on first principles calculations, Pickett et al. predicted that tetragonal La_2CuO_4 should be superconducting.[7] However, resistance measurements of Jorgensen et al. on La_2CuO_4 indicated that the material is metallic down to about 100 K, below which it behaves like a doped semiconductor.[4] Most recently Grant et al. reported evidence of superconductivity below 40 K of 1 part in 6000 of La_2CuO_4.[8] In consideration of the presence of both metal-like and semiconductor-like behavior in this material, Kasowski et al. performed band structure calculations and group theoretical analyses.[9] From this, they suggested that La_2CuO_4 may undergo a structural phase transition at lower temperatures from the orthorhombic phase to a lower symmetry phase, possibly monoclinic. We have found evidence of such a transition and find that it is correlated with a change in the resistance near 30 K.

EXPERIMENTAL PROCEDURES

Test samples were prepared by mixing appropriate proportions of reagent grade powders of La_2O_3 and CuO to yield a product of La_2CuO_4.

The La_2O_3 was 99.99% pure and contained 1 ppm of Ca, with no Sr or Ba detected; the CuO contained 1 ppm Ba and less than 1 ppm of Sr. The powders were reacted in air at 950° C for 6 hr, with one grinding after 3 hr. The powders were again ground and pressed at 20 kpsi into pellets, sintered at 950° C in air for 15 hr, and then slowly cooled (2° C/min).

Simultaneous resistance and x-ray diffraction measurements were performed in a temperature controlled cryostat. The resistance measurements were made using standard ac, four probe methods with 100 microamps of current at a frequency of 31 hz. The x-ray data were collected on a computer controlled diffractometer using Cu K-alpha radiation. Additional details are given on our earlier report on the superconductor $La_{1.9}Ba_{0.1}CuO_4$.[10]

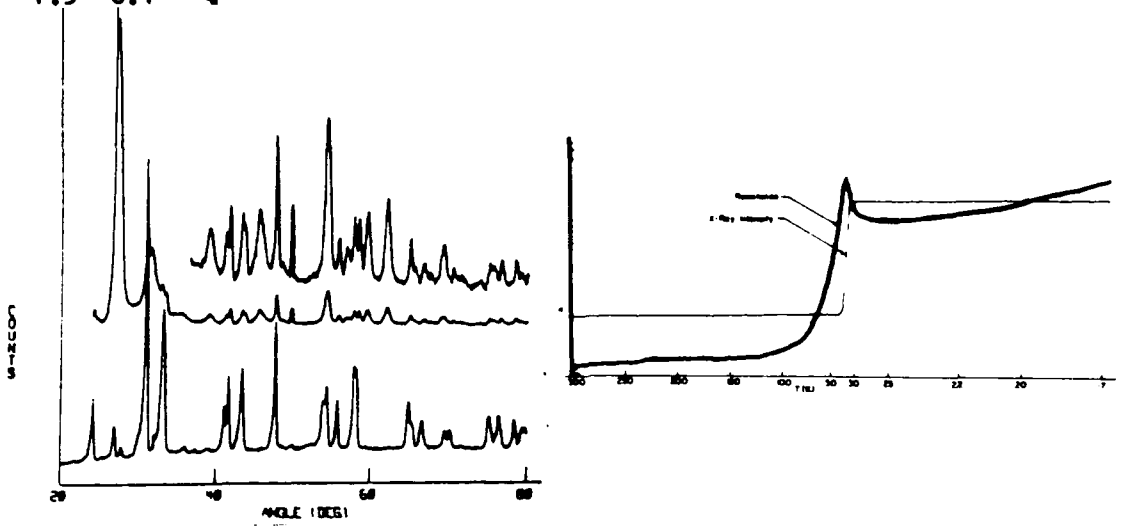

Fig. 1(left): X-ray diffraction spectra recorded at 295 K (lowest curve) and 10-12 K (upper curves). Fig. 2(right): Temperature dependence of the electrical resistance and x-ray intensity at 27.3° 2θ.

RESULTS AND DISCUSSION

A diffraction spectrum taken at 295 K is shown in Fig. 1 (lowest curve). The positions of all the major peaks are in agreement with the orthorhombic lattice reported by Grande et al.[3] and our measured intensities agree with those calculated from their structure. Expressed in the standard setting, the space group is Cmca; a least-squares fit to 37 diffraction peaks between 60° and 120° yields the following unit cell parameters: a = 5.361±0.001; b = 13.151±0.003; c = 5.408±0.001 A.

The temperature dependence of the resistance is plotted in Fig. 2. On cooling from room temperature, there is initially a gradual increase in the resistance, near 100 K a significant increase begins which peaks to a local maximum near 36 K, the resistance then drops until about 25 K below which it monotonically rises. The resistance curves are reversible and seen in every sample. A crystallographic phase transformation accompanies this resistance anomaly. The upper diffraction spectra shown in Fig. 1 are of the same material, but recorded at 10-12 K. There are 17 additional diffraction peaks between 20° and 80° 2θ. We have tentatively indexed these peaks to a monoclinic lattice; attempts to fit lower symmetry lattices were unsuccessful. We are in the process of determining the structure of this new phase.

Magnetization measurements made on a squid susceptometer show a diamagnetic onset at about 35 K. The magnitude of the signal indicates that one part in 5000 of the sample expells flux, if the diamagnetism is due to superconductivity.

To determine the temperature at which the structural transition occurs, the x-ray detector was centered on the prominent diffraction peak in the low temperature phase at 27.3° 2θ. The other curve shown in Fig. 2 represents the temperature dependence of this peak and hence the relative amount of the low temperature phase. Repetitive cycling through the transition clearly establishes a connection between the two phenomena. However, the magnitude of the resistive anomaly near 30 K shows no measurable relationship to the magnitude of the x-ray peak at 27.3°. But, the magnitude of the low temperature resistance does increase with increasing magnitude of the x-ray peak. This implies that this new phase is responsible for the semiconductor-like behavior at low temperatures. The kinetics of the structural transition are very sluggish on cooling. Moreover, in addition to the new diffraction peaks in the specta at low temperatures, remanents of the orthorhombic structure could always be seen. Comparisons of peak intensities in the vicinity of the transition reveals that the low temperature phase grows at the expense of the orthorhombic phase.

It is our belief that these observations confirm the predictions of Kasowski et al.[9], viz. that it is this new phase which is responsible for the low temperature semiconductive behavior of La_2CuO_4. We further speculate that this phase transition inhibits the superconducting transition in most of the material; as noted above, superconductivity has been reported only in small fractions of these materials.[8] We, as well as others, have searched without success for structural transitions in the superconductor $La_{1.9}Ba_{0.1}CuO_4$.[4,10] We believe that one effect of the introduction of the metal inpurity (Ba, Ca, or Sr) is to suppress this phase transition and thereby allow a substantial portion of the orthorhomibic phase to become superconducting. A series of low concentration alloys is under preparation to test this hypothesis.

REFERENCES

1. J. G. Bednorz and K. A. Müller, Z. Phys. B64, 189 (1986)

2. M. K. Wu, J. R. Ashburn, C. J. Torng, P. H. Hor, R. L. Meng, L. Gao, Z. J. Huang, Y. Q. Wang, and C. W. Chu, Phys. Rev. Lett. 58, 908 (1987)

3. V. B. Grande, H. Müller-Buschbaum, and M. Schweizer, Z. Anorg. Allg. Chem. 428, 120 (1977)

4. J. D. Jorgensen, H. -B. Schuttler, D. G. Hinks, D. W. Capone, II, K. Zhang, M. B. Brodsky, and D. J. Scalapino, Phys. Rev. Lett. 58, 1024 (1987)

5. U. Geiser, M. A. Beno, A. J. Schultz, H. H. Wang, T. J. Allen, M. R. Monaghan, and J M. Williams, Phys. Rev.-B 35, 6721 (1987)

6. M. Onoda, S. Shamoto, M. Sato, and S. Hosoya, Jpn. J. Appl. Phys. 26, 363 (1987)

7. W. E. Pickett, H. Krakauer, D. A. Papaconstantopoulos, and L. L. Boyer, Phys. Rev.-B 35, 7252 (1987)

8. P. M. Grant, S. S. P. Parkin, V. Y. Lee, E. M. Engler, M. L. Ramirez, J. E. Vazquez, G. Lim, R. D. Jacowitz, and R. L. Green, Phys. Rev. Lett. 58, 2482 (1987)

9. R. V. Kasowski, W. Y. Hsu, and F. Herman, Solid State Commun. -in press

10. E. P. Skelton, W. T. Elam, D. U. Gubser, S. H. Lawrence, M. S. Osofsky, L E. Toth, and S. A. Wolf, Phys. Rev.-B 35, 7140 (1987)

Formation of the Structure of the Superconducting Phase of La-Sr-Cu-O by DC Sputtering

A. S. Edelstein, S.B. Qadri, R.L. Holtz, P.R. Broussard, J.H. Claassen,

T.L. Francavilla, D.U. Gubser, P. Lubitz, E.F. Skelton and S.A. Wolf

Condensed Matter and Radiation Sciences Division

Naval Research Laboratory, Washington, DC 20375

DC sputtered filrn samples of La-Sr-Cu are found to be noncrystalline. Annealing in air at temperatures as low as 350° C yields crystallization of the structure of the superconducting phase of La-Sr-Cu-O. We present x-ray spectra showing the continuous development of the La-Sr-Cu-O phase and a decrease in the c/a ratio upon further annealing in air for temperatures up to 600 °C.

The discovery[1,2] of high temperature superconductivity in La-Sr-Cu-O and in the Y-Ba-Cu-O system has created an enormous research effort directed at understanding and utilizing these materials. We report here on one aspect of our effort. Specifically, in order to study the formation of the superconducting phase of La-Sr-Cu-O, we have annealed sputtered metallic films of La-Sr-Cu. We have found that these films are initially noncrystalline, but begin to crystallize at a low temperature, 350° C, into the necessary[3] tetragonal K_2NiF_4 structure type for superconductivity at 35 K. Subsequent annealing at higher temperatures improves the long range order as evidenced by additional diffraction peaks. The information we are reporting should prove useful in understanding the superconducting phase of La-Sr-Cu-O.

The films were prepared by DC sputtering from a single inhomogeneous target of the three metals onto quartz substrates. Some control of the sample composition could be achieved by varying the substrate position and the argon pressure. The base pressure before admitting the argon was $2\text{-}3\text{x}10^{-7}$ mm of Hg. Typical film thicknesses were in the range of several thousand Angstroms. Before annealing all the films were metallic and noncrystalline.

The annealing was done in air by raising the film temperature to the annealing temperature (T_a) over a period of one to two hours. The films were cooled from T_a in a shorter time, usually in approximately one half hour.

Figure 1 shows a series of x-ray scans of one of our films taken with Cu radiation and a graphite monochromator as deposited and after it had been annealed

in air at successively higher temperatures for 15 minutes at each temperature. We found that annealing the film for an additional hour had a negligible effect on the x-ray pattern. Seven of the peaks have been identified as belonging to the superconducting K_2NiF_4-type phase of La-Sr-Cu-O. Four of the peaks we have tentatively identified as belonging to either LaO or SrO. After annealing at only 350 °C, the prominent peaks belonging to the superconducting K_2NiF_4-type structure can be seen. The growth of this phase is enhanced at higher annealing temperatures.

The intensities of the peaks belonging to the superconducting K_2NiF_4-type structure change after being annealed at succesively higher temperatures and begin to approach the intensities expected for a polycrystalline sample of the superconducting K_2NiF_4-type structure. However, the intensities have not reached the calculated intensities of the superconducting K_2NiF_4-type structure at 600 °C. At least part of the reason for this is that the crystallites comprising the film have a preferred orientation. The effect of this preferred orientation is demonstrated in Fig. 2 which shows a Read camera x-ray photograph of the film after it had been annealed at 600 °C. The non-uniformity of the rings shows that the crystallites are not randomly oriented and that they have a preferred orientation. In contrast to the low temperature at which the superconducting K_2NiF_4-type structure appears, the LaO phase only starts forming at 500 °C.

By fitting the position of the peaks in Fig. 1 to the superconducting K_2NiF_4-type structure we have obtained values for the tetragonal lattice constants, a and c. These values are plotted as a function of T_a in Figures 3 (a) and 3 (b). One sees that as T_a is increased, c and a decrease and increase, respectively. Presumably this implies that atoms move out of the spaces between the planes in the superconducting

K_2NiF_4-type structure and the planes become better formed.

The average composition of the metals in the film was determined by x-ray fluorescence to be $(La_{0.959}Sr_{0.041})_2Cu_1$. This is the average composition. Because of the inhomogeneous nature of our target, the copper composition varied by approximately 40% over the length of the film. Although our average Ba composition is above the minimum Ba composition for which van Dover et al. observed[4] superconductivity, it is not much above it. In any case we did not observe a resistive superconducting transition in this film. The c/a ratio is approximately 3.57 after the 350 °C anneal. The value of c/a after the 600 ° C anneal is 3.47 which is below the values for which superconductivity has been observed.[5] The composition variation within our films may be responsible this low value of c/a and the absence of superconductivity. The unit cell volume decreases approximately 1% as we increased the annealing temperature.

We have found the K_2NiF_4 structure type is also formed in other La-Sr-Cu-O films at approximately the same low annealing temperature. We infer that this result can be expected to occur rather generally in this system. We have obtained quite different results in our investigation of Y-Ba-Cu-O films. In this case, we started with a film with the composition $Y_1Ba_2Cu_3$, i.e. the correct composition for obtaining a superconducting transition temperature above 90 K. Again crystallization occurs at a low temperature of 300 °C. However for the Y-Ba-Cu-O film, the structure formed at 300 °C was not the correct structure for observing high temperature superconductivity. Further annealing this film at temperatures as high as 850 °C did not produce the correct structure.

In conclusion we have found that the superconducting K_2NiF_4-type structure

starts forming at a remarkably low temperature, 350 °C. The structure starts forming at a lower temperature than LaO. The low temperature required to activate crystallization, shows that the activation barrier that must be overcome in going from the noncrystalline phase to the structure of the superconducting phase is very low. Considering the complexity of the structure, it is perhaps surprising that it forms at such a low temperature.

Refrences

1. J.G. Bednorz and K.A. Muller, Z. Phys. B 64, 189 (1986).

2. M.K. Wu, J.R. Ashburn, C.J. Torg, P.J. Torng, P.H. Hor, R.L. Meng, L.Gao, Z.J. Huang, Y.Q. Wang and C.W. Chu, Phys. Rev. Lett. 58, 908 (1987).

3. H. Takagi, S. Uchida, K. Kitazawa and S. Tanaka (unpublished?).

4. R.B. van Dover, R.J. Cava, B. Batlogg, and E.A. Rietman, Phys. Rev B 35, 5337 (1987).

5. D.U. Gubser, R.A. Heine, S.H. Lawrence, M.S. Osofsky, D.J. Schrodt, L.E. Toth, and S.A. Wolf, ibid, p. 5350.

Figure Captions

1. X-ray scans of the film after annealing for 15 minutes at the temperatures indicated. (See the text for a more complete description of the annealing procedure.) The peaks corresponding to the superconducting K_2NiF_4-type structure have been identified by their Miller indices. The peaks that we associate with LaO and SrO are also labeled.

2. Read camera photograph taken with x-rays from a Cu tube of the La-Sr-Cu-O film after it had been annneal at 600 C.

3. Variation of the tetragonal unit cell parameters, a (upper) and c(lower), with annealing temperature, T_a. The straight lines represent linear fits to the data.

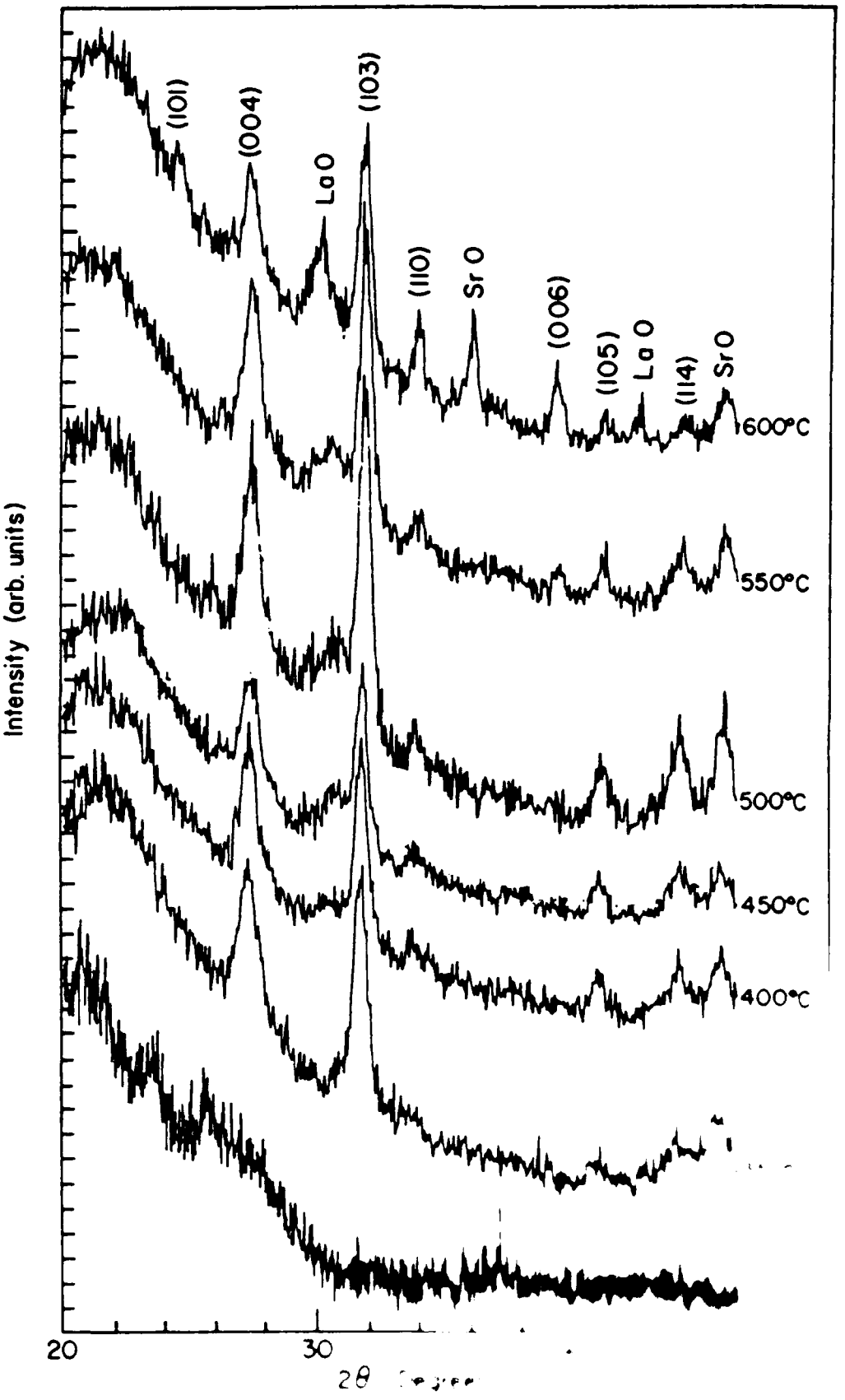
(101)
(004)
La O
(103)
(110)
Sr O
(006)
(105)
La O
(114)
Sr O
600°C
550°C
500°C
450°C
400°C
Intensity (arb. units)
20
30
2θ

AD-A189 137 COMPILATION OF NRL PUBLICATIONS ON HIGH TEMPERATURE SUPERCONDUCTIVITY(U) NAVAL RESEARCH LAB WASHINGTON DC D U GUBSER 1987 3/3

UNCLASSIFIED F/G 20/3 NL

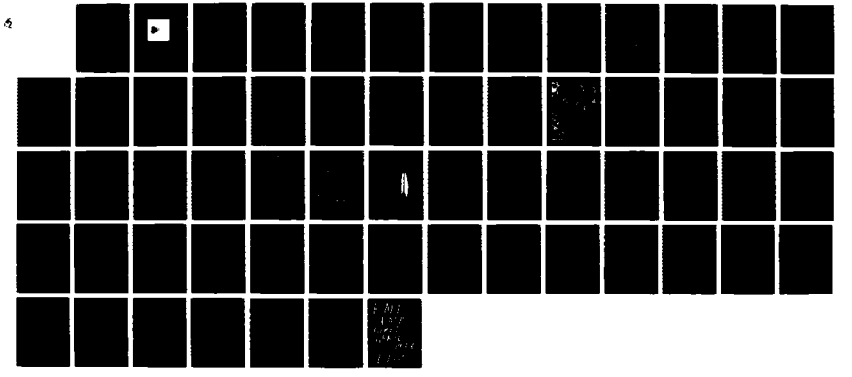

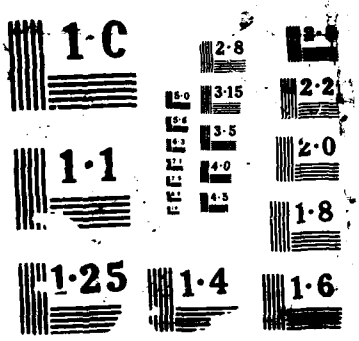
1·C
1·1
1·25
1·4
1·6
2·8
3·15
3·5
4·0
4·5
2·2
2·0
1·8

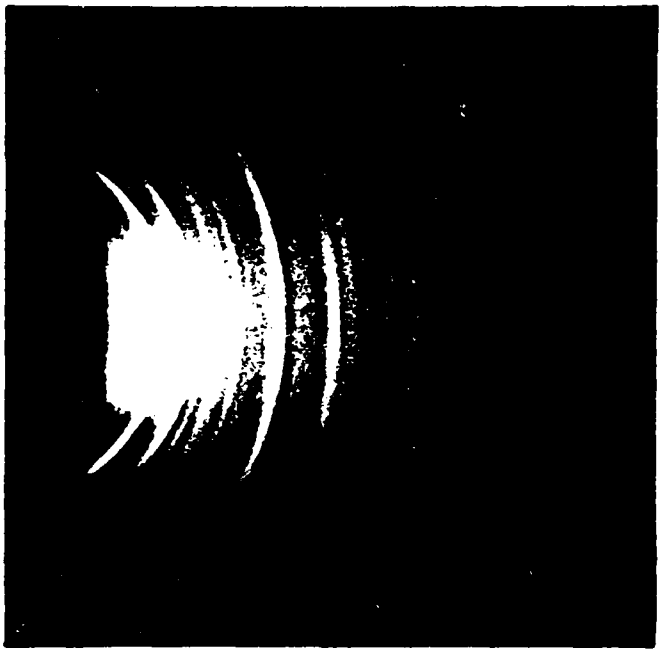

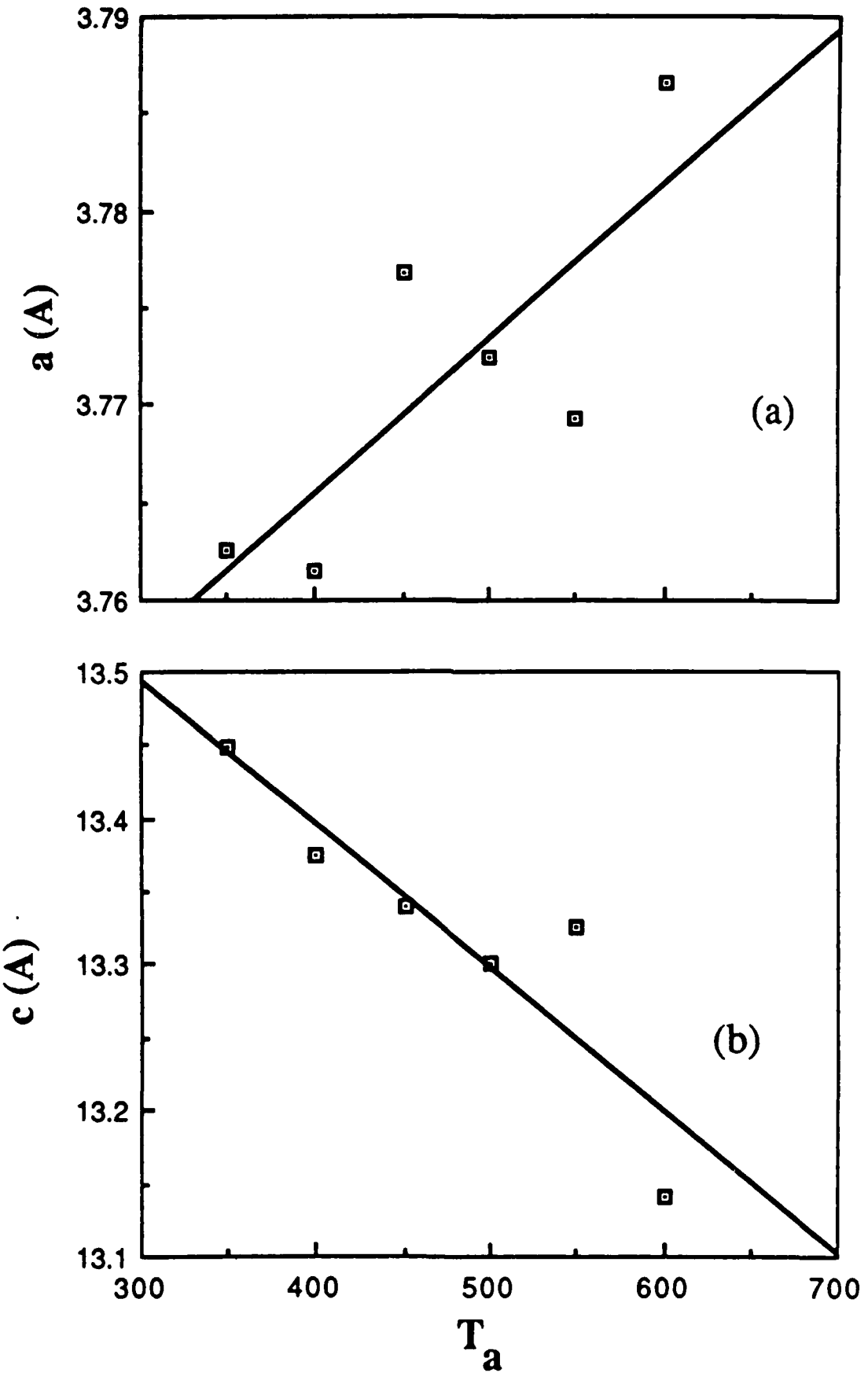
3.79
3.78
3.77
3.76
a (A)
(a)
13.5
13.4
13.3
13.2
13.1
c (A)
(b)
300
400
500
600
700
T_a

Plasma Sprayed Superconducting Oxide Coatings

R.A. Neiser[a,b], J.P. Kirkland[b], H. Herman[a],
W.T. Elam[c], E.F. Skelton[c]
State University of New York at Stony Brook,
and the Naval Research Laboratory

Abstract

A new technique for plasma spray processing high temperature superconducting oxides is discussed. Powdered superconducting material is fed into the plasma flame and can be deposited onto suitably prepared substrates. A post-spray anneal yields coatings with transition temperatures above the boiling point of liquid nitrogen.

Introduction

Superconductivity above 30 K was reported by Bednorz and Muller in the La-Ba-Cu-O system [1]. Subsequently, Wu and co-workers announced the discovery of a 93 K transition temperature in the closely related Y-Ba-Cu-O system [2]. Cava et. al. identified the superconducting phase as a layered, orthorhombic perovskite with stoichiometry $YBa_2Cu_3O_x$ where x is around 6.9 [3]. Other work indicated that the critical fields associated with these new metallic oxide superconductors were very high [4]. With the announcement of critical temperatures above the boiling point of liquid nitrogen at 77 K, the need to develop technologies capable of processing these brittle ceramics into commercially usable forms became apparent. This

letter presents the results of a study in which plasma spraying was used to produce superconducting coatings of Y-Ba-Cu-O. These plasma sprayed coatings offer the advantages of high density, which will lead to the ability to carry high currents; high mechanical strength and durability; applicability to a wide range of substrate materials; and flexibility in spraying a large range of geometries and thicknesses.

Experimental Procedure

The powder for plasma spraying was prepared by mixing high purity Y_2O_3, $BaCO_3$, and CuO in the correct ratios and reacting the mixture in a fashion similar to those described elsewhere [3,4]. The reaction yielded a hard, brittle, and black material which was reduced to powder by grinding.

The substrates selected for spraying were steel rectangles 12 mm x 51 mm x 3 mm thick. The coupons were degreased and grit blasted with coarse SiC and then bond coated with a 0.13 mm thick layer of NiCrAlY. The coupons were mounted on a carousel for spraying the superconducting powder.

The powder was fed into the plasma flame and was deposited onto the substrates. During the spraying process, the plasma gun moved slowly up and down in front of the rapidly spinning carousel. The deposited coatings were uniform, 0.13 mm thick, black, and essentially non-conducting.

After spraying, the coupons were heat treated to restore the superconducting properties of the sprayed material. Temperatures as low as 600 C and as high as 1100 C were used for times as short as 5 minutes and as long as 60 hours.

Results and Discussion

Figure 1 shows a typical x-ray diffraction pattern from an as-sprayed Y-Ba-Cu-O coating. Note the presence of a broad peak extending from 28 to 35 in 2 , indicating that the coating contains highly distorted, poorly crystallized material. Such broad maxima are commonly observed in plasma sprayed coatings and result from the rapid solidification (as high as 10^6 degrees/sec) of the molten droplets on the cold substrate. The as-sprayed coating is not superconducting.

In order to recover the superconducting properties of the Y-Ba-Cu-O, the coating must be annealed. Figure 2 is an x-ray diffraction pattern taken after a five minute exposure at 950 C followed by an air quench. The pattern shows that the Bragg peak intensities have increased considerably as compared with Figure 1 and that the broad maximum is gone. These results show that the coating has recrystallized into the superconducting crystal structure. Closer examination of the x-ray diffraction data shows that the crystal structure is not tetragonal, but rather that there is an orthorhombic distortion in the crystal which grows larger with longer annealing times. This result can be explained by the diffusion of oxygen from the air into preferential sites in the copper oxygen planes of the layered perovskite structure. Work by Skelton et. al. showed that larger distortions gave rise to sharper transitions at higher temperatures [5].

The annealing temperature has been found to be critical to the recovery process. X-ray patterns taken from samples annealed at 600 C show that the amount of

superconducting phase continually decreases with time and that $BaCO_3$, Y_2O_3, and CuO appear and grow. Presumably the barium reacts with CO_2 in the air to form the carbonate. At temperatures above about 1000 C, the superconducting phase is observed to disappear. After even short exposures to these high temperatures, the superconducting phase is replaced by several poorly identified phases. In the temperature range from 850 C to 1000 C, the coatings recrystallize into the proper structure.

Figure 3 is a resistance versus temperature plot for one of the heat treated coatings. The data was taken using a standard 4 point ac resistance probe. The coating shows a two degree wide transition which is complete by 86 K. Magnetic susceptibility measurements have not been made on this coating, but a measurement done on the feedstock powder exhibits a broad transition indicating the presence of diamagnetic material.

Conclusions

It has been found that plasma spray processing can be used to fabricate superconducting coatings. The as-sprayed coatings are not superconducting, but a post-spray anneal in the appropriate temperature range can restore or improve the superconducting properties of the original material. Because of the highly flexible nature of the spraying system, virtually any substrate material which can survive the post-spray heat treatment, and a wide range of substrate geometries can be given a superconducting coating. The plasma spray approach has many potential applications including the fabrication of high strength superconducting magnets, coatings for the electronics industry, and superconductor coated wires.

References

a) State University of New York at Stony Brook, Stony Brook, NY

b) Sachs/Freeman Associates, Landover, MD

c) Naval Research Laboratory, Washington D.C.

1 J.G. Bednorz and K.A. Muller, Z. Phys. B 64, 189 (1986).

2 M.K. Wu, J.R. Ashburn, C.J. Torng, P.H. Hor, R.L. Meng, L. Gao, Z.J. Huang, Y.Q. Wang, and C.W. Chu, Phys. Rev. Lett. 58, 908 (1987).

3 R.J. Cava, B. Batlogg, R.B. van Dover, D.W. Murphy, S. Sunshine, T. Siegrist, J.P. Remeika, E.A. Rietman, S.Zahurak, and G.P. Espinosa, Phys. Rev. Lett. 58, 1676 (1987).

4 J.Z. Sun, D.J. Webb, M. Naito, K. Char, M.R. Hahn, J.W.P. Hsu, A.D. Kent, D.B. Mitzi, B. Oh, M.R. Beasley, T.H. Geballe, R.H. Hammond, and A. Kapitulnik, Phys. Rev. Lett. 58, 1574 (1987).

5 E.F. Skelton, S.B. Qadri, B.A. Bender, A.S. Edelstein, W.T. Elam, T.L. Francavilla, D.U. Gubser, R.L. Holtz, S.H. Lawrence, M.S. Osofsky, L.E. Toth, S.A. Wolf, "Structural Considerations of Cu-oxide Based High T_c Superconductors", to be published.

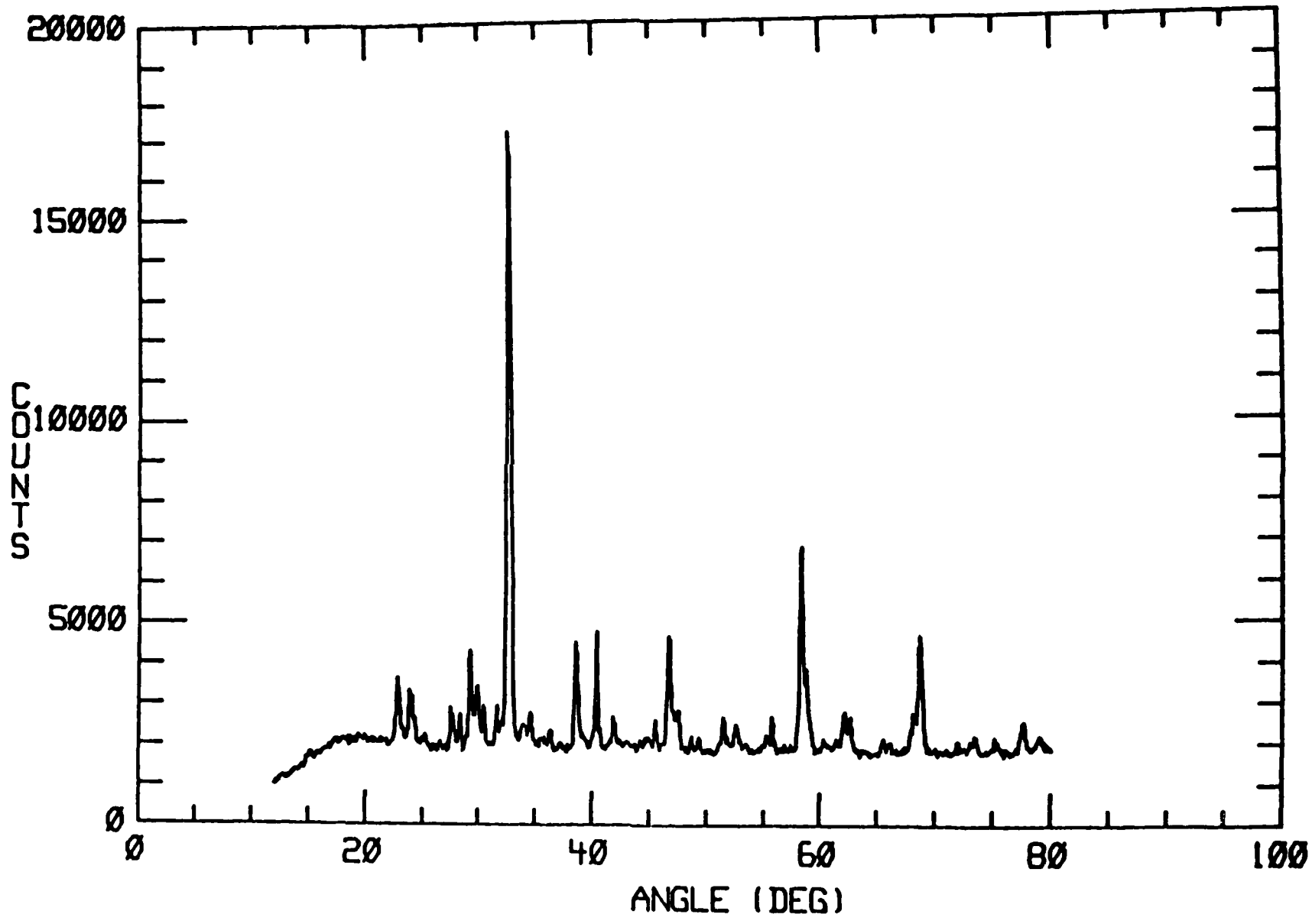
20000
15000
10000
5000
0
COUNTS
0
20
40
60
80
100
ANGLE (DEG)

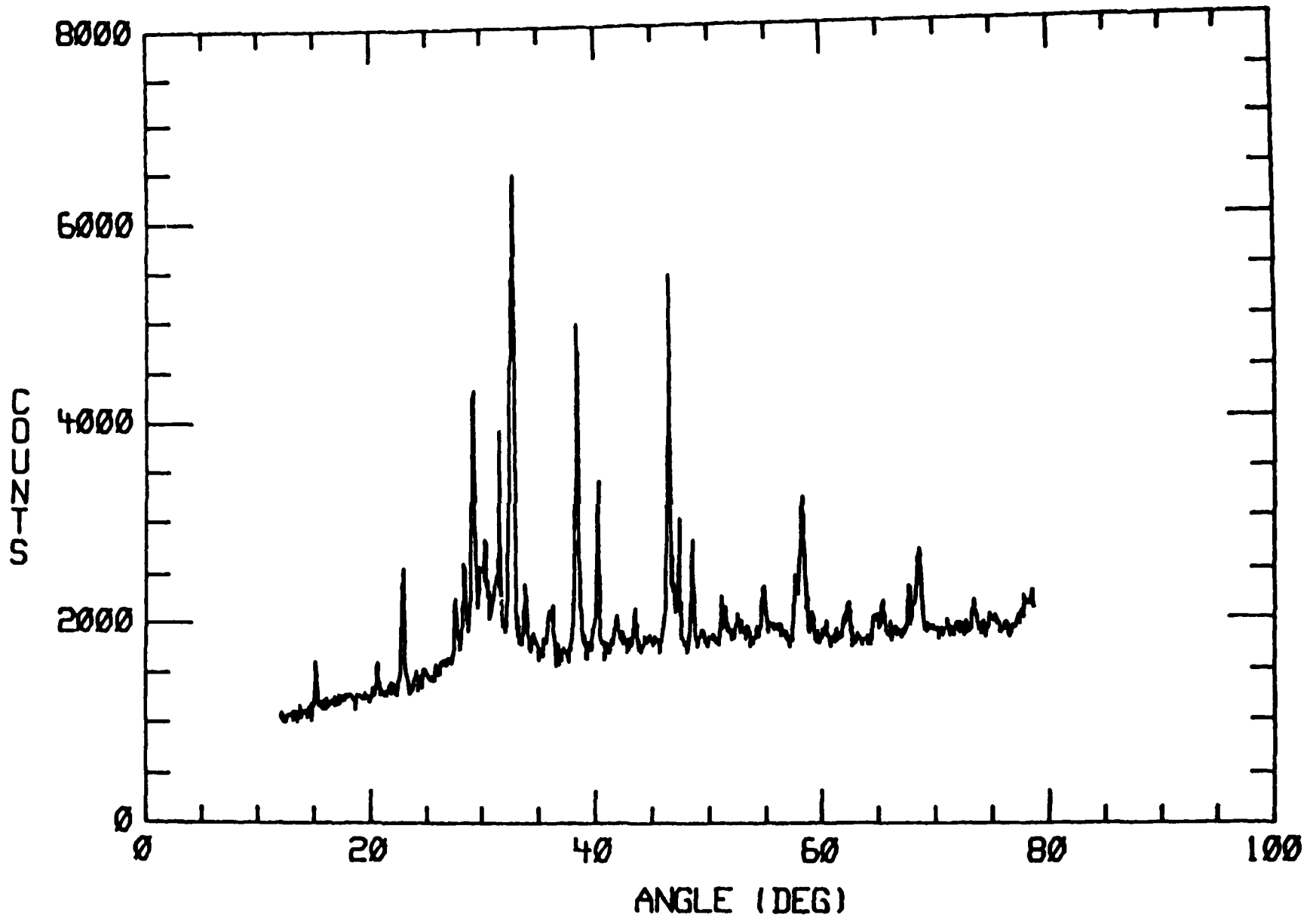
8000
6000
4000
2000
0
COUNTS
0
20
40
60
80
100
ANGLE (DEG)

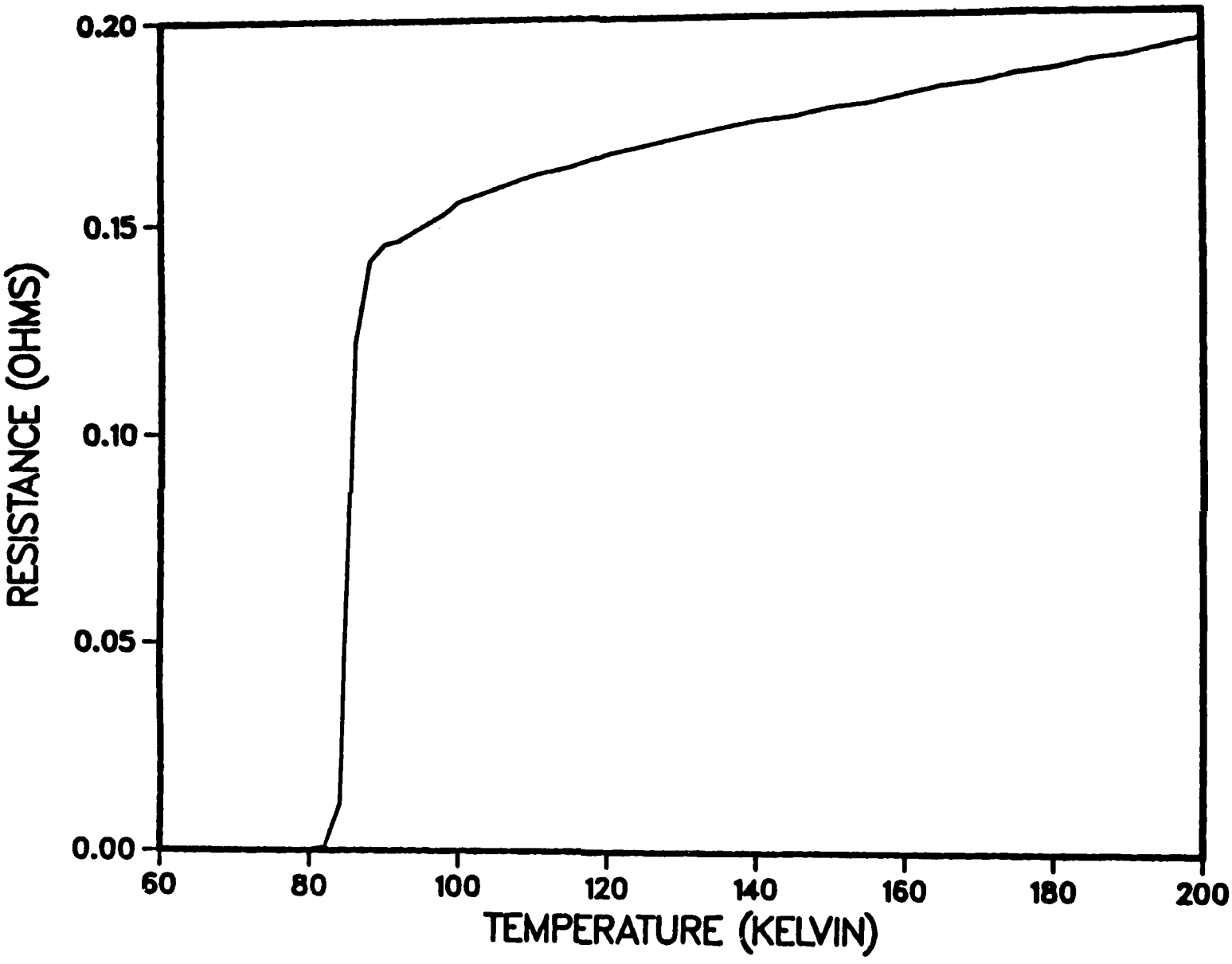
0.20
0.15
0.10
0.05
0.00
RESISTANCE (OHMS)
60
80
100
120
140
160
180
200
TEMPERATURE (KELVIN)

PLASMA SPRAYED HIGH T_c SUPERCONDUCTORS

W. T. Elam, J. P. Kirkland*, R. A. Neiser*, and E. F. Skelton
Condensed Matter and Radiation Sciences Division
Naval Research Laboratory
Washington, DC 20375-5000

S. Sampath and H. Herman
Department of Materials Science and Engineering
State University of New York at Stony Brook
Stony Brook, NY 11794-2275

*Sachs/Freeman Associates, Landover, MD

Abstract

Coatings of Y-Ba-Cu-oxide superconductors have been produced by plasma spraying the reacted powders. The spraying process disrupts both the structural and the electrical properties of the material, however the desired properties can be restored by heat treatment. Short times (5 to 20 min.) at high temperatures (900° to 1000° C) produce coatings which are predominantly the desired $YBa_2Cu_3O_7$-phase and exhibit on-set of

superconductivity above 80 K. Details of the effects of heat treatment on the structural, electrical, and chemical properties are reported.

I. Introduction

The discovery of superconductivity in La-Ba-Cu-oxides at temperatures in excess of 30 K [1] and in Y-Ba-Cu-oxides at temperatures in excess of 90 K [2] has spawned a flurry of research directed toward these materials. The preparation procedures used to produce most of the samples used for this work involve reaction of appropriate combinations of the metal oxides at sufficiently high temperatures in a series of heating and grinding operations yielding brittle pellets. An alternative method which can be used to prepare these superconductors is by injecting the reacted powder directly into a plasma flame and spraying onto a suitable surface.[3] One advantage of this method is that it can be used on a variety of surfaces, regardless of their texture and shape.

II. Sample Preparation

The feedstock powder for plasma spraying was prepared by mixing high purity Y_2O_3, $BaCO_3$, and CuO in the correct ratios. The powders were mixed in a ball mill with methanol as a mixing fluid and reacted above 900° C for several hours. The hard, black, brittle material thus formed, which was not necessarily superconducting, was re-ground and sized to form powder suitable for the spray feeders.

Substrates were 12 mm x 51 mm x 3 mm steel rectangles. The substrates were degreased, grit-blasted, and sprayed with a 1 mm thick coating of spinel (Al_2O_3 + MgO). The Y-Ba-Cu-oxide powder described above was then deposited approximately 0.13 mm thick over the white spinel substrate. The deposited coatings were uniform, black, physically durable, and essentially non-conducting.

At this point, several heat treatments were used to restore the

superconducting properties. This paper gives comprehensive data on the effects of some of these treatments. In particular, treatment at 950° C for various times was carefully studied. Lower temperatures caused the coatings to break down into simple oxides of the elemental metals. Higher temperatures caused melting and/or paratectic reactions.

III. Sample Characterization

A. Structural

All of the samples were measured on a computer controlled diffractometer using filtered radiation from a Cu x-ray tube. Diffraction spectra from three samples are shown in Fig. 1: one as-sprayed, i.e., without any annealing, one after 20 min at 950° C in air, and the third after annealing at 890° C in O_2 for 16 hours. The desired $YBa_2Cu_3O_7$-phase is present and the dominant component in all samples. Excellent agreement is obtained between the measured peak positions and intensities for this phase with those calculated on the basis of the crystal structure as determined by Rhyne et al. from neutron diffraction data.[4] Additional diffraction peaks present in all spectra can be largely associated with the compound $BaCuO_2$ [JCPCS card #30-123]. Peaks observed near 31.6° cannot be associated with either of these phases, but do agree with the strongest peaks in both the Y_2BaCuO_5 structure, as determined by Michael and Reaveau [5], and the $YBa_3Cu_2O_x$-phase recently proposed by Frase, Liniger, and Clarke.[6] We cannot distinguish between these phases from our data. We also note that, although the annealed phases appear to be stable, the presence of the $YBa_2Cu_3O_7$-structure in the as-sprayed coating tends to degrade with time, concomitant with the growth of the other phases.

It is clear from an examination of the diffraction spectra that the relative amounts and quality of the $YBa_2Cu_3O_7$-phase are enhanced by increased annealing times, up to about 20 min. To further quantify this, we have examined the relative intensities of the $YBa_2Cu_3O_7$-phase (013,103,110) peaks and the $BaCuO_2$-(600) peaks as a function of anneal time. These data are plotted in Fig. 2. Clearly, the greatest changes are affected during the first 20 min., as evidenced by the growth of the

$YBa_2Cu_3O_7$-peaks and the decay of the $BaCuO_2$-peaks. There appears to be a subsequent increase in the $BaCuO_2$-phase for longer anneals; a corresponding loss of the $YBa_2Cu_3O_7$-phase is uncertain.

Contrary to expectations, annealing the samples does not appear to have any effect on the $YBa_2Cu_3O_7$ orthorhombic lattice. The unit cell parameters (a,b,c) as determined from 30 to 35 diffraction peaks between 40° and 80° for each of the samples are listed in Table 1. To within the uncertainty of the fits, all the values are in agreement, indicating that there are no measurable changes in the lattice dimensions with annealing. This observation may be in conflict with an orthorhombic-tetragonal transition reported by Schuller et al.[7] Based on high temperature x-ray diffraction experiments, Schuller et al. find that at about 750° C, the $YBa_2Cu_3O_7$-phase undergoes an orthorhombic-to-tetragonal transition. This is presumed to arise from a disordering of oxygen atoms on the a,b-axes. In the ordered, orthorhombic structure, which is considered favorable to the superconducting properties, the (0,1/2,0)-sites on the b-axes are fully occupied by oxygen atoms and the (1/2,0,0)-sites on the a-axes are vacant. It is presumed that at temperatures above 750° C, a disordering takes place, leading to the orthorhombic-to-tetragonal transition. Although all our heat treatments were at temperatures well above this and the samples were quenched, we did not see any evidence of a tetragonal phase for $YBa_2Cu_3O_7$.

B. Electrical

The temperature dependence of the electrical resistance of all the samples, except the as-sprayed sample, was measured down to 20 K. All showed an initial increase in resistance as the temperature dropped to about 80 K. At this point, the resistance began to decrease; for 2 to 5 min. anneal times, this decrease extended indefinitely, with the resistance never reaching zero. For the 10, 20, and 49 min. anneal times, the samples became superconducting at various temperatures. The 20 min. sample had the highest onset and the narrowest transition, as well as the lowest room temperature resistance. The sample annealed for 85 min. was not superconducting and showed a double transition. The temperature dependence of resistance for the 20 min. and 85 min. samples is shown in Fig. 3. The onset, as determined by a change in sign of the slope, and width of the transitions, and the room-temperature resistance are given in Table

1.

C. Chemical and Microstructure

Bulk compositions measured by x-ray fluorescence showed some deviation from the YBa_2Cu_3-stoichiometry by a few atomic percent. This effect was observed in the feedstock powder as well as in all the sprayed coatings. It is not known at what stage the composition changes, but there is no evidence that spraying or annealing has any effect on the bulk stoichiometry.

On a microscopic scale however, many things are happening. The as-sprayed coating shows several chemical phases, with the desired $YBa_2Cu_3O_7$-phase being the most abundant. The composition of other areas implies $BaCuO_2$ and Y_2BaCuO_5, in agreement with both the x-ray diffraction results and predictions based on the phase diagram of Schuller et al..[7] A backscatter electron micrograph of the as-sprayed sample is shown in Fig. 4, revealing contrasting regions of different composition.

As little as 5 min. of annealing time produces a sample which shows little of these compositional variations and is predominantly the desired $YBa_2Cu_3O_7$-phase. Figure 5 shows a similar backscatter electron image of the sample annealed for 20 min., exhibiting relatively little contrast and a good uniformity of composition. The series from 5 to 49 min. shows very little change with time.

It is noted that the electron microprobe images indicate the presence of cracks in the coating. These cracks are more easily visible in the SEM pictures, and form either during annealing or during cooling. (The samples were allowed to cool in air after removal from the hot furnace.) Cross-section images of the samples broken in half show the cracks extending through the entire coating, although this may be an effect of the stress induced in breaking the sample. These samples show no significant compositional changes with depth.

IV. Discussion and Conclusions

The plasma-spraying process disrupts the structure of the Y-Ba-Cu-oxide superconducting powder, but the structure can be recovered and even improved by appropriate heat treatment. The disruption takes the form of both amorphizing the crystal structure and forming grains of other phases, particularly $BaCuO_2$.

Relatively short times at high temperature are required to produce

coatings which are predominantly the $YBa_2Cu_3O_7$-phase in the orthorhombic structure. This structure seems to form immediately, without any evidence of a tetragonal intermediate or any slow cooling necessary. The coatings have uniform composition, are durable both with respect to time and physical abuse, and show high superconducting onset temperatures. At present, their resistance still shows activated behavior below room temperature, as well as broad superconducting transitions. The physical morphology of the coatings, especially cracks, may be responsible, in part. Slight errors in the stoichiometry also may play a role. Future research will be aimed at correcting these problems.

V. Acknowledgement

We are grateful to P. R. Bartholemew for helpful suggestions and assistance with the microprobe measurements.

3. R. A. Neiser, J. P. Kirkland, H. Herman, W. T. Elam, and E. F. Skelton, Materials Science and Engineering **91**, L13-15 (1987).

4. J. J. Rhyne, D. A. Neumann, J. A. Gotaas, F. Beech, L. Toth, S. Lawrence, S. Wolf, M. Osofsky, and D. U. Gubser, submitted to Phys. Rev. Lett. (1987).

5. C. Michel and B. Raveau, J. Solid State Chem. **43**, 73 (1982).

6. K. G. Frase, E. G. Liniger, and D. R. Clarke, submitted to Commun. Am. Ceramic Soc (1987).

7. I. K. Schuller, D. G. Hinks, M. A. Beno, D. W. Capone-II, L. Soderholm, J. -P. Locquet, Y. Bruynseraede, C. U. Segre, and K. Zhang, submitted to Solid State Commun. (1987).

VII. Figure Captions

Fig. 1: X-ray diffraction spectra of the as-sprayed coating (bottom curve), after 20 min. anneal at 950° C (middle curve), and after 16 hr. anneal at 890° C (top curve). The Miller indices correspond to the structure of the $YBa_2Cu_3O_7$-phase as reported in Ref. [4].

3. Geiser

4. Herman -

Fig. 2: Fractional intensities of the $YBa_2Cu_3O_7$-phase (130,310,110)-diffraction peaks and the $BaCUO_2$-phase (600)-diffraction peaks as a function of anneal time.

Fig. 3: Temperature dependence of the resistance of the plasma-sprayed coatings after annealing at 950° C for 20 min. and for 85 min. Note the negative coefficient between room temperature and 80 K. The sample annealed for 20 min. shows the best superconducting transition, while the 85 min. sample is not a superconductor above 20 K.

Fig. 4a: Backscatter electron micrograph of the as-sprayed coating with the electron microprobe set for a magnification of 800X. The contrasting regions are indicative of different compositions.

Fig. 4b: Backscatter electron micrograph of the sample annealed for 20 min. at 950° C. The desired $YBa_2Cu_3O_7$-phase predominates with very little evidence of regions with altered composition. Some cracking is evident and is more pronounced in SEM images.

Anneal Times versus Unit Cell and Transition Parameters

Δt	a (Å)	b (Å)	c (Å)	R(300K)	T(onset),K	ΔT,K
0	3.843±0.026	3.852±0.028	11.581±0.099	—	—	—
2	3.826±0.007	3.889±0.007	11.683±0.016	16	58	a
5	3.834±0.009	3.893±0.008	11.693±0.022	3.2	83	a
10	3.826±0.006	3.896±0.006	11.689±0.013	6	83	50
20	3.827±0.006	3.898±0.006	11.678±0.015	1	85	20
49	3.829±0.008	3.896±0.010	11.703±0.019	1.5	80	40
85	3.839±0.006	3.883±0.005	11.699±0.013	6.3	80	b
16h[c]	3.831±0.005	3.894±0.005	11.680±0.011	2.7	90	10

a = resistance never reaches zero above 20 K
b = double transition, resistance never reaches zero above 20 K; see Fig. 3
c = 16 hour anneal in O_2

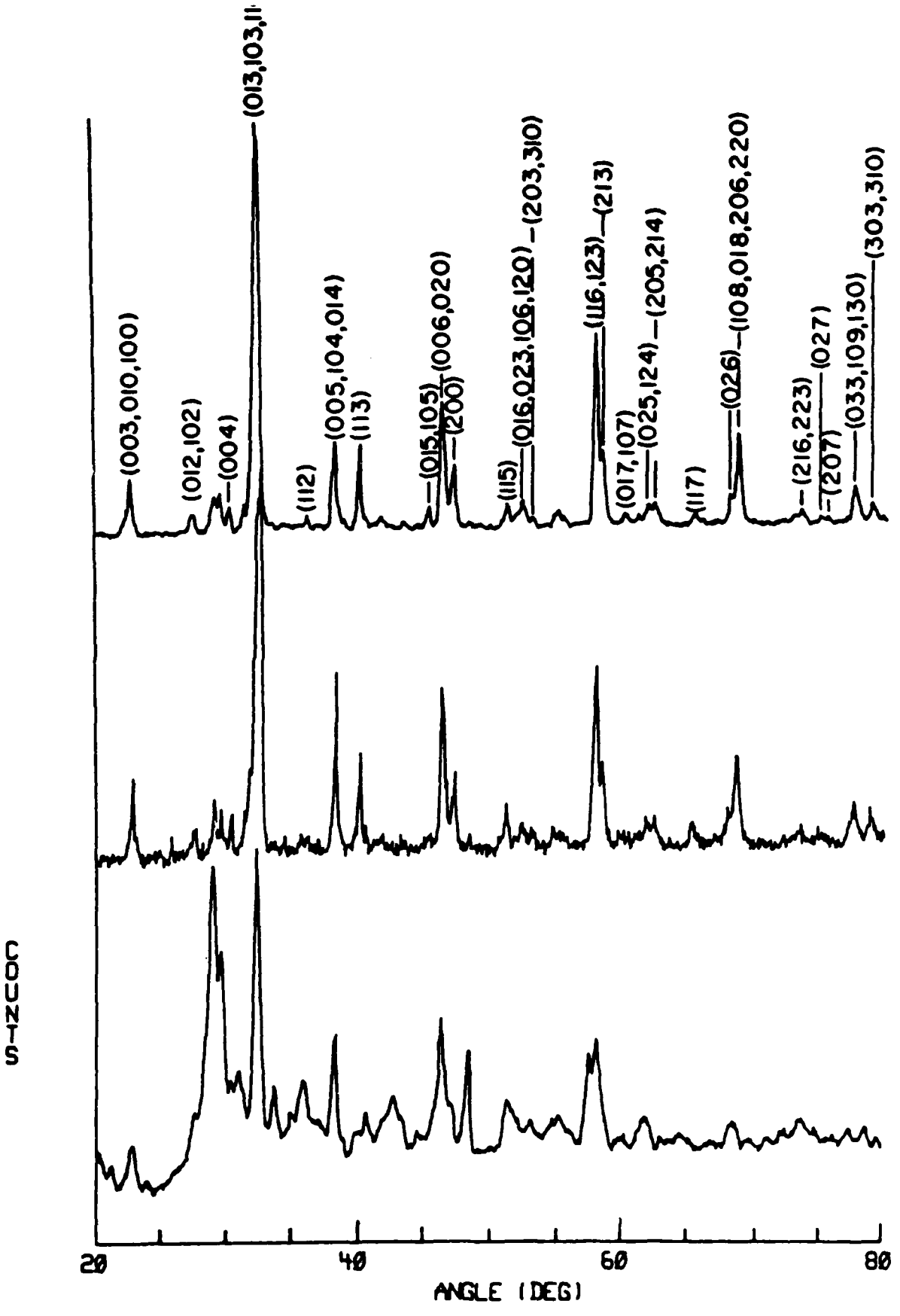
(003,010,100)
(012,102)
(004)
(013,103,11
(112)
(005,104,014)
(113)
(015,105)
(006,020)
(200)
(115)
(016,023,106,120)
(203,310)
(116,123)
(213)
(017,107)
(025,124)
(205,214)
(117)
(026)
(108,018,206,220)
(216,223)
(027)
(207)
(033,109,130)
(303,310)
S-1ZCOC
20
40
60
80
ANGLE (DEG)

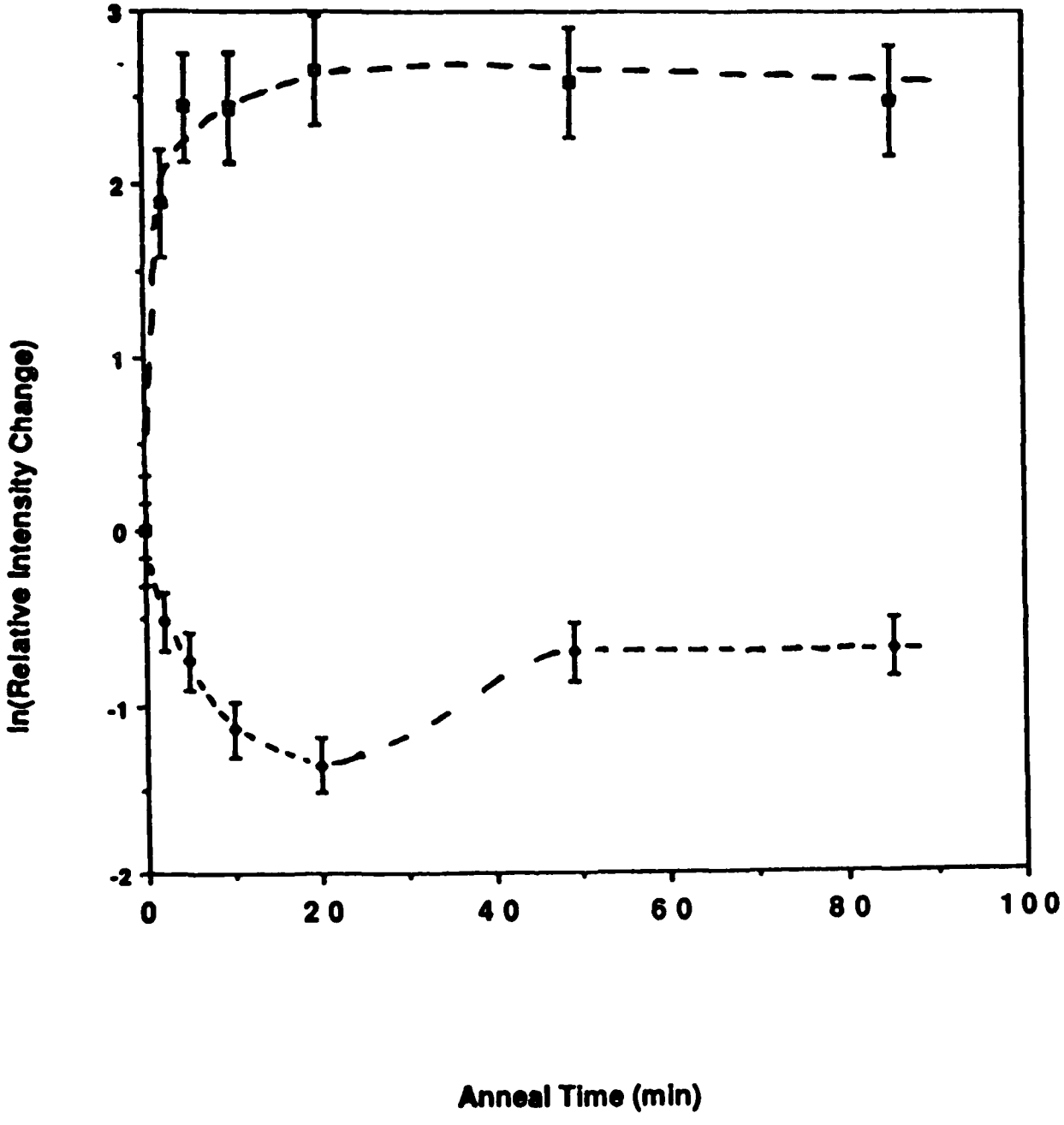
3
2
1
0
-1
-2
0
20
40
60
80
100
ln(Relative Intensity Change)
Anneal Time (min)

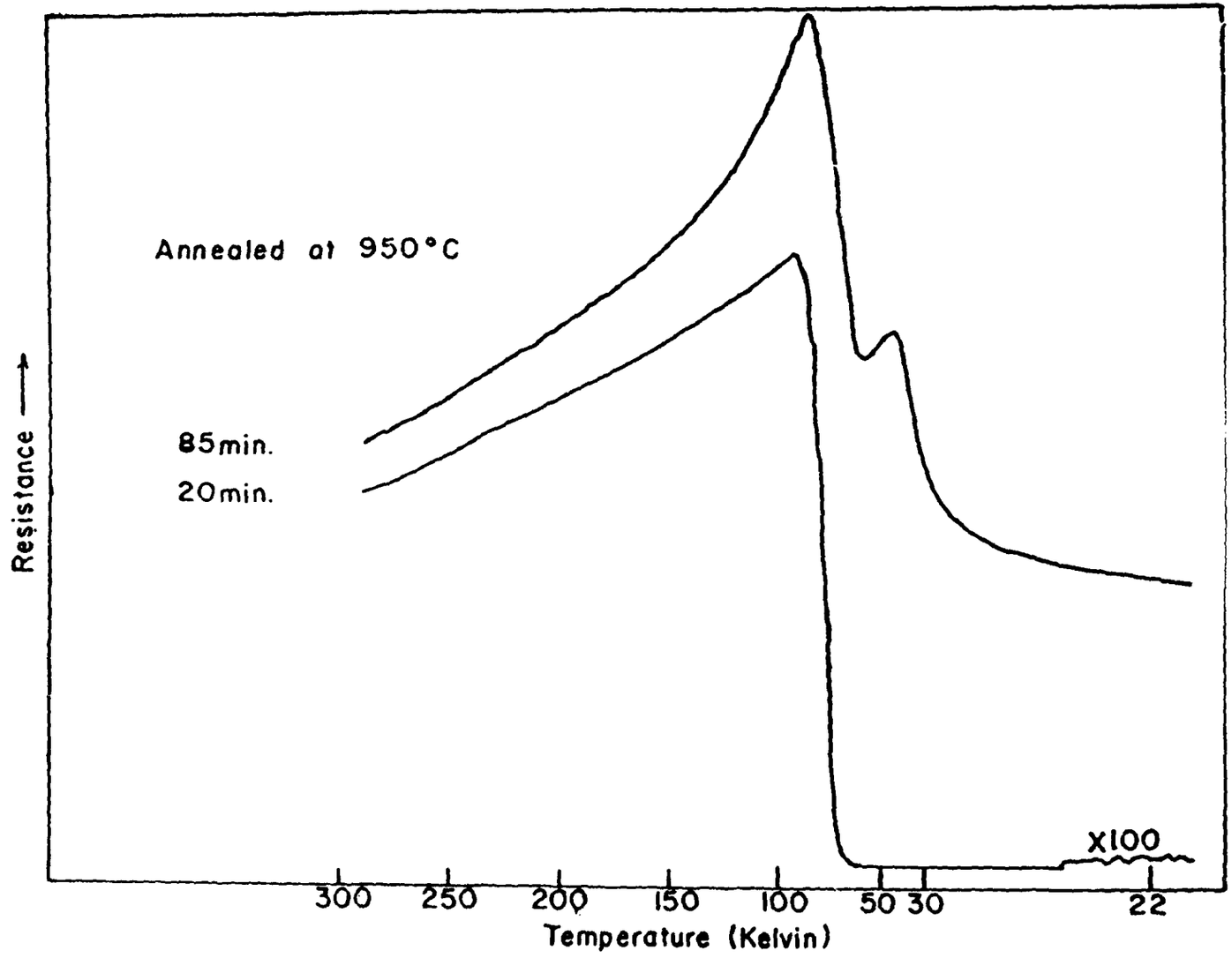
Annealed at 950°C
85min.
20min.
Resistance ⟶
X100
300
250
200
150
100
50
30
22
Temperature (Kelvin)

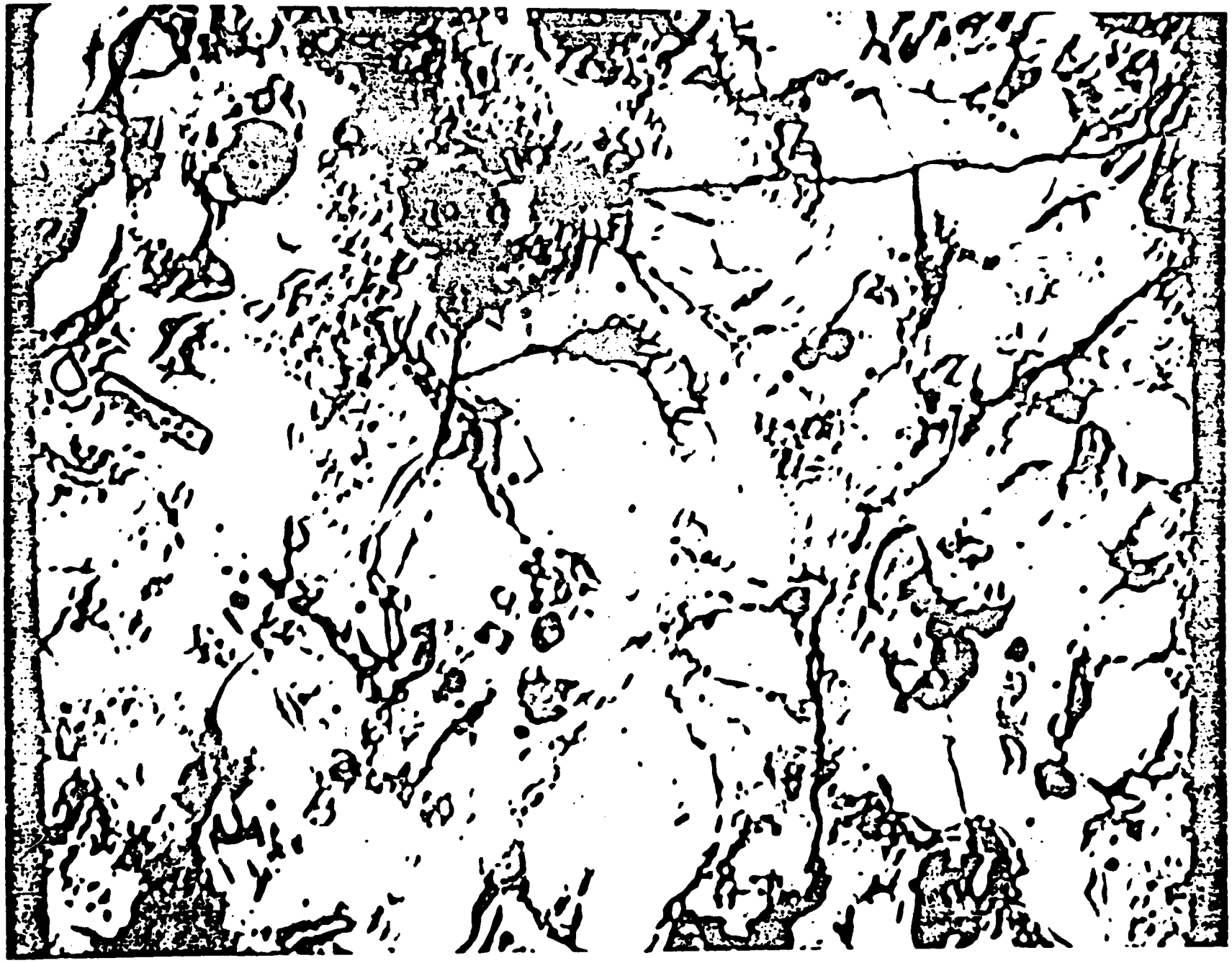

Resonant Photoemission Study of Superconducting Y-Ba-Cu-O

Richard L. Kurtz and Roger L. Stockbauer
Surface Science Divison
National Bureau of Standards
Gaithersburg, Maryland 20899

Donald Mueller[†] and Arnold Shih
Lewis E. Toth,[††] Michael Osofsky,[†††] and Stuart A. Wolf
Naval Research Laboratory
Washington, DC 20375

(Received April __, 1987)

Abstract

Ultraviolet photoelectron spectra of a 93 K superconducting compound, $YBa_2Cu_3O_7$ have been obtained using photon energies ranging from 25 to 180 eV. Resonant photoemission is used to identify the chemical origin of the features in the valence band electronic structure.

Accepted Phys. Rev. B. Rapid Communications, 1 June 1987.

Recent developments in the production of high T_c superconductors have spurred the rapid development of theories of the geometric and electronic structure of these compounds. A number of theoretical calculations of the band structures of La-Ba-Cu-O have been produced and studied in an effort to understand the nature of the superconducting process.[1] These calculations have not been supported by direct measurements of the band structures, however. With the production of the series of Y-Ba-Cu-O materials and their critical temperatures above 77 K, measurements of the electronic structures below T_c have become experimentally more tractable.[2] An essential component of the interactions that produce the superconductivity is the electronic structure yet measurements of this structure have not been made.

In this letter, we report the first measurements of the electronic structure of $YBa_2Cu_3O_7$ using synchrotron radiation in the range 25-180 eV. In this photon energy range, we are able to use resonant photoemission in order to assist in the chemical identification of the Cu and Ba features observed in the valence band spectra.

The samples of $YBa_2Cu_3O_7$ were prepared by mixing oxides and carbonates of the metals in the appropriate atomic ratios, and calcining in air. The samples were pressed into pellets and sintered in air and O_2. The structure is that determined by Beech et. al.[3] Four-point a.c. resistance measurements show a sharp drop in the resistance at 93K and zero resistance is attained at 91K. Neutron scattering measurements are currently being performed at NRL and NBS to determine in detail the crystal structure.

The photoemission measurements were made using the National Bureau of Standards SURF-II Synchrotron Light Source, a toroidal grating monochromator and a double-pass cylindrical mirror analyzer (CMA). Base pressures were ~ 1×10^{-10} Torr. The sample normal was at an angle of 45° to both the photon beam and the axis of the analyzer; the spectra obtained are angle integrated. Calculated photon resolution is 350 meV at $h\upsilon$=60 eV. The CMA was

operated with a constant pass energy giving a constant resolution of 240 meV; the data are presented uncorrected for CMA transmission. Samples were mounted on a liquid nitrogen cooled manipulator using Ta foil and soldered into an Al ring with In in order to produce good thermal contact. The temperatures were measured with a W-5%Re, W-26%Re thermocouple imbedded in the In. The surfaces were prepared in ultra-high vacuum (UHV) by fracturing the microcrystalline needles with a stainless steel blade. Measurements were made on two separate batches of oxide superconductor. Spectra from both samples showed the same features at identical binding energies, however, the sample that had been sintered longer showed sharper peaks.

Figure 1 shows a survey of ultraviolet photoelectron spectra from the first sample in the photon energy range 60-104 eV in 2 eV increments. At a photon energy of 60 eV (top curve), we observe primarily two valence band features centered at 5 eV and at 9.4 eV. As the photon energy is increased, the 9.4 eV peak is enhanced slightly and an additional feature at 12.4 eV is introduced. This peak rises to a maximum at a photon energy near 74 eV and then decays in intensity, along with a portion of the 9.4 eV feature. With increasing photon energy, two additional peaks become apparent, centered at 15.0 and 28.8 eV. Over the photon energy range spanned by fig.1, several low energy Auger features are also observed; they appear at constant kinetic energy or at 2 eV higher binding energy in successive curves.

Figure 2 shows, in more detail, photoemission spectra obtained from the second sample with $h\upsilon$=74 and 94 eV, resonant energies for Cu and for Ba, resopectively. The long dashed curves represent an approximation to the secondary electron contribution and the multiple features observed in these curves are fit using simple Gaussian lineshapes. The detailed form of the secondary background does not, to first order, affect the locations or widths of the features but it can influence their intensities. Here, we are primarily interested in locating the energies of these features and this decomposition allows a better estimation.

The primary photoelectron feature, located immediately below E_F, contains at least two contributions that are centered at 2.3 and 4.5 eV. These states are identified as a combination of the Cu 3d and O 2p orbitals. The upper edge of the valence band nearly coincides with the Fermi level and the density of states at E_F is small; there is no distinctive edge. This valence band is not observed to resonate with photon energy. The other O-related feature in the binding energy region shown in these spectra is the O 2s level, observed with a low cross-section at 20.1 eV.

As indicated above, the intensities of several of the photoemission features are observed to resonate with the photon energy. This resonant enhancement is observed both for Cu 3d satellites and for Ba 5s and 5p levels. The Cu satellite resonant enhancement occurs as a result of an interference between an Auger process and a shake-up effect.[4(a)] This enhancement occurs at a photon energy of 74.2 eV in CuO and results in two satellites whose apparent binding energies are 12.9 and 10.5 eV with respect to the Fermi level.[4(b)] In Cu metal, the enhancement occurs at a photon energy of 75.6 eV and results in two satellites at 14.6 and 12.0 eV.[4(b)] In Cu_2O enhancement occurs at 76.5 eV and results in a single satellite at an apparent binding energy of 15.3 eV.[4(b)]

To better characterize the photon energy dependence of the 12.4 and 9.4 eV satellites observed here, we have fit these features with Gaussian peaks as shown in fig. 2 but in order to use consistent secondary electron approximations, a "Shirley method" background was used.[5] This gives a reasonable approximation to the form of the secondary background for energies near E_F. Figure 3 shows the photon energy dependence of the two Cu satellites over the energies where resonance is expected. Structure in the curves is consistent with the precision of the intensity determinations. The enhancement of the 12.4 eV feature is much stronger than for the 9.4 eV feature however the latter feature is likely to contain overlapping contributions from this satellite and a multi-electron feature that has been observed in

photoemission from metallic Y.[6] Both of these satellites are strongly enhanced at photon energies near 74.5 eV. Based on these observations, we assign the feature at 12.4 eV and a portion of the feature at 9.4 eV to resonantly enhanced satellites of Cu in a CuO-like oxide. At the lowest photon energies, the majority of the intensity of the 9.4 eV feature is likely to be due to Y.[6]

The apparent binding energies of the satellites in the oxide superconductor are significantly lower than the energies of the CuO satellites, indicating that the U_{eff} for the Cu cation in this material is smaller than that of CuO. The resonant energy, however is in good agreement with that of CuO.

When the photon energy exceeds 94 eV, the features at 15.0 and 28.8 eV are observed to be resonantly enhanced. This enhancement may be due to an interference with the excitation of the Ba 4d levels (whose binding energies are 91 and 93.1 eV[7]) and the two peaks are identified as Ba 5p and Ba 5s levels, respectively. This identification is confirmed by comparison of these valence levels with x-ray photoelectron (XPS) data from BaO. There, the Ba 5s has a binding energy of 30.6 eV and the Ba 5p level is observed at 15.2 eV, essentially in agreement with the observations made here.[7] Also observed in the spectrum shown in fig. 2(b) is a feature located at an apparent binding energy of 37.6 eV or a kinetic energy of 51.1 eV. This is identified as a Ba NOO Auger electron feature. Table 1 presents a listing of the energies and identifications of the valence features observed in this study.

Within the resolution of this study, there is no evidence for valence band structural changes associated with superconductivity as the temperature is lowered below T_c. In these measurements, the lowest temperatures attained were 88K. There are other effects of operating at low temperatures, though, especially the increased sticking probability of H_2O. Even at $1x10^{-10}$ Torr, the contamination of the surface due to H_2O adsorption was observed over time periods as short as 30 minutes. This surface contamination is observed both as a reduction of

the intensity of the 2.3 eV Cu/O valence band and in the introduction of the b_2, a_1, and b_1 molecular orbitals.

In conclusion, we have measured the valence electronic structure of $YBa_2Cu_3O_7$ above and below the critical temperature. The Cu/O valence band edge is located immediately below the Fermi level; a sharp Fermi edge was not observed. The features observed in the spectra have been identified with the use of resonant photoemission. The Cu oxide is similar to CuO however the U_{eff} is lower, as indicated by the lower satellite energies.

† Naval Research Laboratory / National Research Council Postdoctoral Associate

†† On a sabattical leave from the National Science Foundation.

††† Office of Naval Technology post-doctoral fellow.

References

1. L. F. Mattheis, Phys. Rev. Lett. 58, 1028 (1987); J. Yu, A. J. Freeman, and J.-H. Xu, Phys. Rev. Lett. 58, 1035 (1987); J. D Jorgensen, et. al., Phys. Rev. Lett. 58, 1024 (1987).

2. M. K. Wu, et. al., Phys. Rev. Lett., 58, 908 (1987).

3. S. Beech, S. Miraglia, A. Santora, and R. S. Roth, submitted.

4(a). M. Iwan, F. J. Himpsel, and D. E. Eastman, Phys. Rev. Lett. 43, 1829 (1979); (b) M. R. Thuler, R. L. Benbow, and Z. Hurych, Phys. Rev. B 26, 669 (1982).

5. D. A. Shirley, Phys. Rev. B 5, 4709 (9172).

6. S. D. Barrett and R. G. Jordan, Daresbury Laboratory Preprint, Feb. 1987.

7. R. E. Thomas, A. Shih, and G. A. Haas, Surf. Sci. 75, 239 (1978).

Table I.

Binding energies (±0.1 eV) referenced to E_F and widths (±0.2 eV) of electronic energy levels of $YBa_3Cu_2O_7$ superconductor

Level	Energy	FWHM
Cu 3d / O 2p	2.3	2.0
Cu 3d / O 2p	4.5	3.0
Y / Cu sat.	9.4	1.9
Cu sat.	12.4	2.5
Ba 5p	15.0	2.9
O 2s	20.1	3.3
Y 4p	24.0	3.1
Ba 5s	28.8	3.6

Figure Captions

1. Ultraviolet photoemission spectra obtained from UHV fractured $YBa_3Cu_2O_7$. The top curve is obtained with $h\upsilon$=60 eV and the lower curve is with $h\upsilon$=104 eV; successive curves are separated by photon energy increments of 2 eV. These data were obtained from the first sample. The spectra obtained from the second sample are essentially identical.

2. Photoemission spectra obtained from the second sample for photon energies of 74 and 94 eV (data points are given by the dots). These are resonant energies for Cu and Ba, respectively. The background of secondary electrons is approximated by the long dashed curve and the features in the spectrum are decomposed into a sum of Gaussian peaks (short dashed curves). The sum of the Gaussian peaks and the secondary background give the solid curve.

3. Intensities of the 9.4 and 12.4 eV features versus photon energy. The feature at 9.4 eV contains contributions from Y and from a Cu 3d satellite. The 12.4 eV feature is due to the second resonant Cu 3d satellite. The shapes and energy locations of these features are consistent with previous observations for the resonant behavior of CuO.

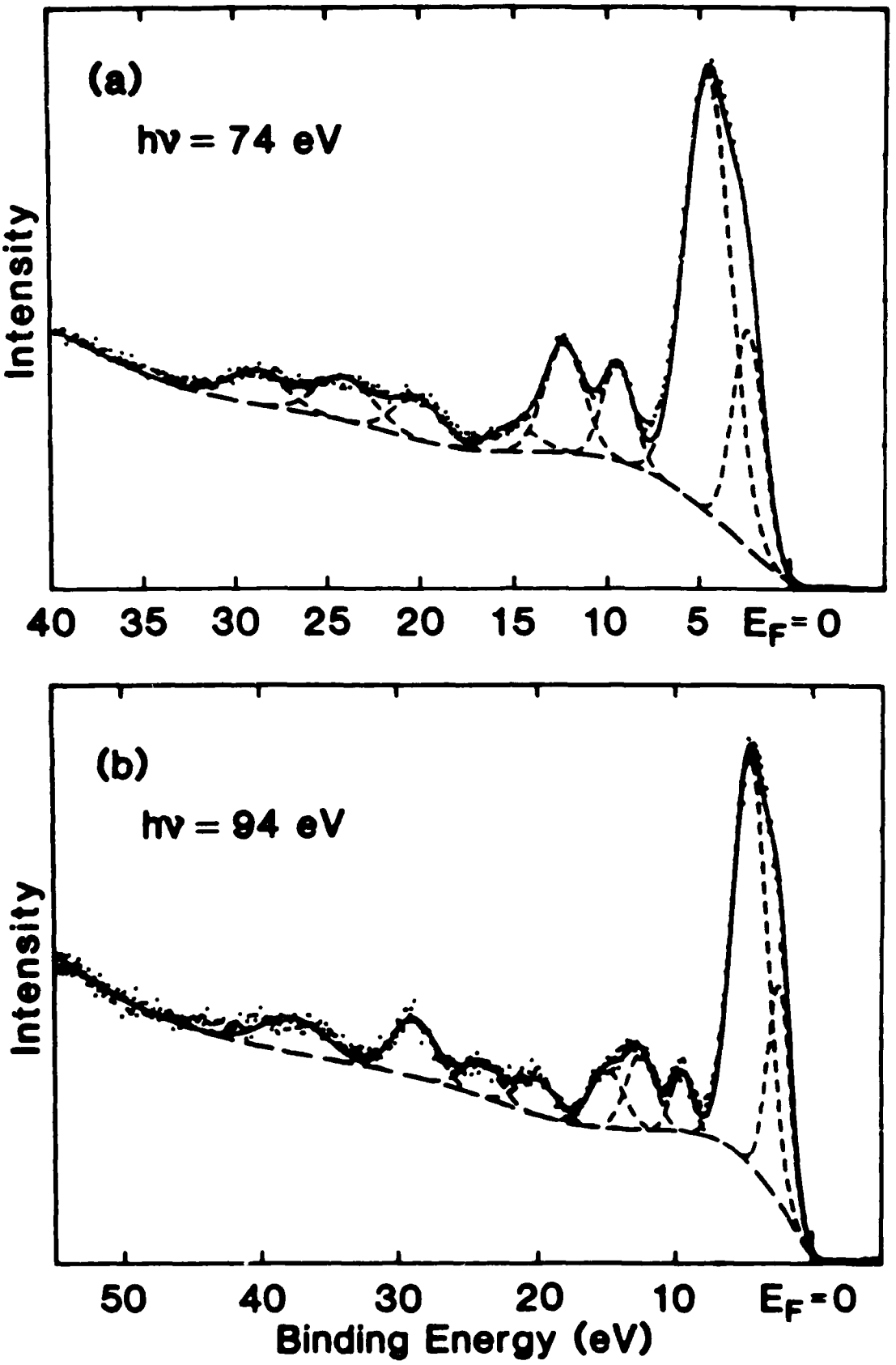
(a)
hν = 74 eV
Intensity
40 35 30 25 20 15 10 5 E_F = 0
(b)
hν = 94 eV
Intensity
50 40 30 20 10 E_F = 0
Binding Energy (eV)

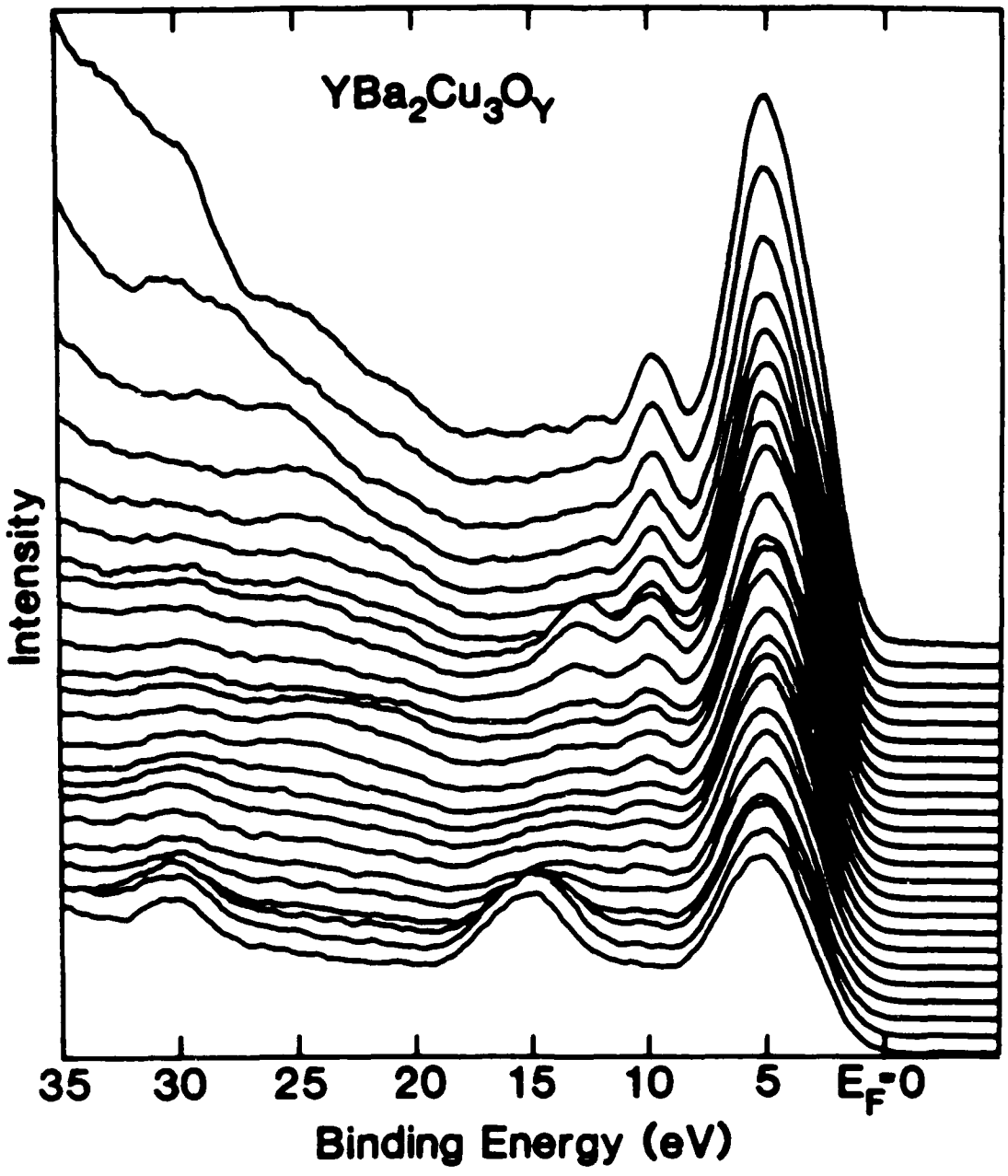
YBa2Cu3OY
Intensity
35
30
25
20
15
10
5
EF=0
Binding Energy (eV)

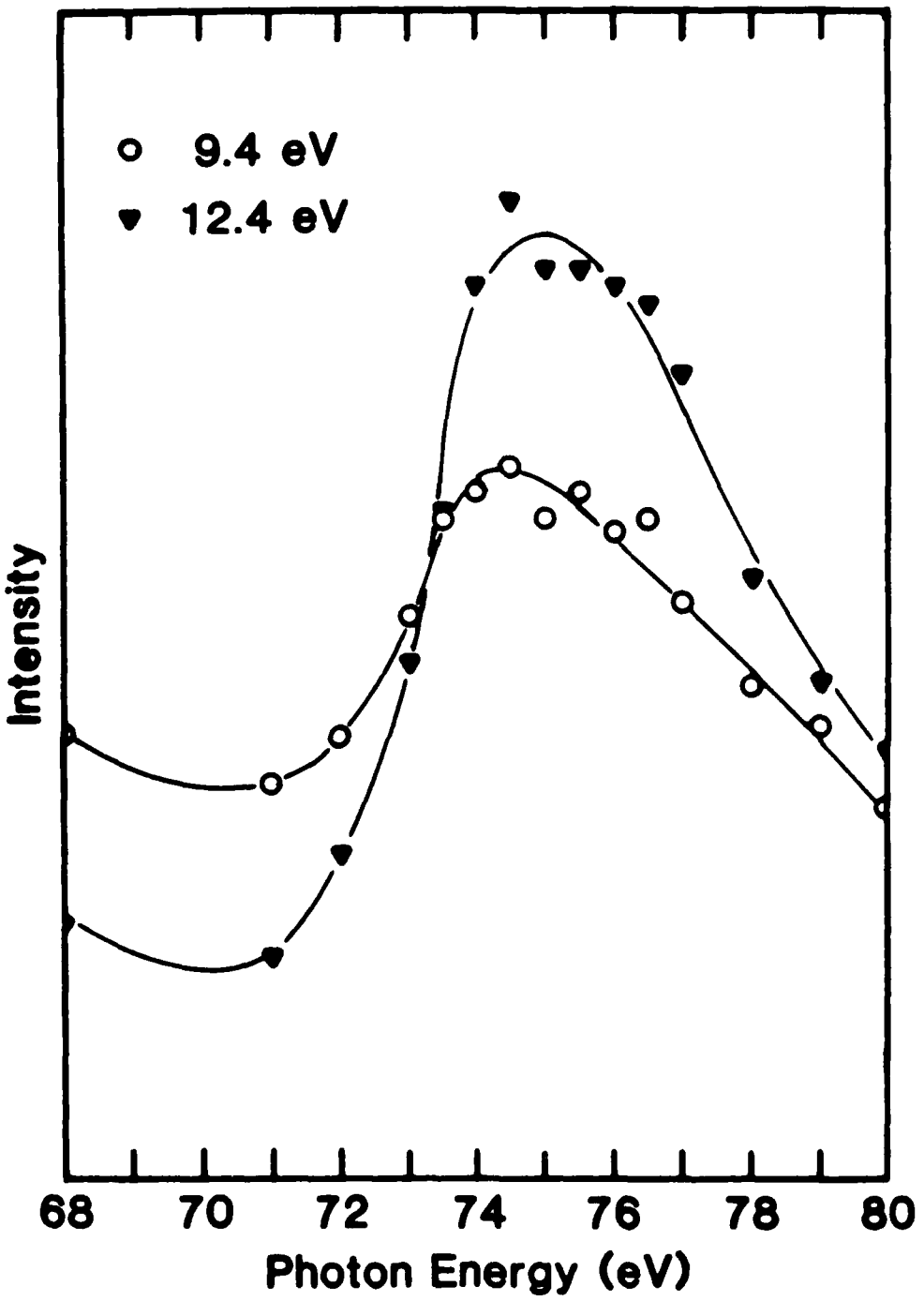
9.4 eV
12.4 eV
Intensity
68
70
72
74
76
78
80
Photon Energy (eV)

A PHOTOEMISSION STUDY OF HIGH T_c OXIDES

Donald Mueller* and Arnold Shih,
Louis E. Toth**, Michael Osofsky*** and
Stuart A. Wolf
Naval Research Laboratory
Washington, D.C. 20375

Richard L. Kurtz and Roger L. Stockbauer
National Bureau of Standards
Gaithersburg, Maryland 20899

INTRODUCTION

A number of ceramic compounds including $YBa_2Cu_3O_7$ have been reported to superconduct at temperatures in excess of 35K [1-9]. A critical feature in the processing of these compounds required to obtain good superconductive properties appears to be a final annealing stage in an oxygen containing atmosphere to increase the oxygen content of the materials [10]. Without the oxygen anneal step, the superconducting transition temperature drops and the drop in the temperature versus resistance curve becomes less defined.

To aid in the development of a better understanding of the electronic structure in this class of materials, we have examined changes in the electronic density of states for $YBa_2Cu_3O_x$ with oxygen content via ultraviolet photoelectron spectroscopy. Samples with x = 6.95, 6.5, and 6.05 were examined.

Photoelectron energy distribution curves provide a semiquantitative measure of the density of occupied electronic states in a material. They differ from the actual density of states in two respects. First, the photoionization cross-sections for different electronic states can be quite different, and their dependence on photon energy can be different as well. For the copper 3d and oxygen 2p levels the photoionization cross sections are approximately equal at a photon energy of 40eV [11]. Secondly, the position of the peaks in a photoelectron energy distribution curve may be shifted slightly with respect to the actual peaks in the density of states due to interaction of the photoelectron with the hole it leaves behind.

Our determination of the electron density of states in $YBa_2Cu_3O_{6.95}$ [12] is in good agreement with similar determinations made by other research groups [12-14]. The

experimentally determined electronic density of states, however, differs from the calculated valence band density of states [15-17], both in terms of the valence band width and in terms of the peak positions relative to the Fermi level.

Although photoemission is a surface sensitive technique, it has been used successfully to examine the bulk electronic structures of a large variety of both metallic and semiconducting compounds [18].

EXPERIMENTAL

In the experiment electrons photoemitteded from the sample were energy analyzed by a double pass cylindrical mirror electron energy analyzer. The source of the photons was the SURF-II storage ring. The energy of the incident light was selected by a toroidal grating monochromator whose energy band width at 60eV photon energy was calculated to be 350meV. At lower energies the resolution was better, at higher energies, worse. Spectra presented below have been normalized to the incident light flux as determined by a calibrated in line tungsten mesh photodiode. The resolution of the electron energy analyzer was fixed independent of the photon energy at 240meV.

The $YBa_2Cu_3O_{6.95}$ sample was prepared as described in reference 10. Other samples prepared in the same batch were characterized by X-ray diffraction, neutron diffraction, resistance versus temperature measurement and Meisner effect [19]. T_c was determined as 93K with a 2K width. The sample was found to have an orthorhombic crystal structure. The $YBa_2Cu_3O_{6.5}$ sample was prepared in the same way as the 93K sample except that the final oxygen anneal step was omitted [10, 20]. Identical samples characterized by resistance measurements and x-ray diffraction were found to have transition temperatures of about 60K with a tetragonal crystal structure. The $YBa_2Cu_3O_{6.05}$ sample was prepared by annealing $YBa_2Cu_3O_{6.5}$ in flowing argon at 750°C for 15 hours. Samples prepared by an identical procedure were found by neutron diffractions to have a tetragonal crystal structure and 6.05 oxygen atoms per unit cell [19]. Auger analysis verified that the last two samples had an oxygen content ratio of approximately 6.5/6.05.

Photoemission measurements were conducted in UHV at pressures from $1x10^{-10}$ to $3x10^{-10}$ Torr. Rectangular samples were cut in air from pellets sintered to approximately 80% density, and mounted rigidly in indium encased in an aluminium holder. Immediately before photoemission measurements were conducted, the samples were fractured in UHV with a stainless steel blade. The samples were positioned so that the photoemitting face was at an angle of 45° with respect to both the photon beam and the analyzer axis. Fermi level determinations were made on the basis of the Fermi edge observed in photoemission spectra from a sputtered gold foil

that was in electrical contact with the samples. The sample holder was mounted on a liquid nitrogen cooled manipulator. Temperatures were determined using a W-5% Re W-26% Re thermocouple imbedded in the sample holder. The measurements were angle integrated throughout the Brillouin zone due to both the large acceptance cone of the CMA and the polycrystalline nature of the sample. No evidence for radiation induced damage was observed in our experiments for any of these samples. Spectra taken immediately after fracturing the sample to expose fresh surface appeared identical to spectra obtained after periods as long as 3.5 hours. This corresponds to a radiation dose of about 10^4 photons/surface atom at photon energies from 30 to 110eV.

RESULTS AND DISCUSSION

Figure 1 shows a series of photoelectron energy distribution curves collected from the $YBa_2Cu_3O_{6.95}$ sample at photon energies from 50 to 108eV. Different features are enhanced at different photon energies. The features at about 14 and 29eV below the Fermi level (E_F) are due to emission from the barium 5p and 5s levels, and are enhanced above the Ba 4d photoionization threshold. The peak at 12.4eV binding energy prevalent in the 76eV photon energy spectrum is assigned to a valence band satellite feature that resonants at the copper 3p threshold. Similar resonance satellites have been observed for CuO and Cu_2O [22]. The binding energy of the satellite feature and the photon energy for which it is most intense depend upon the charge state of copper. The binding energy and photon energy dependence of the satellite observed here are most nearly matched by CuO, although oxidation states other than Cu^{++} cannot definitely be ruled out on the basis of our data. The features that appear at 28 and 31eV in the 60eV photon energy spectrum and at 24 and 27eV in the 64eV photon energy spectrum are due to the barium 4d core level excited by second order light. Above 70eV photon energy the intensity of second order light transmitted by the monochromator is essentially zero. The features at 20 and 24eV binding energy visible particularly in the low energy spectra arise from the oxygen 2s and yttrium 4p levels. The main valence band photoemission feature occurs with a binding energy 4.5eV below the Fermi level. Two smaller peaks with binding energies of 9.4 and 2.3eV also occur. Both these peaks drop more rapidly in intensity than the 4.5eV feature with increasing photon energy. At photon energies of approximately 40eV, the photoionization cross-sections of oxygen and copper are approximately equal. At photon energies below 40eV, emission from predominantly oxygen derived levels is more intense than from levels of predominantly copper character [11]. At photon energies above 40eV, emission from predominantly copper derived levels is more intense than emission from oxygen derived levels. This observation together with the behavior of the spectra in figure 1 suggests a greater oxygen contribution for the levels at 2.3

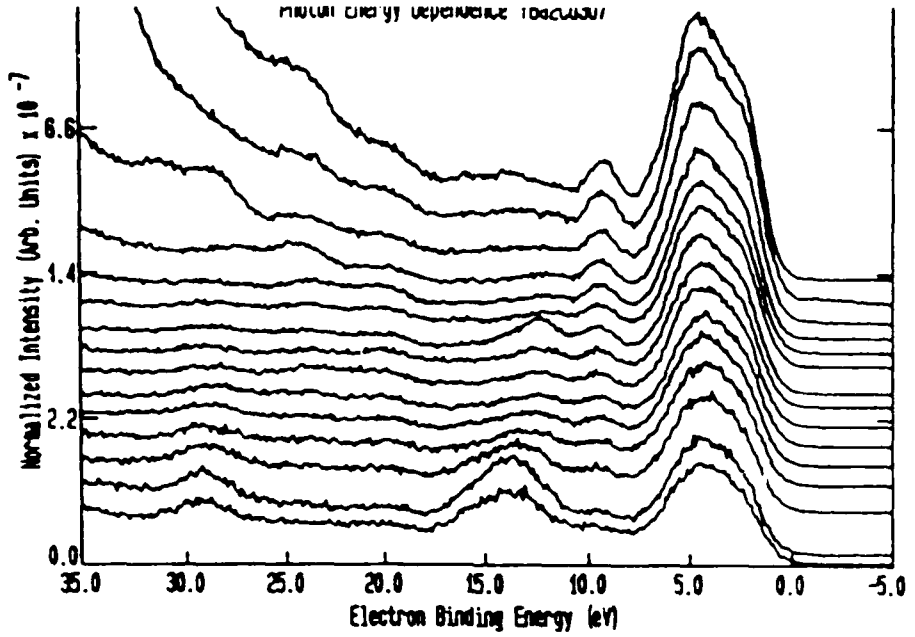

Figure 1. Photoelectron energy distribution curves from $YBa_2Cu_3O_{6.95}$ at photon energies from 50 to 108eV. The electron binding energies are measured with respect to the Fermi energy (0.0eV). The curves have been offset vertically for clarity. Photon energies were 50eV (top curve), 55, 60, 64, 68, 72, 76, 80, 84, 88, 92, 96, 100, 104, and 108eV (bottom curve).

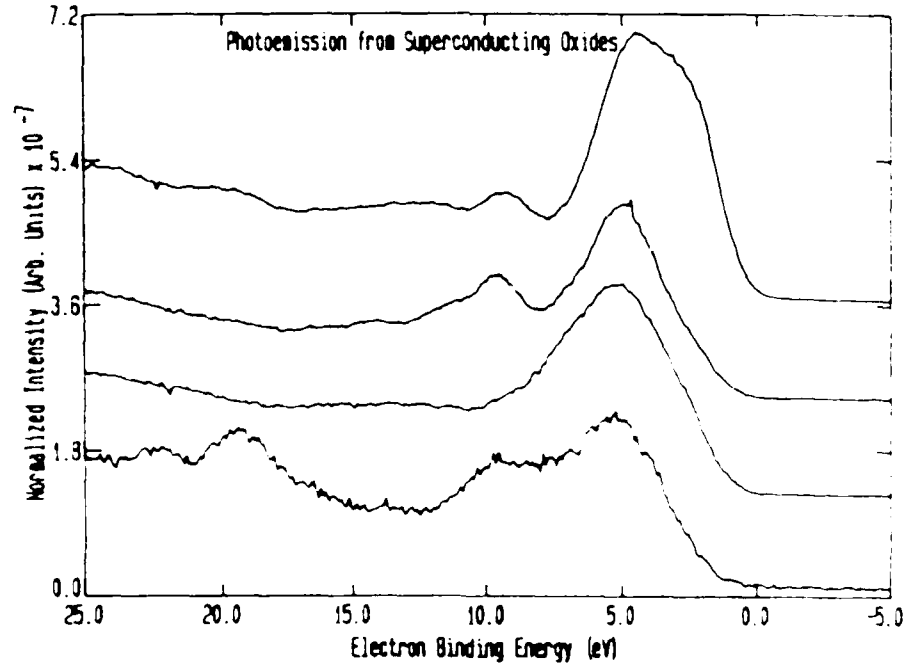

Figure 2. Photoemission spectra (photon energy=60eV) are compared for the compounds $YBa_2Cu_3O_{6.95}$ (top curve), $YBa_2Cu_3O_{6.5}$, $YBa_2Cu_3O_{6.05}$ and La_2CuO_4 (bottom curve).

and 9.4eV binding energy than to the main peak. On cooling the 93K superconductor to 88K, no changes in the valence band photoemission spectra were noted. The 2.3eV peak was particularly sensitive to water adsorption. After exposure of the sample to 1 L water vapor this peak was significantly reduced in intensity.

Figure 2 shows photoemission spectra of the valence band region for the three $YBa_2Cu_3O_x$ samples together with a spectrum from a non-superconducting La_2CuO_4 sample. All four spectra show the main peak in the electron energy distribution curves 4.5 to 5eV below the Fermi level. This peak is shifted slightly toward higher binding energies in the oxygen deficient compounds and in La_2CuO_4. The feature at 9.4eV binding energy is also present in all the spectra except that of $YBa_2Cu_3O_{6.05}$, where it appears to be shifted to 8.8eV and reduced in intensity. The main difference between the 93K superconductor and other compounds is the presence of the feature at 2.3eV binding energy. It is much less intense in the $YBa_2Cu_3O_{6.5}$ spectrum where it appears to be shifted slightly toward higher binding energy (2.6eV) and has all but vanished in the $YBa_2Cu_3O_{6.05}$ spectrum (See figure 3). Minor shifts in the O 2s, Y 4p and Ba 5s and 5p levels also take place with changes in the oxygen concentrations. These shifts may be due to a combination of changes in the atomic charge states and changes in the hole screening. The levels of binding energies are summarized in table I.

The measurements presented here provide two constraints on theoretical treatments aimed at understanding the electronic structure of $YBa_2Cu_3O_x$. (1) The presence of the 2.3eV feature in spectra from the 93K compound implies a higher charge carrier concentration at the Fermi level in this compound than in the related lower T_c and non-superconductive compounds. (2) The oxygen-like cross sectional dependence of the 2.3eV states implies a large contribution from oxygen toward the density of states near the Fermi level in the 93K compound. In agreement with the measurements, calculations by Massidda et. al. [16] and Krakauer et. al. [17] show that the density of states near the Fermi level are mainly derived from the oxygen in the Cu-O chain. More significantly, the observed 2.3eV feature is intense in the orthorhombic sample, but very weak or absent in the tetragonal samples. The X-ray and neutron diffraction data [10, 19] as well as Cu-O vibrational spectra [22] indicated that the linear Cu-O chains are removed by the orthorhombic to tetragonal phase transition. The measurements however disagree with the calculations in terms of the locations of peaks in the electronic density of states with respect to the Fermi level. The measured levels lie roughly 2eV further below E_F than the calculated peaks. Part of this shift may be due to interaction between the photoemitted electron and the hole it

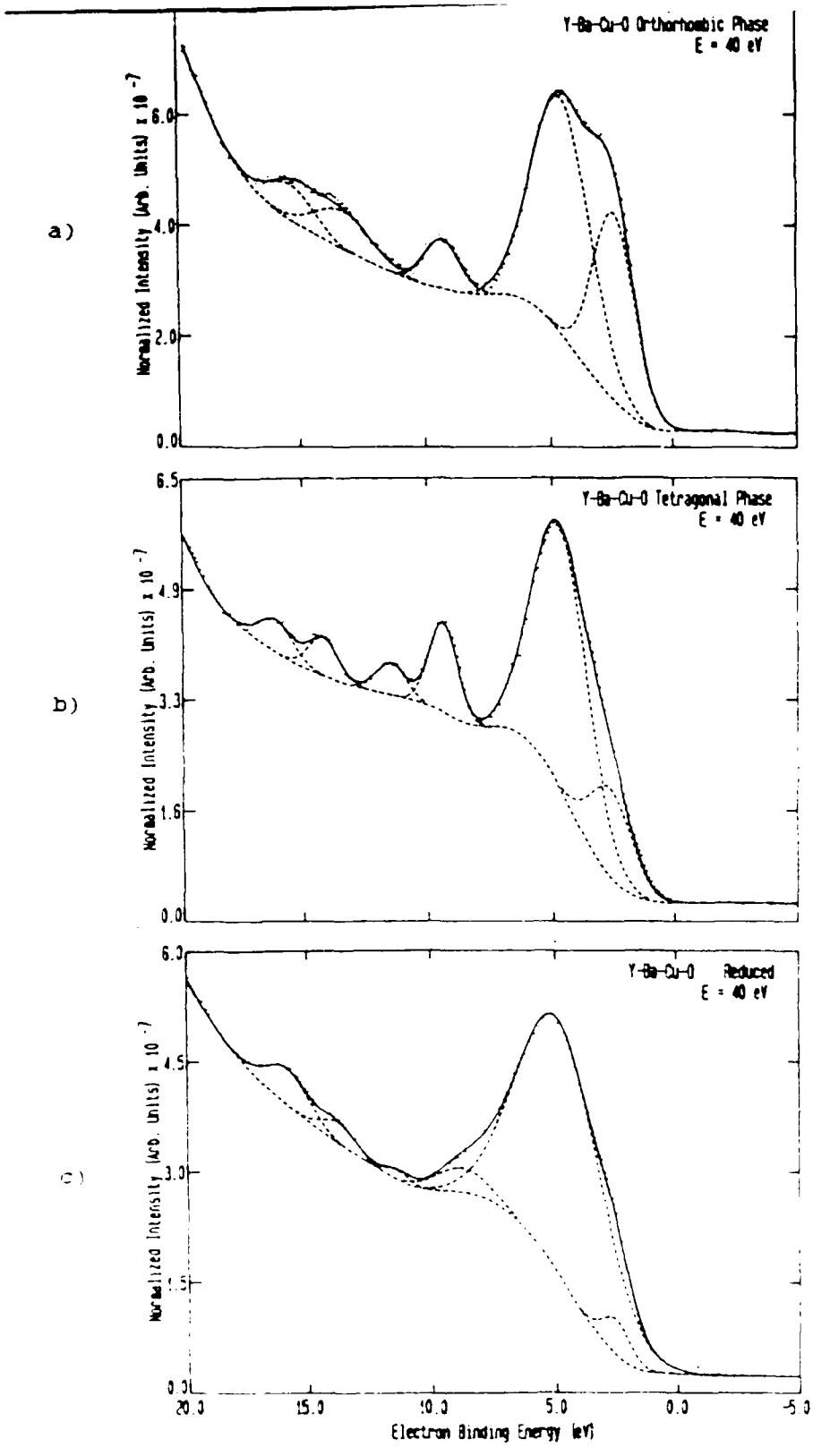

Figure 3. Deconvolution of the 40eV spectra into a background and Gaussian peaks. a) $YBa_2Cu_3O_{6.95}$, b) $YBa_2Cu_3O_{6.5}$, c) $YBa_2Cu_3O_{6.05}$

Table 1. Comparison of electronic binding energies for $YBa_2Cu_3O_x$ Compounds (in units of eV)

Levels	Orthorhombic x = 6.95	Tetragonal x = 6.5	Tetragonal x = 6.05
Valence	2.3	2.6	—
Valence	4.5	4.7	4.8
Valence+ Satellite	9.4	9.4	8.8 (?)
Ba 5p $_{3/2}$	13.3	14.2	13.7
Ba 5p $_{1/2}$	15.3	16.2	15.8
O 2s	20.1	20.5	21.0
Y 4p	24.0	24.0	24.5
Ba 5s	28.8	28.8	29.8

leaves behind in the final state. But, further investigations are needed to determine the source (or sources) of this shift.

* National Research Council Postdoctoral Fellow.
** On sabbatical leave from the National Science Foundation.
*** Office of Naval Technology Postdoctoral Fellow.

ACKNOWLEDGMENT

RLK and RLS wish to acknowledge support from the United States Office of Naval Research. One of the authors (AS) wishes to thank his daughter, Tina, for typing the manuscript.

REFERENCES

1. M. K. Wu, J. R. Ashburn, C. T. Torng, P. H. Hor, R. L. Meng, L. Gao, Z. Huang, Y. Q. Wang and C. W. Chu, Phys. Rev. Lett. 58:908 (1987).
2. P. M. Grant, S. S. P. Parkin, V. Y. Lee, E. M. Engler, M. L. Ramirez, J. E. Vazquez, G. Lim, R. D. Jacowitz and R. L. Greene, to be published Phys. Rev. Lett. (1987)
3. S. Uchida, H. Takagi, K. Kitazawa and S. Tanaka, Jpn. J. Appl. Phys. Lett. 26:L1 (1987).
4. C. W. Chu, P. H. Hor, R. L. Meng, L. Gao, Z. J. Huang, and Y. Q. Wang, Phys. Rev. Lett. 58:405 (1987).
5. D. U. Gubser, R. A. Hein, S. H. Lawrence, M. S. Osofsky, D. J. Schrodt, L. E. Toth and S. A. Wolf, Phys. Rev. B35: 5350 (1987).
6. P. H. Hor, R. L. Meng, Y. Q. Wang, L. Gao, Z. J. Huang, J. Bechtold, K. Forster and C. W. Chu, Phys. Rev. Lett. 58: 1891 (1987).
7. D. W. Murphy, S. Sunshine, R. B. VanDover, R. J. Cava, B. Batlogg, S. M. Zhurak and L. F. Schneemeyer, Phys. Rev. Lett. 58:1888, (1987).
8. D. B. Mitzi, A. F. Marshall, J. Z. Sun, D. J. Webb, M. R. Beasley, T. H. Geballe and A. Kapitulnik (submitted to Phys. Rev.)
9. Shiou-Jyh Hwu, S. M. Song, J. Thiel, K. R. Poeppelmeier, J. B. Ketterson and A. J. Freeman, Phys. Rev. B35:7119 (1987).
10. L. E. Toth, M. Osofsky, S. A. Wolf, E. F. Skelton, S. B. Qadri, W. W. Fuller, D. U. Gubser, J. Wallace, C. S. Pande, A. K. Singh, S. Lawrence, W. T. Elam, B. Bender, and J. R. Spann, submitted to Proceeding of Journal of Chemistry, the American Chemical Society meeting, to be held in New Orlean, Aug. 20, 1987.
11. J. A. Yarmoff, D. R. Clarke, W. Drube, U. O. Karlesson, A. Taleb-Ibrahimi, and F. J. Himpsel, private communication.

12. R. L. Kurtz, R. L. Stockbauer, D. Mueller, A. Shih, L. E. Toth, M. Osofsky and S. A. Wolf, to appear in Phys. Rev. B., Rapid Communication, June 1, 1987.
13. P. D. Johnson et. al., to appear in Phys. Rev. B, Rapid communication, June 1, 1987.
14. F. C. Brown, T. C. Chiang, T. A. Friedmann, D. A. Ginsberg, G. N. Kwawer, T. Miller, M. G. Mason, submitted for publication.
15. L. F. Mattheiss and D. R. Hamann, submitted for publication.
16. S. Massidda, Jaejun Yu, A. J. Freeman, D. D. Koelling, Submitted for publication.
17. H. Krakauer and W. E. Pickett, Noval Mechanisms of Superconductivity, ed. by S. A. Wolf and V. Z. Kresin, this issue.
18. E. W. Plummer and W. Eberhardt in "Angle-Resolved Photoemission as A Tool For Study of Surfaces", Advances in Chemical Physics XLIX:533.
19. J. J. Rhyne, J. Gotaas, F. Beech, L. Toth, S. Lawrence, M. Osofsky, and S. A. Wolf, submitted for publication in Phys. Rev. B, Rapid communication.
20. A. M. Kini, U. Geiser, H-C. I. Kao, K. D. Carlson, H. H. Wang, M. R. Monaghan, and J. M. Williams, submitted for publication in Inorg. Chem., communication, (1987).
21. M. R. Thuler, R. L. Benbow and Z. Hurych, Phys. Rev. B26: 669 (1982)
22. M. Stavola, D. M. Krol, W. Weber, S. A. Sunshine, A. Jayaraman, G. A. Kourouklis, R. J. Cava and E. A. Rietman, submitted for publication.

OBSERVED TRENDS IN THE X-RAY PHOTOELECTRON AND AUGER SPECTRA OF HIGH TEMPERATURE SUPERCONDUCTORS

D.E. Ramaker[a], N.H. Turner[a], J.S. Murday[a],

L.E. Toth[b], and M. Osofsky[b]

Naval Research Laboratory, Washington, DC 20375

and

F.L. Hutson[c]

Chemistry Department,

George Washington University, Washington, DC 20052

X-ray photoelectron spectra and Auger electron spectra are reported for La_2CuO_4, and $YBa_2Cu_3O_4$ in the tetrahedral and orthorhombic crystal structures; they are compared to previously reported data for Cu, Cu_2O, and CuO. These data reveal large electron-electron interaction effects. The magnitude of these interaction effects correlate with the transition temperatures of the superconducting oxides.

[a]Chemistry Division

[b]Materials Science and Technology Division

[c]Supported by the Office of Naval Research

The recent discoveries of superconductivity above 30 K in $La_{2-x}Ba_xCuO_4$ [1] and above 90 K in a mixed-phase Y-Ba-Cu-O compound [2] (subsequently shown to be $YBa_2Cu_3O_{7-\delta}$ [3]), have generated a great interest in elucidating the electronic structure of these materials. The high transition temperatures (T_c) and the lack of an isotope effect [4] have suggested that the electron-phonon interaction, as indicated by the conventional Bardeen-Cooper-Schrieffer (BCS) mechanism [5], may not be dominant. Rather electron-electron interactions, such as in the "resonanting valence bond" (RVB) mechanism, may dominate [6]. Recent band-structure calculations and published density-of-states (DOS) have provided great insight into the electronic structure of these materials [7,8]. However, the one-electron nature of the band-structure calculations do not provide much insight as to the nature of the electron-electron interactions.

Auger electron spectroscopy (AES) is unique as an experimental tool in this regard, since the Auger lineshape reflects a two-hole (or two-electron) DOS [9]. Certain satellite features in x-ray photoelectron spectroscopy (XPS) also reflect a two-hole, one-electron final state. We report Cu $2p_{1/2}$ and $2p_{3/2}$ ($L_{2,3}$) XPS and Cu $L_{2,3}VV$ AES data for three superconducting (SC) materials having the nominal composition La_2CuO_4 (herein call the La material), and $YBa_2Cu_3O_7$ with the tetrahedral (123-t) and orthorombic (123-o) crystal structures. We compare this data with previously reported data [10] for Cu, Cu_2O, and CuO (herein called non-SC materials). Briefly, these data suggest the following: 1) the covalency of the Cu-O bond increases in the

order CuO < La < 123-t < 123-O (i.e. proportional to T_c), 2) the localized nature of the antibonding Cu3d-O2p σ^* band decreases with covalency, and 3) the electron-electron interaction energy in the Cu3d-O2p σ bonding band decreases with covalency (i.e. screening increases).

The La, 123-t, and 123-o materials were prepared from the high-purity powders La_2O_3, Y_2O_3, $BaCO_3$, CuO. These powders were mixed and calcined at 940° C for 3h (with an intermediate mixing), pressed into 1.2 cm diameter pellets and sintered for 12h at 940° C in air, reheated to 900° C in oxygen for 3h, and finally slow cooled at 1°/min. The 123-t material was air quenched from 900° C instead of slow cooling. Structures were determined by x-ray and neutron diffraction. The superconducting T_c's were determined resistively. Table 1 gives the temperature for each SC material at which the resistance begins to drop with cooling, and the temperature at which the resistance drops to zero. The La material exhibits only a filamentary superconductivity [11] and a resistance minimum at 29 K. Both the AES and XPS spectra were taken with Al Kα excitation at room temperature with a Surface Science Laboratories Model SSX-100-03 spectrometer . The samples were scraped with a diamond tip within five minutes of insertion into vacuum. XPS indicates that surface adventitous carbon was present, but this is not expected to alter any of our conclusions.

Fig. 1 and Table 1 show the XPS data comparisons. Note that large satellites are present in the Cu $L_{2,3}$ XPS spectra except for Cu metal and Cu_2O. This is apparently because the Cu 3d band is

filled in these two materials so that the previously identified 3d to $3d^9$ or σ to σ^* shakeup process, which may occur upon core excitation in CuO, cannot occur [12]. Larsson [12] has summarized the satellites observed in a large number of other systems as follows: 1) spectra with atomic ligands typically have one satellite peak associated with L_2 and two with L_3, 2) the satellite intensity is strongest if the ligands are highly electronegative (i.e. ionic bonding), 3) the energy separation between satellite and main peak increases with electronegativity. Table 1 indicates that the ionicity of the Cu-O bond must decrease (covalency increase) in the order as described above.

The $L_{2,3}VV$ Auger data are shown on the left in Fig. 1. Only the lineshape for Cu [10] has been quantitatively interpreted previously [13,14]. The Cu lineshape has been interpreted within an atomic picture, where the final state holes are assumed to remain on the atom with the initial core hole. The main feature at 918.8 and a smaller feature just 2.7 eV higher in kinetic energy arise from atomic multiplets within the principal L_3VV lineshape; a similar main feature for the L_2VV lineshape falls at 938.7 eV. Satellite features identified as arising from the LV-VVV process lie just to the left of the principal L_2 and L_3 features [13,14].

The lineshapes for Cu_2O [10] and CuO [10] are very similar to that for Cu; however the lineshapes measured in this work for the La and 123 SCs are very different. There are two reasons for this. First, becasue of the Al Kα x-ray source used in this work, the Auger lineshapes of the 3 SCs lie on top of a large

contribution arising from O 1s (kinetic energy = 951 eV) photoelectrons which have suffered inelastic loss processes on their way out of the sample. In a standard procedure [15] for Auger spectra, we deconvolved the entire spectrum (O 1s XPS plus Cu Auger region) with a backscattered electron spectrum taken such that the elastic peak had the same energy as the O 1s photoelectrons. This process removes most of the XPS-loss contribution as well as the Auger-loss contribution (this latter contribution is present also in the Cu, Cu_2O and CuO spectra). The L_3 portions of these deconvolved spectra are given in Fig. 2.

Comparison of Figs. 1 and 2 reveals that the relative sizes of the satellite and principal Auger contributions in the 3 SCs are very different from those for the 3 non-SCs. To understand how this can be true, we need to itemize those processes which can create the initial valence hole in the LV-VVV satellite. The relative total core ionization cross-sections under Al Kα x-rays are $L_1:L_2:L_3$ = 26:54:100 [13]. The L_1 and L_2 core holes may undergo Coster-Kronig (CK) decay ($L_{1,2}L_3V$). The resultant L_3 core hole may subsequently Auger decay, and because of the valence hole, this results in the satellite contribution. We assume that CK decay dominates for the L_1 core level, and that the level degeneracy dictates the relative final state populations (i.e. 9 L_2V to 18 L_3V) [13,14]. The relative intensities of the L_3VV and L_2VV contributions in the Cu Auger lineshape are approximately $L_3:L_2$ = 5:1 [13], hence we allot 18 to the L_2VV Auger and 36 to the L_2L_3V CK process. The theoretical probablity for shakeoff of a valence electron upon

"sudden" creation of a core hole in a Cu atom has been estimated to be around 10% [16]. Since this probabililty is nearly independent of the molecular environment [17], we allot 10 to the L_3V-VVV satellite from shakeoff. The total satellite contribution is then 70% of the principal contribution in close agreement with experiment for the non-SCs.

Table 1 shows that the relative satellite contribution for the 3 SCs is very much larger. This cannot arise from an increase of the L_2 CK decay since the experimental L_3VV:L_2VV intensity ratio in the SCs is similar to that for the non-SCs. Another possibility is that some of the principal Auger intensity goes elsewhere, for example at higher energy just below the L_2VV lineshape. We do see some contribution here, but it is not any bigger than that seen in the CuO lineshape, yet CuO does not show the enhanced satellite. We conclude that some intensity from the principal L_3VV contribution must be transfered to the satellite L_3V-VVV contribution.

The transfer of principal to satellite intensity can arise from the s to s^* shakeup process discussed above. Normally, shakeup does not cause a satellite Auger contribution since the shakeup electron remains localized and thus the shakeup-Auger final state still contains only two holes [17]. However, if the s^* electron should propagate away before the core hole decay, we then have a local three hole state, as in the shakeoff process. We suggests that the increased intensity of the L_3V-VVV satellites for the SCs results from delocalization of the σ^* shakeup electron before the Auger decay. This does not happen in

CuO, because in that material the σ^* orbital on the atom with the core and valence holes drops out of the conduction band and becomes a localized excitonic-like state with a binding energy of around 1.4 eV. [18]. In the SCs no band gap exists [7,8]; however, evidence for a $3d^*$ resonance does appear in recent x-ray absorption spectra for the La material [19]. Since the XPS satellite decreases (i.e. decreasing shakeup) while the Auger satellite increases with increasing T_c in the SCs, not all of the σ^* shakeup electrons must escape before the Auger decay. The escape probability must increase with covalent character, a trend one might expect as the electrons become more delocalized. Table 1 gives the relative amount of intensity transfer, from principal line to satellite, required to give agreement with experiment.

Finally we consider the spectral feature seen in Figs. 1 and 2 between the L_3 and L_2 Auger contributions. This very small feature for Cu has been interpreted as a delocalized band-like (as opposed to the atomic-like) contribution to the Auger lineshape [13]. This feature has increased intensity for the remaining oxide materials, suggesting that the larger intensity arises when one of the final state holes is delocalized onto a neighboring O atom (i.e. an effective two-center Auger final state, but not necessarily involving a two-center Auger process). Such a final state might arise when the σ Cu-O bonding band is involved in the Auger decay. Fig. 1 and Table 1 show that the energy of this two-center feature relative to the Fermi level (i.e. $E_{tc}-E_F$) decreases with increasing covalency. We have modeled this contribution in Fig. 2 for the SCs by applying the

Cini-Sawatzky expression [20] to the self-fold of the Cu DOS [7] with an effective hole-hole repulsion, U_{eff}, chosen to provide optimal agreement with experiment. Table 1 reveals that U_{eff} decreases as the covalency increases (i.e. as T_c increases), consistent with the increased screening of the Cu-O valence holes by the more delocalized electrons in the covalent systems.

In an ionic vs. covalent (i.e. local vs.non-local) description of the bonding, we have shown that the covalency of the Cu-O bond increases with T_c. This is reflected in the intensity and energy of the XPS satellites, in the intensity of the Auger satellites, and in the effective hole-hole repulsion energies reflected in the "two-center" Auger contribution. Increased covalency usually reflects increased interorbital overlap, in this case between the Cu 3d and O 2p orbitals. This increasing 3d-2p overlap is consistent with the decreasing interatomic distances (the shortest Cu-O distance is 1.95 A° in CuO, 1.95 in La [21], and 1.85 in 123-t and 123-o [1,3]) and the decreasing dimensional character of the Cu-O lattice (nominally 3D in CuO, 2D in La and 123-t, and both 2D and 1D in 123-o [7,8]) in the higher T_c SCs. Increased covalency suggests increased mobility of the electron pairs. Electron-electron interactions dominate the Auger and XPS satellite spectra for all of these materials, and these interactions may play a significant role in the electron pair binding [6].

We thank D.U. Gubser for providing the most recent literature supporting this work.

TABLE 1 Summary of the XPS and AES data for the six materials studied.

Item	Cu	Cu_2O	CuO	La	123-t	123-o
T_c(K)	-	-	-	43-29	80-70	93-91
XPS						
[E(sat) - $E(L_3)$] (eV)	8.5-9	-	-	8.5	9	9.2
$I(sat)/I(L_3)$	-	-	0.58	0.49	0.43	0.37
AES						
$I(L_3VV)$[a]	90	90	90	90	90	90
$I(L_3V\text{-}VVV)$ from L_1 & L_2 CK and shakeoff	64	64	64	64	64	64
$I(L_3V\text{-}VVV)/I(L_3VV)$, Theory	0.70	0.70	0.70	0.70	0.70	0.70
$I(L_3V\text{-}VVV)/I(L_3VV)$, Exp.	0.75	0.75	0.75	1.3	1.5	1.6
% of shakeoff transfer	0	0	0			
E_{tc}-E_F (eV)	-	-				
U_{eff}. (eV)	-	-	-	2	≈0	≈0

aThe total L_3 ionization cross for each material is normalized to 100. This cross-section is then divided among the possible L_3 processes (e.g. for Cu we have [normal:shakeup:shakeoff]= 60:30:10)

References

1. J.G. Bednorz and K.A. Muller, Z. Phys. B64, 189 (1986).
2. M.K. Wu et al, Phys. Rev. Lett. 58, 908 (1987).
3. R.J. Cava, Phys. Rev. Lett. 58, 1676 (1987).
4. B. Batlogg et al, Phys. Rev. Lett. 58, 2333 (1987); L.C. Bourne et al, Phys. Rev. Lett. 58, 2337 (1987).
5. J. Bardeen, L.N. Cooper, and J.R. Schrieffer, Phys. Rev. 106, 162 (1957), and 108, 1175 (1957).
6. P.W. Anderson, Science 235, 1196 (1987).
7. J. Yu, A.J. Freeman, and J.H. Xu, Phys. Rev. Lett. 58, 1035 (1987); S. Massidda et al, to be published.
8. L.F Matteiss, Rev. Lett. 58, 1028 (1987).
9. D.E. Ramaker, Appl. Surf. Sci. 21, 243 (1985).
10. P.E. Larson, J. Electron Spectrosc. Related Phenom. 4, 213 (2974).
11. J. Beille et al, to be published.
12. S. Larsson, Chem. Phys. Lett. 40, 362 (1976).
13. P. Weightman and P.T. Andrews, J. Phys. C: Solid State Phys. 12, 943 (1979).
14. N. Martensson and B. Johansson, Phys. Rev. B28, 3733 (1983).
15. D.E. Ramaker, J.S. Murday, and N.H. Turner, J. Electron. Spectrosc. Related Phenom. 17, 45 (1979).
16. T.A. Carlson et al, Phys. Rev. 169, 27,(1968).
17. D.E. Ramaker, Phys. Rev. B25, 7341 (1982).
18. M.R. Thuler, Phys. Rev. B26, 669 (1982).

19. J.M. Tranquada et al, Phys. Rev. B35, 7187 (1987); E.E. Alp et al, Phys. Rev. B35, 7199 (1987);

20. M. Cini, Solid State Commun. 20, 650 (1976); Phys. Rev. B17, 2788 (1978); G.A. Sawatzky, Phys. Rev. Lett. 39, 504 (1977).

21. E. Skelton, private communication.

Figure Captions

Fig. 1 Comparison of the previously published Cu $L_{2,3}VV$ Auger spectra (left) and x-ray photoelectron spectra (right) for Cu, Cu_2O, CuO [10] with those obtained in this work for the superconducting materials La_2CuO_4 and $YBA_2Cu_3O_7$ in the tetrahedral and orthorhombic crystal structures (i.e. the La, 123-t, and 123-o materials). The principal components, L_2 and L_3, and satellites for each case are indicated. The vertical marks indicate the energy of the L_3 Fermi level, E_F, and the "two-center" feature, $E_{t.c.}$.

Fig. 2 Comparison of the Cu L3VV Auger spectra for the La, 123-t, and 123-o superconducting materials after deconvoluting out the inelastic contributions as described in the text. A least squares fit of the L_3V-VVV and L_3VV components [14] for Cu metal is shown. Slight relative shifts in the two components were required to obtain optimal fits. Also shown is a self-fold of the Cu DOS [7] after including correlations effects via the Cini-Sawatzky expression [20] with an optimal U_{eff} as tabulated in Table 1.

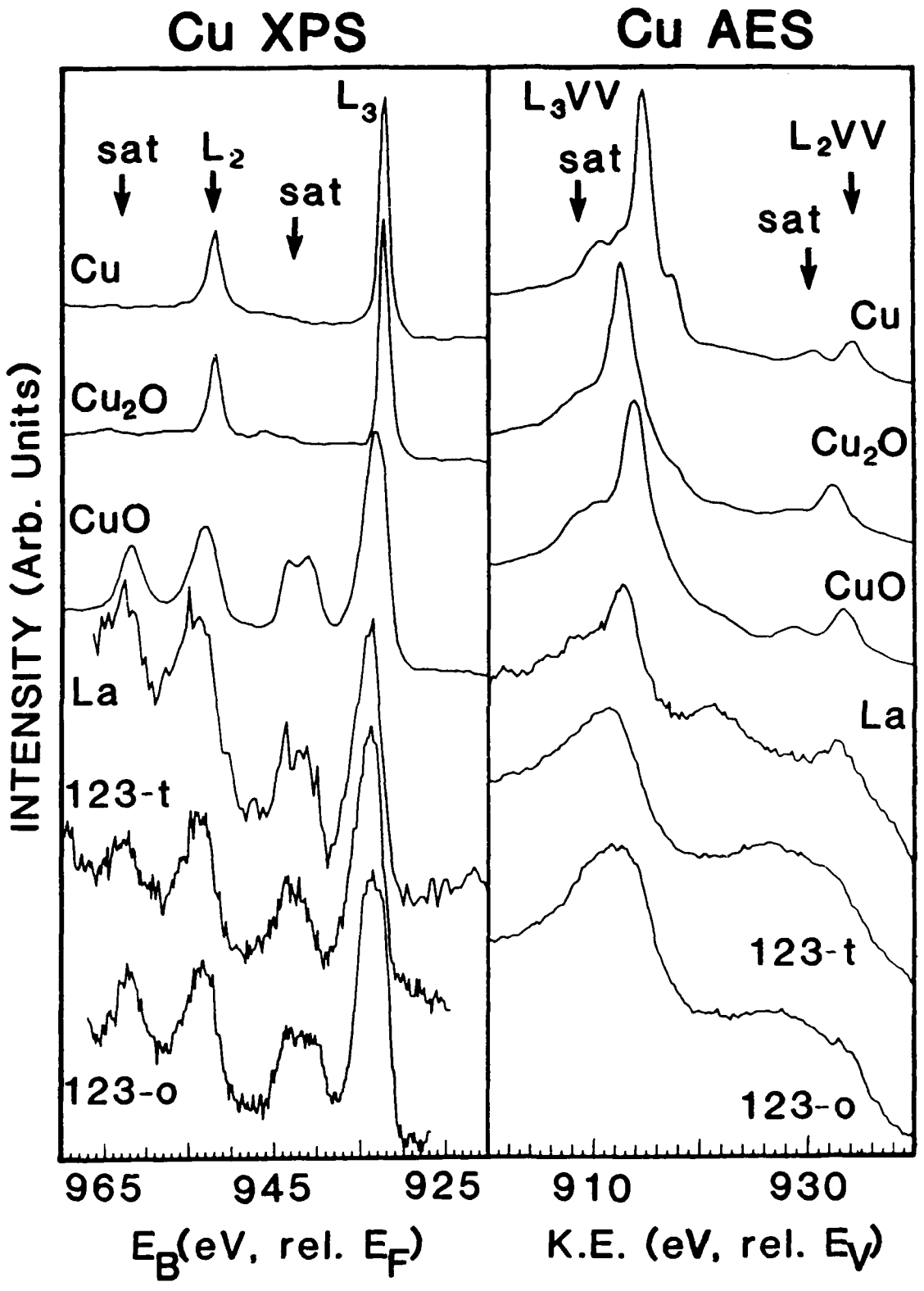
Cu XPS
Cu AES
L3
sat
L2
sat
L3VV
sat
L2VV
sat
Cu
Cu2O
CuO
La
123-t
123-o
INTENSITY (Arb. Units)
965
945
925
910
930
EB(eV, rel. EF)
K.E. (eV, rel. EV)

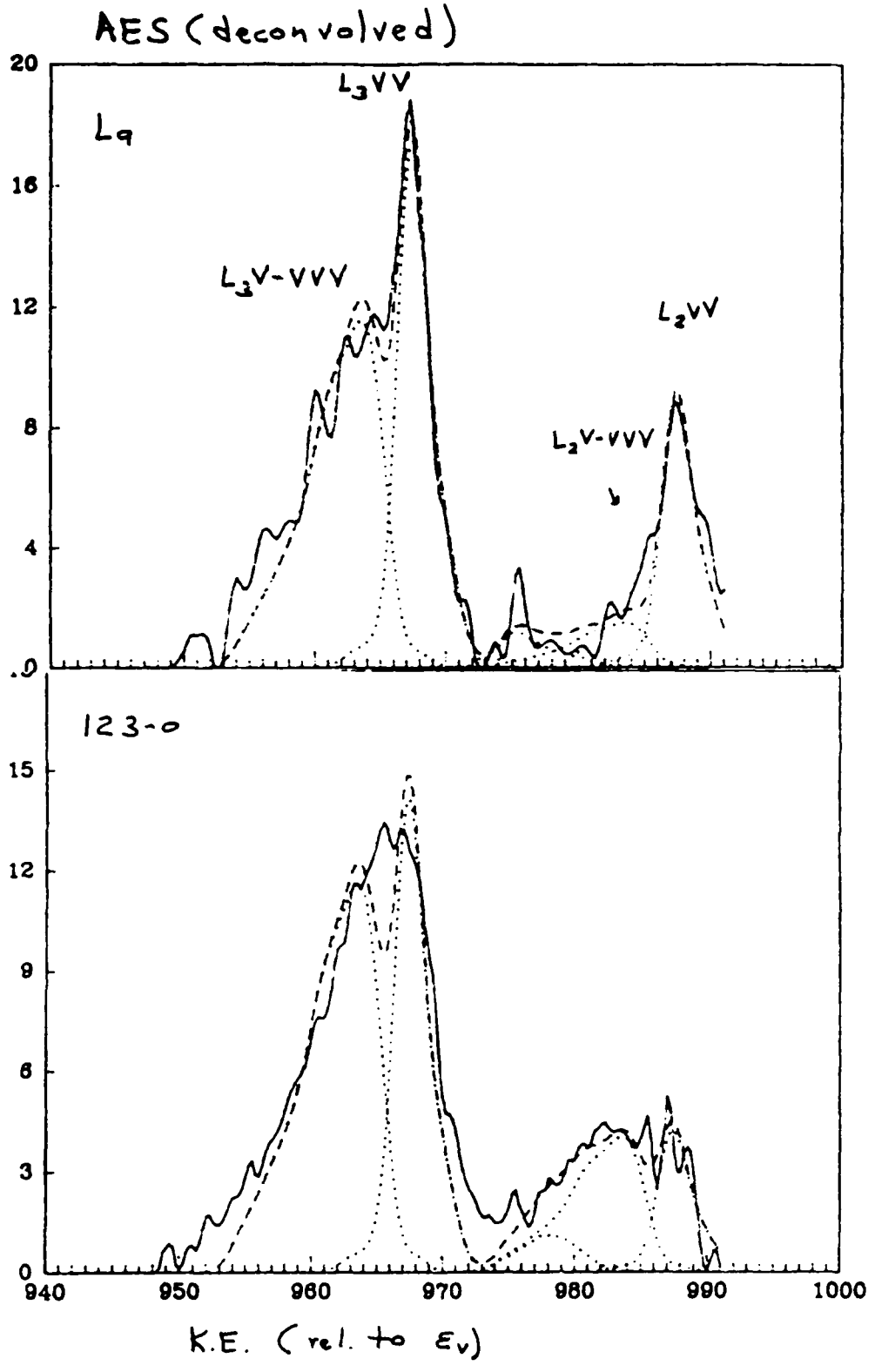
AES (deconvolved)
Li
L3VV
L3V-VVV
L2VV
L2V-VVV
123-o
20
16
12
8
4
0
15
12
9
6
3
0
940
950
960
970
980
990
1000
K.E. (rel. to εv)

IMPACT OF HIGH-TEMPERATURE SUPERCONDUCTORS ON HIGH POWER, MILLIMETER WAVE SOURCE TECHNOLOGY

Recent discoveries of compounds having superconducting transition temperatures above 77K has led to the distinct possibility that in the near term practical liquid N_2 cooled superconducting magnets will be available. The advent of liquid nitrogen cooled superconducting magnet technology will have an immediate impact on high power mm-wave source technology. The main problem that has faced the development of microwave/mm-wave sources employing conventional liquid He cooled superconducting magnets has been the coolant cost and/or the complexity of the cyrogenic system. By combining high temperature superconducting technology with advanced cyrogenic techniques these problems will be eliminated. Using present cyrogenic technology it should be possible to construct liquid N_2 cooled magnets which remain superconducting for months at a time without requiring additional coolant. The magnets then function as tunable, high field, permanent magnets. By eliminating the refrigeration system and the magnet power supply this would be the key towards extending superconducting technology to airborne applications.

High magnetic fields are advantageous for the operation of many advanced mm-wave devices. MM-wave devices can be broken down into two classes, slow wave or fast wave, depending on whether the phase velocity of the EM circuit wave is less than or greater than the speed of light in vacuum. Conventional slow wave devices use fragile periodic rf structures, such as a wire helix or corrugated metal wall, to slow down the EM wave. At mm-wave frequencies these structures are exceedingly small, on the order of a free space wavelength. Furthermore the electron beam must be placed very close to the structure for a strong interaction. The main problem plaguing high power slow wave mm-wave operation is heating of the slow wave structure due to electron beam interception. Better focusing of the beam is required therefore for high power mm-wave operation. The simplest way to accomplish this is to increase the strength of the confining magnetic field. Water cooled solenoids are typically employed in conventional power tubes requiring strong magnetic fields. High field operation ,however, results in excessive ohmic heating losses. For Naval applications where prime power usage is key these power losses can be unacceptable. Successful development of liquid N_2 cooled superconducting magnets would eliminate these problems. This technology would then result in an immediate advance in the performance of high power, mm-wave slow wave devices.

The advent of high temperature superconducting magnets will make many advanced fast wave, high power, mm-wave devices attractive for Naval applications. Electron cyclotron maser devices(gyro-devices) are typically operated at the fundamental harmonic where the gain, bandwidth and efficiency are greatest. High frequency operation at the fundamental ,however, requires very strong magnetic fields (40kG @ 100GHz). High temperature superconducting coils could make high field gyrotron operation feasible and thereby extend the performance of gyro-devices in the mm-wave regime. Free electron lasers(ubitrons) could also benefit from high temperature superconducting technology. In an FEL the interaction occurs between an electromagnetic wave and an electron beam undulating in a periodically varying magnetic field. The strength of the interaction depends on the wiggler magnetic field strength. By using small period, superconducting wiggler magnets high efficiency, moderate voltage mm-wave operation becomes possible. Furthermore, recent studies have shown that the efficiency and bandwidth of the free electron laser can be significantly enhanced by applying an axial magnetic guide field. High field strengths are typically required however to access the high efficiency mode of operation. Superconducting coils are therefore required for the practical implementation of such a device.

by: Carter Armstrong

SECURITY CLASSIFICATION OF THIS PAGE

REPORT DOCUMENTATION PAGE

Form Approved
OMB No 0704-0188

1a REPORT SECURITY CLASSIFICATION UNCLASSIFIED	1b RESTRICTIVE MARKINGS
2a SECURITY CLASSIFICATION AUTHORITY	3 DISTRIBUTION / AVAILABILITY OF REPORT
2b DECLASSIFICATION / DOWNGRADING SCHEDULE	
4 PERFORMING ORGANIZATION REPORT NUMBER(S)	5 MONITORING ORGANIZATION REPORT NUMBER(S)
6a NAME OF PERFORMING ORGANIZATION Naval Research Laboratory 6b OFFICE SYMBOL (If applicable)	7a NAME OF MONITORING ORGANIZATION
6c ADDRESS (City, State, and ZIP Code) Washington DC 20375-5000	7b ADDRESS (City, State, and ZIP Code)
8a NAME OF FUNDING / SPONSORING ORGANIZATION Office of Naval Research 8b OFFICE SYMBOL (If applicable)	9 PROCUREMENT INSTRUMENT IDENTIFICATION NUMBER
8c ADDRESS (City, State, and ZIP Code) Arlington, VA 22217	10 SOURCE OF FUNDING NUMBERS PROGRAM ELEMENT NO / PROJECT NO / TASK NO / WORK UNIT ACCESSION NO

11 TITLE (Include Security Classification)
Compliation of NRL Publications on High Temperature Superconductivity

12 PERSONAL AUTHOR(S)
Guber, Donald U. Editor

13a TYPE OF REPORT	13b TIME COVERED	14 DATE OF REPORT (Year, Month, Day)	15 PAGE COUNT
Compilation	FROM 1/1/87 TO 7/1/87		254

16 SUPPLEMENTARY NOTATION

17 COSATI CODES			18 SUBJECT TERMS (Continue on reverse if necessary and identify by block number)
FIELD	GROUP	SUB-GROUP	

19 ABSTRACT (Continue on reverse if necessary and identify by block number)

20 DISTRIBUTION / AVAILABILITY OF ABSTRACT ☒ UNCLASSIFIED/UNLIMITED ☐ SAME AS RPT ☐ DTIC USERS	21 ABSTRACT SECURITY CLASSIFICATION UNCLASSIFIED
22a NAME OF RESPONSIBLE INDIVIDUAL Donald U. Gubser	22b TELEPHONE (Include Area Code) (202) 767-2600 Code 4630

DD Form 1473, JUN 86 Previous editions are obsolete

S/N 0102-LF-014-6603

END

DATE

FILMED

APRIL

1988

DTIC